



<https://theses.gla.ac.uk/>

Theses Digitisation:

<https://www.gla.ac.uk/myglasgow/research/enlighten/theses/digitisation/>

This is a digitised version of the original print thesis.

Copyright and moral rights for this work are retained by the author

A copy can be downloaded for personal non-commercial research or study,
without prior permission or charge

This work cannot be reproduced or quoted extensively from without first
obtaining permission in writing from the author

The content must not be changed in any way or sold commercially in any
format or medium without the formal permission of the author

When referring to this work, full bibliographic details including the author,
title, awarding institution and date of the thesis must be given

Enlighten: Theses

<https://theses.gla.ac.uk/>
research-enlighten@glasgow.ac.uk

TRACER APPLICATIONS OF SELLAFIELD RADIOACTIVITY
IN BRITISH WEST COASTAL WATERS

Thesis submitted to the University of Glasgow in
fulfilment of the requirements for the degree of
Doctor of Philosophy

By

BEATRICE ECONOMIDES

OCTOBER 1986

CHEMISTRY DEPARTMENT
UNIVERSITY OF GLASGOW
GLASGOW G12 8QQ

ProQuest Number: 10991881

All rights reserved

INFORMATION TO ALL USERS

The quality of this reproduction is dependent upon the quality of the copy submitted.

In the unlikely event that the author did not send a complete manuscript and there are missing pages, these will be noted. Also, if material had to be removed, a note will indicate the deletion.



ProQuest 10991881

Published by ProQuest LLC (2018). Copyright of the Dissertation is held by the Author.

All rights reserved.

This work is protected against unauthorized copying under Title 17, United States Code
Microform Edition © ProQuest LLC.

ProQuest LLC.
789 East Eisenhower Parkway
P.O. Box 1346
Ann Arbor, MI 48106 – 1346

To my parents

"One of the greatest pains to
human nature is the pain of
a new idea".

Walter Bagehot

ACKNOWLEDGEMENTS

I gratefully acknowledge the invaluable advice and encouragement given by Professor M.S.Baxter throughout this project. Special thanks are also due to Mr.D.J.Ellett for his considerable kindness and help during this project.

I wish to thank Brian Miller (CRPB) and the SMBA for provision of ship time, hydrographic data and collection of water samples, the glassblowing and mechanical workshops (GU) for construction and maintenance of equipment and Dr.W.Jack for provision of counting facilities.

Pleasant social and working environments were created by the former Nuclear Geochemistry Group, Alison, Keith, Richard, Tam, Paul, Joe, Francis, Gordon, Mike, Andrew and Phil, by Kirsty, Colin, Joe, Anton, Dave M. and Roy of the SMBA and also by the "Hostel Mob and associates" in particular, Jenny, Sally, Mark, Chris M, Chris S, Yin, Nick, Gidon & Co. and Janet; thanks also to Jen for the use of the word-processor.

I owe inestimable gratitude to my family and my boyfriend, Tim, for continual encouragement and support and to my mother for typing of tables.

Finally, I acknowledge the support of a N.E.R.C. grant for this project.

INDEX

	<u>PAGE</u>	
CHAPTER 1	INTRODUCTION	
1.1	Releases of Artificial Radioactivity into the Marine Environment	1
1.2	Behaviour of Radionuclides in the Marine Environment	9
1.3	Effects of Artificial Marine Radioactivity on Man	19
1.4	Artificial Marine Radioactivity as Tracers	24
1.5	Aims	28
CHAPTER 2	EXPERIMENTAL	
2.1	Introduction	31
2.2	Pre-counting Procedures	32
2.3	Detectors and Counting Techniques Used	54
CHAPTER 3	COASTAL REGIONS	
3.1	Clyde Sea Area (CSA)	75
3.2	Loch Etive	95
3.3	Summary and Conclusions	98
CHAPTER 4	HEBRIDEAN SEA AREA	
4.1	Introduction	101
4.2	Research Vessel Cruises	102
4.3	Time Trends	205
4.4	Deep Samples	237
4.5	Summary and Conclusions	275
CHAPTER 5	SEAWEEDES	
5.1	Introduction	281
5.2	Radiological Investigations	287
5.3	Tracer Applications of Seaweeds	295
5.4	Half-distances, Residence-Times and Concentration Factors	321
5.5	Summary and Conclusions	330
CHAPTER 6	OVERVIEW	333
REFERENCES		339
APPENDICES		
Appendix I	Radiocaesium Levels in Surface Waters of Clyde Sea Area and Loch Etive	A1
Appendix II	Radiocaesium and Salinity Levels in Seawater for Research Vessel Cruises	A4
Appendix III	Environmental Appearance Factors (Ea)	A35
Appendix IV	¹³⁷ Cs Data for MAFF/GU Calibration	A46

cont'd...

INDEX Continued

	<u>PAGE</u>
Appendix V Seaweed Data	A47
Appendix VI Computer Programmes	A49
Appendix VII Reference Standards for Ge(Li)	A54

LIST OF FIGURES

	<u>PAGE</u>
1.1 UK nuclear establishments giving rise to principal discharges of liquid radioactive waste	2
1.2 Annual ¹³⁷ Cs discharges, 1971-1984	5
1.3 Radioactive discharges from Magnox ponds before and after installation of Zeolite skips	7
1.4 Impact of Windscale liquid effluent on the marine environment	20
1.5 Map showing areas studied	29
2.1 Map of Clyde Sea Area	33
2.2 Map of Loch Etive and surrounding area	35
2.3 Typical sampling stations in HSA	36
2.4 Outline of ¹³⁷ Cs analysis	38
2.5 Filtering of sea water samples	40
2.6 Gravity filtration of sea water through KCFC ion-exchange column	41
2.7 Sampling sites for soils, grasses and seaweeds	46
2.8 Outline of Pu analysis	48
2.9 Electroplating cell	52
2.10 An alpha particle spectrum	65
3.1 Concentration of ¹³⁷ Cs (pCi l ⁻¹) in UK coastal waters, May/July 1972	76
3.2 CSA (b) and modelled (a) ¹³⁷ Cs curves	80
3.3 Matching of Sellafield ¹³⁷ Cs discharge record with CSA ¹³⁷ Cs trend	82
3.4 CSA (b) and modelled (a) ¹³⁴ Cs: ¹³⁷ Cs ratio trends	86
3.5 Matching of CSA and Loch Etive ¹³⁷ Cs records	96
4.2.a1 Station positions - May 1983 cruise	103
4.2.a2 Salinity contours (‰) - May 1983 cruise	104
4.2.a3 ¹³⁷ Cs contours (dpm/l) - May 1983 cruise	105
4.2.a4 Salinity profile across (i) transect Z and (ii) transect A, May 1983	108

	<u>PAGE</u>
4.2.a5 Salinity profile across (i) transect B and (ii) transect D, May 1983	110
4.2.a6 Salinity profile across transect K, May 1983	113
4.2.a7 Salinity profile across transect J, May 1983	114
4.2.a8 ¹³⁷ Cs against distance from North Channel	116
4.2.a9 ¹³⁷ Cs along main path of plume (from North Channel), May 1983	118
4.2.a10 ¹³⁷ Cs/salinity plot to illustrate mixing between water types	120
4.2.a11 ¹³⁷ Cs/salinity curve, May 1983	122
4.2.a12 ¹³⁷ Cs/salinity plots illustrating (i) perfectly conservative Cs with fresh water influence and (ii) no fresh water influence with Cs removal	124
4.2.b1 Station positions, August 1983 cruise	130
4.2.b2 Salinity contours (‰) - August 1983 cruise	131
4.2.b3 ¹³⁷ Cs contours (dpm/l) - August 1983 cruise	132
4.2.b4 ¹³⁷ Cs/salinity curve - August 1983	134
4.2.b5 Salinity profile (‰) across (i) transect Z and (ii) transect A, August 1983	136
4.2.b6 ¹³⁷ Cs along main path of plume (from North Channel), August 1983	138
4.2.c1 Station positions, January 1984 cruise	142
4.2.c2 Salinity contours (‰) - January 1984 cruise	143
4.2.c3 ¹³⁷ Cs contours (dpm/l) - January 1984 cruise	144
4.2.c4 Salinities (‰) across transect G (17/11/83)	146
4.2.c5 Concentration (Bq kg ⁻¹) of caesium-137 in filtered surface water from the north-west of Scotland, October 1983	148
4.2.c6 ¹³⁷ Cs along main path of plume (from North Channel), January 1984	151
4.2.c7 ¹³⁷ Cs/salinity curve, January 1984	153
4.2.d1 Station positions - April/May 1984 cruise	156
4.2.d2 Salinity contours (‰) - April/May 1984 cruise	157
4.2.d3 ¹³⁷ Cs contours (dpm/l) - April/May 1984 cruise	158

	<u>PAGE</u>
4.2.d4 ¹³⁷ Cs along main path of plume (from North Channel), April/May 1984	159
4.2.d5 ¹³⁷ Cs/salinity curve, April/May 1984	160
4.2.d6 ¹³⁷ Cs/salinity plot for mixing of three water types (A, B and C)	162
4.2.e1 Station positions - June/July 1984 cruise	166
4.2.e2 Salinity contours (‰) - June/July 1984 cruise	167
4.2.e3 ¹³⁷ Cs contours (dpm/l) - June/July 1984 cruise	168
4.2.e4 ¹³⁷ Cs/salinity curve, June/July 1984	170
4.2.e5 ¹³⁷ Cs along main path of plume (from North Channel), June/July 1984	173
4.2.e6 Salinity contours (‰) - June/July 1984 cruise (Irish Sea section)	175
4.2.e7 ¹³⁷ Cs contours (dpm/l) - June/July 1984 cruise (Irish Sea section)	176
4.2.f1 Station positions - November 1984 cruise	180
4.2.f2 Salinity contours (‰) - November 1984 cruise	181
4.2.f3 ¹³⁷ Cs contours (dpm/l) - November 1984 cruise	182
4.2.f4 Salinity profile (‰) across (i) transect Z and (ii) transect A, November 1984	184
4.2.f5 Salinity profile (‰) across (i) transect B and (ii) transect F, November 1984	185
4.2.f6 ¹³⁷ Cs/salinity curve, November 1984	187
4.2.f7 ¹³⁷ Cs/salinity curves, June/July 1984 and November 1984	188
4.2.f8 ¹³⁷ Cs along main path of plume (from North Channel), November 1984	190
4.2.h1 Station positions - May 1982 cruise	195
4.2.h2 Salinity contours (‰) - May 1982 cruise	196
4.2.h3 ¹³⁷ Cs contours (dpm/l) - May 1982 cruise	197
4.2.h4 ¹³⁷ Cs/salinity curve, May 1982	198
4.2.h5 ¹³⁷ Cs/salinity curves, May 1982 and May 1983	200
4.2.h6 ¹³⁷ Cs along main path of plume (from North Channel), May 1982	202

	<u>PAGE</u>
4.3.1 ^{137}Cs /salinity curves for transect Z	209
4.3.2 ^{137}Cs /salinity curves for transect A	210
4.3.3 ^{137}Cs /salinity curves for transect B	211
4.3.4 ^{137}Cs /salinity curves for transect G	212
4.3.5 Isopleths of ^{137}Cs (Bq/l) and salinity ($\times 10^3$) against time for section D, west of Islay	214
4.3.6 Current speed at Tiree and wind speed ² at Tiree and Colerance	218
4.3.7 Temporal trend of ^{137}Cs levels at transects Z, A and D	222
4.3.8 Temporal trend of ^{137}Cs levels at transects B, E, G and K	223
4.3.9 Isopleths of ^{137}Cs peak values (Bq/l) on the sampling sections against time, 1983-85	233
4.4.1 ^{137}Cs /salinity curve - August 1983	241
4.4.2 ^{137}Cs /salinity curve - April/May 1984	243
4.4.3 ^{137}Cs /salinity curve - June/July 1984	247
4.4.4 ^{137}Cs profile across transect W (Irish Sea), June/July 1984 (dpm/l)	248
4.4.5 Three-dimensional ^{137}Cs distribution in the North Channel, June/July 1984 (dpm/l)	250
4.4.6 Salinity/Temperature profiles for stations (i) B2 and (ii) B4, June/July 1984	252
4.4.7 Profiles of transect D, June/July 1984 for (i) ^{137}Cs and (ii) salinity	253
4.4.8 Salinity profiles across transect D for (i) February 1985, (ii) May 1983 and (iii) August 1983	255
4.4.9 ^{137}Cs /salinity curve - November 1984	259
4.4.10 ^{137}Cs profiles across (i) transect W and (ii) transect X (Irish Sea), November 1984 (dpm/l)	260
4.4.11 Salinity and ^{137}Cs profiles across transect Z, February 1985	264
4.4.12 Salinity and ^{137}Cs profiles across transect Z, June/July 1984	268
4.4.13 Salinity and ^{137}Cs profiles across transect Z, November 1984	269
5.1 Sampling sites for seaweed, grass and soil samples	286

	<u>PAGE</u>
5.2 ^{137}Cs activity of seaweeds (mBq g^{-1})	293
5.3 Normalised ^{137}Cs levels in seaweeds ($^{137}\text{Cs}/^{40}\text{K} \times 10^3$)	294
5.4 Normalised radioactivity levels in seaweeds against distance from Sellafield	305
5.5 Radionuclide levels in seaweeds - (x) - standardised against ^{137}Cs plotted against distance from Sellafield	311
5.6 $\text{Pu}(\alpha)$ activity of seaweeds (mBq g^{-1})	314
5.7 Normalised $^{239/240}\text{Pu}$ levels in seaweeds ($^{239,240}\text{Pu}/^{40}\text{K} \times 10^3$)	319
5.8 Normalised radionuclide levels - (x) - against distance from Sellafield	320
5.9 $^{239,240}\text{Pu}/^{137}\text{Cs}$ ratios in seaweeds ($\times 10^2$)	325
5.10 $^{239,240}\text{Pu}$ and ^{106}Ru levels in seaweeds - (x) - standardised against ^{137}Cs plotted against distance from Sellafield	329

	<u>PAGE</u>
1.1 Annual discharges of ^{137}Cs from Sellafield, UK and from La Hague, France nuclear reprocessing plants, 1970-1982	3
1.2 ^{137}Cs and total (α and β) radioactivity discharged annually from Sellafield pipeline, Cumbria 1974-1984	4
1.3 Annual discharges of major radionuclides from Sellafield pipeline for 1983 and 1984	8
1.4 Distribution coefficients (Kds) for various elements	12
1.5 Concentration factors used for radiological assessment	17
2.1 Details of sample collections - seaweeds, soils and grasses	44
2.2 Details of gamma-counting facilities	58
2.3 Summary of NaI (Tl) system constants for 8mm (9mm) tubing	59
2.4 Counts under Cs peaks on system A NaI(Tl) (during ^{137}Cs spike counting) illustrating spectrum shift	73
3.1 Environmental Appearance (Ea) factors for the CSA - corresponding to a transit time of 4.8 months - and discharges, 1982-1984	89
3.2 Environmental Appearance (Ea) factors for Seascale obtained by averaging of 2 months' discharges 1982-1984	91
3.3 Environmental Appearance (Ea) factors for Loch Etive - corresponding to a transit time from Sellafield of 6.4 months	93
3.4 Dilution factors of CSA and Loch Etive radiocaesium levels from corresponding Seascale levels (1982-1984 discharges)	97
3.5 Summary of estimated transit times from Sellafield to the CSA / North Channel and residence times within the Irish Sea	99
4.2.a1 Mean ^{134}Cs : ^{137}Cs ratio across each transect	126
4.2.c1 ^{137}Cs levels across transect G, October/November 1983, as determined by MAFF	149
4.3.1 Dilution factors of radiocaesium levels between the North Channel - transect A - and various sites	207
4.3.2 Span of Islay Front along transect D ($55^{\circ}46'N$)	216
4.3.3 Intensity of Islay Front (salinity and ^{137}Cs gradients) and Tiree current speeds	217
4.3.4 Transit times from Sellafield to various transects	224

4.3.5	Environmental Appearance (Ea) factors for various transects for corresponding lag-times from Sellafield	226
4.3.6	Dilution factors of ^{137}Cs between the North Channel (transect A) and various transects, as derived from respective Ea values	229
4.3.7	Dilution factors of radiocaesium between Seascale and transect A and Seascale and transect G	231
4.4.1	Results of deep samples, August 1983	240
4.4.2	Results of deep samples, April/May 1984	242
4.4.3	Results of deep samples, June/July 1984	245
4.4.4	Results of deep samples, November 1984	257
4.4.5	Results of deep samples, February 1985	262
4.4.6	Estimated radiocaesium and water fluxes through the North Channel using 2.7 km day^{-1} current velocity (1.7 km day^{-1})	271
4.4.7	Estimates of northward water flux through the North Channel	272
5.1	Artificial radioactivity in seaweeds collected on 3/4 January 1983, counted on Ge(Li) detector - units in mBq/g dry weight	283
5.2	Gamma-emitting radionuclides found in seaweeds from Dunstaffnage and Northern Ireland - units in mBq/g dry weight	289
5.3	Gamma-emitting radionuclides found in environmental samples from the Isle of Man - units in mBq/g dry weight	290
5.4	Gamma-emitting radionuclides found in environmental samples from Barra, Outer Hebrides - units in mBq/g dry weight	291
5.5	Reduction factors for most abundant radionuclides in seaweeds	296
5.6	Transit times from Sellafield pipeline calculated from decay of $^{134}\text{Cs}/^{137}\text{Cs}$ ratio	299
5.7	^{134}Cs activities corrected for radioactive decay (mBq/g) and corresponding $^{134}\text{Cs}:^{137}\text{Cs}$ ratios	301
5.8	Data from Table 5.1 normalised with respect to ^{40}K	303
5.9	Levels of most abundant radionuclides in seaweeds, standardised with respect to ^{137}Cs levels	309

	<u>PAGE</u>
5.10 Pu activities found in seaweeds (mBq/g dry weight)	313
5.11 Reduction factors for Pu activities in seaweeds in relation to activities for the Ravenglass sample	315
5.12 Pu activities in seaweeds normalised with respect to ^{40}K	316
5.13 Reduction factors for Cs and Pu nuclides in seaweeds with activities normalised with respect to ^{40}K	317
5.14 Reduction factors for ^{106}Ru , ^{95}Nb and ^{60}Co nuclides in seaweeds with activities normalised with respect to ^{40}K	322
5.15 Pu activities in seaweeds standardised with respect to ^{137}Cs levels	323
5.16 $^{239,240}\text{Pu}$ reduction factors compared to ^{137}Cs reduction factors	324

ABSTRACT

In this research study, Sellafield - discharged radioactivity, in particular radiocaesium, is used to trace water movement in west British coastal waters.

Data on radiocaesium levels in surface waters of the Hebridean Sea Area, Clyde Sea Area, North Channel and Irish Sea are interpreted along with salinity and other hydrographic results. These data provide information on spatial and temporal property distributions whilst subsurface radiocaesium levels help to improve knowledge of the three-dimensional transport of these waters. In parallel, seaweeds from the west coast of Britain (including N. Ireland, the Isle of Man and the Outer Hebrides) have been analysed for their radionuclide contents.

Matching of radiocaesium time-trends at various sites has provided estimates of water transit times between stations (e.g. 4.8 months from Sellafield to the Firth of Clyde) and thus has allowed calculation of nuclide Appearance (Ea) Factors. A 14.4 months' residence time for water in the Irish Sea / Clyde Sea Area system and a maximum decay-time of 17 months between Sellafield and the Clyde Sea Area have been estimated; evidence from sea water and seaweed radionuclide levels suggests that most of this residence occurs in the north eastern Irish Sea.

It is proposed that a fraction of the Sellafield - discharged material, particularly in the Irish Sea and probably in surface waters, remains relatively undiluted during transport of the radioactive plume from Sellafield to The Minches, whilst some extensive mixing may occur in deeper and surrounding waters.

Restriction of the radioactive plume to the Scottish coast is observed when Atlantic water incursion into the Hebridean Sea Area is strong and the Islay Front attains an easterly position. When Atlantic water influence in the area is weak, the front has a more westerly position and coastal confinement of the plume is less obvious. Observations show that, when the gradient across the front is strong, nearby current velocities are slow and vice versa; current velocity is found to show good correlation with wind speed.

Radiocaesium dilutions estimated from Ea values and measured sea water and / or seaweed radiocaesium levels indicate relatively high (~twentyfold) dilutions from Sellafield to the North Channel and the Clyde Sea Area but slow dilutions (~two-threefold) from the North Channel to The Minches. This finding is confirmed by the observation from radiocaesium and plutonium half-distances, of higher (13 and 4 times) dilution rates within the Irish Sea and Clyde Sea Area (respectively) relative to those in the Scottish coastal current.

From the observed Sellafield-Clyde Sea Area transit time, a mean velocity of 1.7 km day⁻¹ is obtained and is applied to the north flowing water of the North Channel to estimate a northwards water flux as 5-10 km³day⁻¹. The corresponding radiocaesium flux, taking account of reduced subsurface radiocaesium levels, is ~1.2 - 4.2 x 10¹⁴ dpm day⁻¹.

During Sellafield - Clyde transport, Pu is estimated to be scavenged from the water column ~5 times faster than Cs, with a half-life of <4.8 months. However, Pu removal, relative to that for Cs, is faster outwith the Irish Sea.

With 30-55% of the Sellafield - discharged radiocaesium estimated to pass through the Clyde Sea Area, mean individual radiation exposures of ~10 times the average U.K. dose from Sellafield are

delivered to the public in this area. This dose is, however, considered negligible. Exposures of ~30% of the principle ICRP-recommended permissible limit of 1mSv year⁻¹ for members of the public would be experienced by critical group members if Fucus seaweeds from Cumbria were to be consumed in the same quantities as Porphyra has been known to be ingested in the past.

CHAPTER 1

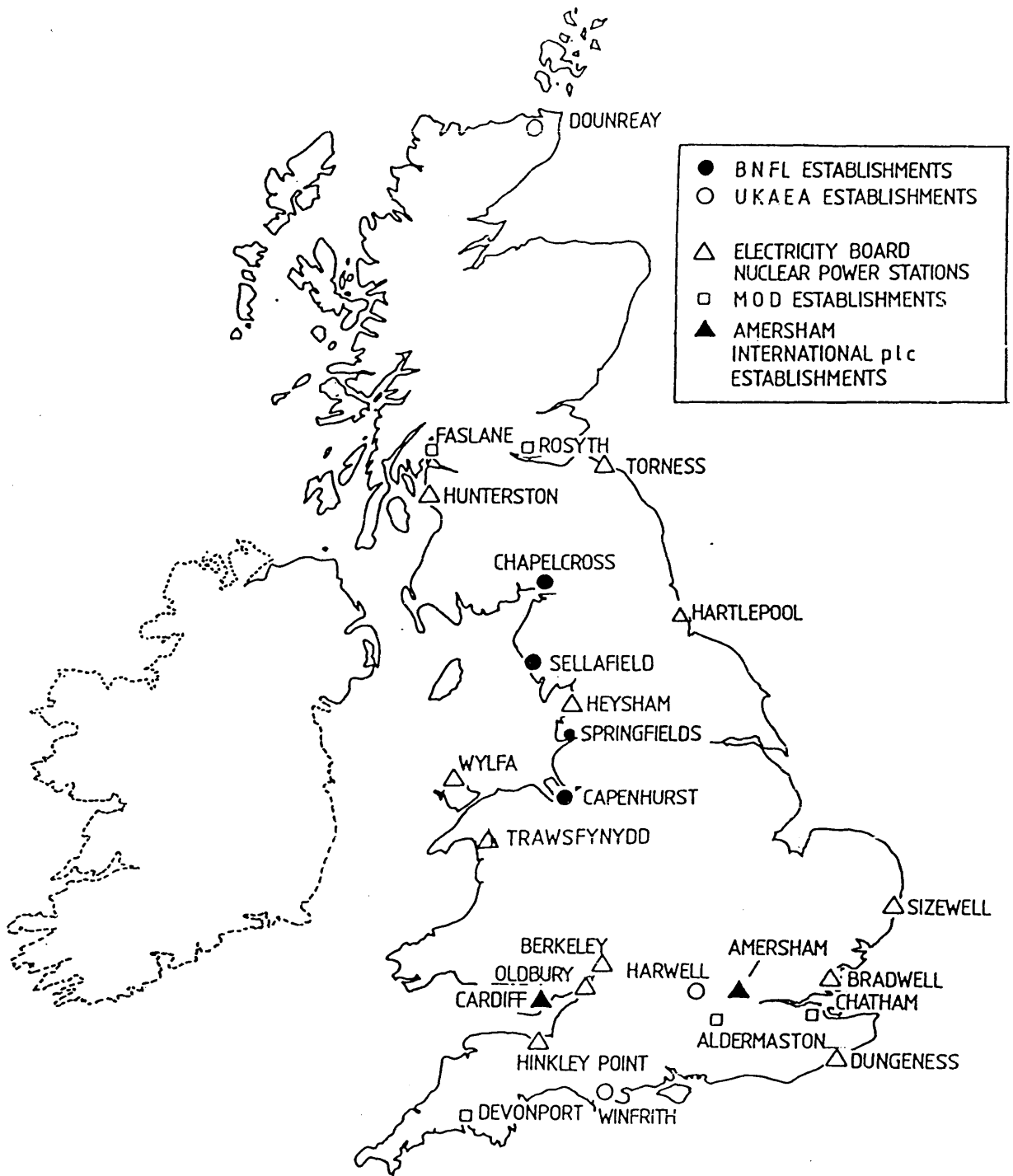
Introduction

1.1 Releases of Artificial Radioactivity into the Marine Environment

Artificial radionuclides have been introduced to the marine environment both indirectly - as fallout from explosion of nuclear weapons - and directly - as waste products from nuclear power stations and from surface and underwater explosions (Burton, 1975). The sites of U.K. establishments authorised to discharge radioactivity are shown in Figure 1.1. The U.K.'s greatest input of liquid radioactive waste into the marine environment is from the Sellafield site (formerly Windscale), the nuclear reprocessing plant in Cumbria, run by British Nuclear Fuels plc (B.N.F.). The discharged waste is largely from reprocessing of irradiated fuel, some of which comes from other countries (Handyside et al., 1982). The nearest foreign discharges are from Cap de la Hague in France. Table 1.1 compares discharges from Sellafield with those from la Hague for the years 1970 - 1982; in 1975 the former exceeded the latter >150 fold.

The distribution of artificial radionuclides in the marine environment depends largely on the source, i.e. whether a single accidental or a long-term release, an input to the atmosphere or an underwater point source. It is the radioactivity discharged continuously via the Sellafield pipeline point source which is considered throughout this project. Of the Sellafield-derived

Figure 1.1



UK nuclear establishments giving rise to principal discharges of liquid radioactive waste (Hunt, 1985).

Table 1.1

Annual Discharges of ^{137}Cs from Sellafield, U.K. and
 from La Hague, France Nuclear Reprocessing Plants,
 1970 - 1982 (TBq).

<u>Year</u>	<u>Sellafield</u>	<u>La Hague</u> *	<u>Sellafield</u> <u>La Hague</u>
1970	1154 ^a	89.1	13
1971	1332 ^a	242.0	5.5
1972	1287 ^a	32.9	39
1973	755 ^a	62.3	11
1974	4040 ^a	56.0	72
1975	5239 ^a	34.5	152
1976	4307 ^a	34.7	124
1977	4484 ^a	50.8	88
1978	4089 ^b	39.0	105
1979	2562 ^b	22.5	114
1980	2966 ^b	26.8	111
1981	2357 ^b	38.6	61
1982	2000 ^b	50.5	40

* Data from Calmet and Guegueniat (1985)

a Data from Mauchline, 1980

b Data from Hunt, 1980 - 1984

Table 1.2

^{137}Cs and Total (α and β) Radioactivity discharged annually
from Sellafield pipeline Cumbria 1974 - 1984 (TBq)

<u>Year</u>	<u>^{137}Cs</u>	<u>Total (α and β)</u>	<u>$^{137}\text{Cs}/\text{Total}(\%)$</u>
1974	4040	7828	52
1975	5239	9156	57
1976	4307	6849	63
1977	4484	7178	63
1978	4089	7192	57
1979	2562	4120	62
1980	2966	4345	68
1981	2357	3861	61
1982	2000	3556	56
1983	1200	2503	48
1984	434	1200	36

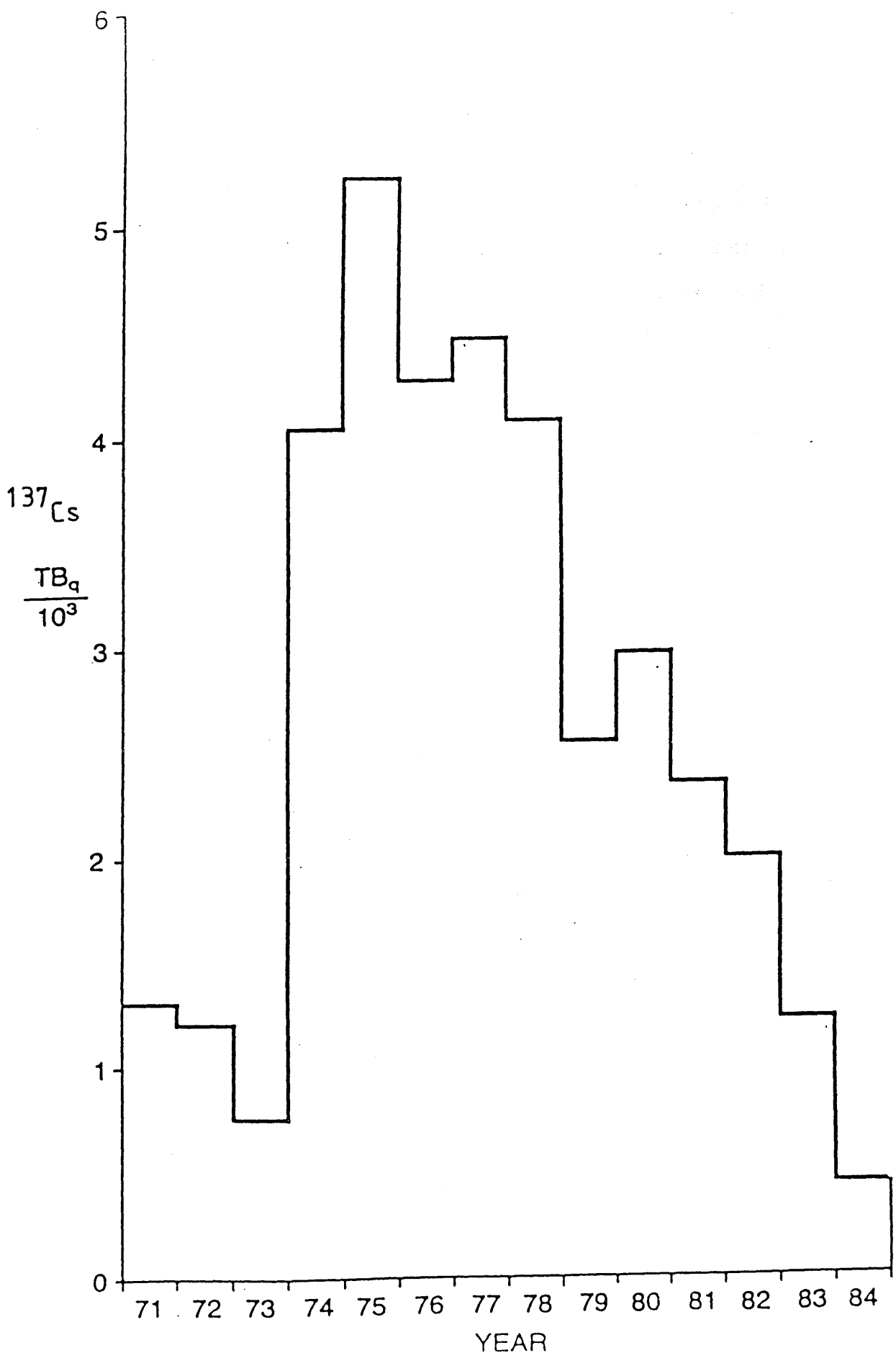
1974 - 1977 Data from Mauchline, 1980

1978 - 1983 Data from Hunt, 1980 - 1985

1984 - BNFL, 1985

Figure 1.2

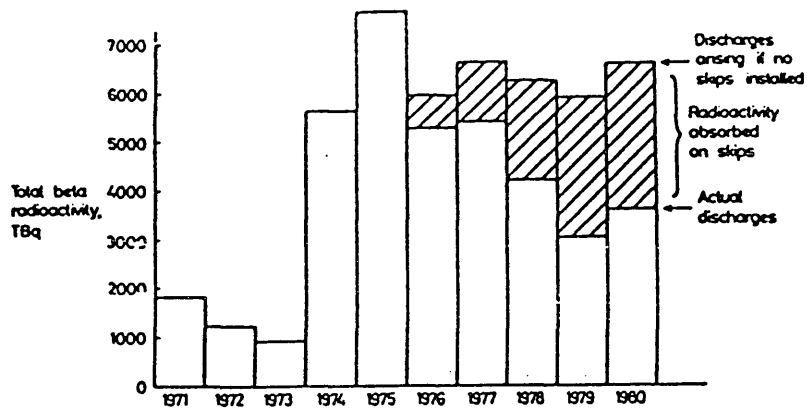
Annual ^{137}Cs Discharges, 1971-1984 (BNFL, 1985)



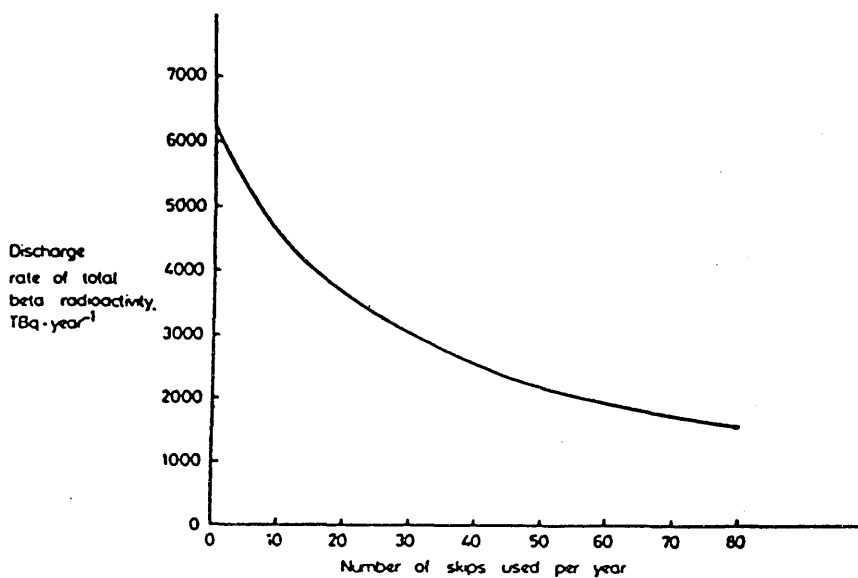
nuclides, the species discharged in greatest quantities is ^{137}Cs which, from Table 1.2, can be seen to have constituted >50% of the total discharges during 1974 - 1982; annual discharges of ^{137}Cs from 1971 to 1984 are shown in Figure 1.2. The fourfold increase in 1974 was caused primarily by corrosion of fuel cladding in the magnox fuel storage ponds (from which the radiocaesium is released) (Handyside et al., 1982) and resulted in increased radiation exposures to the general public. Consequently it was decided by BNFL and the Authorising Government Departments that an ion-exchange treatment plant, SIXEP (Site Ion Exchange Plant), should be installed to actively remove radioactivity from storage pond effluents. From 1976 until the plant was ready, however, zeolite skips were introduced into the pond water to reduce the levels of radiocaesium in the discharge. The radioactive water in the cooling ponds was allowed to circulate through the skips so that a large proportion of the radiocaesium was removed by ion-exchange. Figure 1.3a compares the levels of total beta radioactivity discharged after installation of the skips to the discharges if no skips had been used and Figure 1.3b shows the discharge rate as a function of the number of skips used. The total beta discharges (excluding tritium and low energy beta-emitting isotopes) were reduced to 1190 TBq in 1984 with the radiocaesium discharges contributing 36% of this total (Table 1.2). The first stage of SIXEP began operation in May 1985. Some of the other more "significant" radionuclides include the beta-emitters ^{90}Sr , ^{106}Ru , ^{95}Zr , ^{95}Nb , ^{134}Cs and ^{241}Pu and the alpha-emitters ^{238}Pu , $^{239/240}\text{Pu}$ and ^{241}Am (see Table 1.3).

Figure 1.3

Radioactive Discharges from Magnox Ponds before and after
Installation of Zeolite Skips (after Handyside et al., 1982)



(a) Discharges of total beta radioactivity from magnox ponds and absorption rate on to zeolite skips.



(b) Discharge rate of total beta radioactivity from magnox ponds as a function of zeolite skip usage on basis of model.

Table 1.3

Annual Discharges of Major Radionuclides
from Sellafield Pipeline for 1983 and 1984 (TBq)

<u>Nuclide</u>	<u>1984</u>	<u>1983</u>
<u>Beta</u>		
^{90}Sr	72	204
^{95}Zr	162	211
^{95}Nb	312	385
^{106}Ru	348	553
^{134}Cs	35	89
^{137}Cs	434	1200
Total β^*	1190	2489
$^{241}\text{Pu}^+$	345	331
<u>Alpha</u>		
^{237}Np	0.3	0.3
^{238}Pu	2.6	2.9
$^{239/240}\text{Pu}$	8.3	8.7
^{241}Am	2.3	2.2

(after BNFL, 1985)

* excluding low energy beta emitters[†] (e.g. ^{241}Pu) not detected by method used for determining "total beta" discharges.

1.2 Behaviour of Radionuclides in the Marine Environment

Once the radionuclides have been discharged from the Sellafield pipeline, it is their physico-chemical behaviour in the marine environment which is crucial in determining their fate. Reasons for interest in the fate of these radionuclides are primarily:

- 1) to understand and predict the extent to which the radioactivity can return to man and its effects on man both via external exposure to radiation (from radioactive sediments and water etc.) and internal exposure (via consumption of seafoods, inhalation of radioactive particles) and hence to a) ensure that radioactive discharges are kept to "safe" levels and b) be aware of the full long-term consequences of discharging/dumping various quantities of radioactivity in the marine environment and
- 2) to learn more about their behaviour and transport processes and to use this information to deduce more about the environment itself, i.e. to use the nuclides as "tracers" in the environment to better our understanding of e.g. water and sediment transport processes.

With regards to the effects on irradiated marine organisms, research in this field (see IAEA, 1976; Woodhead, 1984; Pentreath 1985) indicates a general consensus view that discharged levels are not sufficiently high for noticeable effects to manifest at the population level.

To begin to understand the behaviour of radionuclides they can be considered, where applicable, to behave identically to the stable elements of which they are radioisotopes but with the addition of physical decay via a specific half-life (Mauchline and Templeton, 1964; Mauchline, 1980). It follows, then, that radioisotopes (of

elements with stable isotopes) can be used as tracers to yield information on their stable counterparts. The main uncertainty in this application is that the physico-chemical forms of the radiotracers may differ from those of the stable elements in the natural system (Duursma, 1976). Hetherington and Harvey (1978) illustrate how radionuclide (plutonium and americium) concentrations in sediments can be used to study other metal pollutants in sediments.

Elements which exhibit conservative behaviour tend (by definition) to remain in the water column in the soluble state whereas non-conservative elements become associated with particulate matter. Hence the "solubility" of an element determines whether most of it remains within the vicinity of the Sellafield pipeline or is transported away by the general water circulation. In addition, marine organisms tend to accumulate metals hence effectively removing them from, or redistributing them within, the water column.

Although considerable research on artificially produced radionuclides has, in recent years, been directed towards understanding their behaviour in aquatic ecosystems (see Onishi et al., 1981; Coughtrey and Thorne, 1983; Sholkovitz and Mann, 1984; Pentreath et al., 1984b, 1985), details of their main transport processes remain poorly understood because of the complexity of the natural marine environment. The effect of one parameter on an element's behaviour can modify or override the effect of another and there are generally several parameters interacting in any natural system. Apart from the individual behaviour of each element in its interaction between the sedimentary and aqueous phases, the preferences which marine organisms exhibit in accumulating the radionuclides vary between species of the same family of organisms and even between individuals of the same species and hence also play a

part in the complex transport modes of radionuclides in the marine environment.

The distribution coefficient (K_d) for each element gives an indication of whether the element behaves conservatively or non-conservatively - see Table 1.4; a high K_d value indicates a tendency to associate with sediments rather than remaining "soluble" in the water column. Generally, the K_d is defined to be the ratio of the concentration of an element in sediments relative to its concentration in the surrounding water; it could, therefore, be described as the concentration factor of an element from seawater to sediment. As can be seen from Table 1.4, the transuranic elements such as Pu, Am and Cm generally have relatively high K_d values and hence can be expected to be scavenged quite rapidly whereas elements such as Sr, I, Cs and Ra have comparatively low K_d 's and thus remain, to a greater extent, in the soluble phase.

The K_d data presented in Table 1.4 represent average values for each radionuclide since, for elements which exhibit more than one oxidation state, a different K_d value may well apply for each. For example, the K_d s for the reduced states of Pu - oxidation states (III) and (IV) - have been found by Nelson and Lovett (1978) to exceed those for the oxidised states - Pu(V) and Pu(VI) - by >1000 and so the overall K_d is largely dependent on the prevailing oxidation state ratio (see section 1.4b). Similarly, values of K_d are dependent on specific environments; for example, the more suspended sediment present the greater the tendency for the radionuclide to associate with this sediment because of the greater number of sites available for sorption (Duursma and Eisma, 1973). Higher resuspension of sediments was found by Santschi et al. (1983) to increase the removal rates of radiotracers from the water column in summer relative to

Table 1.4

Distribution Coefficients (Kds)
for Various Elements (IAEA, 1978)

<u>Element</u>	<u>Sediment</u>
H	1.OE 00
C	(1.OE 02)
Na	(1.OE 02)
P	(1.OE 02)
S	(1.OE 02)
Cl	(1.OE 02)
Ca	(5.OE 02)
Cr	(1.OE 04)
Mn	1.OE 04
Fe	1.OE 04
Co	1.OE 04
Ni	1.OE 04
Zn	1.OE 04
Se	1.OE 04
Br	(1.OE 02)
Sr	5.OE 02
Y	1.OE 04
Zr	1.OE 04
Nb	1.OE 04
Tc	1.OE 04
Ru	1.OE 04
Pd	(1.OE 04)

Cont.'d.

Table 1.4 cont.'d.

Distribution Coefficients (Kds)
for Various Elements (IAEA, 1978)

<u>Element</u>	<u>Sediment</u>
Ag	1.0E 04
Sn	1.0E 04
Sb	1.0E 04
Te	1.0E 04
I	1.0E 02
Cs	5.0E 02
Ce	1.0E 04
Pm	1.0E 04
Sm	(1.0E 04)
Eu	1.0E 04
Au	1.0E 04
Pb	1.0E 04
Po	1.0E 04
Ra	5.0E 02
Ac	1.0E 04
Th	5.0E 06
Pa	5.0E 03
U	5.0E 02
*Np	1.0E 04
*Pu	3.0E 05
*Am	2.0E 06
*Cm	1.0E 06
Cf	(5.0E 04)

* Pentreath et al., 1985.

winter due to increased benthic activity in the former, with the radiotracers of higher removal rates generally corresponding to those of higher K_d s. The nature of the sediment, e.g. percentage of organic, oxide and carbonate phases (McKay and Baxter, 1985b), mineral composition and grain size (Duursma and Eisma, 1973; McKay and Baxter, 1985b) and the presence of other ions which could be "competing" with the radionuclides for sites in/on particles (Duursma and Eisma, 1973; Stanners and Aston, 1981b) have all been found to influence K_d values. Similarly, Duursma and Eisma (1973) found that redox conditions in the sediment affect K_d s whilst Murray et al. (1973) have shown that pH modifies some metal solubilities which, as already mentioned, are very important in determining the degree of particulate scavenging.

The movement of radionuclides within the marine environment is therefore difficult to predict since many factors must be taken into account. Even for radionuclides with high K_d values, removal from the water column by sediment particles is not the end of the story since remobilisation from the sediments may occur following chemical diagenetic processes in the "new" environment - parameters such as oxygen content and pH are invariably different in the sediment column from those of the overlying water. Hence the K_d of an element may change once it is incorporated into the sediment column and thus the equilibrium between soluble and non-soluble states changes and radionuclides may be effectively released into the pore water and thereafter into the water column above.

Studies of the remobilisation of radionuclides and of the events leading up to it have concentrated largely on the transuranics and radiocaesium. Livingston and Bowen (1979) suggested that $^{239,240}\text{Pu}$ undergoes diagenetic chemistry resulting in upward transport of soluble organic complexes of the Pu and that ^{137}Cs is not remobilised

in Atlantic ocean sediments. Livingston and Anderson (1983) also suggest significant remobilisation of particulate Pu in the deep ocean relative to ^{137}Cs . However, other workers disputed these findings (Carpenter and Beasley, 1981; Beasley et al., 1982; Santschi et al., 1983; Sholkovitz et al., 1983; Santschi et al., 1984; Sholkovitz and Mann, 1984.), concluding that $^{239,240}\text{Pu}$ shows no diagenetic chemistry and no significant mobility within coastal sediments, whereas ^{137}Cs is preferentially transported downwards in the sediment column, the latter phenomenon causing the decreasing $^{239,240}\text{Pu} : ^{137}\text{Cs}$ ratio with depth observed in Atlantic ocean sediments by Livingston and Bowen (1979). Aston and Stanners (1981) also conclude that there are negligible diagenetic changes in phase association of Pu after burial in oxic sediments and that post-depositional migration is also negligible. Santschi et al. (1984) suggest that anoxic sediments may retain many nuclides such as Cs, Zn, Mn, Co and Cd - the more soluble radionuclides - which would not be fixed in oxic conditions. These workers also found that high sediment resuspension and / or anoxic bottom waters increase the retention and storage capacity of coastal sediments. From laboratory studies on sediments from near Sellafield, Stanners and Aston (1982) found that radiocaesium nuclides show at least partial reversibility whilst ^{106}Ru , ^{144}Ce and ^{241}Am do not show significant desorption. Pentreath et al. (1985) conclude that Pu, in particular, undergoes changes in chemical form following discharge and that the greatest transitions for Pu and Np occur in interstitial waters and are dependent on the prevailing Eh and pH conditions.

Whilst discussing the sediment column, it is worth briefly referring to the subject of bioturbation (mixing of the sediment column by benthic fauna). Kershaw et al. (1983) have shown that the echinoid, Maxmulleria lankesteri, can remove Pu to at least 35cm

depth in sediment. This mechanism can be of vital importance for the observed distribution of radionuclides within the sediment column and for their potential for remobilisation.

As already mentioned, the radionuclides may be taken up by marine organisms; in fact, most radionuclides are concentrated to some degree by marine organisms relative to their concentration in surrounding seawater. Table 1.5 presents data of concentration factors for 45 elements by the five groups of marine organisms, molluscs, crustaceans, fish, plankton and seaweeds. The concentration factor refers to the ratio of the level of the element in the organism (dry weight) to the level of the element in the surrounding water. In the latter context, the water should be filtered prior to analyses since the presence of suspended sediments generally increases the measured sea water levels quite significantly and hence the concentration factor will appear to vary with suspended sediment concentration. Since, in practice, the water may or may not be filtered before analysis, then concentration factors obtained by different workers for different conditions are not necessarily comparable. Other variables (e.g. radionuclide input, chemical forms of nuclides, size of organism and the rate of change in its size) will affect the observed concentration factor; hence it is impossible to define an absolute and unique concentration factor value for any given element and organism for application to all conditions. Similar to the K_d value, then, these concentration factors are "averaged" values which give some idea of the relative affinities of various organisms for particular elements/ radionuclides; they are not absolute values.

Superimposed on the behaviour of individual elements is the process of radioactive decay since, in many cases, this leads to a change in the actual element and hence to a change in its behaviour.

Table 1.5

Concentration Factors Used for Radiological Assessment
(IAEA, 1978)

<u>Element</u>	<u>Fish</u>	<u>Crustacea</u>	<u>Molluscs</u>	<u>Seaweed</u>	<u>Plankton</u>
H	1.0E 00	1.0E 00	1.0E 00	1.0E 00	1.0E 00
C	5.0E 04	4.0E 04	5.0E 04	4.0E 03	3.0E 03
Na	1.0E-01	3.0E-01	2.0E-01	1.0E 00	1.0E 00
P	2.0E 04	1.0E 04	1.0E 04	1.0E 04	1.0E 04
S	1.0E 00	1.0E 00	1.0E 00	1.0E 00	1.0E 00
Cl	1.0E 00	1.0E 00	1.0E 00	1.0E 00	1.0E 00
Ca	1.0E 00	1.0E 01	1.0E 00	1.0E 00	1.0E 01
Cr	1.0E 02	5.0E 02	5.0E 02	(3.0E 04)	(3.0E 03)
Mn	5.0E 02	1.0E 04	1.0E 04	1.0E 04	1.0E 03
Fe	1.0E 03	1.0E 03	1.0E 03	1.0E 04	1.0E 04
Co	1.0E 02	1.0E 03	1.0E 03	1.0E 03	1.0E 03
Ni	5.0E 02	1.0E 02	1.0E 02	5.0E 02	1.0E 03
Zn	2.0E 03	4.0E 03	1.0E 05	1.0E 03	1.0E 04
Se	1.0E 02	1.0E 03	1.0E 03	1.0E 03	1.0E 04
Br	(3.0E 00)	(1.0E 01)	(1.0E 01)	(3.0E 01)	(3.0E 01)
Sr	1.0E 00	1.0E 01	1.0E 01	1.0E 01	(1.0E 01)
Y	1.0E 00	1.0E 03	1.0E 03	1.0E 03	1.0E 02
Zr	1.0E 00	1.0E 02	1.0E 03	5.0E 02	(1.0E 04)
Nb	1.0E 00	1.0E 02	1.0E 03	5.0E 02	(1.0E 03)
Tc	1.0E 01	1.0E 03	1.0E 03	1.0E 05	1.0E 03
Ru	1.0E 00	6.0E 02	2.0E 03	2.0E 03	(1.0E 03)
Pd	(3.0E 02)	(3.0E 02)	(3.0E 02)	(1.0E 03)	(1.0E 03)
Ag	1.0E 03	5.0E 03	1.0E 05	1.0E 03	1.0E 03

cont.'d

Table 1.5 cont.'d.

Concentration Factors Used for Radiological Assessment
(IAEA, 1978)

<u>Element</u>	<u>Fish</u>	<u>Crustacea</u>	<u>Molluscs</u>	<u>Seaweed</u>	<u>Plankton</u>
Sn	1.0E 03	3.0E 02	1.0E 02	1.0E 02	1.0E 03
Sb	1.0E 03	3.0E 02	1.0E 02	1.0E 02	1.0E 03
Te	1.0E 03	1.0E 03	1.0E 03	1.0E 04	1.0E 03
I	1.0E 01	1.0E 02	1.0E 02	1.0E 03	1.0E 03
Cs	5.0E 01	3.0E 01	1.0E 01	1.0E 01	1.0E 02
Ce	(1.0E 01)	1.0E 03	1.0E 03	1.0E 03	1.0E 03
Pm	1.0E 02	1.0E 03	1.0E 03	1.0E 03	1.0E 03
Sm	(1.0E 02)	(1.0E 03)	(1.0E 03)	(1.0E 03)	(3.0E 03)
Eu	1.0E 02	1.0E 03	1.0E 03	1.0E 03	1.0E 04
Au	1.0E 02	1.0E 03	1.0E 03	1.0E 03	1.0E 04
Pb	3.0E 02	1.0E 02	1.0E 02	1.0E 03	1.0E 04
Po	2.0E 03	2.0E 04	2.0E 04	1.0E 03	1.0E 04
Ra	1.0E 02	1.0E 02	1.0E 02	1.0E 02	1.0E 02
Ac	3.0E 01	1.0E 03	1.0E 03	1.0E 03	1.0E 04
Th	1.0E 03	1.0E 03	1.0E 03	1.0E 03	1.0E 04
Pa	1.0E 01	1.0E 01	1.0E 01	1.0E 02	1.0E 03
U	1.0E-01	1.0E 01	1.0E 01	1.0E 01	5.0E 00
Np	(1.0E 01)	(1.0E 02)	(1.0E 03)	(1.0E 03)	(2.0E 03)
Pu	1.0E 01	1.0E 02	1.0E 03	1.0E 03	(2.0E 03)
Am	1.0E 01	2.0E 02	2.0E 03	2.0E 03	(2.0E 03)
Cm	(1.0E 01)	(2.0E 02)	(2.0E 03)	(2.0E 03)	(2.0E 03)
Cf	(1.0E 01)	(2.0E 02)	(2.0E 03)	(2.0E 03)	(2.0E 03)

Concentration Factors in parentheses are based on educated guesswork only.

Limits depending on such values are flagged with an asterisk on output.

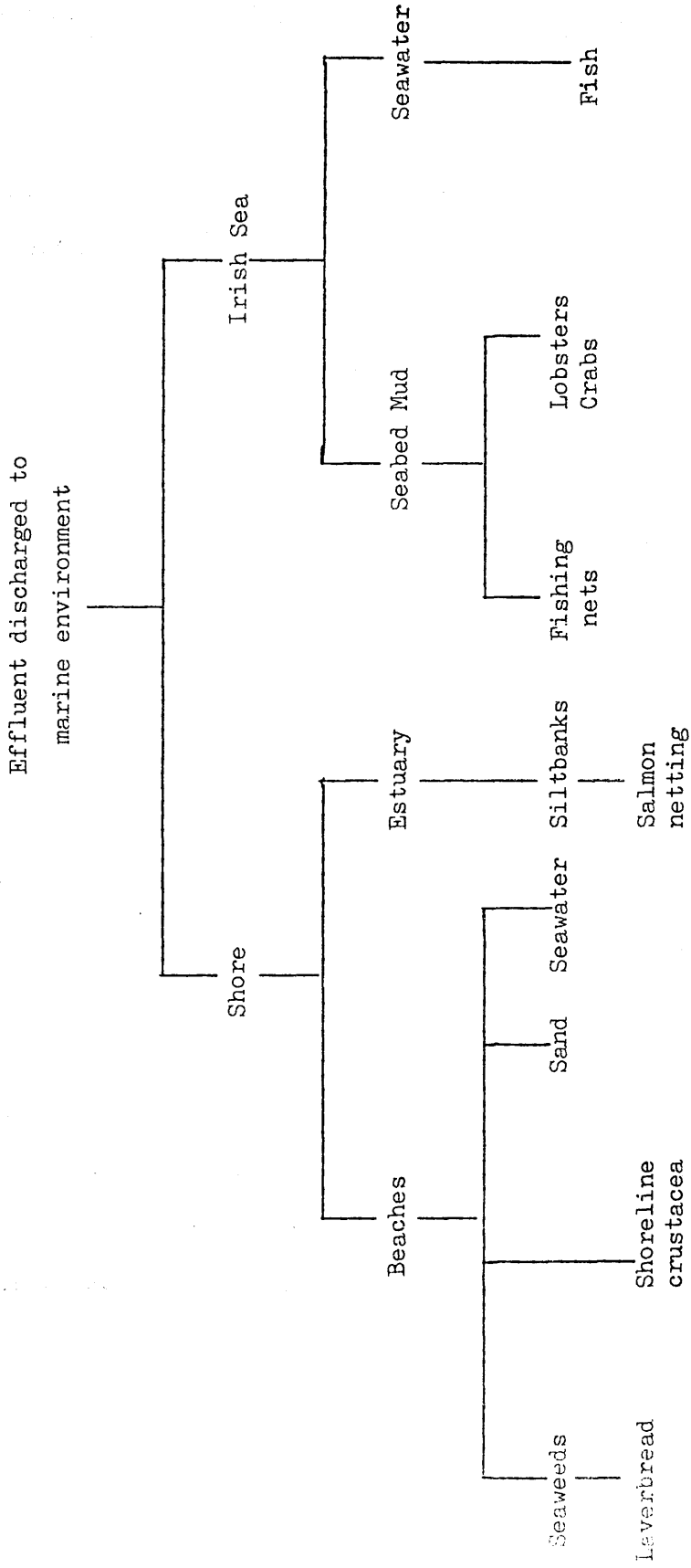
This transmutation complicates matters further in trying to follow / define the movements of certain radionuclides in the marine or terrestrial environments. In Irish Sea sediments, for example, it may be necessary to determine how much of the observed ^{95}Nb is due to decayed ^{95}Zr released from Sellafield and how much is due to ^{95}Nb discharged directly from the pipeline. This phenomenon applies to other radionuclides such as ^{241}Pu which decays into ^{241}Am which in turn decays to ^{237}Np ; each of these radionuclides behaves differently, Np being the most conservative of the three ($K_d \sim 10^3 - 10^4$).

1.3 Effects of Artificial Marine Radioactivity on Man

Damage by radiation to human tissue depends on a number of factors such as the type of radiation and its energy; the amount of total radiation received and its intensity; the duration of exposure to the radiation; whether the exposure was internal or external; whether it was received in one or several doses. Figure 1.4 illustrates the various possible pathways for return of marine radioactivity to man. The pathway which leads to the greatest radiation exposure of an identifiable group of the general public is termed the critical pathway and the section of the population receiving this maximum estimated dose is referred to as the critical group. Between 1966 - the time of the first M.A.F.F. (Ministry of Agriculture Fisheries and Foods) report for monitoring of radionuclide levels in the Sellafield area - and 1972, the pathway of most concern was consumption of laverbread produced from Porphyra, an alga collected from near Sellafield (Mitchell, 1967). In 1972, however, harvesting of Porphyra was discontinued and the most important pathway became the external dose to fishermen in the Ravensglass estuary from

Figure 1.4

IMPACT OF WINDSCALE LIQUID EFFLUENT
ON THE MARINE ENVIRONMENT



radionuclides in the local sediments (Mitchell, 1975). By 1974, increased discharges of radiocaesium (Figure 1.2) led to a new dominant critical pathway, that of consumption of fish and shellfish caught off the Cumbrian coast (Hetherington, 1976b). Until 1980, then, the radionuclide causing most concern was ^{137}Cs . In 1976 a peak in estimated maximum dose to members of the fish-eating critical group occurred, reaching 44% of the ICRP's (International Committee on Radiological Protection) Annual Limit on Intake (A.L.I.) for members of the public; this was largely attributable to the two radiocaesium nuclides (Mitchell, 1977).

MAFF authorises and monitors the Sellafield discharges, setting limits of permissible levels for discharge. In 1980, MAFF was advised by NRPB (National Radiological Protection Board) that the figure for Pu uptake in the gut should be increased by a factor of 5, leading to an overall total exposure to members of the critical group (fish, crustacean and mollusc eaters) of 39% of the ICRP-recommended limit for the public of 5mSv year^{-1} (see below) of which the largest contributors were the Pu alpha-emitters. Data for 1981 included a new, higher consumption rate by mollusc-eaters (Hunt, 1983), producing an estimated dose of 69% of the appropriate ICRP limit to the critical group members. ^{241}Am contributed 20% whilst the plutonium and radiocaesium nuclides contributed 29.4% and 9.3% respectively. A new critical pathway, was therefore recognised and focused attention on the mussel eating community and on the transuranic nuclides. The most recent Maff report (Hunt, 1985) estimated a maximum critical group exposure of 45% of the ICRP-recommended annual limit for the public of 5mSv whilst, for the critical group for external exposure - persons living on board their boats in Whitehaven harbour -, a total of 11% of the ICRP-recommended limit of 5mSv year^{-1} was received from

Sellafield-derived nuclides. Of this, 7% was from external exposure and the additional 4% was from consumption of fish and shellfish. Recently, ICRP has stated (ICRP, 1985) that the principal limit for the annual committed effective dose equivalent received, by a member of the public, is 1mSv and that the limit of 5mSv year⁻¹ may be used in the short-term, i.e. for a number of years, provided that, over a lifetime, the average annual dose does not exceed the principal limit, 1mSv.

The critical pathway concept relates to the maximum dose of radiation likely to be received by the critical group and thus involves individual / specific monitoring of radioactivity levels both in the foodstuffs eaten by critical group members and in the contaminated sediments to which the critical group members are exposed. Habit surveys are necessary to recognise critical groups, to determine consumption rates of the relevant foodstuffs and obtain details of exposure times to external irradiation from radioactive sediments etc.

For assessment of health detriment on a national (or international) scale, however, the concept of "collective dose" is adopted whereby the dose received by large populations (e.g. the whole country) is calculated. This calculation is performed using fish landing data - compiled by ICES (International Council for the Exploration of the Sea) - and measurements of radioactivity in fish. For these collective dose assessments data on radionuclide levels in fish do not need to be as accurate as those required for critical group dose calculations and hence data on measured radioactivity levels in fish are supplemented by applying concentration factors of radionuclides in fish to the known radionuclide concentrations in water from various areas. Extensive mathematical modelling of the

marine environment is basic to the collective dose predictions. The collective effective dose equivalent, measured in units of man-Sv, can then be divided by the population to find the mean dose received by each member of the general public.

The ICRP has prescribed a system of dose limitation which states that "all exposures shall be kept as low as reasonably achievable.." (ALARA). Included in the requirements for ALARA, then, is the requirement that collective doses be reasonably minimised and the ICRP conclude that, by its system of dose limitation, the annual dose equivalent averaged over the population will not exceed 0.5mSv. The NRPB (National Radiological Protection Board), however, consider it unlikely that average doses will reach a tenth of this, that is 0.05mSv.

In its annual report, (e.g. Hunt, 1985) MAFF publishes the calculated collective doses from fish and shellfish for the U.K. and for other European countries. The main contribution to the collective dose is from the radiocaesium nuclides in fish; the contribution from shellfish is minor and that from other pathways is also relatively small (Hunt and Jefferies, 1981).

For the period 1974 to 1978, the ratio of the collective effective dose equivalent from radiocaesium in fish for the U.K. to that for western Europe was $\sim 0.55:1$ whilst the corresponding population ratio is $\sim 0.08:1$. This gives an average effective dose equivalent per person in the U.K. of 6.9 times that per person in western Europe. However, of the total dose to the U.K., it is "guessed" that approximately half is delivered to the population of Scotland (Mitchell, 1983; pers. comm.). Considering the relatively small population of Scotland (compared to that of Britain), the actual average dose to the general public in Scotland is thus higher (by

~*10) than that to the rest of Britain.

A maximum contribution to the U.K. collective dose from radiocaesium in edible fish occurred in 1976 and was 133 man-Sv (Pentreath, 1985). Since then, values have been steadily decreasing: a reflection of the decreasing radiocaesium discharges in the Sellafield liquid effluent. In 1983 collective doses from fish and shellfish to the U.K. and to other European countries were 70 and 110 man-Sv respectively. This annual collective effective dose equivalent averaged over the population is equal to 0.00125mSv for the U.K. (and even less for Europe), corresponding to less than 3% of the NRPB suggested limit of 0.05mSv.

Clearly, for both critical group and collective dose rates, exposures to the general public are largely determined by the distribution of radioactivity in the marine environment and, in the case of collective doses, it is the distribution of radiocaesium in particular which is of primary importance. Indeed, the U.K. collective dose from fish consumption has been shown in the past to depend critically on water transport characteristics within the Irish Sea / North Channel system (Hunt, 1985).

1.4 Artificial Marine Radioactivity as Tracers

a) Radiocaesium

^{137}Cs is suitable as a tracer of water movement because of 1) its aforementioned conservative nature - it remains largely in the water column in its monovalent (hydrated) cationic form, $\text{Cs}(\text{aq})^+$ and can be detected as far afield as the Arctic (Livingston, 1981; pers. comm.),

2) its relatively high and known discharges from Sellafield and 3) its relative ease of accurate measurement (see Chapter 2). In addition, it does not occur naturally and hence any detectable levels are from an anthropogenic source. The quantities released from Sellafield are far higher (50 - 100 fold) than from the next nearest source (Cap de la Hague - see Table 1.1) and therefore levels detected in most north and west British coastal waters can be considered, as a first approximation, to have arisen from this point source alone. In addition to ^{137}Cs , the radionuclide ^{134}Cs can be determined simultaneously by the method used here (extraction by ion-exchange using KCFC resin - see Chapter 3).

^{134}Cs , like ^{137}Cs , does not occur naturally. It is an activation product (as opposed to a fission product) arising from the nuclear fuel cycle and is therefore not produced in significant quantities during nuclear weapons testing. Thus any ^{134}Cs detected can safely be assumed to have been produced from the nuclear fuel cycle (Burton, 1975); it, too, is discharged from Sellafield in significant quantities (see Table 1.2). The ratio $^{134}\text{Cs} : ^{137}\text{Cs}$ can therefore be used as a guide as to whether the detected levels are due to fallout from nuclear weapons testing or to waste products from the nuclear fuel cycle. Furthermore, if $^{134}\text{Cs} : ^{137}\text{Cs}$ ratios can be measured with sufficient precision (particularly in the past when the radiocaesium levels in Sellafield discharge were significantly higher than at present), they provide an inbuilt timeclock for radiocaesium and hence water transport, the ratio halving every 2.2 years after release.

^{137}Cs is a soft β -emitter: it predominantly decays to the metastable $^{137\text{m}}\text{Ba}$ ($t_{1/2} = 2.6$ minutes), an intermediate step in decaying to the stable ^{137}Ba isotope. The γ -emissions detected during counting of ^{137}Cs , then, are actually emitted from $^{137\text{m}}\text{Ba}$.

Sellafield radiocaesium has been used by numerous workers in tracer studies of water movement around Britain (Templeton and Preston, 1966; Jefferies et al., 1973, 1982; Wilson, 1974; Livingston and Bowen, 1977; Baxter et al., 1979; Baxter and McKinley, 1978; Mauchline, 1980; McKinley et al., 1981a,b; Livingston et al., 1982b; Prandle, 1984; McKay and Baxter, 1985a; McKay et al., 1986) and has also been detected further afield in the North and Baltic Seas (Kautsky, 1973, 1976, 1985; Kautsky et al., 1980; Kautsky and Eicke, 1982; Livingston et al., 1982b) and along the Norwegian Coastal Current to East Greenland (Dahlgaard et al., 1984; Aarkrog et al., 1983). Radiocaesium has also been employed to study sedimentation processes (Livingston and Bowen, 1977; Baxter et al., 1978; Aston and Stanners, 1979; MacKenzie et al., 1979; McKinley and Baxter, 1980; Stanners and Aston, 1981; Clifton and Hamilton, 1982). Its detection in algae has likewise been applied to tracer studies (Thompson et al., 1982). The aims of this project include exploring further the applications of radionuclide levels in seaweeds for tracer work and carrying out detailed investigations of ^{137}Cs distributions in Scottish coastal waters as an indicator of water movement (see section 1.5).

b) Plutonium

Plutonium occurs naturally only in very small (negligible) quantities, produced by neutron capture in uranium ores (UNSCEAR, 1981). Environmental levels, therefore, can safely be assumed to have arisen solely from anthropogenic sources, i.e. from nuclear weapon tests, production of nuclear weapons and operations of the nuclear fuel cycle. The Pu produced from nuclear explosions mainly consists of ^{239}Pu and ^{240}Pu - the latter two being indistinguishable by alpha

spectrometry - and the ratio of ^{238}Pu : $^{239,240}\text{Pu}$ activities resulting from fallout is 0.025 - 0.050. The corresponding ratio in the Sellafield discharges, however, is ~ 0.3 , hence providing a useful method for distinguishing between the two sources. The Pu produced in the nuclear fuel cycle is released mainly during reprocessing of fuel rather than during the operation of nuclear reactors. The major Pu isotopes discharged from Sellafield are ^{238}Pu , $^{239,240}\text{Pu}$ and ^{241}Pu (see Table 1.2). The former two decay by alpha-emission whilst the latter decays by beta-emission into ^{241}Am which, in turn, is an alpha-emitter.

Relatively recently, Pu has attracted increased attention from research workers (see section 1.3). As already explained (section 1.2) it has a high K_d value and hence tends to accumulate on particulate matter, with approximately 95% of the Sellafield Pu being removed from the water column to the Irish Sea sediments (Hetherington et al., 1975) whilst the other 5% remains in the soluble phase. As indicated earlier, this differentiation is caused by the occurrence of different oxidation states of Pu, oxidation states +3 and +4 showing non-conservative behaviour ($K_d \sim 10^6$) and states +5 and +6 having more conservative behaviour with a K_d of $\sim 1.4 \times 10^4$ (Nelson and Lovett, 1978). Hence the latter are assumed to represent the 5% remaining in the "soluble" phase in the water column. The reduced forms of Pu are the most abundant and rapidly form oxides, oxyhydroxides, polymers and organic complexes; Pu complexed with biological ligands may become incorporated in micro-organisms or in plant and animal tissues (UNSCEAR, 1981).

Work thus far on plutonium in the marine environment has, like that for caesium, been concerned either with determining the levels and behaviour of Pu (Fowler et al., 1975; Hetherington, 1976a;

Hetherington et al., 1976; Aston and Fowler, 1984; Pentreath et al., 1984a; Sholkovitz and Mann, 1984; Hunt, 1985; Pentreath, 1985;) or with tracer use to reveal more about the environment (Hetherington, 1976a, 1978; Aston and Stanners, 1981; Cross and Day, 1981; Livingston et al., 1982b; Thompson et al., 1982; Hallstadius et al., 1986). During this project, both approaches are applied.

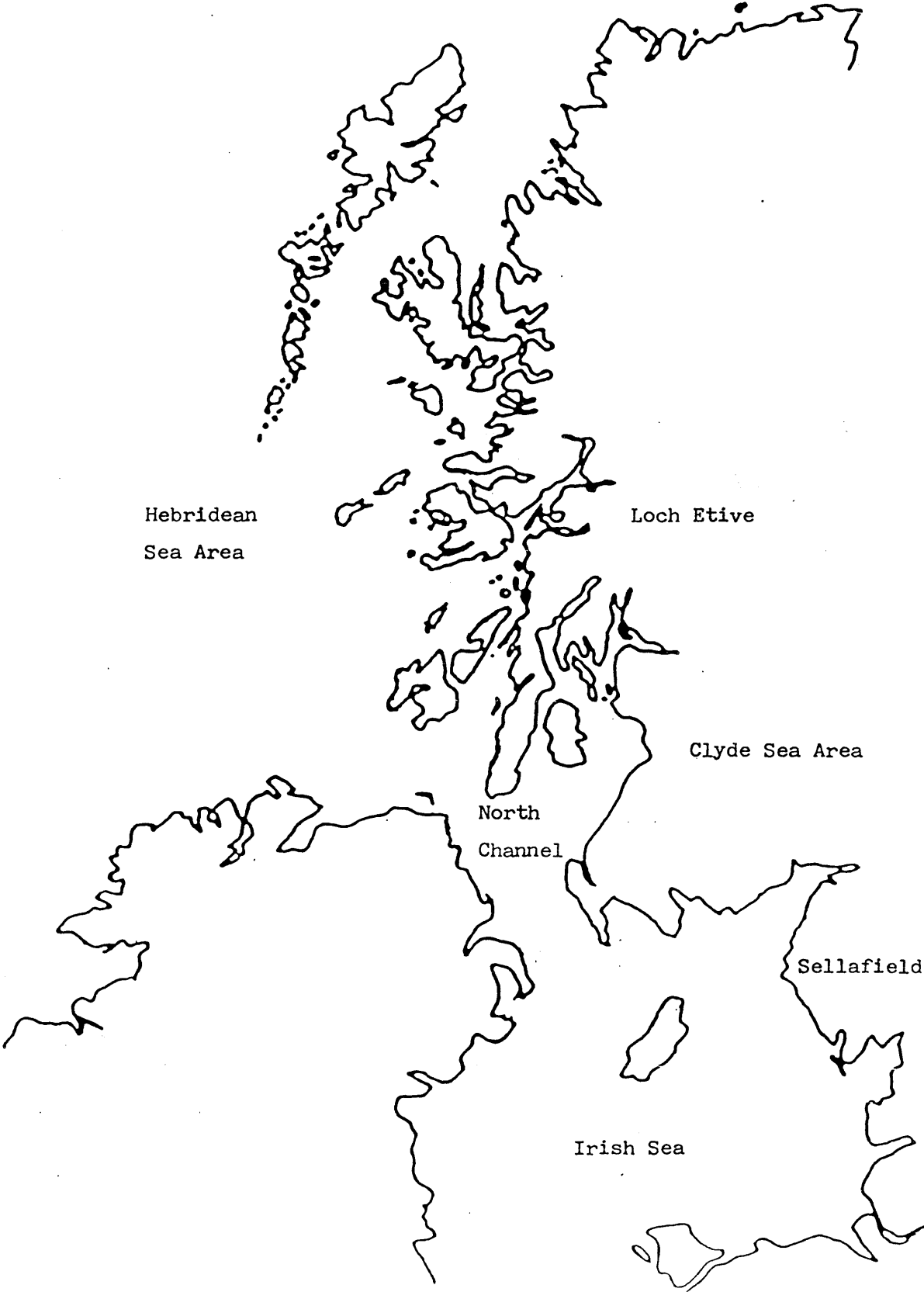
1.5 Aims

The main objectives of this research are summarised as follows:

- 1) detailed study of the Hebridean Sea Area (HSA) (Figure 1.5) and surrounding waters using radiocaesium and salinity distributions obtained by regular sampling during research cruises. Data interpretation concentrates on radiocaesium trends with time and depth and on short-term spatial distributions;
- 2) measurement of radiocaesium levels and trends in Clyde Sea Area (CSA) surface waters (Figure 1.5) to allow assessment of a) transit times for water reaching the CSA from Sellafield and b) residence times of water in the northern Irish Sea;
- 3) similarly to characterise radiocaesium trends in Loch Etive waters (Figure 1.5) to allow estimation of transit times from the CSA or Sellafield to the Loch;
- 4) investigation of the possible return of Sellafield radioactivity (Cs, Pu etc.) to man via the use of seaweeds as fertilisers; in

Figure 1.5

Map Showing Areas Studied



parallel, to explore the value of seaweeds as indicators of radionuclide levels in sea water and hence to deduce information on radionuclide behaviour in the sea water during transit between sites.

In experimental work, seaweeds of various species were collected from the sea and analysed for radionuclides. The results showed that seaweeds are good indicators of radionuclide levels in sea water and that they are particularly good for the detection of ^{137}Cs and ^{90}Sr . The seaweeds were analysed for radionuclides by the following methods:

Sample	Radionuclides Assayed
Sea water	^{137}Cs , ^{90}Sr
Seaweed	^{137}Cs , ^{90}Sr , ^{226}Ra
Seaweed	^{137}Cs , ^{90}Sr , ^{226}Ra
Seaweed	^{137}Cs , ^{90}Sr , ^{226}Ra
Seaweed	^{137}Cs , ^{90}Sr , ^{226}Ra

The results of the above work are given in the following tables. The seaweeds were analysed for radionuclides by the following methods:

CHAPTER 2

Experimental

2.1 Introduction

The experimental section describes 1) sampling procedures, 2) analytical methods, including nuclide separation and counting techniques, and 3) result calculation and errors assessment. The samples were of 2 types, namely 1) sea water samples and 2) solid samples, e.g. seaweeds, soils, and grasses.

These were radiochemically analysed as follows:

<u>Sample</u>	<u>Radionuclides Assayed</u>
sea water	^{134}Cs , ^{137}Cs
seaweeds	all γ -emitting isotopes
soils	all γ -emitting isotopes
grasses	all γ -emitting isotopes
some seaweeds	Pu α -emitting isotopes

Thus all the solid samples were analysed for γ -emitting radionuclides and the most active seaweeds were further assayed for Pu α -emitting isotopes; water samples were assayed for their radiocaesium content alone.

First to be described here is the procedure applied, from sampling through to preparation for counting, in radiocaesium analysis

of sea water samples, followed by the corresponding method for solid samples. The next stage of sample counting and, finally, the methods of calculation of activities and their associated errors are then described.

Basically, the multinuclide analysis of γ -emitting radionuclides involves non-destructive counting of samples in their original forms, leaving them available afterwards for further specific analyses if required. On the other hand, radiocaesium or plutonium assays involve destructive radiochemical separations prior to counting.

2.2 Pre-counting Procedures

2.2(a) Water samples

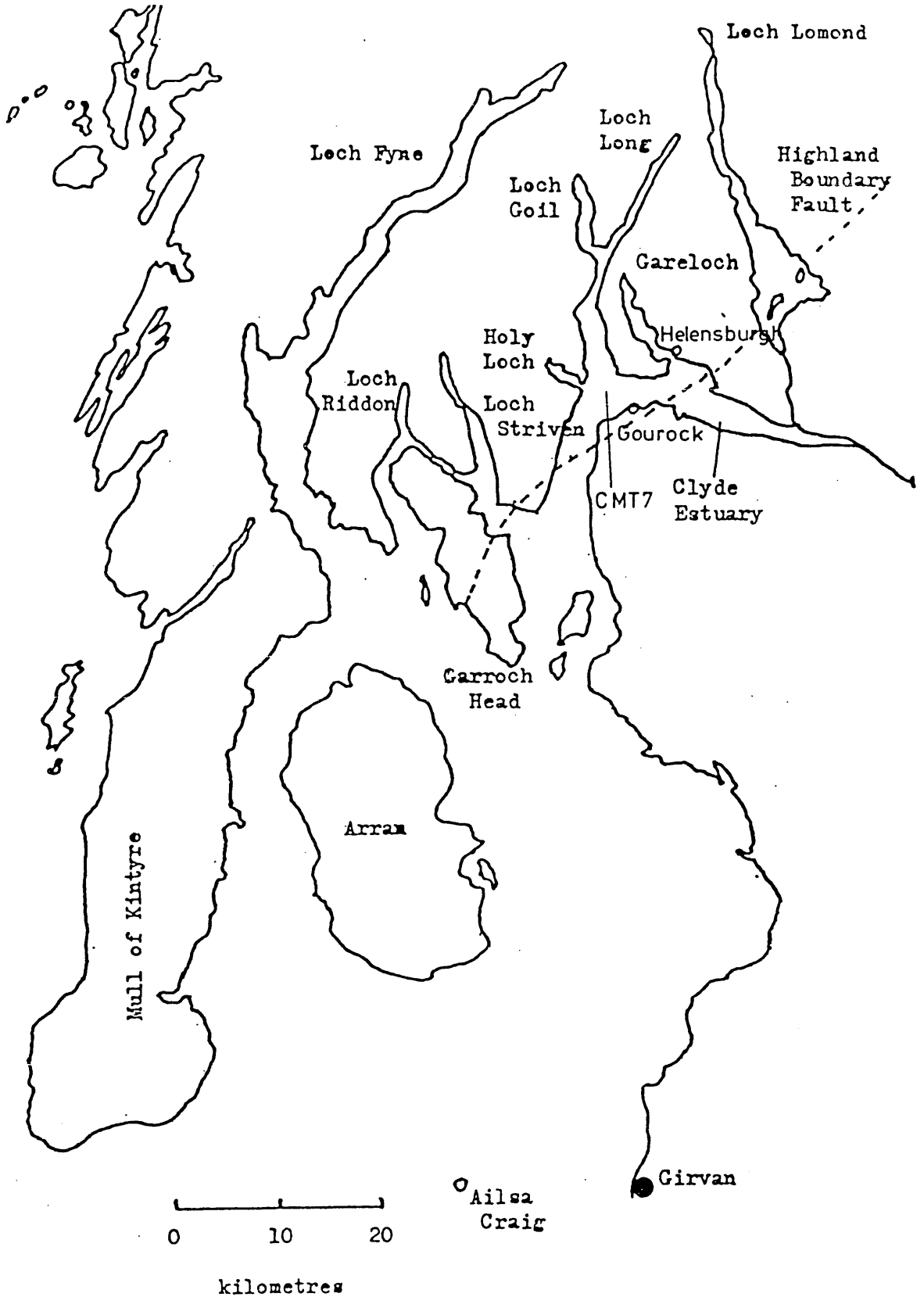
i) Sampling

The three main areas from which water samples were collected are: a) the Clyde Sea Area (CSA), b) the Hebridean Sea Area (HSA) and c) Loch Etive. Further samples were taken from the North Channel and the Irish Sea. Details of dates and stations of samples collected in each region are presented in the appropriate chapters.

In the CSA, samples - all from the surface of the water column - were obtained monthly, mainly by pumping sea water, from a few metres' depth, via a salt water sampling line on board Endrick II - the research vessel of the Clyde River Purification Board. Ten litre samples were collected. Simultaneous "in-situ" measurements of temperature and salinity of the water column were made at the time of sampling, whilst collection of small auxiliary water samples (400ml) allowed more accurate conductivity measurements to be carried out

Figure 2.1

Map of Clyde Sea Area



later in the laboratory using a BREMMER Inductive Salinometer, providing salinity data of precision $\pm 0.0005\%$. The main sampling station, "CMT 7", was used in the majority of cases; other samples were obtained from nearby station CMT7, off Gourock and Helensburgh quaysides (Figure 2.1). Previous work at GU (Baxter et al., 1979; McKinley, 1979) has implied that, on a monthly basis, the CSA is well-mixed and absolute ^{137}Cs levels can be considered uniform throughout the area. Exceptions to this are fresh water diluted areas and the deeper sections of the northern sea lochs. To eliminate the former effect, the radiocaesium measurements have been normalised to a constant salinity, 33.9‰.

Loch Etive sampling was also carried out on a monthly basis whenever possible. Two sites were used, one at Aird's Bay - about 45 metres deep - and one in the inner basin - about 125 metres deep (Figure 2.2). Samples of 20-25 litres were collected regularly from depths of 35, 85 and 125 metres and on two occasions were taken at 10 metre intervals between 15 and 125 metres. Since these samples were from depth, multiple water bottles (I.O.S.* 7.5 litres capacity), attached to a hydrographic wire and closed by a "messenger", were deployed from the NERC[#] research vessel "Calanus" during SMBA[†] surveys in the lochs.

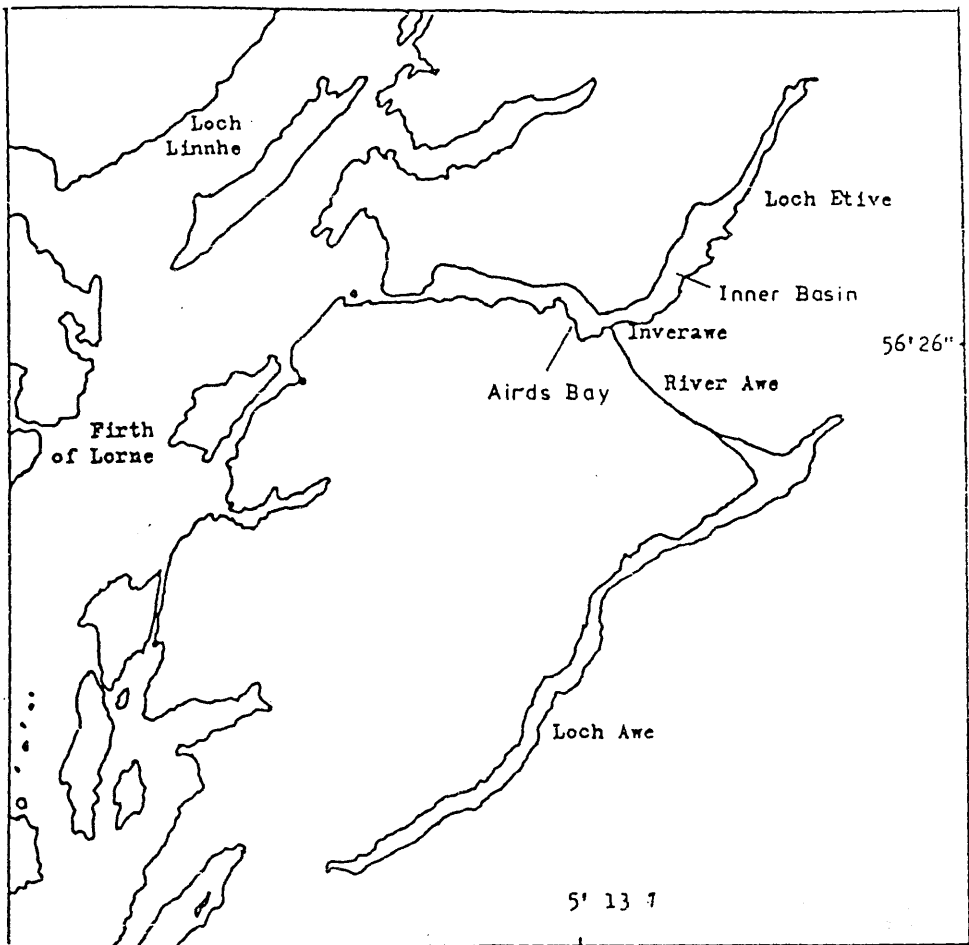
Samples from the HSA were collected on board the NERC research vessels RRS Shackleton (1 cruise), RRS Frederick Russel (1 cruise), RV Calanus (2 cruises) and RRS Challenger (4 cruises) during SMBA (7) and UCNW Marine Science Labs. (1) research cruises. Figure 2.3 shows a

* Institute of Oceanographic Sciences

Natural Environment Research Council

† Scottish Marine Biological Association

Figure 2.2



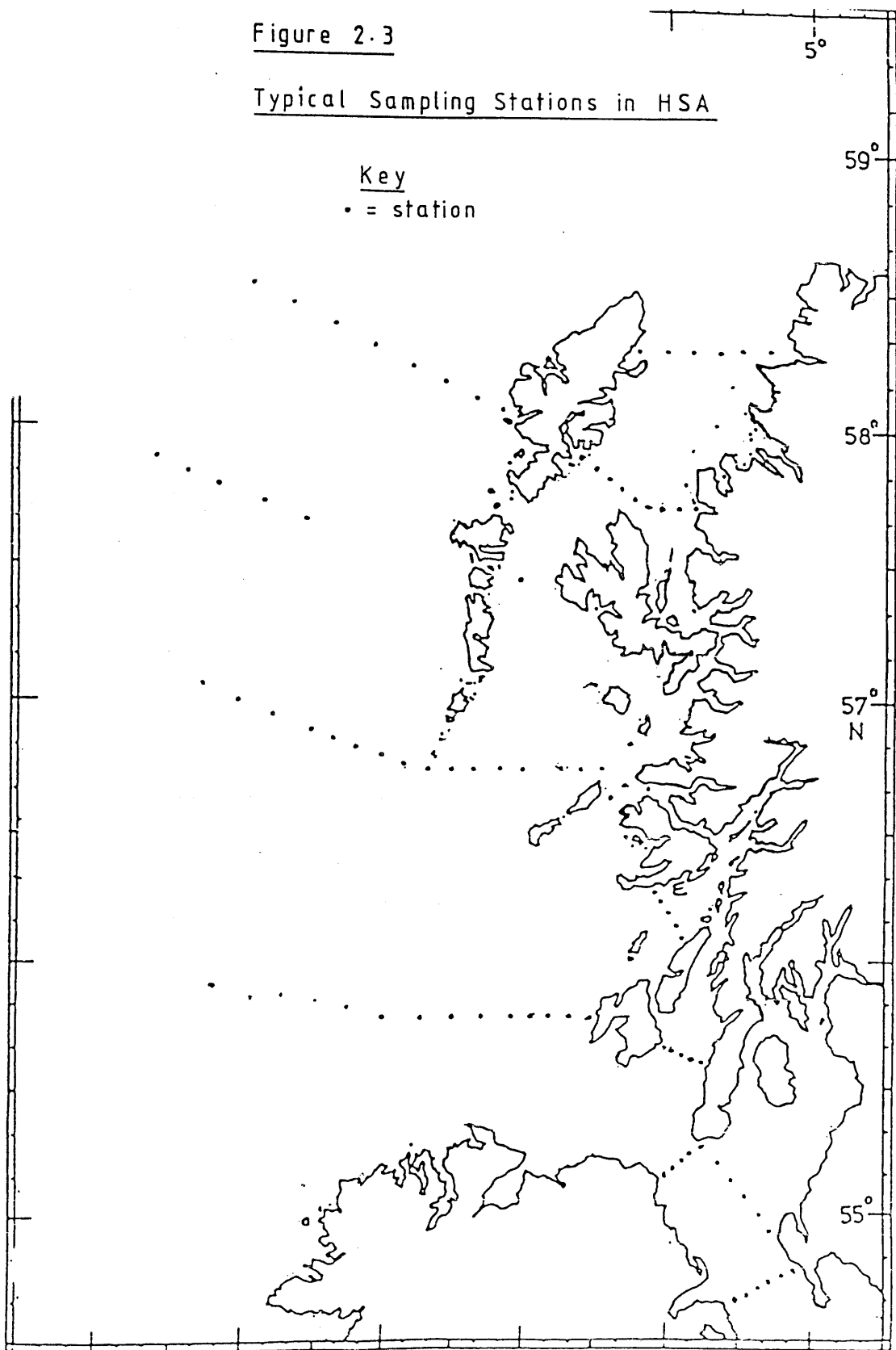
MAP OF LOCH ETIVE AND SURROUNDING AREA

Figure 2.3

Typical Sampling Stations in HSA

Key

• = station



typical sampling grid used. Surface samples were obtained by pumping from about 5 metres, whilst deep samples were collected - as for Loch Etive samples - in IOS bottles on a hydrographic wire. To obtain 25 litre samples at each depth it was, in practice, found necessary to perform 2 drops with 2 bottles on the wire for each drop. Once the sea water has been transferred to a plastic carbuoy - previously thoroughly washed with water and rinsed with 2M HNO_3 - conc. HNO_3 is added to acidify the water sample to pH2 (10ml acid required per 10 litres of sea water) and so prevent any removal of the caesium in solution on to suspended particulates in the sample or on to the walls of the plastic container.

ii) Laboratory Analysis

Radioanalysis of a typical water sample involves 1) extraction of the radiocaesium from the sea water on to an ion-exchange resin such as KCFC (Potassium Hexacyanocobalti II Ferrate II) and 2) γ -spectroscopy of the KCFC sample. The method adopted for this project is based largely on that used by McKinley (1979) and McKay (1983) and summarised by MacKenzie et al., (1979) but with some modifications; the flow diagram in Figure 2.4 outlines the procedure. The efficiency of KCFC in extracting radiocaesium from sea water has been found to be 99.7 +/- 0.2 % for ^{137}Cs and 97.3 +/- 2.6 % for ^{134}Cs with effectively all the radioactivity being retained within the top 1cm of the KCFC column (McKinley, 1979). Comparison of KCFC with other ion-exchange resins has been discussed by McKinley (1979).

Briefly, then, the water sample is first filtered, with flow augmentation from a water pump, through a cellulose nitrate membrane filter of pore size $0.2 \mu\text{m}$ (Whatman WCN, 90mm diam.). Such

Figure 2.4Outline of ^{137}Cs Analysis

Sea water sample

Filter

KCFC

Ion - exchange resin

Dry and seal

Count on

NaI gamma-detector

elimination of larger particulate matter minimises 1) confusion with regard to the source of radiocaesium, i.e. is it derived from the water alone or both the water and the particulate load? - interest here, from the water-tracing viewpoint, being solely in the fraction of Cs in solution and 2) particulates becoming trapped in the KCFC column firstly, restricting water flow, and secondly, partially giving rise to an increase in the background level of radioactive contaminants. This filtration process takes about one hour for a 10 litre sample and about 3 hours for a 20 litre sample; for the more turbid waters, Glass Microfibre Filters (Whatman GF/D, 90mm diam.) were placed on top of the membrane filter in order to retain the bulk of the larger particles and hence slow down clogging of the membrane filter. The apparatus is shown in Figure 2.5.

This "prefiltering" stage is followed by gravity-fed ion-exchange of the sea water through a KCFC column as shown in Figure 2.6. The column is prepared by transferring KCFC resin - slurried with distilled water - into plastic tubing (8 or 9mm diam., blocked at one end with cotton wool) to a depth of 5 cm. The prefiltered sample is measured out using 5 litre volumetric flasks and transferred to a 10 litre round-bottomed flask which feeds the ion-exchange column at a rate of about one litre per hour. After ion-exchange, the KCFC column in the polythene tubing is air-dried using a water pump, air-drying being preferable to oven-drying since the latter leads to incorporation of salt from residual sea water on the column and so increases the ^{40}K background of the sample. Once dried, the KCFC column is stoppered at the open end with a small block of dowelling of length 5mm and appropriate diameter (9 or 8mm, depending on the diameter of the available tubing). The latter is then trimmed at either end and sealed with sellotape ready for counting.

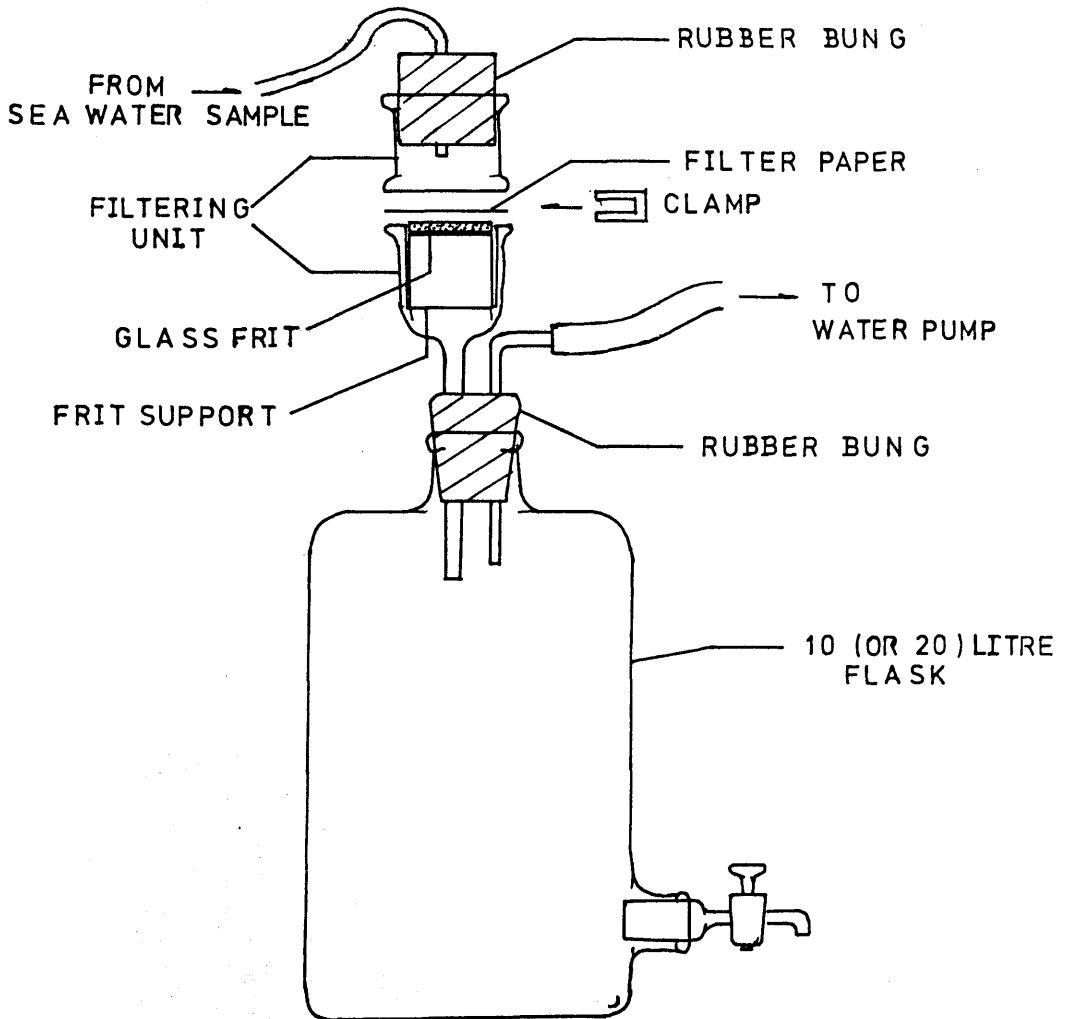
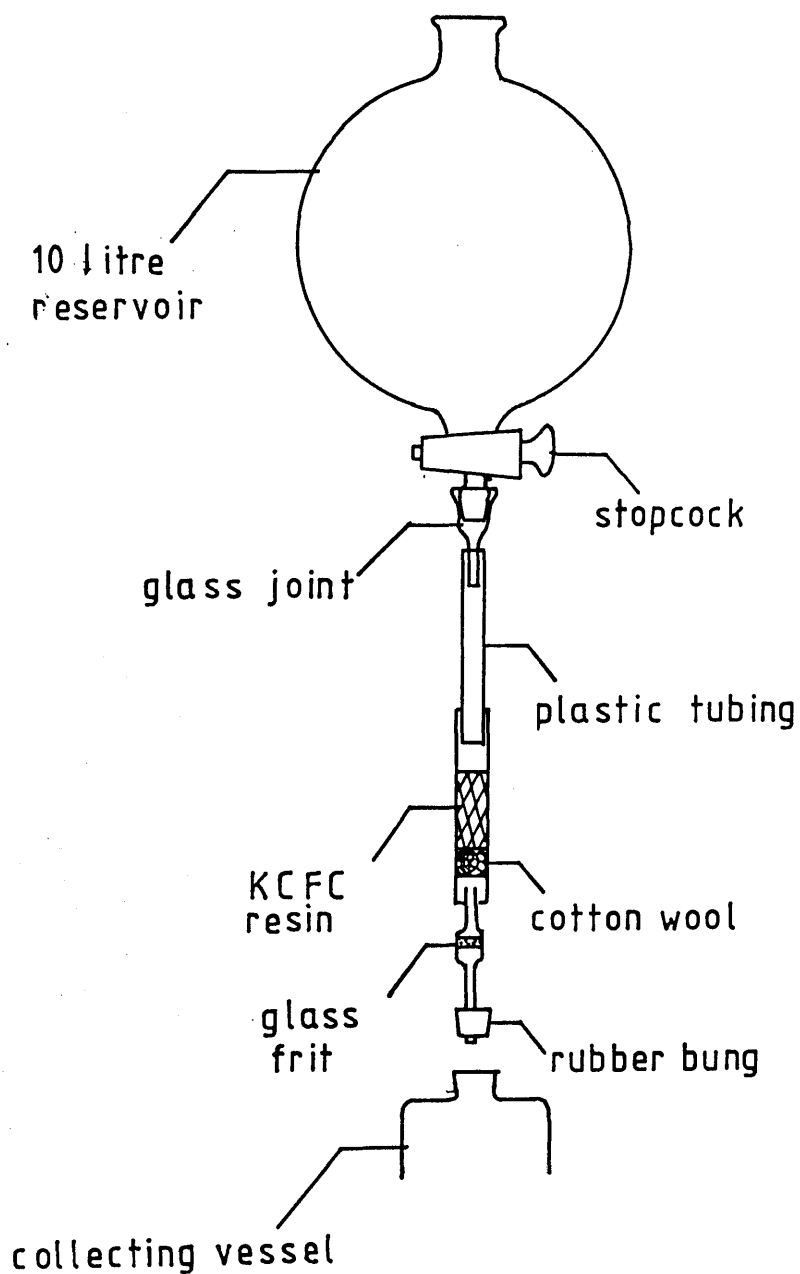
Figure 2.5Filtering of Sea Water Samples

Figure 2.6

Gravity Filtration of Sea Water Through
KCFC Ion-exchange Column



All the glassware used was periodically soaked in DECON cleaning fluid and, between samples, was washed thoroughly with tap water and rinsed with 2M HNO_3 and distilled water; the radiocaesium concentration in Glasgow tap water has been found to be negligible (McKinley, 1975). Overall, the pre-counting procedure takes about 14 hours per sample. Three sets of prefiltering apparatus were set up so that three samples could be prefiltered simultaneously; up to eight gravity filtrations could be run in parallel.

2.2(b) Soils, Grasses and Seaweeds

i) Sampling

Seaweeds (Fucus species) were obtained from sites from the west mainland coast of Britian as well as from Northern Ireland*, the Isle of Man* and the Outer Hebrides* whilst soil and grass samples were collected from the Isle of Man and the Outer Hebrides. Details of the types of samples collected, sampling dates and regions of origin are presented in Table 2.1 whilst the actual sampling sites are shown in Figure 2.7 (see also chapter 5). All samples were collected either in polythene bags or plastic containers and laboratory analysis performed soon after sampling, before decomposition set in.

ii) Laboratory Analysis

For the soils, laboratory treatment simply involved weighing the samples, drying them - though some were quite dry when collected - and reweighing, then sieving to remove stones and pebbles and reweighing again; these weights were recorded with an accuracy of +/- 0.005 grams. The samples were then ready to be packed into small-sized counting vials - consisting of a dish and lid. To accommodate for the

* Isle of Man samples were provided by Mr. A.Walton, Marine Biology Station, Port Erin, Isle of Man.

N.Ireland samples were provided by Miss J. Lennon, Marine Biology Station, Portaferry.

Outer Hebrides samples were provided by Mr. Buchanan, Isle of Barra.

Table 2.1Details of Sample Collections - Seaweeds, Soils and Grasses

<u>Date</u>	<u>Site</u>	<u>Sample</u>
January 1983	<u>West Coast Britain :-</u>	<u>Seaweeds :-</u>
	Ravenglass Estuary	<u>Fucus vesiculosus</u>
	Sellafield pipeline	<u>F. vesiculosus</u>
	St. Bees	<u>Fucus spiralis</u>
	Annan	<u>F. vesiculosus</u>
	Balcary Bay	<u>F. spiralis</u>
	Sandhead	<u>F. vesiculosus</u>
	Turnberry	<u>F. spiralis</u>
	Saltcoats	<u>F. spiralis</u>
	Gourock	<u>Fucus serratus</u>
	Loch Fyne	<u>Ascophyllum nodosum</u>
June 1983	<u>Barra,</u> <u>Outer Hebrides</u>	<u>Seaweeds, soils</u> <u>and grasses :-</u>
		* grass
		# grass
		* soil
		# soil
		dried seaweed
		fresh seaweed
		(<u>A. nodosum</u>)
June 1983	<u>Isle of Man</u>	<u>Seaweeds, soils</u> <u>and grasses :-</u>
		* grass
		# grass

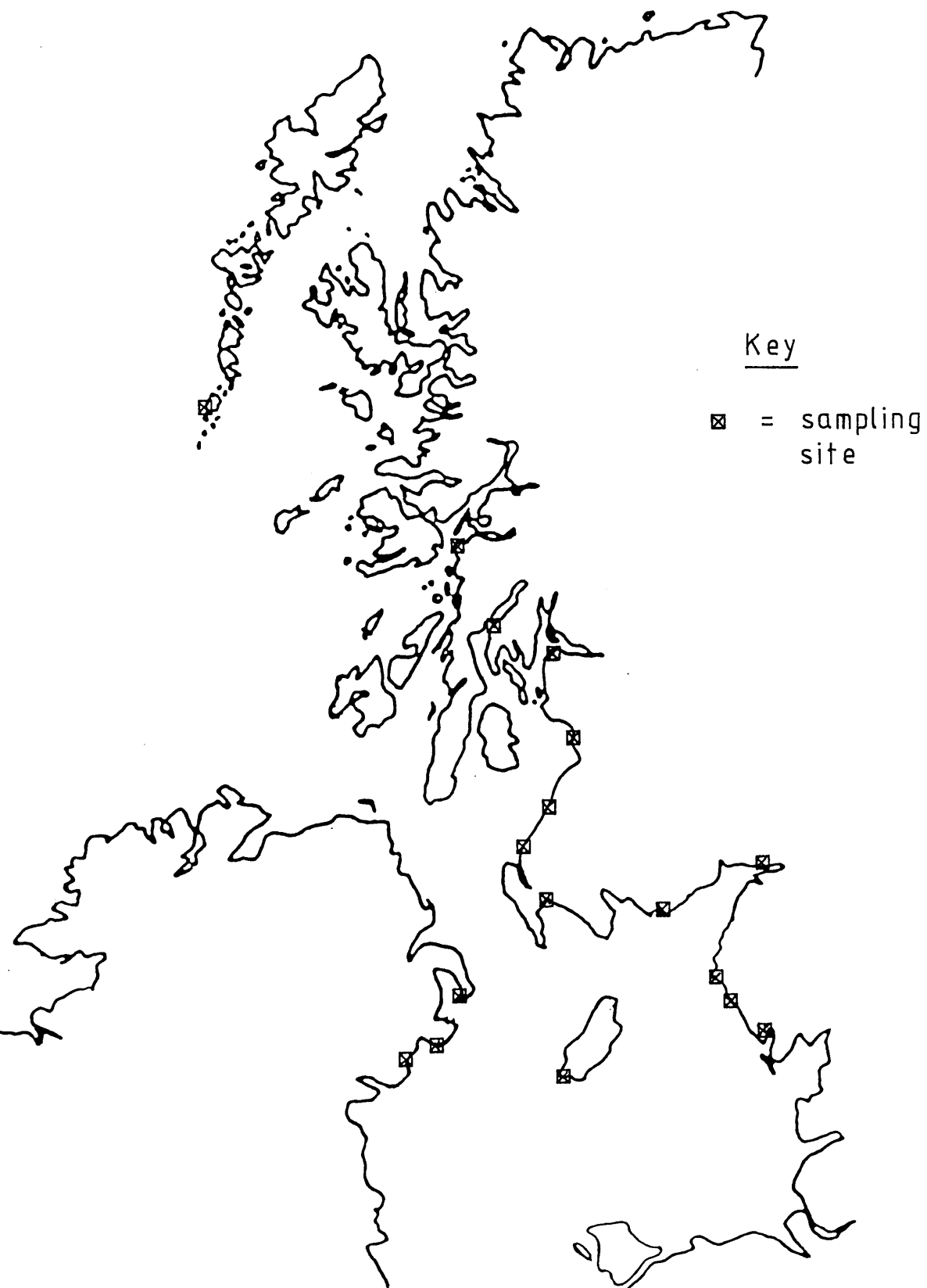
Table 2.1. cont'dDetails of Sample Collections - Seaweeds, Soils and Grasses

<u>Date</u>	<u>Site</u>	<u>Sample</u>
		* soil
		# soil
		seaweed (<u>F. spiralis</u>)
August 1983	<u>Dunstaffnage,</u> <u>Scotland</u>	<u>Seaweeds :-</u> <u>Pelvetia caniculata</u> <u>F. spiralis</u> <u>A. nodosum</u>
November 1983	<u>Cumbria :-</u> Sellafield pipeline Ravenglass Estuary	<u>Seaweeds :-</u> <u>F. vesiculosus</u> <u>P. caniculata</u> <u>F. vesiculosus</u> <u>A. nodosum</u>
April 1984	<u>N. Ireland :-</u> Portaferry St. John's Point Newcastle	<u>Seaweeds :-</u> <u>F. vesiculosus</u> <u>F. serratus</u> <u>F. vesiculosus</u> <u>F. vesiculosus</u>

* fertilised with seaweed

not fertilised with seaweed

Figure 2.7

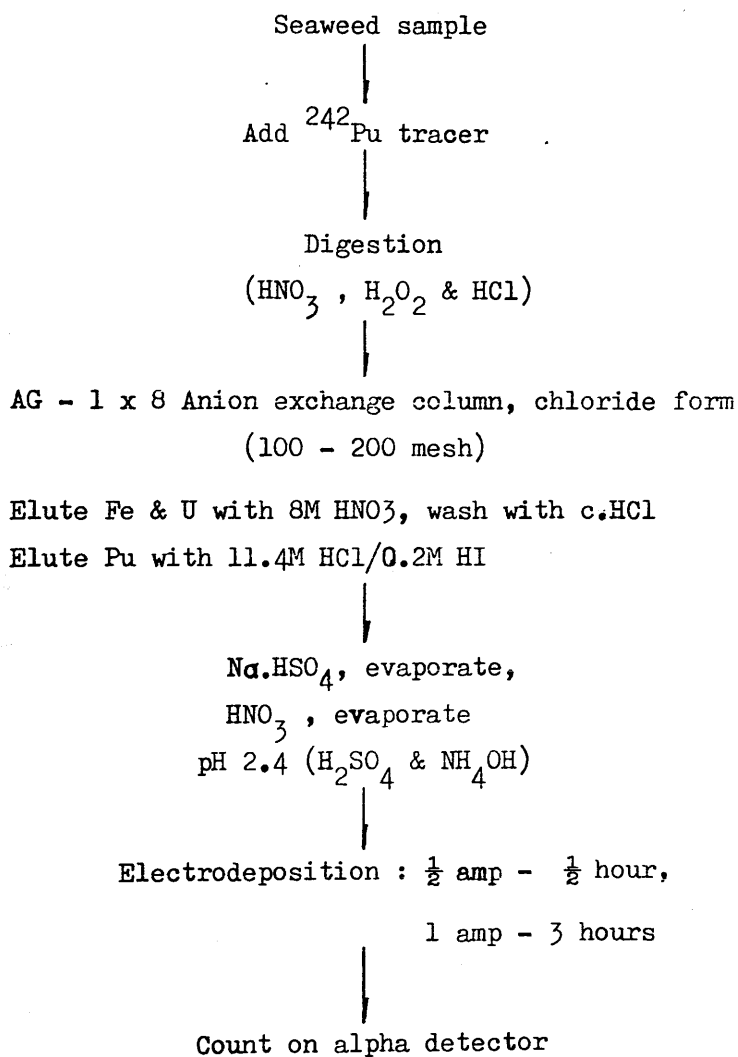
Sampling Sites for Soils, Grasses and Seaweeds

same sample geometry for which the Ge(Li) detector system had been calibrated, the vials were filled with approximately 30 grams of sample. The soil was thus carefully transferred to the labelled, tared dish which was then accurately reweighed, labelling of the dish being performed, before weighing the dish, by scratching and/or writing on the lid and dish. Each of these weighings was accurate to ± 0.0005 grams, so that the final recorded weight of sample in the dish had an associated error of 0.007 grams. The lid was then very carefully sealed on to the dish with sellotape ensuring that none of the sample escaped from the container. The sample was now ready for gamma-counting on a Geli counter (see section 2.3).

Grasses were also weighed and then air-dried - in an oven at 50 degrees Celsius - and reweighed. Samples were then ground in a Moulinex coffee grinder and transferred to a counting dish. The samples were weighed and prepared for gamma-counting in the same way, as explained above, as for soil samples.

The first steps involved in preparing the seaweeds for counting were 1) definitive identification of species obtained and 2) washing to remove barnacles or other associated organisms or sediment particles. The seaweeds were then weighed, dried, reweighed and ground in a Moulinex coffee grinder. From here, preparation for gamma-counting was identical to that already described for soils whilst preparation for plutonium alpha-counting involved prior radiochemical extraction of the plutonium from the sample.

The plutonium method used is outlined in the flow diagram in Figure 2.8 and is based on the method described by Lally and Eakins (1978). The latter method, however, involves initial ashing of the sample (2-50 grams depending on expected activity, see below) overnight in a furnace at 500 degrees Celsius - to oxidise organic

Figure 2.8Outline of Pu Analysis

matter. Then a plutonium spike and HF are added. However, in this work, oxidation of organics was often found to be incomplete and a "wet ashing" method was substituted. Thus the spike (1ml of ^{242}Pu of activity 4.02pCi/ml) was added and the sample treated with an oxidising solution (see below) by refluxing for about 2 days. This "wet ashing" was found to be more satisfactory, not only because it was more effective in destroying organic matter, but also because it avoided multiple transfers of sample between different containers. Thus the sample remains in the same vessel from the stage of adding the spike and digesting the sample until the latter is prepared for the first ion-exchange column; the original method involves transfer of the sample about 6 times to different vessels before the first anion column stage is reached. Samples losses are thus minimised.

A few steps of the original method were omitted, for example, the extraction of Fe with di-isopropyl ether conditioned with 8M HCl was not necessary for seaweeds because of their low iron contents. Similarly, the addition of aluminium chloride to remove any remaining HF was unnecessary.

The procedure, then, was begun by weighing out (+/- 0.0005 g) the required amount of sample and transferring it to a 1 litre wide-necked conical flask using distilled water for the washings. The spike (1ml of activity 4.02pCi/ml ^{242}Pu) was then pipetted into the seaweed sample and 150ml of distilled water added to make up a slurry. Next, 60ml of c.HNO₃ were added carefully - to avoid excessive frothing. The sample was then left overnight to oxidise gently, helped by stirring. After this initial stage of digestion, heat was applied and the sample refluxed for about half a day before any (60ml) c.HCl and (40ml of 30%) H₂O₂ were introduced; the refluxing henceforth was continued for about 18 hours. Once digestion of the sample was complete, it was

prepared for the first anion exchange column by making up in 500ml of 10.7M HCl and adding 10ml c.HNO₃ - the latter in order to ensure the plutonium is in the (IV) oxidation state (+4) and thus remains on the column.

The column has a glass frit at its base. It is filled (12cm length by 3.3cm internal diameter) with the resin (BIO-RAD, DOWEX 1-x8, chloride form, 100-200 mesh) - prewashed to remove the fines and slurried with distilled water - to a height of 4.5cm. A glass wool plug sits above the resin. The column is prewashed with 200ml 8M HCl from a 500ml reservoir above the column. The sample is then transferred to the column with washings - using 10ml 8M HCl. The column is then washed with 200ml 8M HCl and the Fe and U eluted with 300ml 8M HNO₃ at a flow rate of ~10 ml min⁻¹. Thereafter the column is converted back to the chloride form by washing slowly, again with 100ml c.HCl (~10 ml min⁻¹). Elution of the Pu is carried out using 200ml 11.1M HCl / 0.2M HI (flow rate of ~5ml min⁻¹). The eluate is collected in a 600ml beaker and boiled down to ~10ml, cooled, and 50ml of c.HNO₃ added. Boiling down again, it is reduced to about 2ml in volume, cooled, and 50ml of 8M HCl added. This procedure generates a solution of 7.8M HCl / 0.5M HNO₃.

A second ion-exchange column, similar to the first but smaller, is now used to purify the sample further. A 1cm (internal diameter) glass tube, fitted above with a 150ml reservoir, is filled to a depth of 4cm with anion exchange resin - BIO-RAD, AG 1x8, chloride form, 100-200 mesh) (fines already removed and slurried with distilled water). Conditioning of this smaller column requires only 20ml 8M HCl.

The solution is transferred, with washings (with 10ml 8M HCl), to the column and the same sequence of steps followed as for the first column. Flow rates are identical but the following smaller volumes of

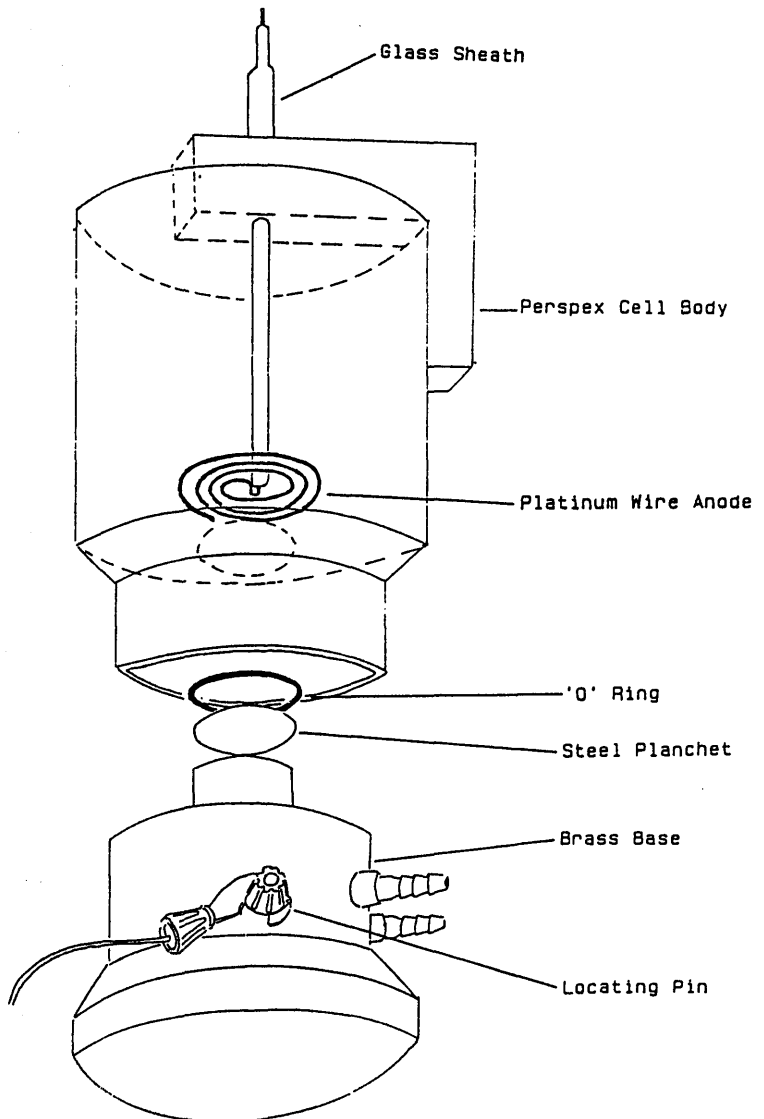
reagents are used:

- 40ml 8M HCl - to wash the column,
- 40ml 8M HNO₃ - to elute Fe and U,
- 20ml c.HCl - to reconvert resin to chloride form,
- 25ml 11.1M HCl/
0.2M HI - to elute Pu.

From here, 5ml NaHSO₄ are added as a carrier and the sample evaporated to dryness under an infra-red lamp - a dirty-white residue is obtained. Then 3mls c.HNO₃ are added and the sample is again evaporated to dryness - this time a pure white residual is obtained, any remaining iodide from the HI having been oxidised by the HNO₃ and liberated as iodine gas. About 2ml 1.8M H₂SO₄ are added and the sample is warmed to dissolve the residue. Addition of a few mls of distilled water makes the volume up to 5ml and 0.2ml saturated EDTA (disodium salt complex) solution are introduced to complex the Pu. Using methyl red as indicator, the solution is then adjusted to the correct pH (2.4) with c.NH₃ solution and 0.5M H₂SO₄. Finally, the solution is made up to 45ml with 40ml distilled water and transferred to an assembled electrodeposition cell (Figure 2.9).

The cell consists of a Perspex tube with a detachable base on which a 2.7cm diameter stainless steel disc is placed as the cathode. The anode is a platinum wire terminating in a platinum tube 1cm long and 1cm in diameter. The distance between the anode and cathode is 3cm and, for best quality of alpha spectrometry, the solution is electrolysed at 0.5 amp for the first 30 minutes and then at 1 amp for 3 hours. Before terminating the electrolysis, 2ml of c.NH₃ solution is added - to provide a basic environment and hence prevent desorption of

Figure 2.9

Electroplating Cell

Pu from the disc - and the sample undergoes a further minute of electrolysis. After completion, the cell and disc are washed with distilled water and the disc is rinsed with methylated spirit and left to dry overnight. The stainless steel disc is now ready to be counted by alpha-spectrometry (see section 2.3).

Recoveries of between 70% and 90% were usually obtained - analyses producing lower recoveries than this were repeated. All samples were analysed in duplicate and it was found possible to carry out 3 sets of duplicate analyses simultaneously having started them 1 day apart. A single duplicate set typically took 6 days to complete unless it was a more active sample, in which case only a small quantity of sample (<5g) was required (as opposed to 30-50g for the less active samples) and the preparation required 4 days. Since gamma-counting of seaweeds preceded Pu analysis it was possible to assess which of the samples were likely to be the "more active" with respect to Pu and therefore required in smaller amounts. When only a few grams of seaweed were used it was considered practicable to omit the first anion exchange stage and to proceed directly to the second ion-exchange step.

rays, will produce electron-positive hole pairs in the sensitive volume of the crystal of such a detector by promoting electrons from the valence band to the conduction band - analogous to ionisation in an atom or molecule - hence leaving a positive hole in the valence band; germanium or silicon is the most widely used material for such detector crystals, lithium being a common (e-donor) doping agent. The above process induces an electrical current in a normally insulating material and the charge can be collected by applying a high voltage across the detector. The electrical pulse produced is proportional in magnitude to the energy of the incident radiation and can be amplified then analysed and stored in a MCA in the same way as above for a scintillation counter.

ii) Detailed Description

The two NaI(Tl) scintillation counting systems (Systems A and B) were both "well" type in design and are described here in more detail. The scintillator used is a NaI crystal activated by trace amounts of thallos iodide. Impinging γ -radiation enters the crystal structure and produces photoelectrons via the photoelectric effect (PEE), the photoelectrons therefore being given all the energy of the γ -ray minus the small electron binding energy. Gamma rays of high energy are more likely to interact via Compton scattering until the scattered photons have lost enough energy to undergo the PEE; in small detectors, however, the more energetic rays may penetrate the crystal without any interaction. Since the main region of interest here is in the γ -radiation of less than 1MeV and since the high atomic number of iodine provides the crystal with a very high absorption efficiency for γ -rays then the absorption coefficients for the γ -rays in question (500-

750keV), for the PEE, are quite high. Some Compton scattering will, however, occur, particularly for the more energetic gammas. A photoelectron thus produced will travel through the crystal and be scattered by the electric fields of other ions. Hence it will deposit some of its kinetic energy in these ions. When all the electron's kinetic energy has been dissipated the electron is brought to rest. At this stage, essentially all the original γ -ray's energy is present as "excitation energy" within the crystal. The energy is distributed throughout the crystal and is transferred to many of the thallous ions which then proceed to de-excite and thus emit light; the amount of light - the number of photons - emitted is therefore proportional to the energy of the original γ -ray. The photons are then directed on to the photosensitive surface - the photocathode - of a photomultiplier tube. Here, photoelectrons are released by the metal surface, the number depending on the intensity of the light from the crystal; it may require 10 photons to release one photoelectron. The photoelectrons are accelerated by a voltage of between 100 and 200 volts to the first electrode (a dynode) behind the photocathode and from here are accelerated by about a further 150 volts to the second dynode, this process being repeated through a total of 10 (sometimes 11) dynodes. At the first dynode, a photoelectron has, by virtue of its acceleration, acquired enough energy to knock out other electrons from the dynode. If one photoelectron from the photocathode knocks out 4 electrons at the first dynode and these 4 electrons proceed to knock out 4 electrons each at the second dynode, then after 10 dynodes about a million electrons have been released; this multiplication factor attained depends on the voltage at each dynode stage.

The electrons from the photomultiplier are detected in the form of a voltage pulse - a current - whose size (height of the pulse) is

proportional, first to the light intensity reaching the photocathode and therefore, second, to the energy of the original γ -ray. A preamplifier receives this high impedance output current from the photomultiplier and matches it to the low impedance input of the main amplifier. After further amplification and pulse-shaping, the voltage pulse in this case enters a 1024 channel ADC (Analogue to Digital Counter) of a MCA - a Canberra Series 80 MCA version 2 was used. The latter acts as a "discriminator", discriminating against pulses that are too small and so limiting the background from "stray" electrons; it also acts as a pulse height analyser, sorting out the pulses according to their energies to provide a pulse height spectrum, i.e. a qualitative as well as quantitative analysis of the γ -energies detected.

Poor resolution of this type of system is largely due to the various conversions of energy from one state to another, i.e. in the crystal, the transfer of the γ -energy to photoelectrons (electrical energy) then to photons (light energy) and at the photocathode, reconversion of this light energy to electrical energy as photoelectrons. Statistical variations occur at each of these steps and also at the dynode stages so that the final γ -spectrum obtained is significantly smoothed out. Resolution at 662keV (the ^{137}Cs peak) was found to be 8.5% for system A and 6.6% for system B. Efficiency, however, is relatively good, especially for the lower γ -energies, since many of the γ -rays undergo the PEE within the crystal hence all of their energy is dissipated and can be detected whereas, at higher energies, Compton scattering occurs more frequently. Since the NaI detector system operates mainly by measuring the energies detected via the PEE then the efficiency is very good - up to 90% for energies below 200keV. For the two systems used during this project (see Table

Table 2.2Details of Gamma-counting Facilities

<u>Detector</u>	NaI (Tl) System A	NaI(Tl) System B	Ge(Li)
<u>Make</u>	Canberra	Bicron (3MW3/P)	Canberra
<u>Specifications</u>	3" x 3" cylindrical well 5/8" diam. x 1 $\frac{5}{8}$ " high		129cc
<u>Resolution</u>	7.5% at 662 keV	7.0% at 662 keV	0.25% at 662 keV
Detection limit for ^{137}Cs (3σ background)	30mBq ($7.9 \times 10^4\text{s}$)	20mBq ($4.8 \times 10^4\text{s}$)	
Detection limit for ^{134}Cs (3σ background)	0.05Bq ($7.9 \times 10^4\text{s}$)	0.04Bq ($4.8 \times 10^4\text{s}$)	

Table 2.3

Summary of NaI (Tl) System Constants for 8mm (9mm) Tubing

<u>Constant</u>	<u>System A</u>	<u>System B</u>
B	17.7283 (18.1949)	6.4138 (6.6850)
B'	22.5906 (23.0377)	8.9800 (9.2600)
e	0.2330 (0.2213)	0.2493 (0.2379)
e'	0.1483 (0.1410)	0.1493 (0.1482)
f ₁	0.3319 (0.3533)	0.3560 (0.3603)
f ₂	0.000321 (0.000933)	0.000322 (0.000700)
R ₁	0.014 (0.020)	0.030 (0.020)
R ₂	0.025 (0.020)	0.030 (0.025)

See text for explanation of symbols.

2.2), System A (Canberra NaI(Tl) with photomultiplier unit) and System B (Bicron Model 3Mw3/P with photomultiplier unit) the efficiencies of ^{137}Cs (662keV) and ^{134}Cs (797keV) detection were found to be about 23% and 14.5% respectively (Table 2.3). These values were, however, found to vary slightly with a change in sample geometry.

The alpha detectors used were EG and G ORTEC Silicon Surface Barrier Detectors made from extremely pure single crystals of silicon (impurities of parts per 10^9) and were mounted in Canberra vacuum chambers. Although perfectly pure silicon is an insulating material, small impurities render it a semiconductor. Whether the impurity donates or "mops up" electrons (e.g. a group V or group III element of the periodic table respectively) will dictate whether the semiconductor is of n-type - with an excess of free electrons within the crystal - or of p-type - an excess of positive holes in the structure, i.e. a lack of electrons. In these detectors, n-type Si is used, with one edge allowed to oxidise and in doing so becomes p-type; a p-n junction has therefore been created. A voltage is then applied to the crystal with the positive potential on the n-type material - which has a layer of aluminium as the terminal - and the negative potential on the p-type side - which has a layer of gold acting as the terminal and also as the window for the detector. Under this voltage, the electrons in the n-type Si are pulled towards the positive electrode and the positive holes in the p-type Si are swept towards the negative electrode. This leaves a region, at the junction of the n- and p-type materials, which is virtually depleted of free charge carriers and is electrically neutral so that the leakage current is very small; this region is called the "depletion layer". When a charged particle enters this depleted region, ionisation occurs and electrons are excited to the conduction band; Si has a band gap of

1.1eV and an average energy of 3.5eV for electron-positive hole pair production. Electron-hole pairs form in the Si and are drawn swiftly towards the electrodes under the applied electric field. The charge produced, i.e. the number of electrons released, by the ionising radiation is proportional to the energy of the ionising particle. The radiation source is placed about 1mm from the gold window of the detector and is counted in vacuum in order to eliminate air scatter. The energy required to produce an electron-hole pair in these semiconductors is 3.6eV. When compared to the energy needed to produce one photoelectron at the photocathode during scintillation counting, 300eV, it is quite clear that more electron-hole pairs are produced in a semiconductor than photoelectrons in a NaI system for the same amount of energy deposited. Hence the resolution is much better in the semiconductor than the NaI(Tl) though efficiency is much lower in the former since its absorbing qualities are poorer due to the less dense crystals used. Background radiation is essentially zero in the alpha detectors.

The depth of the depletion layer depends on the voltage applied to the crystal which is limited by the onset of breakdown across the junction (Friedlander et al., 1964) and also on the resistivity of the crystal. The higher the energies of radiation expected, the deeper the depletion layer required to ensure the radiation does not travel through the crystal's sensitive region (the depletion layer) without being detected hence the higher crystal resistivity required. For the purpose of detecting γ -radiation, therefore, this is precisely what is required. Instead of the p-n junction described above, it is possible to start off with p-type material for the crystal with a thin n-type surface; again a reverse bias is applied and a p-n junction is formed.

In order to increase the resistivity of the crystal the small

leakage current must be made even smaller, i.e. the excess of acceptors in the p-type must be compensated for. This can be done by the introduction of donor atoms, e.g. lithium. The Li is allowed to diffuse into the crystal under reverse bias and at an elevated temperature when the mobile Li^+ ions travel towards the negative electrode. When essentially perfect balance has been attained, i.e. all the positive holes have been taken up by the electrons "donated" by the lithium atoms, then the current reads zero. The crystal is cooled to liquid nitrogen temperature (-196°C) and the Li is fixed in the crystal structure.

An additional way of obtaining higher resistivity is to use germanium instead of silicon since it is denser and therefore has better γ -absorption qualities than the silicon. The energy needed to produce an electron-hole pair for the Ge is only 2.9eV so its resolution is even better than that of the Si surface barrier detector although its very small band gap of 0.66eV means that excessive thermal excitation of electrons across the gap at room temperature can occur. Hence by cooling the detector to liquid nitrogen temperature this thermal noise is prevented.

The detector is mounted in vacuum to prevent absorption of impurities on the surface (Faires and Boswell, 1981) and a voltage of about 4000 volts is applied.

For the alpha detectors, the charge obtained from ionisation in the crystal goes, via a preamplifier, to a main amplifier which feeds the pulses to a MCA - a pulse height analyser and an ADC which gives out a digital signal proportional to the pulse height. The MCA accumulates a spectrum of the frequency of photons versus photon energy. Details of the Canberra Ge(Li) used are given in Table 2.2. All the gamma detectors were surrounded by 10cm of lead shielding -

with an additional 5cm on top for the NaI(Tl)'s - in order to reduce background radiation. In the case of System B, "pre-war" lead was used whilst that used for System A was more recent and, from Table 2.3, it can clearly be seen that System A has background count rates of about 3 times higher than those of System B. The most probable explanation is that the modern lead has a higher activity due to ^{210}Bi , a decay product of ^{210}Pb , and that the steel frame of the shielding in System A contains a contribution from fallout-derived fission products.

2.3(b) Calibration of Detectors and Counting of Samples

Calibration of the alpha detectors for measurement of Pu alpha nuclide activities (^{238}Pu and $^{239/240}\text{Pu}$) was relatively straightforward since the use of ^{242}Pu as a spike (known activity) in each sample provided a direct proportional relationship between counts in the ^{238}Pu (or $^{239/240}\text{Pu}$) energy range, the number of counts in the ^{242}Pu range and the known activity corresponding to the latter such that :

$$\text{Activity of } ^{238}\text{Pu} = \frac{\text{counts in } ^{238}\text{Pu peak}}{\text{counts in } ^{242}\text{Pu peak}} \times \text{activity of } ^{242}\text{Pu}.$$

The activity for $^{239/240}\text{Pu}$ is deduced in the same way using the counts in the $^{239/240}\text{Pu}$ peak. This assumption of equal efficiencies for all 3 peaks is reasonable since the peaks occur at very similar energies, as follows:

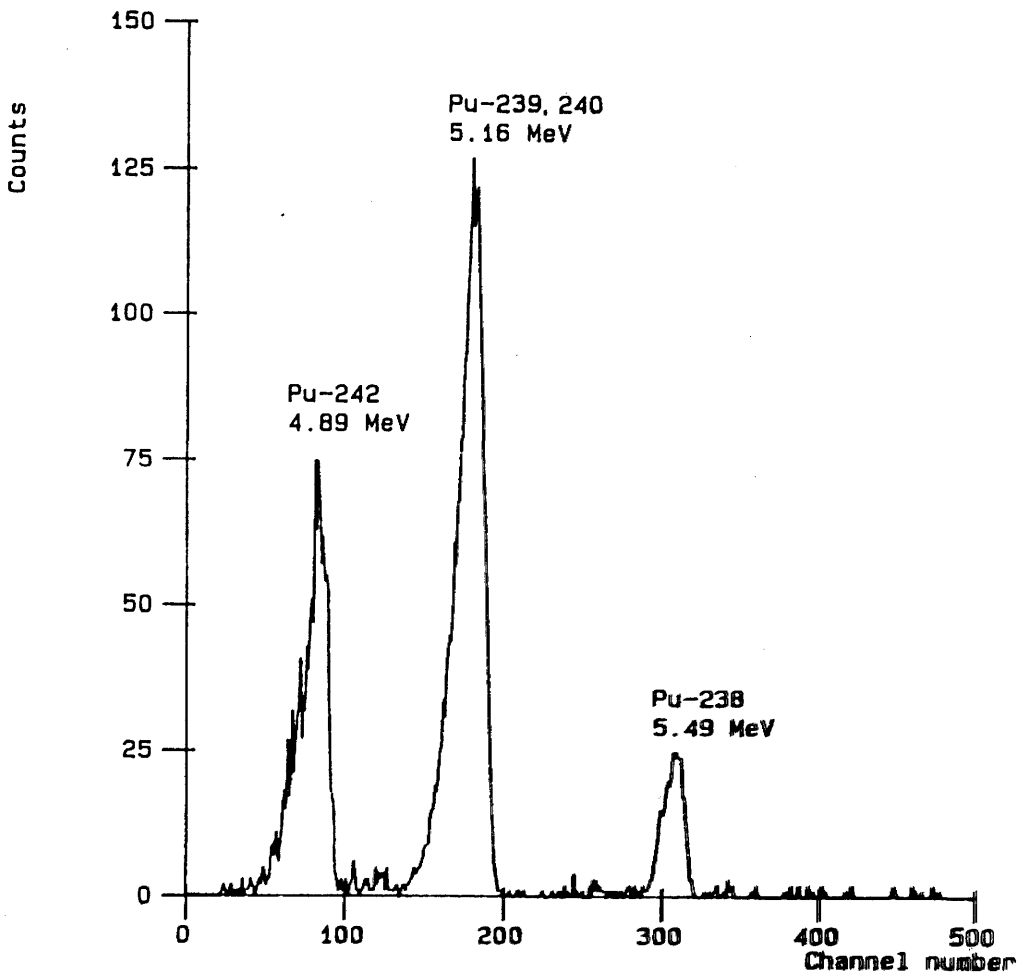
<u>Isotope</u>	<u>α-energy</u>
^{242}Pu 4.903 MeV

$^{239/240}\text{Pu}$.5.157/5.168 MeV
^{238}Pu 5.499 MeV

Since plutonium is selectively extracted from environmental samples, counting of this source of α -radiation by the detector is expected to give 3 clear peaks. If resolution is found to be poor then this could reflect the presence of impurities in the extract or previous contamination of the detector. However, background readings were taken regularly and at random to ensure that the detectors had not been contaminated. Thus poor resolution generally implied a poor chemical analytical technique. A typical α -spectrum obtained is shown in Figure 2.10.

Bearing in mind that the ^{242}Pu activity was known and constant for all samples (4.02pCi, see subsection 2.2(b)), the count rate obtained was usually about 1.7 cpm for ^{242}Pu since the counting efficiency of the α -detectors was about 20%. Hence the source would be counted for 86400 seconds (24 hours) resulting in about 2500 counts for the ^{242}Pu peak. To achieve reasonable errors on the Pu counts in each peak the aim was to obtain a $^{239/240}\text{Pu}$ peak of magnitude about 3 times larger than the ^{242}Pu peak (the ^{238}Pu : $^{239/240}\text{Pu}$ ratio was around 1:4) so that attainment of a reasonable number of counts in the ^{242}Pu peak would give a similar number of counts in the ^{238}Pu peak. This was achieved by rough estimation of the Pu activity expected in the sample and by using an appropriate amount of sample (subsection 2.2(b)), i.e. active samples required smaller amounts.

Associated errors for the Pu activities derived were calculated as follows:

Figure 2.10An Alpha Particle Spectrum

$$S_a = (C_a/C_s \times A)^2 (1/C_a + 1/C_s)$$

$$S_b = (C_b/C_s \times B)^2 (1/C_b + 1/C_s)$$

where S_a is the counting error (1σ) for the ^{238}Pu activity

S_b is the counting error (1σ) for the $^{239/240}\text{Pu}$ activity

C_a is the number of counts in the ^{238}Pu peak

C_b is the number of counts in the $^{239/240}\text{Pu}$ peak

C_s is the number of counts in the ^{242}Pu spike peak

A is the ^{238}Pu activity of the sample

B is the $^{239/240}\text{Pu}$ activity of the sample

In addition, the ratio, R , of ^{238}Pu to $^{239/240}\text{Pu}$ in each sample was calculated and the associated error, S_r , was derived in the following manner:

$$[(A^{1/2}/A)^2 + (B^{1/2}/B)^2]$$

The errors involved in weighing the sample were, at most, only $\pm 0.0007\text{g}$ (subsection 2.2(b)) which, even for the smallest sample (2g), represent an error of $<0.04\%$ which is negligible relative to the counting errors. All other quantifiable errors were also found to be negligible in comparison with the counting errors, e.g. activity of spike ^{242}Pu present in 1.000 ± 0.0005 ml has an associated error of 0.05% .

For the Ge(Li) detector, both energy and efficiency calibrations were carried out so that the efficiency at each energy was known; in general, efficiency decreases with increasing energy. Calibrations were performed using a standard gamma source, the data being processed by the Canberra Ge(Li)'s computer. The following two different gamma

sources were available and were used at different times:

- 1) a mixed radionuclide gamma-ray reference standard
- 2) a ^{152}Eu gamma standard.

The multi-nuclide standard contained 9 isotopes and provided 11 major energy peaks ranging from 0.088MeV to 1.836 MeV (Appendix VII.1) with an overall uncertainty for each peak $\ll 3.8\%$. The europium spike provided 11 gamma energy peaks ranging from 0.122MeV to 1.528 MeV (Appendix VII.2). The data for these calibrations was stored on a floppy disc and recalled for analysis of sample-spectra. Energy calibration of the Ge(Li) is independent of sample geometry whereas efficiency very much depends on the latter; hence the efficiency calibration was carried out for the particular geometry used (subsection 2.2(b)).

In the case of the NaI(Tl) counter, it was only necessary to calibrate the efficiencies at energies of around 662keV and 797keV since these were the only regions of interest. In order to do this, background readings were obtained by counting blanks containing no detectable amounts of radiocaesium and then counting spiked samples (standards), some containing ^{137}Cs , some containing ^{134}Cs and others containing both. The blanks and standards were prepared and subjected to the routine analytical procedures. The blank counts provided an assessment of the background count rate for the regions of interest whilst the spikes provided count rates of known concentrations of γ -radiation for known energies.

Preparation of blanks and standards was as follows. Several 10 litre volumes of artificial sea water were prepared by the method described by Lyman and Fleming (1940). To the samples intended as

"blanks" only the 10ml of c.HNO₃ was added whilst, to the samples for the standards, aliquots of known ¹³⁷Cs and / or ¹³⁴Cs activity, as well as the acid, were added. Primary standards of ¹³⁷Cs and ¹³⁴Cs - obtained from Amersham International Ltd. - were diluted one hundredfold from their respective activities, 4.62kBq/ml (on 1/7/78) and 4.60kBq/ml (on 1/7/79), to provide secondary standards; thus a 0.1ml aliquot of each primary standard was taken and diluted to 10ml with HCl. From here, 0.4ml of the ¹³⁷Cs secondary standard were added to the 10l of artificial sea water intended for ¹³⁷Cs calibration whilst 0.2ml of the ¹³⁴Cs secondary standard were added to a 10l volume of sea water for ¹³⁴Cs calibration. Two ¹³⁷Cs, two ¹³⁴Cs and three ¹³⁷Cs and ¹³⁴Cs (i.e. mixed) standard sea water samples as well as two blanks were prepared. The resulting activities in the spiked samples, taking into account radioactive decay, were 16.72Bq (1003dpm) / 10l of ¹³⁷Cs and 3.00Bq (180dpm) / 10l of ¹³⁴Cs on the day of preparation, 1/11/82; these activities were about equal to the highest environmental levels expected to be measured (assessed from previous measured levels by GU and MAFF, e.g. McKinley et al. (1981a,b); Hunt (1985). The 10 litre volumes of artificial sea water - blanks and spikes - were subjected to the pre-counting procedure already described and were then ready to be counted.

A further set of blanks and standards was prepared later in the project to recalibrate the system for the use of the new, smaller-sized diameter tubing for KCFC containment - 8mm as opposed to the original 9mm diameter tubing; such a change in sample geometry could cause a change in counting efficiency. This second preparation of blanks and standards was carried out on 10/5/84, with final activities of the latter being 16.15Bq (969dpm) / 10l of ¹³⁷Cs (0.4ml of secondary standard used) and 2.687Bq (161dpm) / 10l of ¹³⁴Cs (0.3ml of

secondary standard used).

^{137}Cs occurs at 662keV whilst the 2 largest ^{134}Cs peaks occur at 605 and 797keV. The 605keV peak of ^{134}Cs , however, is not distinguishable from the ^{137}Cs 662keV peak since the two peaks overlap because of the inherent low resolution of the detector. The 797keV peak is therefore used to determine the ^{134}Cs concentration even though it is smaller than the 605keV peak. This still leaves the problem of some of the counts under the ^{137}Cs peak corresponding to the ^{134}Cs 605keV peak. The extent of this overlap can be quantified by determining, from the ^{134}Cs spikes, the constant ratio of the ^{134}Cs occurring in the 797keV peak to that occurring in the fraction of the 605keV peak which overlaps with the ^{137}Cs peak. Thus the number of counts in the 605keV peak which overlap into the ^{137}Cs region can be defined. This number can then be subtracted from the total counts in the ^{137}Cs region to leave the number of counts arising from ^{137}Cs radiation alone. The equations used to treat the data from the relevant regions of the spectrum are shown below, incorporating also a correction for a slight overlap occurring between the 662keV ^{137}Cs peak and the 797keV ^{134}Cs peak - about 0.03% of the total 662keV counts occurring in the energy range of the ^{134}Cs 797keV peak. In comparison, for the larger, more important overlap, the ratio of the counts in the 797keV peak to the counts from the 605keV peak occurring in the 662keV peak was found to be about 3:1 for the energies chosen. The actual energies were chosen so as to minimise the overlap as much as possible and, at the same time, retain the good ^{137}Cs efficiency.

The equations used to quantify the radiocaesium activities of a KCFC sample counted on a NaI(Tl) detector are as follows:

$$C7 = \frac{C - B.T - f_1 (C' - B'.T)}{1 - f_1 f_2} \times \frac{\exp(\lambda t)}{e.T} \quad \dots\dots\dots(1)$$

$$C4 = \frac{[(C' - B'.T) - f_2 A] \times \exp(\lambda' t)}{e'.T} \quad \dots\dots\dots(2)$$

where C7 is the ^{137}Cs activity (dpm)

C4 is the ^{134}Cs activity (dpm)

C is the count integral in the ^{137}Cs window

C' is the count integral in the ^{134}Cs window

B is the background of the ^{137}Cs window (cpm)

B' is the background of the ^{134}Cs window (cpm)

T is the count time (mins)

e is the detector efficiency for ^{137}Cs (fractional)

e' is the detector efficiency for ^{134}Cs (fractional)

f_1 is the fractional overlap of ^{134}Cs in the ^{137}Cs peak

f_2 is the fractional overlap of ^{137}Cs in the ^{134}Cs peak

λ is the decay constant for ^{137}Cs (days⁻¹)

λ' is the decay constant for ^{134}Cs (days⁻¹)

t is the time elapsed between sampling and counting (days)

and
$$A = \frac{(C - B.T) - f_1 (C' - B'.T)}{1 - f_1 f_2}$$

$$s_{C7} = [C + E_1^2.T^2 + f_1^2(C' + E_2^2.T^2) + R_1^2 A^2]^{1/2} \times \frac{\exp(\lambda t)}{(1-f_1 f_2)e.T} \quad \dots(3)$$

$$s_{C4} = [C' + E_2^2.T^2 + \frac{f_2^2}{(1-f_1 f_2)^2} (C + E_1^2.T^2) + f_1^2(C' + E_2^2.T^2) +$$

$$R_2^2 B] \times \frac{\exp(\lambda' t)}{e' \cdot T} \quad \dots(4)$$

where s_{C7} is the associated random error for C7 (dpm)

s_{C4} is the associated random error for C4 (dpm)

E_1 is the random error on the ^{137}Cs background (cpm)

E_2 is the random error on the ^{134}Cs background (cpm)

R_1 is the residual error in the ^{137}Cs window (%)

R_2 is the residual error in the ^{134}Cs window (%)

and $B - C' - B' \cdot T - f_2 \cdot A$.

The above constants used during this project are given in Table 2.3 and a fortran computer programme (listed in Appendix VI.1), incorporating these equations, was used to calculate the radiocaesium activities and their errors. The residual errors, R_1 and R_2 , were obtained from analysis of replicate spiked samples whilst random errors on the background, E_1 and E_2 , are calculated as follows:

$$E_1 = (\text{counting error on background}^2 + \text{residual error on background}^2)^{1/2}$$

Quite frequently, the gamma spectrum obtained on System A would shift from the calibrated channels. A total of 1024 channels covered the whole energy spectrum and, whilst the channel, "x", was calibrated to correspond to the energy of maximum ^{137}Cs activity, in practice, the channel of maximum activity varied by +/-4 channels though it remained mostly within +/-2. It also became apparent that, accompanying this change in channel of maximum activity, was a change in background of the two Cs windows and that this difference was

outwith the calculated error of the background. This drift implied that the calibration carried out for the maximum activity channel at "x" was not applicable when this channel was at "x+/-4". Since a "shifting" of the spectrum is equivalent to a change in gain it was decided to compensate for this change in the following manner if the channel deviated from "x" by more than 2 channels either way (i.e. >1% change in gain):-

<u>Channel of Maximum ^{137}Cs Activity</u>	<u>Channel Limits used for ^{134}Cs Peak (1) and ^{137}Cs Peak (2)</u>			
x	a	to	b	...(1)
	c	to	d	...(2)
x+4	$\frac{(x+4)}{x}$ a	to	$\frac{(x+4)}{x}$ b	...(1)
	$\frac{(x+4)}{x}$ c	to	$\frac{(x+4)}{x}$ d	...(2)

Essentially, a shift along the energy spectrum towards the higher energies (an increase in gain) leads to a decrease in the number of background counts whilst a shift towards the lower energies (a decrease in gain) results in higher background counts. Rigorous examination of this method of correction was carried out on various samples including spikes and blanks. Table 2.4 shows the results of one set of samples studied.

The same problem was not encountered with System B since the channel of maximum activity always occurred at channel "x +/- 1" which corresponded to a maximum deviation from "x" of 1%.

Table 2.4

Counts under Cs peaks on System A NaI (Tl)
 (during ^{137}Cs spike counting) illustrating spectrum shift

Channel of Maximum Activity (relative to "x")	Counts in ^{134}Cs integral	Counts in ^{137}Cs integral
x	31365	339075
x	31262	338228
x-1	31533	338511
x-2	31294	337682
x+2	30815	335325
x+2	31003	336336
x+2	31068	331886
x-1	31735	337856
x-2	31155	337844
x+1	31375	334894
x+2	31375	334656
x+1	31307	334137
x+3	31388(31147)	333539(334435)
x+4	30456(30829)	330052(332783)
x+4	30503(30881)	328459(330262)
x+3	30964(31162)	337044(337921)
x+3	31139(31407)	333310(334222)

() = corrected for spectrum shift as
 explained in text.

Some radiocaesium data obtained by MAFF have kindly been provided for interpretation with the GU data. It has been necessary, however, to standardise the two data sets since minor analytical differences are apparent. This was achieved by comparing a range of ^{137}Cs results from duplicate samples collected during various cruises, i.e. MAFF and GU results. Such data were obtained from samples collected during cruises in August 1983, January 1984 and June 1984 (Appendix IV).

Since no errors have been provided with the MAFF data they have been assumed to be equal to those of the GU data (Appendix IV). The maximum systematic error was found to be 13.0%, with MAFF data higher than GU data. A previous intercalibration between GU and MAFF data by McKay (1983) revealed a maximum systematic error of 10% with, again, MAFF data being greater than GU data. From Appendix IV, the correlation coefficient, obtained from 21 points, is 0.997. The equation used to standardise MAFF data to the GU data is presented in Appendix IV.

CHAPTER 3

Coastal Regions

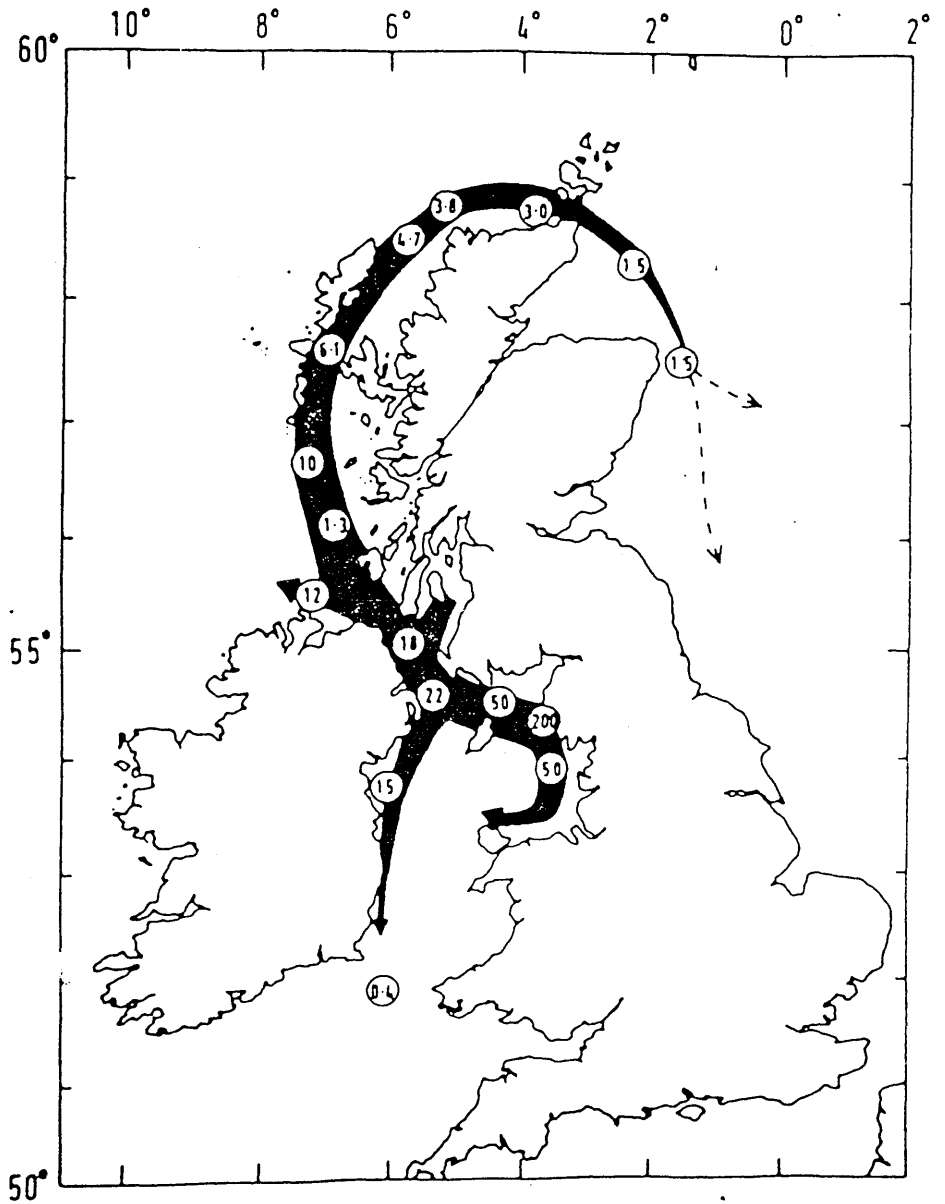
3.1 Clyde Sea Area (CSA)

The major route for dispersal of Sellafield radiocaesium from the Irish Sea is via the North Channel (Jefferies et al., 1973; McKinley et al., 1981b), with only about 5% of the discharge being washed out through the southern exit of the Irish Sea, the St. George's Channel (Jefferies et al., 1982). This northward transit of the main radiocaesium plume is largely maintained by prevailing south westerly winds and thus follows the coastline of the west of Scotland (Figure 3.1) entering, in part, the Clyde Sea Area (CSA). McKinley et al. (1981b) estimated that approximately 50% of Sellafield's radiocaesium discharged through the pipeline passed through the CSA during the period 1974 - 1977 whilst McKay and Baxter (1985a) found this to be ~35% for the period 1978 - 1981.

Results of radiocaesium analyses of CSA water samples collected monthly have allowed an improved understanding of water flow patterns from the Irish Sea, hence helping to explain the fate of soluble pollutants discharged into the latter and providing information for radiological assessment purposes.

Previous workers have estimated transit times for water flow from Sellafield to the North Channel, CSA, HSA and regions further along the main path of the radioactive plume. In most cases, direct advection has been assumed to dominate water transport, mixing "en

Figure 3.1



Concentration of ^{137}Cs (pCi l⁻¹) in UK coastal waters, May/July 1972 (from Jefferies *et al.*, 1973).

route" playing a minor role (Jefferies et al., 1973; Livingston and Bowen, 1977; MacKenzie, 1977; Mauchline, 1980; Jefferies et al., 1982; Livingston et al., 1982a,b), whilst McKinley et al. (1981b) and, more recently, McKay and Baxter (1985a) placed emphasis on mixing processes within the Irish Sea. In the latter context, mixing of newly discharged activities with residual waters effectively lowers observed nuclide concentrations and $^{134}\text{Cs} : ^{137}\text{Cs}$ ratios at source if the discharge ratios and nuclide activities are constant or increasing with time; with an adequately sharp decrease in discharge ratios and nuclide activities with time then mixing with older waters may increase the source water values of these two parameters. Thus, on an advection-only basis, "low" measured ratios along the plume path probably indicate erroneously long transit times for the water mass. Thus, Livingston and Bowen (1977)'s estimated transit time of ~2 years from Sellafield to north west Scottish coastal waters, derived by considering only $^{134}\text{Cs} : ^{137}\text{Cs}$ ratio decay between Sellafield and the Minch, had errors arising both from averaging the varying source terms and from the neglected mixing in the Irish Sea. Jefferies et al. (1982) used the $^{134}\text{Cs} : ^{137}\text{Cs}$ ratio to evaluate a 1 year transit time from Sellafield to the North Channel (1972 - 1973) and suggested a shorter time for later years. More recently, Prandle's numerical model (Prandle, 1984) of water circulation for waters of the British Isles includes the Irish Sea and the west and north coasts of Scotland. In identifying the main driving forces of the system and their relative strengths, Prandle concludes that, although in the North Sea area advection dominates over diffusion, in the Irish Sea the two transport processes are of equal importance.

By incorporating a residence time in a single-box model (see below) for the period 1974-1977, McKinley et al. (1981b) found the

transit time from Sellafield to the North Channel to be 6 months and from the North Channel to the CSA 2 months. Associated with this transport, a residence time of 17 months ($t_{1/2}$ of ~ 12 months) within the Irish Sea was estimated. McKinley et al. (1981b) postulated an increase in North Channel current velocities after early 1977, when Atlantic incursion into the southern Irish Sea flushed out northern Irish Sea waters through the North Channel. This outflow generated a peak in radiocaesium levels in Scottish waters as seen in a spring 1977 cruise. The immediate "post-flushing" period (i.e. 1978 - 1981) was studied by McKay and Baxter (1985a) using the same box model but ignoring the North Channel stage since mixing between the North Channel and the CSA had been found negligible ($t_{1/2} \sim 2$ months) by McKinley et al. (1981b) relative to that in the Irish Sea. McKay and Baxter found, by comparing monthly CSA radiocaesium trends with modelled radiocaesium curves, a lag-time of 4 months between the two sites. The accompanying residence half-time of 8 months (residence time ~ 12 months) in the northern Irish Sea was assessed by matching the observed and decay-corrected (modelled) $^{134}\text{Cs} : ^{137}\text{Cs}$ ratio curves which, it was found, would not match without a significant residence time being incorporated into the model. McKay and Baxter (1985a) thus suggested that the mean flows of Atlantic water through the St. George's Channel and of northern Irish Sea water via the North Channel had doubled after 1977. The latter, shorter residence time value found by McKay and Baxter supports the concept of an increased flux through the North Channel (or shorter lag-time). In parallel, it was also suggested that greater dilution of Irish Sea water by Atlantic water occurred after 1977. From the lag-time estimate, the mean water flow velocity for the Sellafield to CSA transect was assessed at 2.1 km day⁻¹, suggesting an average volume outflux from the Irish Sea of

7.8km³ day⁻¹.

Data on volume flows from the Irish Sea have also been generated by Jefferies et al. (1982) who, for the October 1971 - May 1978 period, found a mean flux of 5km³ day⁻¹, with means of 3.4 and 7.9 km³ day⁻¹ for the pre- and post- January 1976 periods respectively. These results, therefore, also indicate that water flows increased greatly after 1977.

In the present study, the subsequent period, 1982-1985, has been investigated and the CSA monthly radiocaesium record extended. In view of its past success in describing flow conditions, the intention was to use the single-box model described by McKinley et al. (1981b) to match the CSA ¹³⁷Cs trend with the modelled curve of best fit, as determined by the residence half-time, t_{1/2}, in the box, and to assess the residence half-time in the northern Irish Sea / North Channel system (i.e. by matching the observed and predicted ¹³⁴Cs: ¹³⁷Cs ratios).

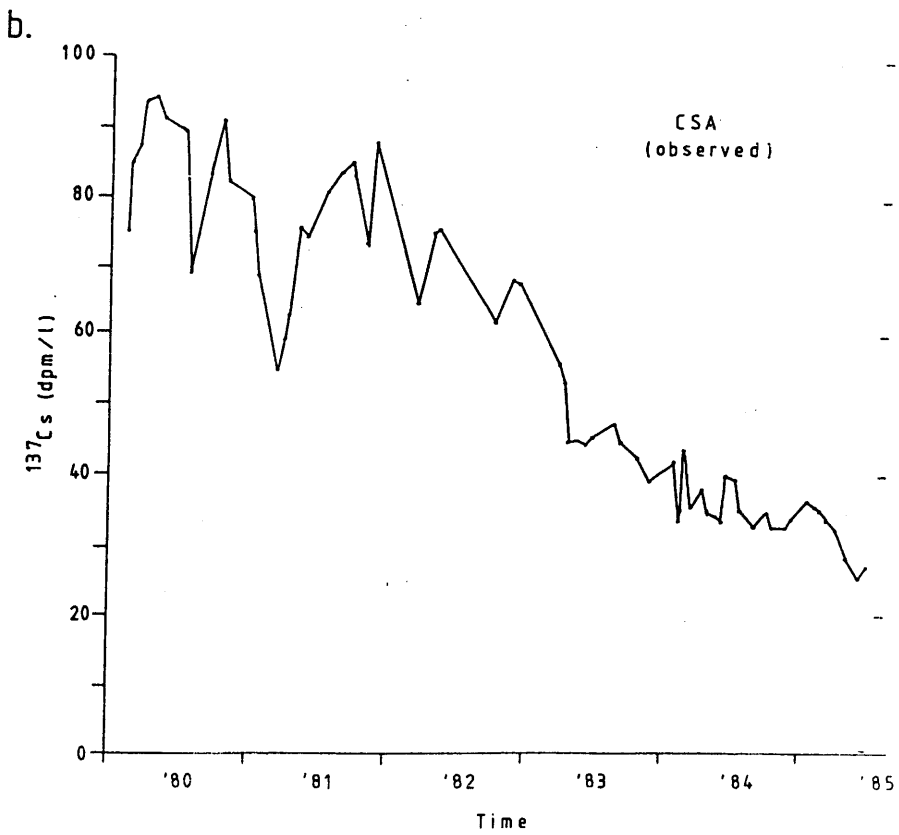
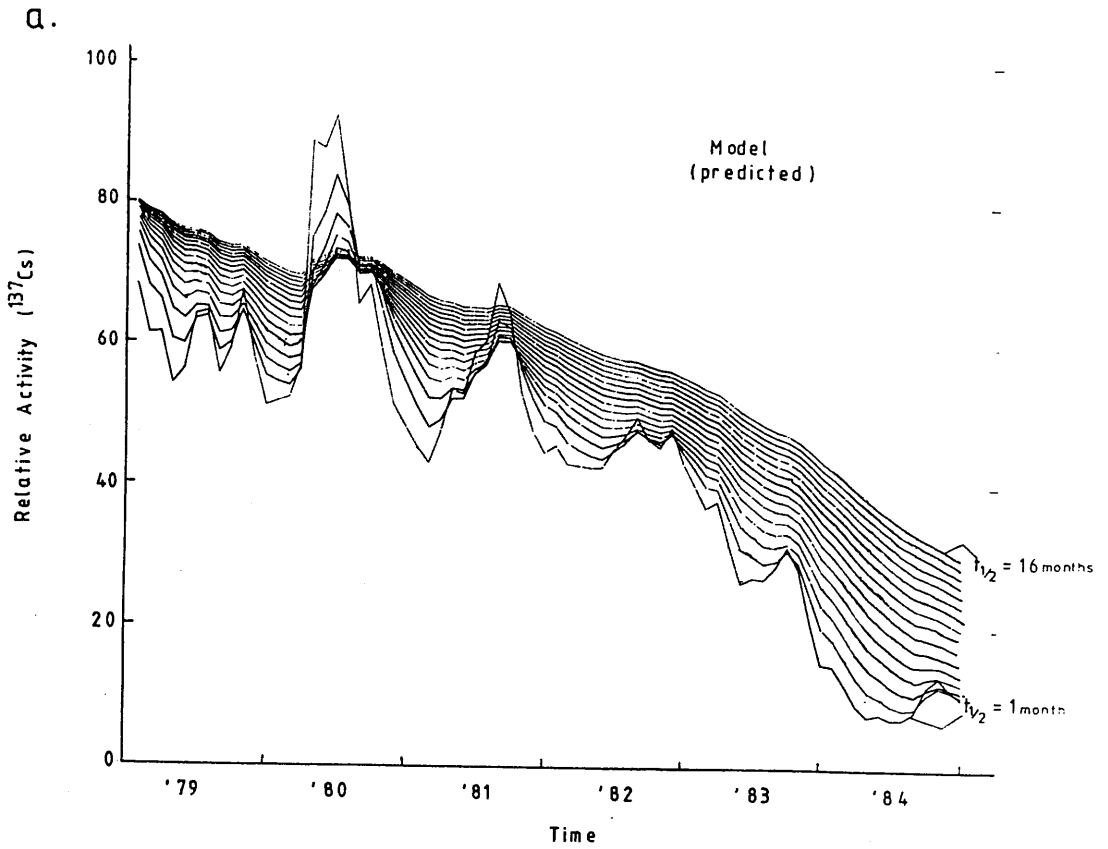
The programme (Appendix VI) was run for 16 values of t_{1/2}, from 1 to 16 months. Monthly radiocaesium discharge values (I), kindly provided by BNFL (Atherton, 1982-1986; pers. comm.), were fed sequentially into the equation:

$$C_t = a C_o + (1 - a)I$$

where C_t is the radiocaesium concentration in the CSA (derived from the previous concentration in the box, C_o),

C_o is the previous concentration in the box,

Figure 3.2

CSA (b) and Modelled (a) ^{137}Cs Curves

and a is the fraction of the box volume remaining in the box each month, i.e.

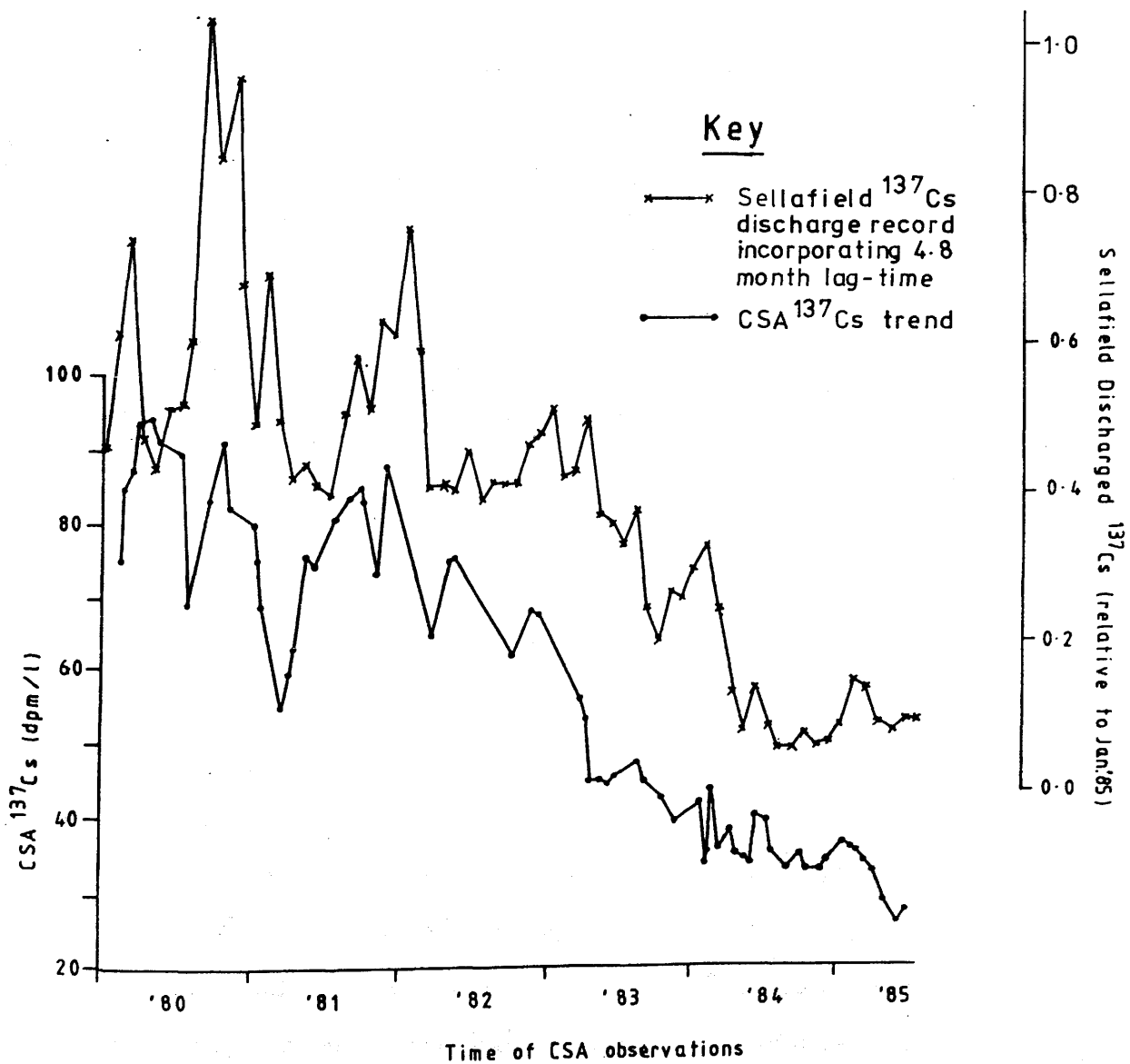
$$a = e^{(-0.693 / t_{1/2})}$$

When attempting to match the CSA ^{137}Cs trend for this period with the modelled curves, the latter were found to have been smoothed so much that, after 1981, virtually no peaks were discernible for any curve corresponding to $t_{1/2} > 5$ months (see Figure 3.2). It was, in fact, found that the CSA ^{137}Cs trend could be more satisfactorily matched with the actual Sellafield ^{137}Cs discharge record, giving a 4.8 (+/- 0.3) months lag-time, i.e. without the use of the model - see Figure 3.3. At first, the unsuitability of the modelled curves appears to imply that water residence in the Irish Sea / North Channel system should be ignored for this period of study. However, the match with the Sellafield record, as discussed below, is imperfect; thus, a 100% advection / 0% residence model is inadequate and some degree of residence / mixing is required. An explanation, therefore, which does not conflict greatly with previous ideas of water residence in the Irish Sea and is also consistent with the complete data set here is as follows.

The model assumes "instantaneous" (within one month of discharge) and complete mixing of newly discharged radiocaesium within the Irish Sea / North Channel "box". However, in practice, there is incomplete mixing, i.e. not all of the discharge is immediately and uniformly mixed with surrounding waters. Coupled with the role of advection within the Irish Sea / CSA system (which, it has been suggested, has increased since 1977), this homogeneity could cause "a fraction" of

Figure 3.3

Matching of Sellafield ^{137}Cs Discharge Record with CSA ^{137}Cs Trend



the Sellafield discharge (probably in surface waters) to reach the CSA, having escaped extensive dilution.

From the salinity and ^{137}Cs contours obtained from cruises and outlined in Chapter 4, the existence of a relatively concentrated plume of radiocaesium travelling along the coast in the northern Irish Sea and into the east side of the North Channel (i.e. approaching the entrance to the CSA) and surrounded by lower radiocaesium, more saline waters, is strongly suggested (see, especially, Figures 4.2.a,2,3, 4.2.e,2,3, and 4.2.f,2,3). Figure 4.4.5 in Chapter 4 is a 3-dimensional representation of the radiocaesium plume in the North Channel (for the June/July 1984 cruise) and clearly shows a surface layer of high radiocaesium activity on the east side of the North Channel curling around the Mull of Kintyre to enter the CSA. Vertical profiles of radiocaesium and salinity across transect Z, shown in Figures 4.4.11-13 (Chapter 4), also clearly show high radiocaesium levels confined to the eastern surface layers of the North Channel. From Figures 4.4.4,10 the vertical radiocaesium sections through the northern Irish Sea transects show isolation of the plume (less pronounced for June/July 1984 and at shallow stations) to surface waters.

This evidence, then, supports the concept that a plume of primarily surface water travels, with some of the Sellafield discharge, from Sellafield to the CSA with relatively little mixing "en route", whilst water nearby, also reaching the CSA, is comparatively well mixed. Therefore, typical CSA water samples do not contain only "recently" released, relatively undiluted, Sellafield discharge nor can residence of water in the Irish Sea be ignored. The ^{137}Cs observed in a CSA sample is most probably a mixture of "old", well-mixed waters of various past discharges and some "new", relatively "unmixed", waters of recent discharge. As explained below,

the sudden, sharp drop in discharges after October 1983 was not observed in the CSA 4.8 months later and this fact is attributed to water residence during transit between Sellafield and the CSA. This water residence must control the overall decrease observed in the CSA radiocaesium levels after April 1984 since the latter is not a result of continued decreasing Sellafield discharges (these had, in fact, levelled out (see Figure 3.3)). This gradual decrease in CSA levels is reproduced by the modelled curve; however, the history of the Sellafield discharges after October 1983 has been fairly well preserved in the CSA record, indicating that some recently discharged material reaches the CSA having avoided mixing with older waters. The latter, being of much higher (>2 times) activities would have "swamped" the newer, lower discharges had extensive / complete mixing occurred (as the model assumes). Hence, the model does not take into account the fraction of unmixed Sellafield discharge which results in a more detailed pattern being superimposed on the "basic" trend - determined by the well-mixed, older waters. Thus the model, in effect, underestimates the fraction of recent discharge and overestimates the fraction of older discharge reaching the CSA (since, in practice, some recent discharge arrives in the CSA mixed with older waters and some arrives relatively concentrated, i.e. not well mixed; therefore the total inventory arriving is more than expected if, as the model assumes, it were all mixed).

In a situation of increasing discharge levels, the model will recognise an increase in levels reaching the CSA and, although it may underestimate this increase, the underestimation may not be obvious / detected. When discharge levels are sharply decreasing, however, the model will "smooth out" the decrease and may not acknowledge any relatively small fluctuations in discharge levels immediately

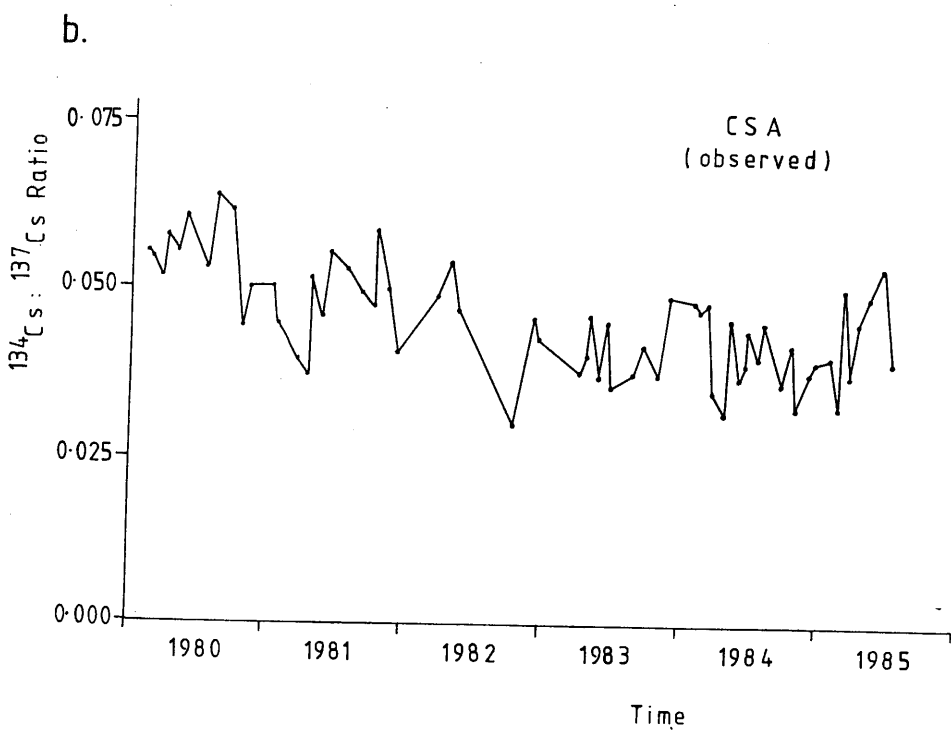
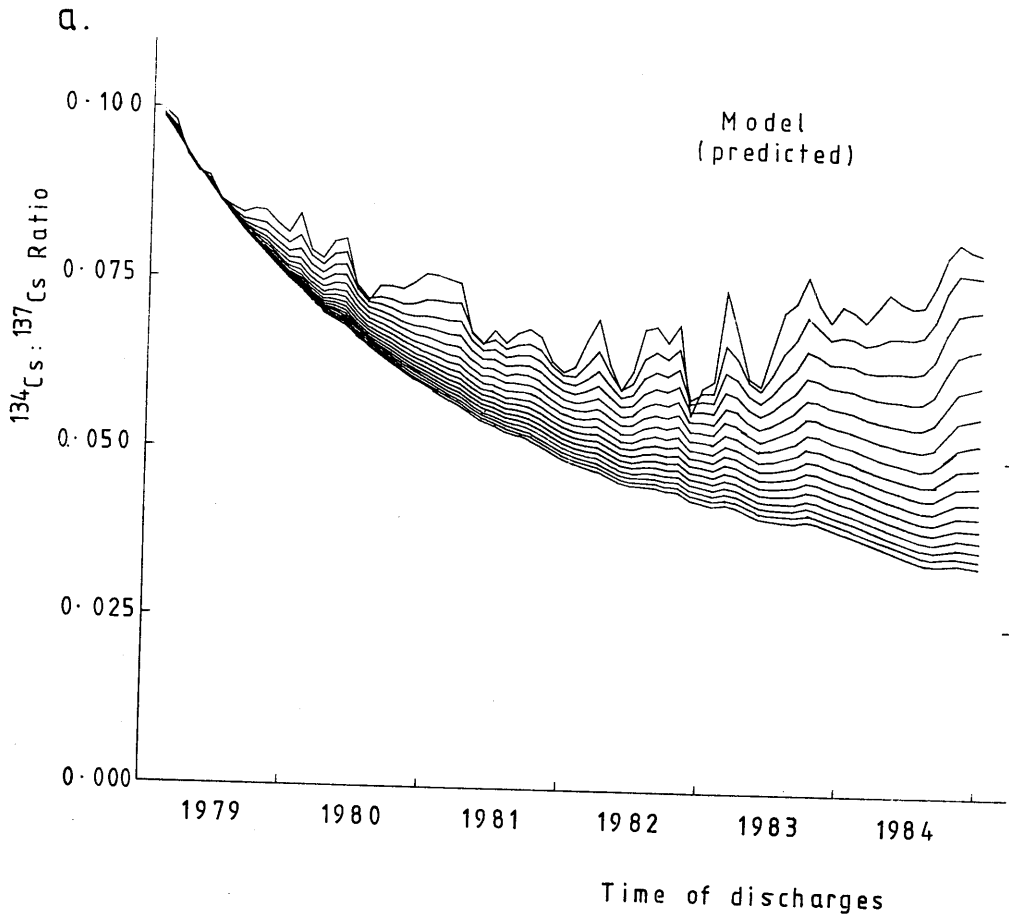
following the sharp decrease; this is because the activity levels in the fraction of the recent discharge which it assumes to reach the CSA may not be sufficiently high to be detected above the relatively high levels from the older discharge.

Effectively, the single-box system can be considered as two boxes - one involving thorough mixing and the other (mostly surface waters) involving comparatively low mixing and possibly faster advection (being affected more by wind stress than are deeper waters). In this case, the two boxes must be treated individually to obtain estimates of residence times, since the rate of decay of a single box comprising two different component boxes, each with a different residence time, is not exponential; thus a true "overall" / "net" residence time cannot be found for the large, single box. However, for the purposes of this study, if the model is assumed to simulate either the "surface" box or the single, large box then matching of the modelled $^{134}\text{Cs}:$ ^{137}Cs ratio curves with the observed CSA $^{134}\text{Cs}:$ ^{137}Cs ratio curve (Figure 3.4) provides a 10 month $t_{1/2}$ value (14.4 months residence time) for either the surface waters / box or the total northern Irish Sea / North Channel system. In the latter case, errors arise as a result of assumptions inherent in the model as already discussed, whilst, in the former case, errors arise from variation (with time) of the "surface box" volume and, again, from overestimation of the extent of mixing within the box. A mean decay-time between the discharged and observed ratios for the period 1983-1985 is about 17 months, thus providing a guide to the maximum limit of residence time involved in this coastal system.

Lack of time and of the necessary information on box volume and exchange parameters have prevented remodelling (using two boxes) of the Irish Sea / North Channel system during this study but it is

Figure 3.4

CSA (b) and Modelled (a) $^{134}\text{Cs} : ^{137}\text{Cs}$
Ratio Trends



suggested for further work in this field. In such a model, the boxes should, at first, be treated individually to obtain mixing times. There is undoubtedly some interaction between the two "boxes" and the extent of this interaction almost certainly varies with time, as does the ratio of the box volumes. Thus, with regard to the relationship between the boxes, a future model should accommodate ranges of box volumes, ratios of box volumes and degrees of interaction between boxes. The predicted curves produced by this model could then be matched with observed data. CSA waters may recently have arisen mostly from surface, relatively unmixed Irish Sea / North Channel waters and therefore its radionuclide levels and trends may be largely dependent on this box.

The transit time found in this study, then, is slightly longer than that estimated by McKay and Baxter (1985a) for the period 1978 - 1981, indicating slightly slower net transit from Sellafield to the CSA during more recent years. The lag-time of 4.8 months from Sellafield to the CSA can be used to derive an average net transport rate of 1.71 km day⁻¹ over this 250 km distance, a value which compares with McKay and Baxter (1985a)'s estimate of 2.1 km day⁻¹ for the preceding period.

The lag-time can also be used to calculate a series of E_a (Environmental Appearance) factor values by dividing each monthly ¹³⁷Cs level measured in the CSA by the corresponding (i.e. 4.8 months earlier) monthly discharge from Sellafield. This, in effect, normalises the observed CSA radiocaesium levels to a common rate of radiocaesium discharge; units are presented as Bq l⁻¹ / TBq day⁻¹. E_a factors for a series of sites can then provide an indication of the extent of dilution occurring during transit between these sites. Values of 0.25 and 0.19 Bq l⁻¹ / TBq day⁻¹ were calculated by

McKinley et al. (1981a) (for the North Channel, 1973 - 1976) and by McKay and Baxter (1985a) (for the CSA, 1978 - 1981) respectively. By comparison with a MAFF-based E_a value of $5 \text{ Bq l}^{-1} / \text{TBq day}^{-1}$ for water close to the discharge pipeline in 1978, estimated dilutions of the water between the discharge pipeline and i) the North Channel and ii) the CSA were found to be $\times 20$ and $\times 26$ respectively.

E_a values can be used to predict radioactivity levels reaching densely populated areas (such as the CSA) as a result of accidental or planned discharges. Their use can also be applied to releases and dispersion of other soluble pollutants, e.g. trace metals.

The full set of E_a values obtained during this study for the range of possible transit times, 4.5 - 5.1 months, is presented in Appendix III.1, whilst the values corresponding to a transit time of 4.8 months are presented in Table 3.1. From the latter, it can be seen that there is a large variation in E_a values throughout the 1982-1985 period, ranging from ~ 0.13 for the November 1982 discharge to ~ 0.77 for the March 1984 discharge. The mean for the November 1981 to October 1983 discharge period, however, is $0.191 (+/- 0.036) \text{ Bq l}^{-1} / \text{TBq day}^{-1}$, in excellent agreement with that found by McKay and Baxter (1985a) for 1978-1981. The values increase noticeably after the discharge of November 1983 (the month of a $> 50\%$ decrease in discharges), the mean E_a values corresponding to $0.193 (+/- 0.038)$ and $0.554 (+/- 0.133) \text{ Bq l}^{-1} / \text{TBq dy}^{-1}$ for the 10 months before and after the November 1983 discharge respectively. This transition would appear to reflect the coincidental, significant drop in discharges, i.e. for the 10 months before and after November 1983 the average discharges were $3.68 (+/- 0.69)$ and $1.11 (+/- 0.34) \text{ TBq day}^{-1}$ respectively. The sharp decrease in discharges, then, had not been immediately reflected in CSA levels and artificially generated an

Table 3.1

Environmental Appearance (Ea) Factors for the CSA -
 Corresponding to a Transit Time of 4.8 months -
 and Discharges, 1982 - 1984

Month of Discharge	Discharge (TBq day ⁻¹)	Ea (Bq l ⁻¹ /TBq day ⁻¹)
<u>1982</u>	Oct.	5.290
	Nov.	6.300
	Dec.	4.581
<u>1983</u>	Jan.	4.419
	Feb.	4.464
	Mar.	4.645
	Apr.	3.153
	May	2.516
	Jun.	3.467
	Jul.	3.197
	Aug.	3.639
	Sep.	4.240
	Oct.	3.055
	Nov.	1.720
	Dec.	1.068
<u>1984</u>	Jan.	1.726
	Feb.	1.197
	Mar.	0.755
	Apr.	0.753
	May	1.000
	Jun.	0.830
	Jul.	0.877
	Aug.	1.126
	Sep.	1.907
	Oct.	1.748
	Nov.	1.217
	Dec.	1.077

increased E_a value because CSA radiocaesium levels - largely due to earlier, higher releases - were normalised with respect to the new, "low" discharges from Sellafield. These results, therefore, indicate the major importance of water "residence" before the water has reached the CSA.

From the data in Table 3.1, it would appear that, after the March 1984 discharge, although radiocaesium levels in the CSA were generally decreasing, the E_a had not settled down to its "pre-November 1983" value, even by December 1984.

If the same E_a value used by McKinley et al. (1981b) and McKay and Baxter (1985a) for waters in the vicinity of the pipeline is used to compare with the post-November 1983 CSA values, then dilutions of as little as $\times 6.4$ would be obtained (March 1984 discharge)! It seems unlikely that the dilution rate would actually change so markedly and exactly in coincidence with the sharp decrease in radiocaesium discharges. It appears, then, that the E_a value for waters close to the pipeline may need revision. For this purpose, data on ^{137}Cs concentrations during January 1980 to December 1985 at a site close to the pipeline were kindly provided by Jefferies (1986, pers. comm.).

If the residence time of water near the discharge point was relatively long, then radiocaesium levels there would not change markedly since any changes in inputs would be dampened and the E_a values would vary inversely with discharge. However, if there is little water residence and mixing occurs further along the plume's path then the radiocaesium levels near the discharge point would vary with the discharges and this, in turn, would result in more or less constant E_a values close to the pipeline. Thus, variation of E_a 's with time, close to the pipeline, provides an indication of water residence time in that sector of the Irish Sea.

Table 3.2

Environmental Appearance (Ea) Factors for Seascale
 obtained by averaging of 2 months' discharges
 (see text) 1982 - 1984 ($\text{Bq l}^{-1}/\text{TBq day}^{-1}$).

	<u>Month of Discharge</u>	<u>Seascale Ea</u>
<u>1982</u>	Oct.	2.165
	Nov.	1.054
	Dec.	1.912
<u>1983</u>	Jan.	3.044
	Feb.	4.481
	Mar.	2.854
	Apr.	4.847
	May	3.345
	Jun.	3.577
	Jul.	4.232
	Aug.	2.894
	Sep.	3.046
	Oct.	2.588
	Nov.	6.492
	Dec.	5.316
<u>1984</u>	Jan.	2.999
	Feb.	3.319
	Mar.	5.840
	Apr.	11.300
	May	7.096
	Jun.	5.301
	Jul.	5.343
	Aug.	6.990
	Sep.	3.587
	Oct.	3.163
	Nov.	3.170
	Dec.	2.180

Table 3.2 presents the E_a values for Seascale (the near-Sellafield site), calculated by dividing the observed ^{137}Cs level by the mean discharge rate of the month of sampling and the previous month, as performed, for earlier data, by Jefferies et al. (1982). Generally, there seems to be considerable variability in the resultant data but an increase can be recognised from the November 1983 discharge onwards, peaking around March / April 1984 discharge. This pattern is indeed similar to that observed in the CSA and indicates the need for "regular" revision of the near-Sellafield E_a value.

Table 3.3 shows the dilution factors between Seascale and the CSA for each month, calculated by dividing the CSA E_a value by the corresponding Seascale E_a value for the same month of discharge. For the 13 months prior to, and 14 months following, the November 1983 discharge, mean dilution factors of 18.8 ± 6.0 and 10.4 ± 2.4 respectively are derived. The decrease in dilution evident after the November 1983 discharge, then, is a result of the increase (1.72 times) in the Seascale E_a being less than that (2.87 times) in the CSA E_a and reflects the longer water residence time inherent in the CSA. However, from these increases in E_a values, it appears that ~60% of the water mixing / residence for waters reaching the CSA had occurred off the Cumbrian coast. Because of the greater variability in E_a values (at both sites) after, relative to before, the November 1983 discharge (see Tables 3.1 and 3.2), it is not clearly defined whether the Seascale value may have returned to its "more usual / pre-November 1983" level sooner than the CSA E_a .

The above estimates of dilution of radiocaesium in the water column (~19) between Sellafield and the CSA compare well with those found in seaweeds (16-23), also between Sellafield and the Clyde Estuary (see Table 5.13, Chapter 5).

Table 3.3

Environmental Appearance (Ea) Factors for Loch Etive -
Corresponding to a Transit Time from Sellafield
of 6.4 months.

	<u>Month of Discharge</u>	<u>Ea (Bq l⁻¹/TBq day⁻¹)</u>
<u>1982</u>	Oct.	0.079
	Nov.	0.060
	Dec.	N.D.
<u>1983</u>	Jan.	0.092
	Feb.	0.110
	Mar.	0.104
	Apr.	N.D.
	May	0.167
	Jun.	0.092
	Jul.	N.D.
	Aug.	0.070
	Sept.	0.060
	Oct.	N.D.
	Nov.	N.D.
	Dec.	0.265
<u>1984</u>	Jan.	N.D.
	Feb.	N.D.

N.D = No data available for this month.

From the mean CSA outflow rate of 1.87×10^{12} l day⁻¹ estimated by McKinley et al. (1981b) and the E_a for the period 1982-1983, 35.7 (+/- 7.5) % of Sellafield's radiocaesium output is estimated to have passed through the CSA during this time. However, by assuming a more recent 2 month residence time of CSA water (Edwards, 1986; pers. comm.) instead of 3 months (as in McKinley et al.'s estimate), a mean outflow rate of 2.75×10^{12} l day⁻¹ is obtained which implies that ~53% of Sellafield's discharged radiocaesium passed through the CSA during the period 1982-1983. The available data do not allow a more precise estimate of the residence time ("t") for CSA water since McKinley et al. (1981b)'s estimate of residence half-time, $t_{1/2}$ - from matching radiocaesium time-trends in the North Channel and the CSA - was 2 (+/- 1) months (i.e. $t = 2.9$ (+/- 1.45) months) and the estimate by Edwards - obtained by comparison of the volume of fresh water in the surface waters to the known fresh water input rate - was $t = 2$ (+/- 0.5) months. Since the water residence time in the Irish Sea is believed to have fluctuated with time, this might also apply to the CSA; hence it is appropriate here to consider a range of values (i.e. 30-55%) for the percentage of Sellafield radiocaesium estimated to pass through the CSA.

As already described, the U.K. collective dose resulting from Sellafield discharges is mainly derived from radiocaesium in consumed fish and it is believed that approximately half of this U.K. dose is delivered to the Scottish population (section 1.3, Chapter 1). Of the latter, about half (~ 3×10^6 people) live in areas around the CSA where radiocaesium levels in water and fish are relatively high. This group of people, then, is the largest encountered by these relatively undiluted radiocaesium waters and receives ~40% of the total U.K. dose from fish and shellfish consumption, i.e. the mean individual dose to

a member of the CSA population is ~ 10 times that within the U.K. as a whole, that is $\sim 13 \mu\text{Sv year}^{-1}$ (see section 1.3, Chapter 1). However, this dose to individuals is negligible relative to the $2000 \mu\text{Sv year}^{-1}$ received in the U.K. from natural background radiation.

3.2 Loch Etive

By similarly matching radiocaesium time-trends between the CSA and Loch Etive, McKay and Baxter (1985a) found a ~ 2 month lag-time during the January 1980 to February 1982 period. The total lag-time from Sellafield to Loch Etive was thus estimated to be ~ 6 months. For the 1981-1984 period, a $1.0 (+/- 1.0)$ month lag-time between the CSA and Loch Etive has been derived here by matching the two radiocaesium time-trends as shown in Figure 3.5. This in turn suggests an overall lag-time and a net transport rate of radiocaesium, from Sellafield to Loch Etive, of $6.4 (+/- 0.7)$ months and $\sim 2 \text{ km day}^{-1}$ respectively, i.e. in excellent agreement with the previous estimates.

The E_a values obtained for Loch Etive (Table 3.3; see Appendix III.2 for E_a 's corresponding to range of lag times) indicate an approximate two-fold ($\times 2.04 +/- 0.38$) dilution in radiocaesium levels from the CSA to Loch Etive, i.e. the Loch Etive E_a values are approximately half those of the CSA (see Table 3.4); hence the overall dilution factor from Seascale is ~ 34 .

From the approximate net daily outflow of Loch Etive of $5.6 \times 10^{10} \text{ l}$ (McKay and Baxter, 1985a) and the mean E_a value, $0.099 \text{ Bq l}^{-1} / \text{TBq day}^{-1}$, for this area before the November 1983 discharge, $< 0.6\%$ of Sellafield's discharged radiocaesium is estimated to have passed through Loch Etive.

Figure 3.5

Matching of CSA and Loch Etive ¹³⁷Cs Records

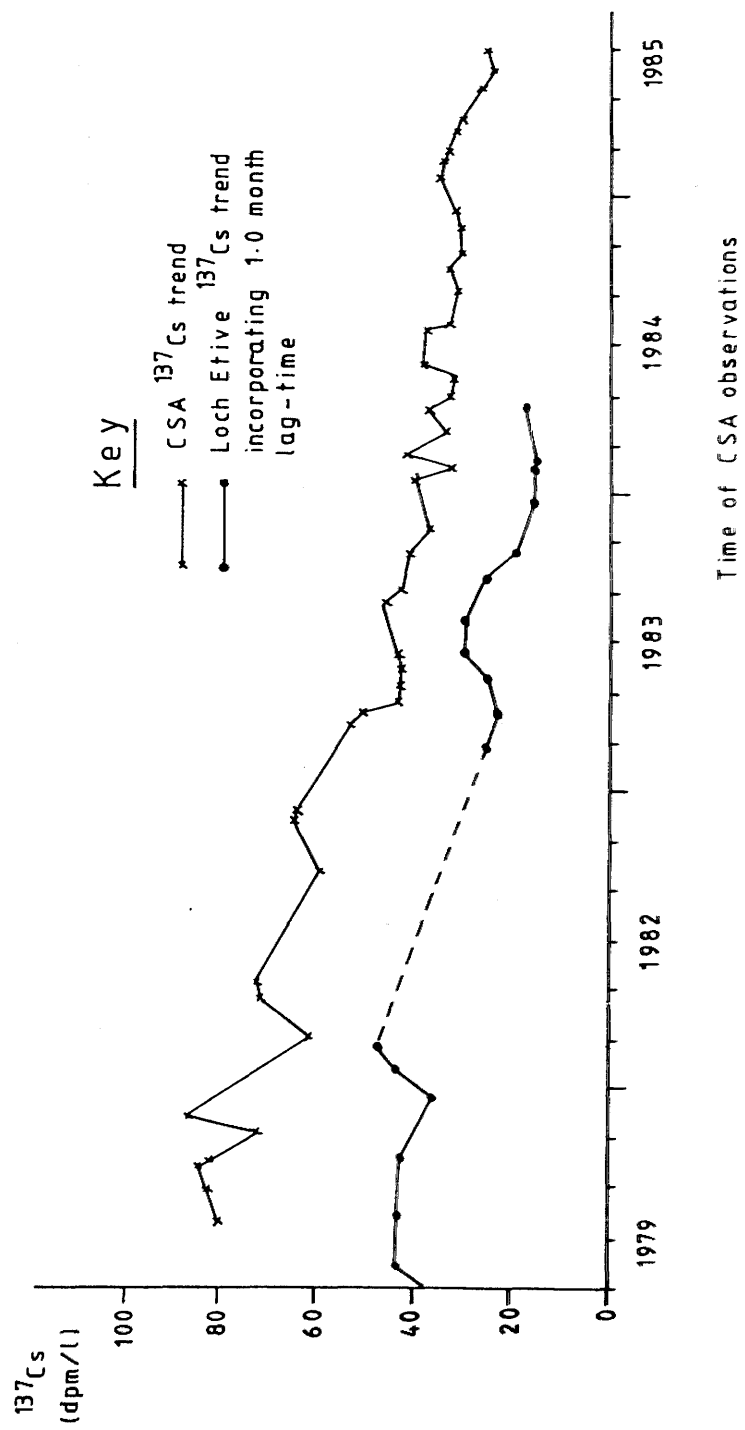


Table 3.4

Dilution Factors of CSA and Loch Etive Radiocaesium Levels
from Corresponding Seascale Levels (1982 - 1984 Discharges)

	Month of Discharge	CSA Dilution Factor	Loch Etive Dilution Factor
<u>1982</u>	Oct.	9.5	20.4
	Nov.	11.5	24.7
	Dec.	15.3	N.D.
<u>1983</u>	Jan.	22.8	40.9
	Feb.	22.4	33.3
	Mar.	23.2	37.0
	Apr.	31.9	N.D.
	May	11.0	18.7
	Jun.	20.8	42.4
	Jul.	17.9	N.D.
	Aug.	15.8	42.4
	Sep.	18.7	47.0
	Oct.	23.7	N.D.
	Nov.	16.6	N.D.
	Dec.	7.7	15.7
<u>1984</u>	Jan.	9.5	N.D.
	Feb.	8.8	N.D.
	Mar.	11.0	N.D.
	Apr.	12.9	N.D.
	May	11.5	N.D.
	Jun.	8.3	N.D.
	Jul.	10.1	N.D.
	Aug.	10.3	N.D.
	Sept.	11.2	N.D.
	Oct.	10.1	N.D.
	Nov.	6.3	N.D.
	Dec.	10.7	N.D.

N.D. = No data available for this month.

3.3 Summary and Conclusions

Transit times required for near-Sellafield waters to reach the CSA (for the period 1982-1985) and Loch Etive (for the period 1982-1984) have been found to be 4.8 (+/- 0.3) and 6.4 (+/- 0.7) months respectively; these values were obtained by matching radiocaesium levels (~monthly) at the destination sites with the (monthly) Sellafield radiocaesium discharge record. These results indicate generally slightly longer timescales than those reported previously (i.e. 4 and 6 months to the CSA and Loch Etive respectively for the period 1980 - 1982 and 8 months' residence time in the Irish Sea (McKay and Baxter, 1985a)).

From the above transit times, mean transport velocities from Sellafield to the CSA and Loch Etive were ~1.7 and 2.0 km day⁻¹ respectively during 1982 -1985.

Table 3.5 summarises transit times from Sellafield to the North Channel or CSA and residence times within the Irish Sea estimated since 1974. These data show that, since 1977, the shorter residence time in the Irish Sea and shorter transit time from Sellafield to the CSA have been maintained. Prandle (1984) also noted the change after 1977 but the cause is uncertain.

It is suggested that a fraction of the Sellafield discharge escapes extensive mixing before reaching the CSA, via surface waters, thus, preserving, to some extent, the details of the radiocaesium discharge history in the CSA radiocaesium record. This means that the one-box model overestimates the role of mixing in the Irish Sea, i.e. it assumes instantaneous (<1 month) complete mixing of all the water in the area. Reduced residence in the Irish Sea / CSA system and a shorter Sellafield - CSA transit time since 1977 could have

Table 3.5

Summary of Estimated Transit Times from Sellafield to the
CSA/North Channel and Residence Times within the Irish Sea

Period of Study	Transit Time (months)	Period of Study	Residence Time (months)	Authors
1971 - 1972	13 - 22 ^a			Jefferies et al. (1973)
1972 - 1973	12 ^a	1970 - 1976	12	Jefferies et al. (1982)
1974 - 1978	<12 ^a	after 1976	<12	
1974 - 1977	6 ^a	1974 - 1977	17	McKinley et al. (1981a)
1974 - 1977	8 ^b	1974 - 1977	20 ^c	
1978 - 1981	4 ^b	1978 - 1981	12 ^c	McKay et al. (1985)
1982 - 1985	4.8 ^b	1982 - 1985	14.4 ^c	Present study

^a Transit Time from Sellafield to North Channel

^b Transit Time from Sellafield to CSA

^c Residence Time in "mixing box", i.e. northern Irish Sea / CSA system

accentuated this condition, thus rendering it more apparent. However, it is more probable that the situation has been revealed as a result of the recently, much lowered discharge levels. An estimated $t_{1/2}$ value of 10 months (residence time of 14.4 months) is obtained by matching the model's predicted ratios with those observed in the CSA. However, a maximum limit for decay-time between discharge and CSA ratios has been estimated as 17 months.

Radiocaesium levels close to the discharge point, prior to the November 1983 discharge, were found to have been diluted ~ 19 and ~ 34 times on reaching the CSA and Loch Etive respectively. After the sharp drop in discharges in November 1983, dilution factors appeared to decrease due to delay in appearance of the lower activities in the CSA and Loch Etive. Ea (Environmental Appearance) values were used to calculate these dilution factors. Water residence which delayed the appearance - in the CSA and Loch Etive - of the November 1983 decrease in discharges largely ($\sim 50 - 60\%$) occurred close to the Cumbrian coast. Hence, the trend in Ea values emphasises the importance of water residence in the northern Irish Sea.

Assuming a residence time for CSA water of 2-3 months, 30-55% of the Sellafield-discharged radiocaesium is estimated to have passed through the CSA at concentrations ~ 20 times diluted relative to levels near the discharge point. In radiological protection terms this indicates that, although the U.K. collective dose when averaged for the dose per person is negligible, proportionally higher (~ 10 times) doses are delivered to locals living around the CSA than to the average member of the U.K. public elsewhere.

CHAPTER 4

Hebridean Sea Area

4.1 Introduction

There are two methods of approach towards establishing the transport paths of the Sellafield radiocaesium source-water and the temporal trends in the physical processes affecting radiocaesium distributions and water movements. They are Lagrangian (following the path of a packet of water in space and time, e.g. dye-tracer or drogoue experiments) and Eulerian (observing the temporal trend of a particular parameter at one point in space, e.g. current meter records or continual or frequent and regular monitoring of a parameter at a particular station). Both types of approach are used in this project in an attempt to unravel, to some degree, a very complex picture of four dimensions - three spatial and temporal.

First, spatial distributions of radiocaesium and salinity have been studied, this being analogous to dye-tracer experiments with radiocaesium representing the "dye". Because of the extensive amount of data collected from the 8 research cruises, the results from individual cruises will be examined in the following subdivisions of section 4.2:

- a) May 1983;
- b) August 1983;
- c) January 1984;

- d) April / May 1984;
- e) June / July 1984;
- f) November 1984;
- g) February 1985;
- h) May 1982.

The circulation patterns observed during each cruise are described and similarities between cruises noted. The station positions occupied during the May 1982 cruise were different from those for all the subsequent cruises and hence direct comparisons of values at specific stations has not been possible. Subsurface samples for radiocaesium analyses were only collected where specified and CTD profiles were taken at every station unless otherwise stated. Section 4.3 presents an overall picture of the variations in circulation and radionuclide dispersion patterns with time by considering simultaneously the results from all cruises presented in section 4.2. Thus it employs the Eulerian approach in monitoring radiocaesium trends at single points through time. Section 4.4 deals with all the deep water ^{137}Cs samples, whilst section 4.5 provides the summary and conclusions for the entire chapter.

4.2 Research Vessel Cruises

4.2(a) May 1983

i) Results and Discussion

The station grid for this cruise is shown in Figure 4.2.a1 whilst Figures 4.2.a2, 3 present the surface salinity and ^{137}Cs contours

Figure 4.2. a1

Station Positions - May 1983 Cruise.

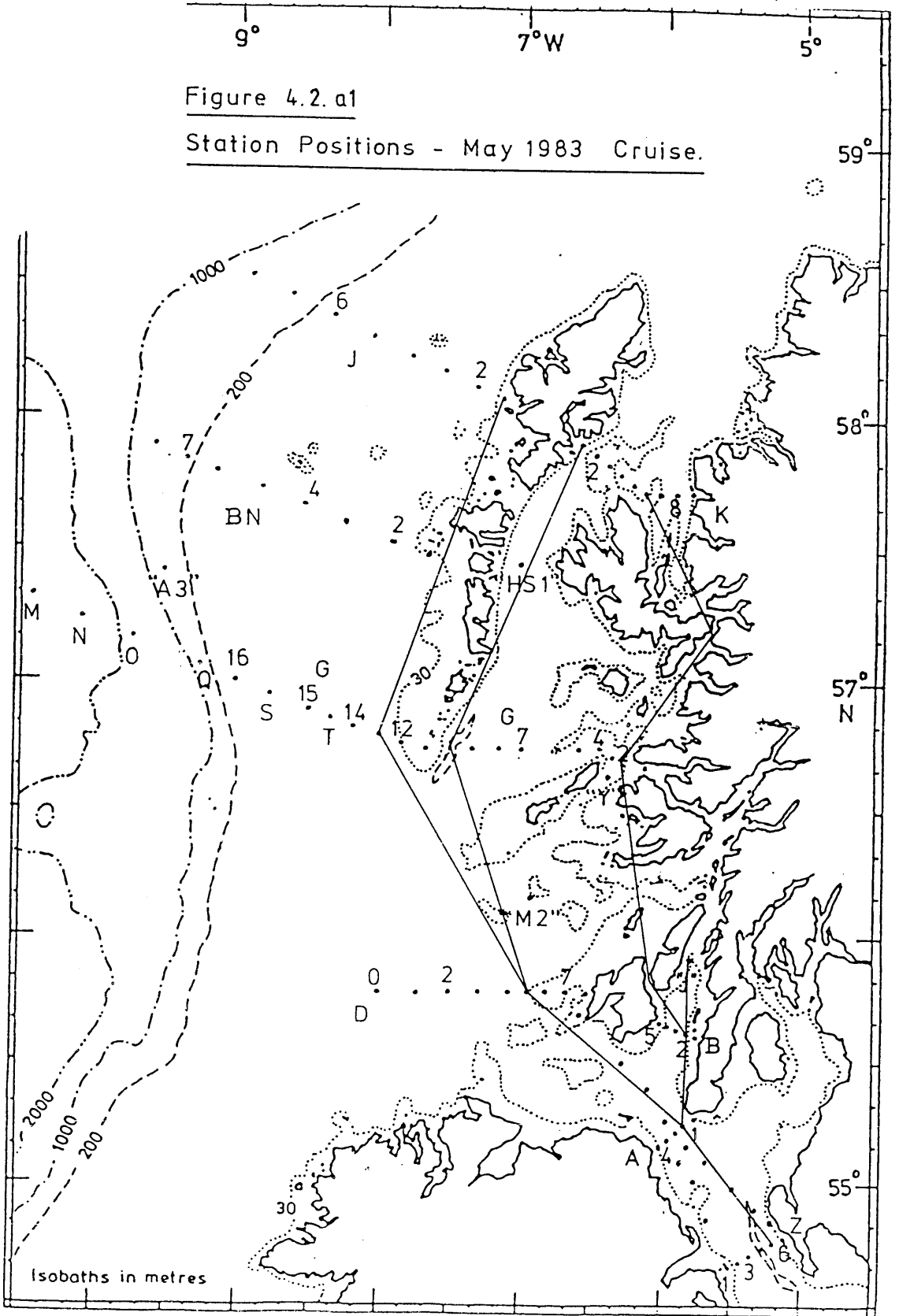


Figure 4.2.a2

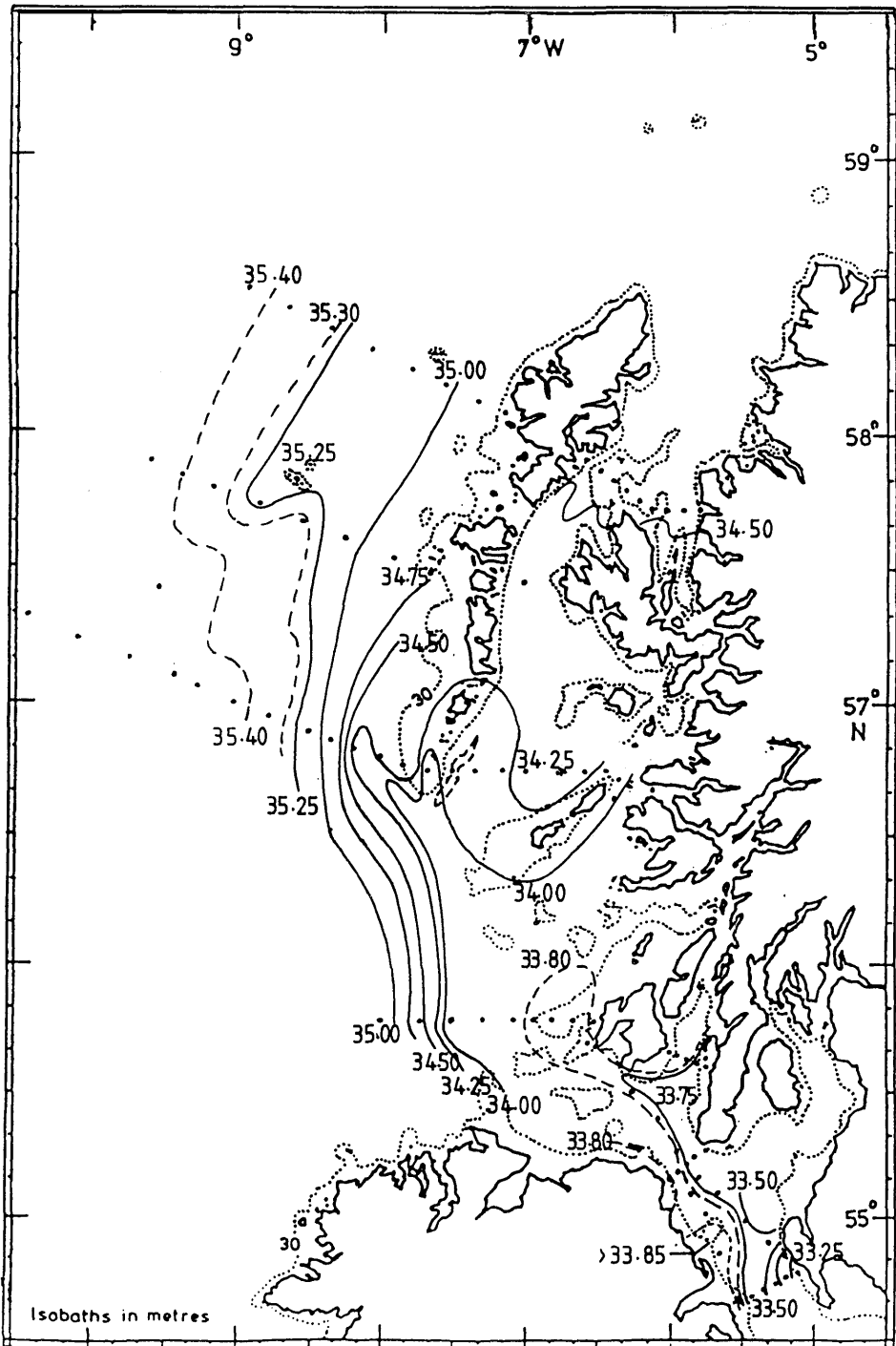
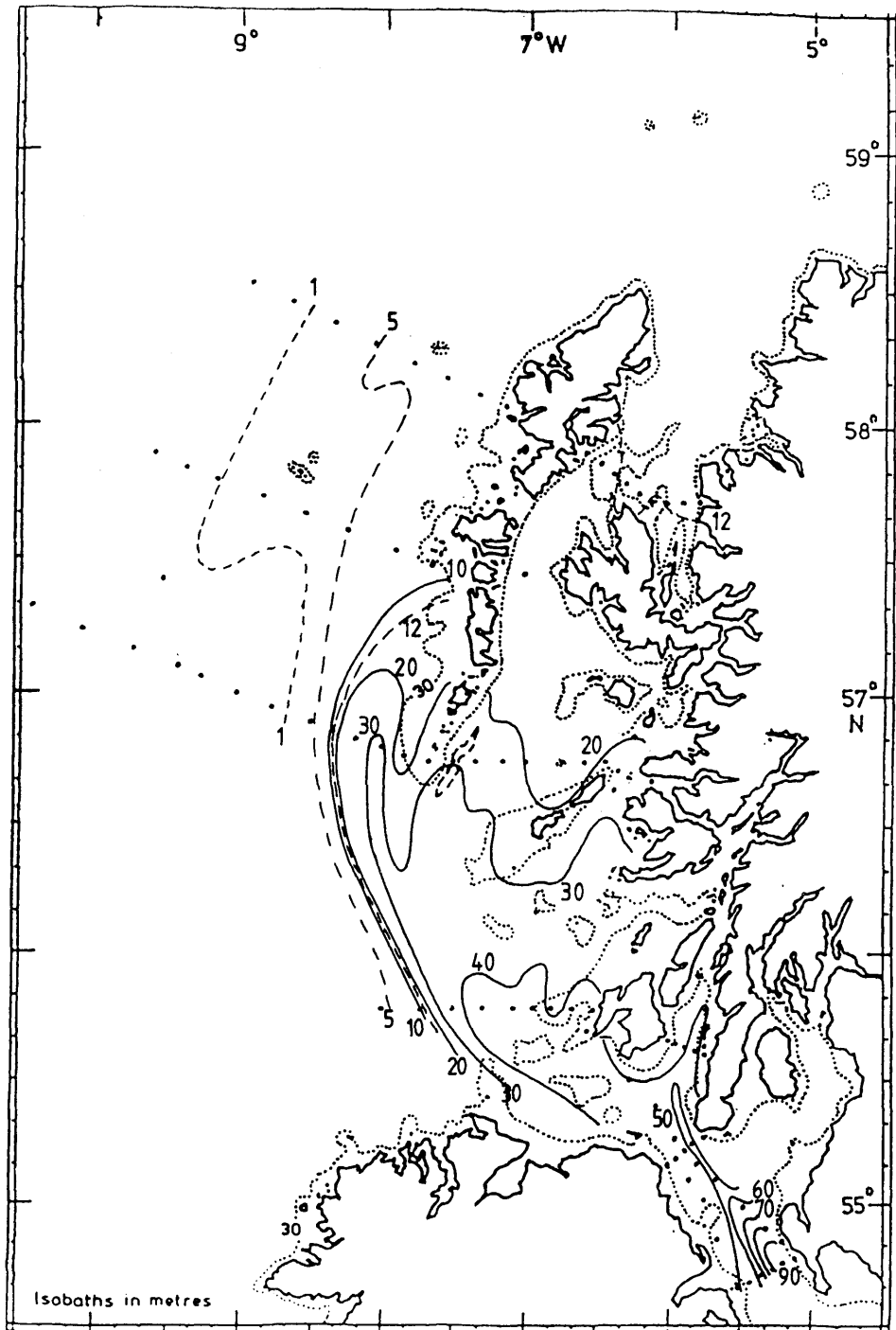
Salinity Contours (‰) - May 1983 Cruise

Figure 4.2. a3

 ^{137}Cs Contours (dpm/l) - May 1983 Cruise

respectively; 57 water samples were analysed for radiocaesium content. From the ^{137}Cs contours, then, levels generally decrease in a northward and westward direction throughout the region of interest, with the highest level (95.7 dpm/l) in the southeastern sector of the North Channel. In the HSA, the westward decline in levels was more rapid than the gradual decrease northward since, to the west, the radiocaesium-rich Irish Sea-derived water encounters low-radiocaesium Atlantic water which dilutes the former with respect to ^{137}Cs . The two water masses meet where the contour lines are close to each other, i.e. where the sharpest change in ^{137}Cs levels occurs; since the mixing processes are not strong enough to achieve homogeneity, a gradient is formed at latitude $55^{\circ}48'\text{N}$ (across transect D) and during this cruise it occurred at $7^{\circ}30' - 8^{\circ}00'\text{W}$. This general pattern of a northward moving radioactive plume of water being diluted during transit by Atlantic water from the west agrees with descriptions by other workers, e.g. Jefferies et al. (1973) - who described the coastal plume as "hugging" the west coast of Scotland - and McKinley et al. (1981a). The corresponding salinity data, (Figure 4.2.a2) complement the ^{137}Cs results similarly showing a marked gradient at about $7^{\circ}30' - 8^{\circ}00'\text{W}$ in the HSA across transect D, where Atlantic water of relatively high salinity ($>35.0\text{‰}$) had mixed with the Irish Sea - derived water of relatively low salinity ($<33.8\text{‰}$).

A more detailed examination of these contours reveals significant dilution of the ^{137}Cs -rich, Irish Sea - derived water during transit through the North Channel. At the southern section - transect Z - of the North Channel the ^{137}Cs levels on the eastern side are twice those on the west whereas across the northern exit - transect A - the levels are more evenly distributed. From south to north of the North Channel, virtually no decrease has occurred along the western side but on the

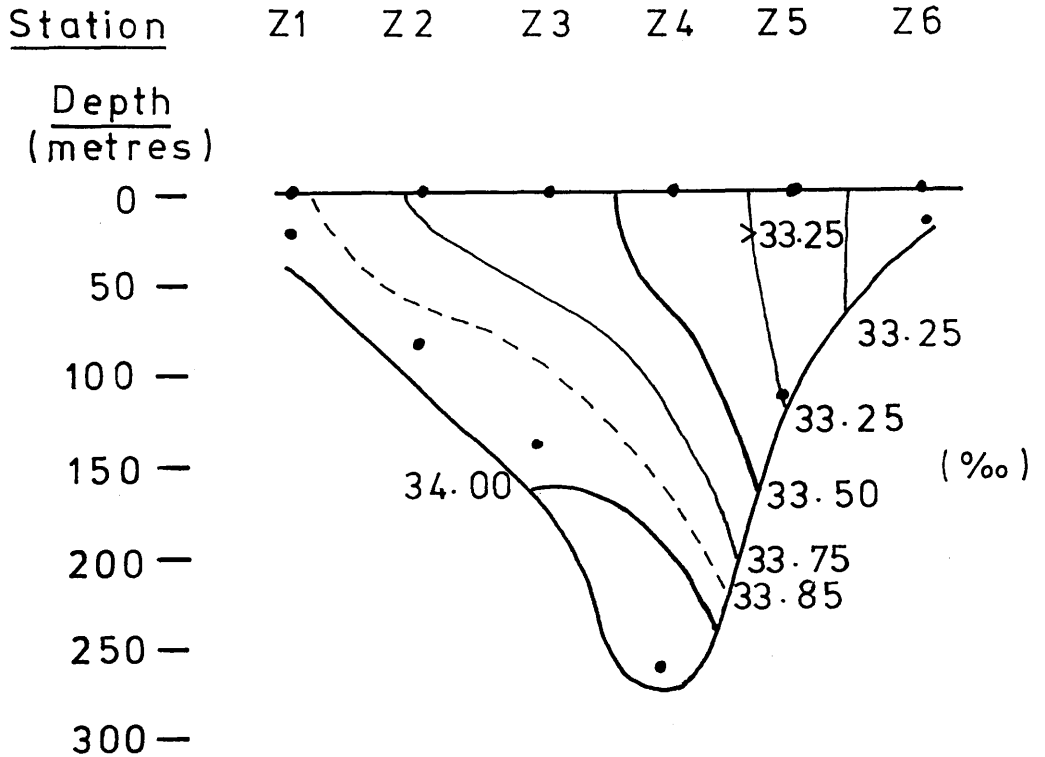
eastern side (i.e. across the entrance of the CSA) a two-fold dilution is observed. Two explanations of the observed pattern in this region are possible at this stage: 1) mixing between relatively low ^{137}Cs content CSA water and high ^{137}Cs content Irish Sea water in the eastern half of the North Channel had diluted the latter during its transit from south to north but the effect of the CSA water had not extended across to the western half of the North Channel, hence a gradient in ^{137}Cs concentration occurred at this latitude or 2) relatively low ^{137}Cs water entering from the north west had diluted the ^{137}Cs concentrations along the west of the North Channel at least as far south as transect Z but had not extended as far south on the eastern side.

By examining the salinity data we find 1) the lowest salinities coincide with the highest ^{137}Cs levels (to the east of transect Z) indicating Irish Sea-derived water here rather than fresh water from the CSA; 2) higher values occur at stations on the western side of the North Channel relative to the eastern side but the fraction of water of highest salinity ($>33.85\%$) occurs between $5^{\circ}30'$ and $5^{\circ}55'$ W south of latitude $55^{\circ}05'$ N. If Irish Sea water was of lower salinity than this, it seems reasonable to assume that this relatively saline water entered the North Channel via the northern exit (transect A). Thus the high salinity, low ^{137}Cs water from the north west had penetrated the North Channel prior to the time of sampling and, at the time of sampling, the net northward movement of the low salinity, high ^{137}Cs Irish Sea water along the eastern side of the North Channel had extended across to the western side at transect A and isolated the high salinity water in the southwestern part of the North Channel. If, however, water in the western half of the Irish Sea was of salinity as high as 33.85% , then this could be the source of the more saline

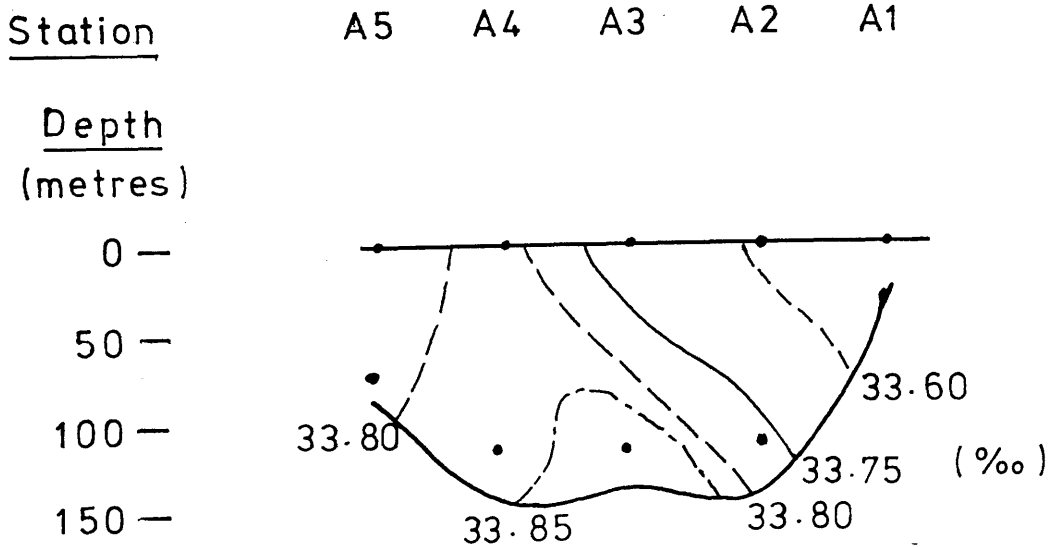
Figure 4.2.a4

Salinity Profile Across(i) Transect Z and (ii) Transect AMay 1983

(i)

Transect Z

(ii)

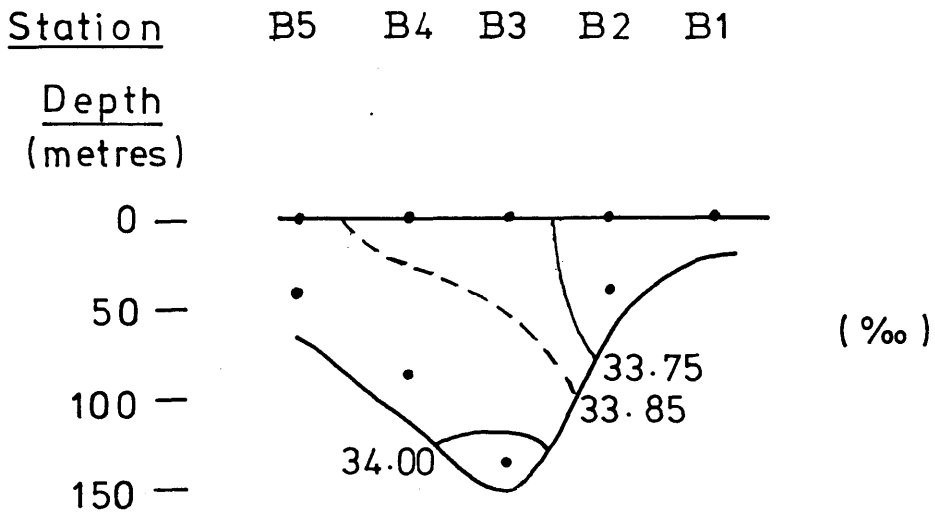
Transect A

water in the southern section of the North Channel. Either way, a slackening off of saline southward moving water along the Irish coast in the North Channel is indicated. Salinity profiles of transects Z and A are presented in Figure 4.2.c4; from these profiles the higher salinity water, $> 34.00\text{‰}$, at the bottom of the North Channel is seen to be trapped below station Z4 and does not occur at transect A, the northern exit of the North Channel (compare with Figure 4.2.b5 for cruise of August 1983). Whether this behaviour is due to relaxation of incoming high salinity, low ^{137}Cs water from the northwest into the North Channel or to increased outflow of Irish Sea derived water through the North Channel is not obvious at this stage. As will be seen from data from other cruises, however, the measured salinities in the North Channel for this cruise are significantly depressed, with a maximum of only 33.810‰ across transect A and an overall maximum in the North Channel of 33.877‰ . These generally low salinities ($< 33.900\text{‰}$) extend northwards to the region between Islay and Northern Ireland and directly westwards of Islay; corresponding ^{137}Cs levels for this region outwith the North Channel lie between 39–45 dpm/l with only marginal dilution of the radioactive plume having occurred. On leaving the North Channel, the radiocaesium plume continued around to the west of Islay with a portion flowing to the east between Islay and the Mull of Kintyre (the Sound of Jura). The ^{137}Cs data show a higher maximum (47.6 dpm/l) across transect B - east of Islay - than across transect D (43.8 dpm/l) - west of Islay - though mean levels across the plume are generally higher across the latter. The salinities show the same relationship to ^{137}Cs levels as in the North Channel, i.e. increasing salinity corresponds to decreasing ^{137}Cs and in contrast to later cruises, higher surface salinities were found east of Islay than for some distance west of Islay (as far as about $7^{\circ}30'W$); this trend

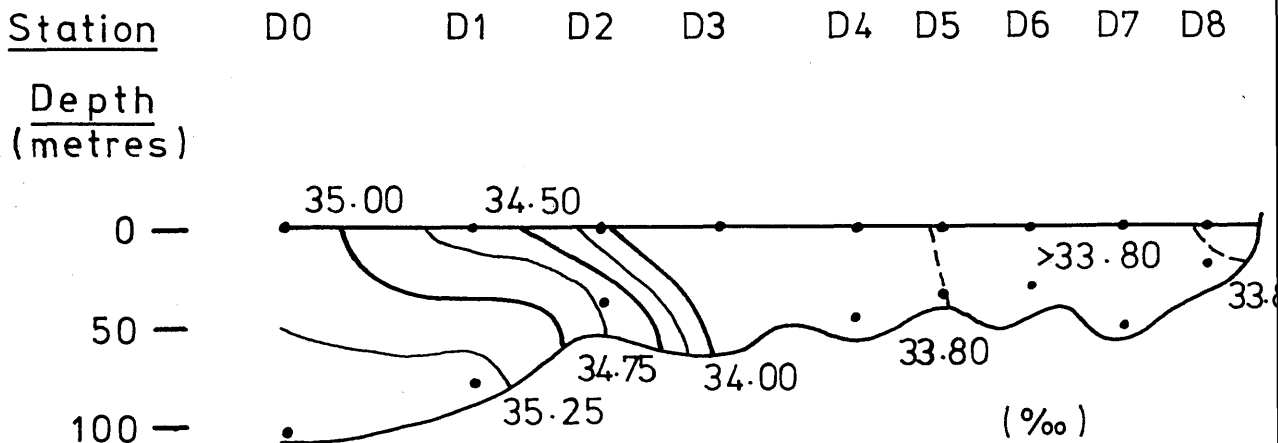
Figure 4.2.a5

Salinity Profile Across(i) Transect B and (ii) Transect DMay 1983

(i)

Transect B

(ii)

Transect D

was also noted in salinities at depth (Figure 4.2 a5). These higher salinities in the Sound of Jura (compared to transect D) can, therefore, be associated with the lower ^{137}Cs levels.

So far the picture is one of generally low salinities and hence of limited dilution of the radiocaesium plume by saline waters - salinities exceeding 34.00‰ occurred only at depth (below 175 metres) so that, at the surface at least, Atlantic influence on the ^{137}Cs levels was relatively small.

On reaching the next sampled transect (G), the radiocaesium plume had split into 2 branches, one either side - east and west - of the Outer Hebrides. The eastern branch entered the Minch whilst the western branch encountered Atlantic water approaching from the west. An estimate made by Craig (1959) for the ratio of coastal water flow west : east of the Outer Hebrides was 3 : 2. More recent work by McKay et al (1986) led to reassessment of this ratio as approximately 1:4.6, i.e. most of the coastal water passing through the Minch. In the latter estimate, the depth of the surface mixed layer (representing the Irish Sea-derived water) was taken into account whereas in the former case a homogenous water column was assumed. However, in assuming the surface mixed layer contained the northward moving radiocaesium, McKay et al. (1986) had no supporting subsurface radiocaesium data.

Although higher ^{137}Cs levels were found in the western branch (relative to the eastern), the levels are reduced faster during northward transport in the former than in the latter. From the salinity contours (Figure 4.2.a2), it is clear that higher salinities were encountered by the western flow north of 57° N (34.25 - >35.00 ‰) than by its eastern counterpart (34.20 - <34.60 ‰) so that, at the surface at least, ^{137}Cs levels were maintained for longer along the

eastern branch, i.e. via the Minch, than along the western route. To indicate the rate of dilution of ^{137}Cs levels from the North Channel to the northernmost transects sampled, a section through the main path of the plume - including both the eastern and western branches at the Outer Hebrides - is presented in Figure 4.2.a8. Maximum ^{137}Cs values were taken across each transect in order to represent, as best possible, the main concentration of the plume during transit (see below).

A point to note at this stage is that low dilution within a region is not necessarily an indication of a quiescent region. The Minch, for example, is generally a well-mixed area compared to that west of the Outer Hebrides because of tidal mixing (Ellett and Edwards, 1983); hence the water is nearly homogenous both horizontally throughout the region (Figures 4.2.a2, 3) and vertically down the water column; with no deep ^{137}Cs data at this stage, it is only possible to gauge from salinity profiles whether the region is homogenous vertically - Figure 4.2.a6 shows a profile for transect K across the Minches. The stronger gradation of ^{137}Cs and salinity in the western branch, then, is a consequence of the encounter of Atlantic water from the west. In the Minches, however, thorough mixing occurs and the influence of low ^{137}Cs , high salinity Atlantic water is less marked; the maximum salinity found in the Minch was $< 34.6\%$. By comparison, on the Hebridean Shelf (west of the Outer Hebrides) - Figure 4.2.a7 - tidal mixing is weaker and stratification occurs. Dilution of radiocaesium from south to north and from east to west in the surface waters of the area is quite significant because of influence here of Atlantic water from the west.

In general, shallow waters with strong tidal streams are usually homogenous whereas deeper waters with weaker tides encourage

Figure 4.2.a6

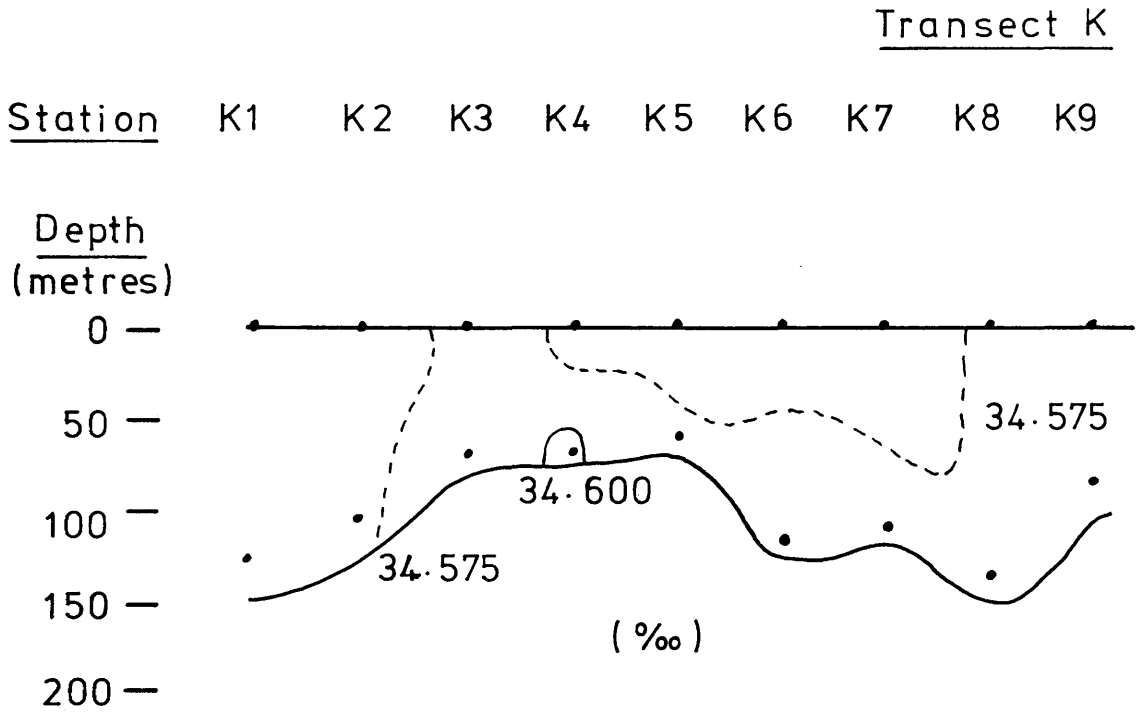
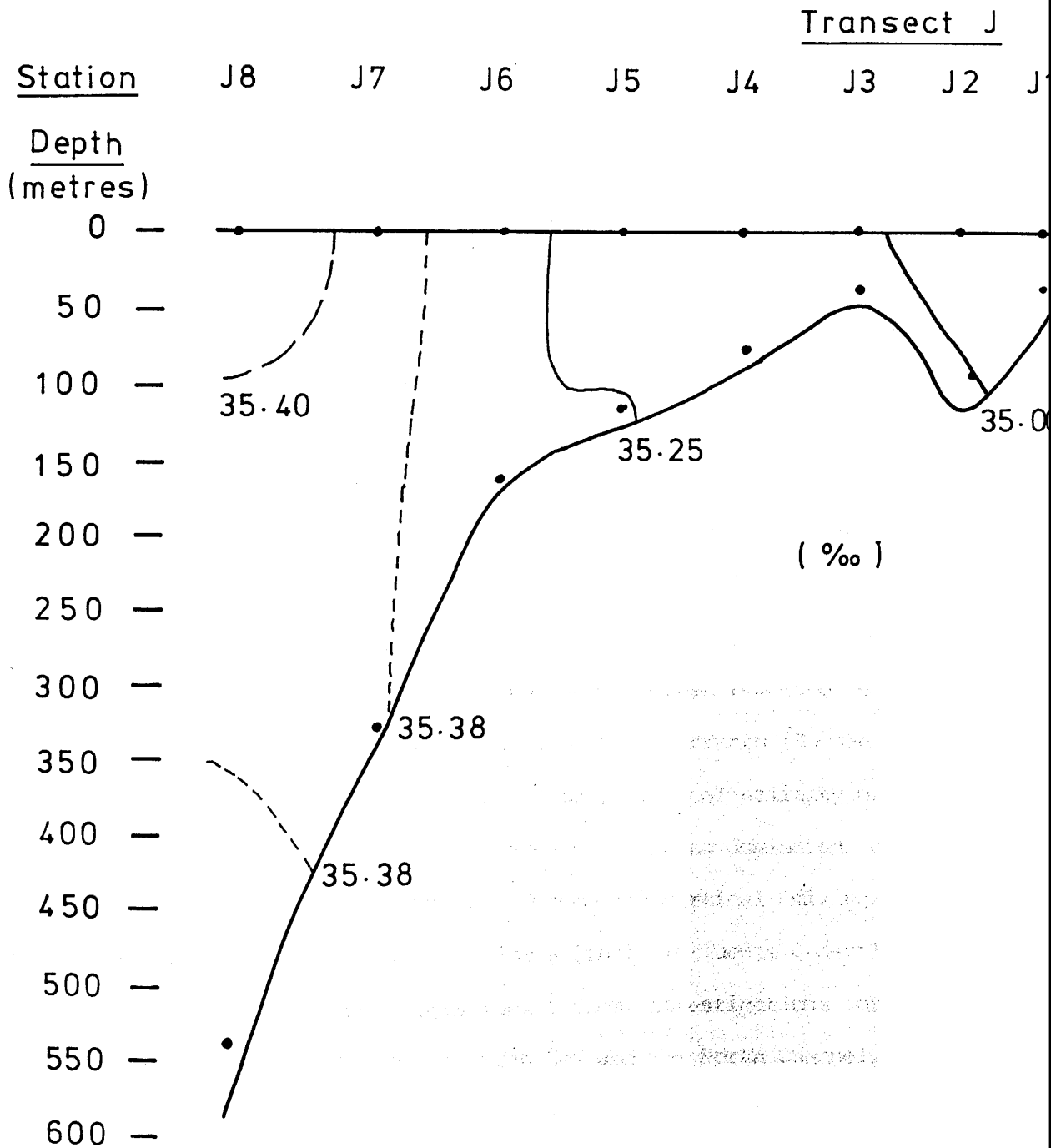
Salinity Profile Across Transect KMay 1983

Figure 4.2.a7

Salinity Profile Across Transect JMay 1983

stratification. Thus, where the coastal current water passes over relatively shallow depths it is well-mixed. Work by Ellett and Edwards (1983) has shown that summer stratification can be present in deeper areas traversed by the current, such as in the approaches to the Firth of Lorn, to the south of Rhum and in the deeper basins. In the sounds, vigorous mixing of water occurs due to strong currents (Ellett and Edwards, 1983).

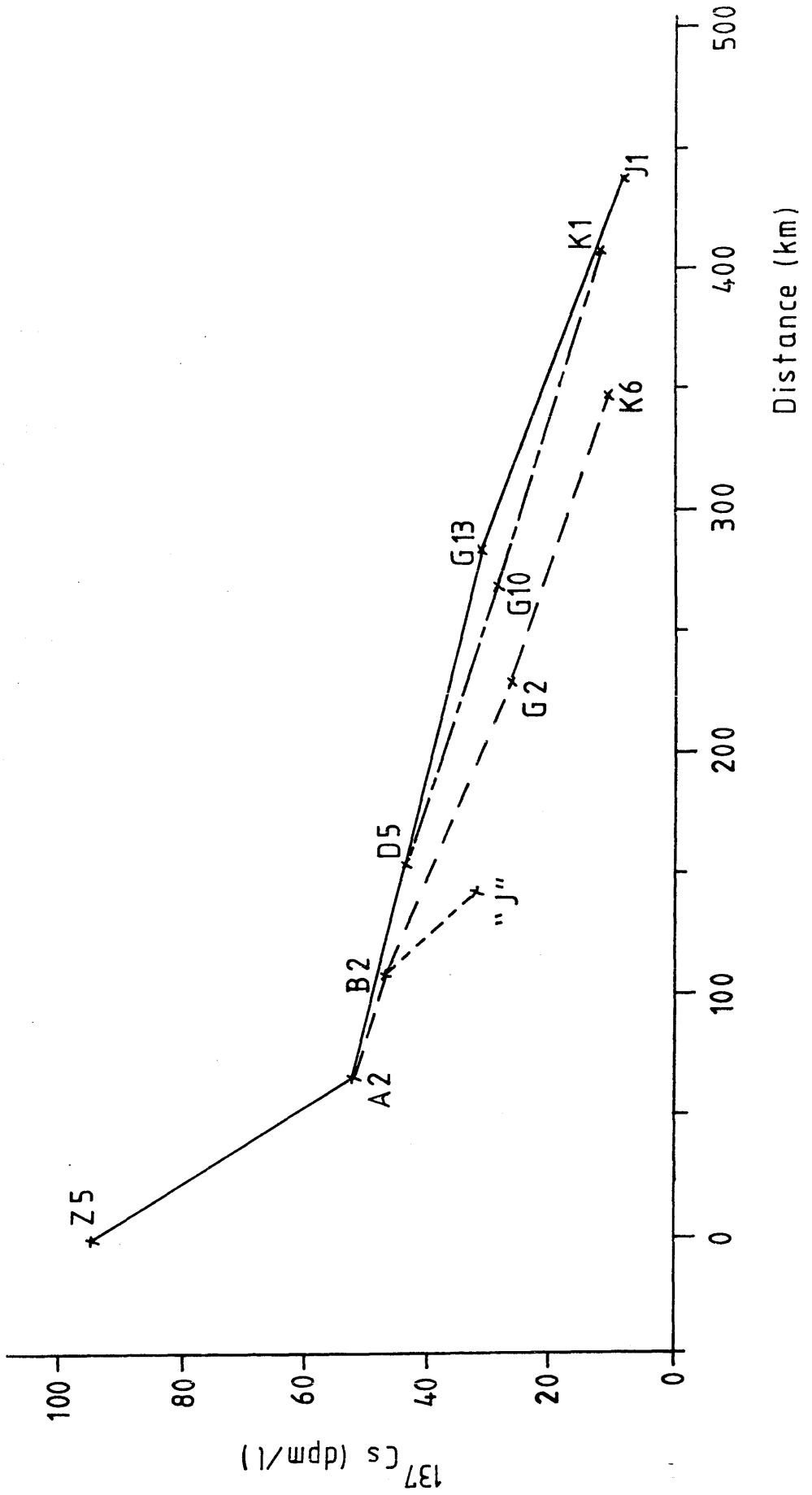
The Islay Front has been described as separating the well mixed, unstratified waters west of Islay from the quiescent, stratified waters further offshore (Fearnhead, 1975; Hughes, 1976; Pingree et al., 1978; Simpson et al., 1979) or marking the boundary between the Atlantic and Irish Sea / CSA water masses (Ellett, 1978; McKinley et al., 1981a).

In the North Channel, the strong gradient (twofold dilution) of ¹³⁷Cs levels observed from south to north and the reduced penetration of high salinity water entering from the west - in turn reflected by the Islay Front lying further to the west than previously reported - seem to imply that, generally, Atlantic water influence in this region at this time was limited. The North Channel has been reported to be a region of extensive mixing due to strong tidal currents (Bowden, 1955; Sager and Sammler, 1968; Howarth, 1982), vertical salinity profiles across transects Z and A in this area often being dominated by the effects of strong tidal currents and complete vertical mixing. Low salinities south of 57° 00' N imply low Atlantic influence generally.

Williamson (1956) suggested, from investigations of the distribution of plankton in the Irish Sea and the North Channel, that the northward flow through the North Channel may, at times, occur in comparatively fast-moving pulses of water separated by periods of reduced flow. Complementary to this suggestion are the variations in

Figure 4.2.a8

^{137}Cs against Distance from North Channel



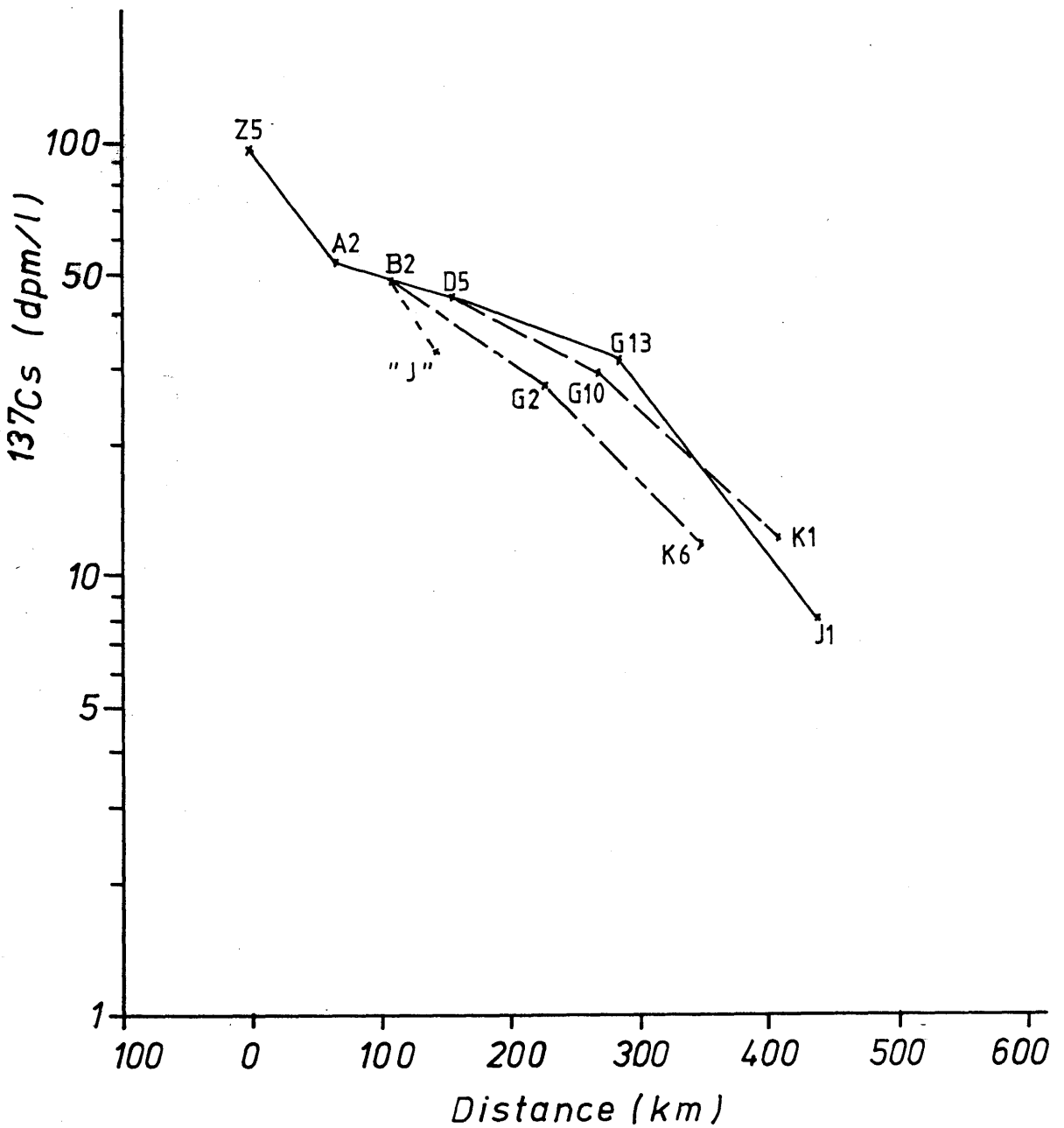
strength of Atlantic incursions into the North Channel as revealed during study of this set of cruises.

To investigate how the surface radiocaesium levels vary along the main path of the plume, the maximum ^{137}Cs levels across each transect have been plotted against distance along the coastal current route (along the sections shown in Figure 4.2.a1) in Figure 4.2.a8. So that ^{137}Cs levels with distance along the coastal current may be related to the water flow characteristics (i.e. degree of mixing) the transit time for water passing through the system must be short enough that the observed levels are not determined by "older" water of different discharge level (this condition is met, as explained below (see also subsection 4.2(d)). As expected, the radiocaesium levels decreased northward from the North Channel, i.e. away from the source. The regions of greatest reduction in levels can be assumed to correspond to areas in Figure 4.2.a3 of noticeable ^{137}Cs gradients in the direction of the plume's path. However, in a plot such as in Figure 4.2.a8, it is not directly clear from the gradients of the different curve regions whether the rate of reduction in levels was increasing or decreasing since, for example, a constant rate of reduction would appear as an exponential decay curve rather than a straight line of constant gradient. Thus, by plotting the ^{137}Cs data on a log scale the gradient of the line indicates, more clearly, the rate of radiocaesium reduction (Figure 4.2.a9). Such reduction is greatest during transit through the North Channel - from station Z5 to A2 - and from transect G, just south of the Outer Hebrides (latitude $\sim 56^{\circ} 45' \text{N}$), to the northernmost sites sampled, in particular, the route to the west of the Outer Hebrides - station G13 to J1. Both regions are typically well mixed due to tidal currents but also they are, at this time, areas where the Irish Sea / CSA waters directly adjoin the Atlantic

Figure 4.2.a9

^{137}Cs Along Main Path of
Plume (From North Channel)

May 1983



water. During transport between these 2 areas, the low salinities indicate relatively little Atlantic influence and relatively slow radiocaesium dilution. Dilution of the Sellafield plume is discussed further in subsections 4.3(b), (e).

Another form of useful data presentation involves plotting ^{137}Cs levels against salinity. Figure 4.2.a10 illustrates how mixing of two water types (i.e. each of characteristic properties) produces water of properties ranging between those of the two end members. Thus, waters of 1) high ^{137}Cs and low salinity and 2) low ^{137}Cs and high salinity mix to produce a water mass with a range of salinities and ^{137}Cs levels. Any proportion of mixing between the two water types will produce water whose characteristics, when plotted on the ^{137}Cs / salinity graph, will fall on the straight line between the two end members. If a third water type is contributing, however, the straight line will be modified to accommodate the new set of characteristic properties introduced. In this study the two sea water end members are Atlantic water - high salinity, negligible levels of ^{137}Cs - and North Channel water - low salinity, high ^{137}Cs - and the third water type is represented by fresh water - zero salinity, negligible ^{137}Cs . The line drawn between the two original end members bows out towards the bottom left hand side, i.e. where low salinity and low ^{137}Cs are represented and thus the "straight line" becomes a curve.

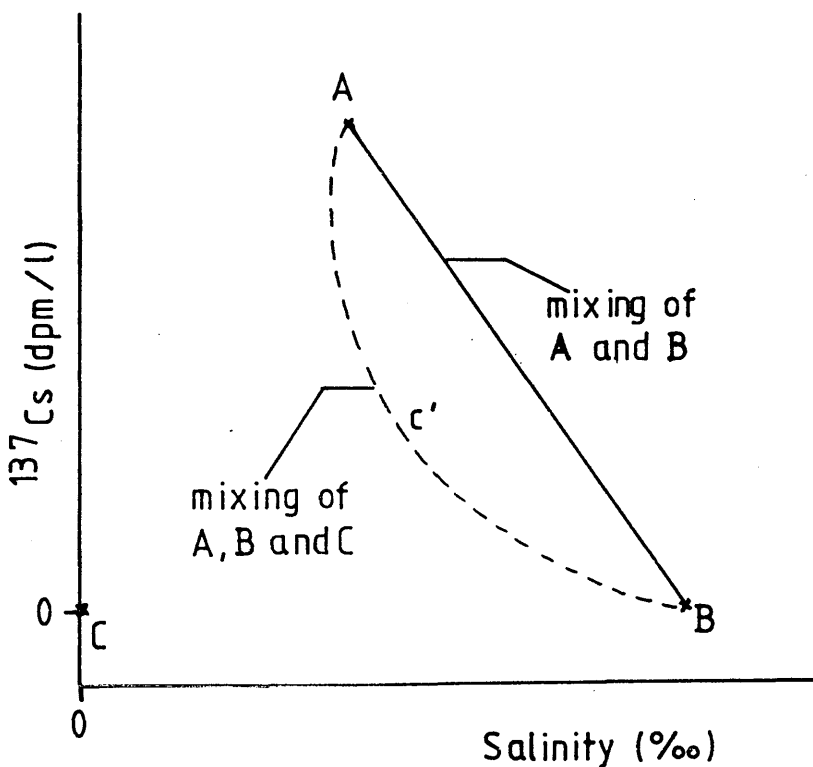
Although a ^{137}Cs / salinity diagram primarily indicates the proportions of the three main water masses of the area of which a particular sample is composed (e.g. 40% Irish Sea / CSA water, 58% Atlantic water and 2% fresh water), such plots of samples taken during a particular cruise serve to present an approximate time history of the modifications to the coastal current water in its journey northwards. Very few samples among the many shown in the following

Figure 4.2. a10

^{137}Cs / Salinity Plot to Illustrate Mixing
Between Water Types

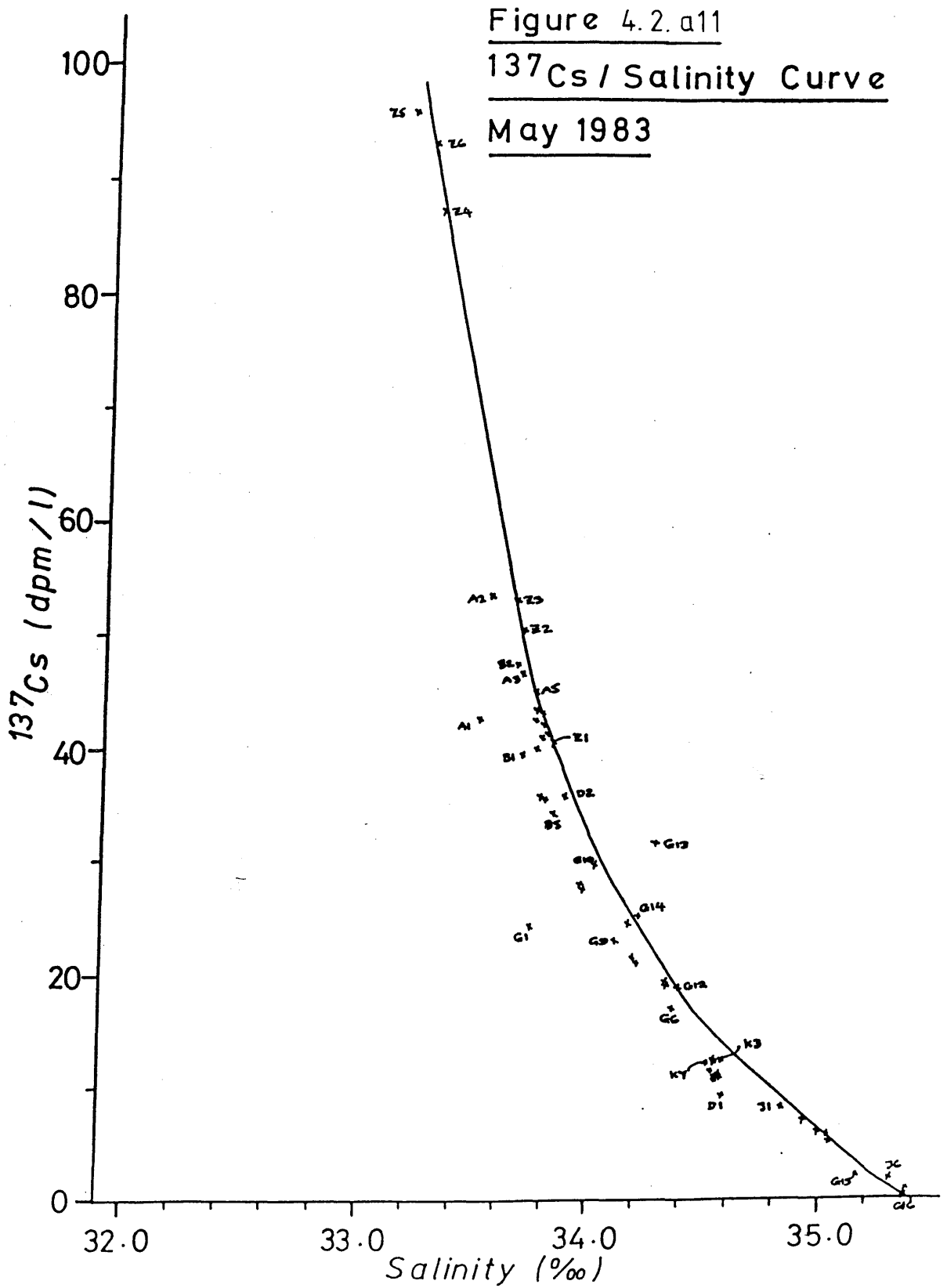
Key

- A = high ^{137}Cs , low salinity,
e.g. Irish Sea / CSA water
- B = negligible ^{137}Cs , high salinity,
e.g. Atlantic water
- C = negligible ^{137}Cs , zero salinity,
e.g. fresh water



^{137}Cs / salinity diagrams indicate direct mixing between the Irish Sea / CSA and Atlantic source waters, i.e. points in Figure 4.2. a10 along the line joining A to B. Instead, the locus traced out by the highest salinity value at any given ^{137}Cs value is a curve which is bowed towards the fresh water source (AC'B in Figure 4.2.a10), showing that the addition of fresh water to the coastal current is significant although small in the region south and east of the Outer Hebrides (A to C'). It is only to the west of the Outer Hebrides where this fresh water addition becomes of decreasing importance with northward transit and linearity between radiocaesium and salinity is restored.

The data from this cruise have been plotted in the manner described and are presented in Figure 4.2.all. Most of the points fall on, or very close to, the curve drawn through them with a few exceptions where fresh water influence is more significant and the points fall to the left of the curve, e.g. A1, G1, two inshore stations - near the Mull of Kintyre and north of Mull respectively. Thus, although the fresh water influence can be assumed negligible for most of the region, its effect can be noticed particularly at coastal stations. The one point noticeably falling to the right hand side of the curve corresponds to station G13, implying low fresh water dilution in relative to nearby stations. It is, however, on the left hand side of a straight line between the two end members - in this case G16 and Z6; falling on the right hand side of this line would imply another input source of either ^{137}Cs or higher salinity (i.e. mixing with a more saline water mass than the Atlantic). Station Z6, then, represents the Irish Sea-derived water entering the North Channel whilst G16 corresponds to the limit of the radiocaesium plume since it exhibits Atlantic type characteristics - high salinity (35.4‰) and very low ^{137}Cs (<1dpm/l).



This form of data presentation may be used to extrapolate ^{137}Cs levels for sites where salinity is known and fresh water influence is considered negligible. This calculation system was performed for transect BN and so allowed more accurate contours to be drawn for the Hebridean Shelf. However, it would not be advisable to apply a similar treatment to, say, transect E - Mull to Jura, Firth of Lorn - since the extent of fresh water dilution on the ^{137}Cs levels is unknown for this region during the time of this cruise. Similarly, it would be inaccurate to extrapolate ^{137}Cs levels from known salinities of, say, the Irish Sea area since it is outwith the region represented by the curve - the ^{137}Cs levels would be expected to be very much higher than those measured in the HSA. Furthermore, there are uncertainties related to the lower salinities of the Irish Sea, i.e. which salinity represents maximum radiocaesium content? For the Irish Sea, then, the end member representing the radiocaesium source would be outside the the HSA North Channel envelope. For deep samples, too, there are uncertainties in extrapolating ^{137}Cs levels from known salinities if there are no known deep ^{137}Cs data already available as a guide to the effect of dilution by fresh water / saline Atlantic water.

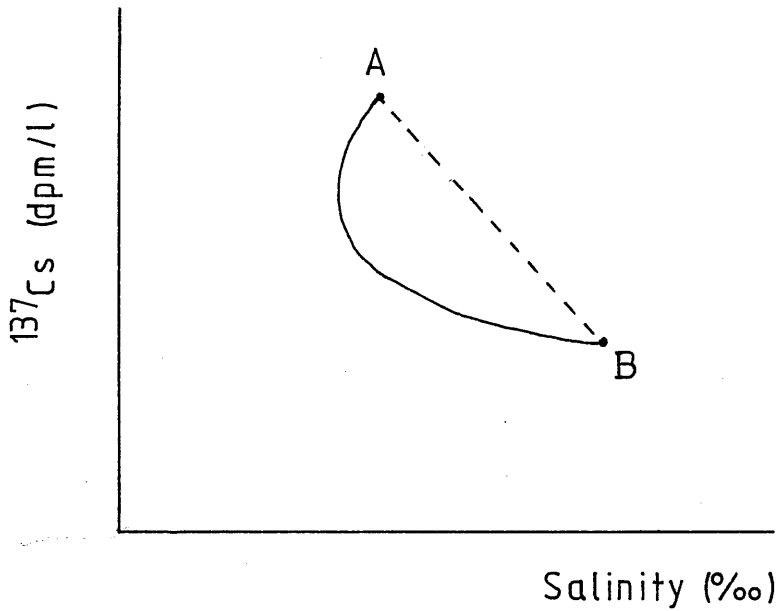
Another use of the ^{137}Cs / salinity curve is as an indicator of the extent of mixing between transects along the the path of the plume and also of whether the radiocaesium dilution achieved on arrival at a particular station has been due mainly to Atlantic or fresh water.

The relationship observed between Cs and salinity in Figure 4.2.all illustrates the relatively conservative behaviour of Cs but we are probably also witnessing a small degree of removal of the caesium from the water column during its northward travel - another reason for the line to curve to the left. Figure 4.2.a12 illustrates the hypothetical situation of two cases: in the first there is no removal

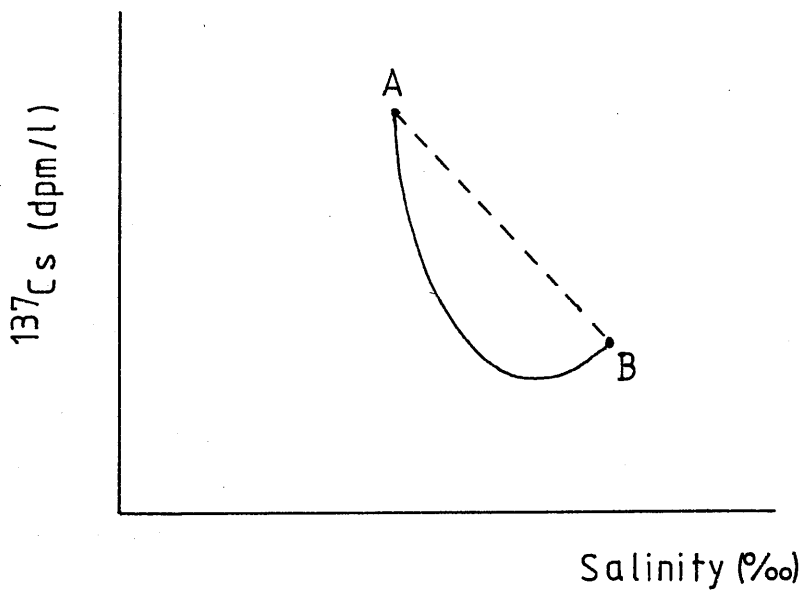
Figure 4.2. a12

^{137}Cs / Salinity Plots Illustrating (i) Perfectly Conservative Cs with Fresh Water Influence and (ii) No Fresh Water Influence with Cs Removal

(i)



(ii)



of ^{137}Cs from the water column, i.e. the element is completely conservative and varies perfectly with salinity, but there exists dilution by fresh water, in the second, there is no fresh water influence but there is some removal of the element from the water column, i.e. it is not completely conservative in behaviour. As can be seen, the two curves produced are not the same - in the first case the curve tends towards the y axis and in the second case it tends towards the x axis. The curve obtained in practice (Figure 4.2.all) is probably a combination of these two processes.

A condition which should be satisfied if the ^{137}Cs / salinity curve may be used to estimate mixing rates between stations is that the flushing time for the whole region is short enough that the measured ^{137}Cs levels are not simply a result of older water recirculating in the area; indeed a time of 2 months has previously been estimated for transit times calculated from ^{134}Cs : ^{137}Cs ratios throughout the area (McKay et al., 1985) and this would seem to satisfy the above condition, bearing in mind that the discharges vary monthly and the pattern of discharge is likely to be somewhat dampened on reaching the HSA. From matching of time trends in this study (section 4.3, Chapter 4), a transit time from transect A of the North Channel to transect G across the entrance to the Minch has been found to be about 2 months with another 2 months within the Minches to reach transect K.

The use of ^{134}Cs : ^{137}Cs ratio values from this cruise has so far not been mentioned. Other workers (e.g. Jefferies et al., 1973; McKinley et al., 1981a; McKay et al., 1986) have used the ratio values to estimate transit times and / or residence times. In this study, however, it has not been possible to use these values to obtain sensitive data, largely because of the increase in counting error

Table 4.2 a1

Mean $^{134}\text{Cs} : ^{137}\text{Cs}$ Ratio Across Each Transect

<u>Transect</u>	<u>Mean $^{134}\text{Cs} : ^{137}\text{Cs}$ Ratio (\bar{X})</u>	<u>Standard Deviation (n)</u>
Z	0.050	0.008
A	0.053	0.006
D	0.046	0.001
B	0.049	0.003
G	0.048	0.003
K	0.053	0.008

since the decrease in Sellafield discharges. From data presented in Appendix II.1, mean ratios across each transect were derived (Table 4.2.a1) (the ratio for station J1 was ignored since the associated counting error exceeded 20%). Assuming advection only from transect Z to transect K and a constant discharge ratio level - hence taking the maximum ratio value ($\bar{x} + n$) at transect Z and the minimum ratio value ($\bar{x} - n$) at transect K - a maximum transit time throughout the area of ~9.7 months is estimated. This is within the estimated transit time from Sellafield to transect K, derived in subsection 4.3(e) from matching of ^{137}Cs time trends, of 6.7 ± 1.0 months, however, the latter is much more sensitive than the estimate obtained here from the ratio data. In the later cruises, errors in ratio values continued to increase (see Appendices II.2 - II.8), providing even less sensitive results, and are therefore not discussed any further.

ii) Summary

1) Atlantic incursion into the southern HSA was low for this cruise with low salinities throughout the region being accompanied by high radiocaesium levels; the western positioning of the Islay Front also reflected the weak intrusion of Atlantic water.

2) A section of high salinity, low radiocaesium water was found isolated in the southwestern part of the North Channel, probably due to withdrawal of Atlantic water from this area.

3) Significant dilution of radiocaesium levels occurred in the North Channel and west of the Outer Hebrides, both being regions where the radiocaesium plume directly encounters Atlantic water.

4) Various forms of data presentation which are referred to again later in this section have been discussed.

4.2(b) August 1983

i) Results and Discussion

The salinity and ^{137}Cs isopleths for this 1983 summer cruise are shown in Figures 4.2.b2 and 4.2.b3 respectively and the stations sampled are shown in Figure 4.2.b1; 73 water samples were analysed for radiocaesium content, 5 of which were subsurface. As found for the May 1983 results, a good correlation exists between ^{137}Cs and salinity data as can be qualitatively observed in the similarity of the two sets of contours.

The general pattern of the radiocaesium contours for the area north of 57°N for this cruise is similar to that observed in May 1983 - decreasing levels both northward and westward of the source region, with a more rapid reduction of levels westwards. The trends can be attributed to the radioactive plume encountering Atlantic water to the west and to stronger mixing in the Minches relative to the Hebridean Shelf area west of the Outer Hebrides (as described for May 1983). Thus, good mixing and a low Atlantic influence prevented formation of marked gradients in the Minches, whereas, west of the Outer Hebrides, considerable dilution occurred - across the path of the radiocaesium plume - where the Atlantic water extended eastwards on to the quiescent shelf region and mixing was insufficient to reduce the gradient between the two water masses. Between the two cruises examined thus far, there are two main notable differences as evidenced in the radiocaesium and salinity contours south of 57°N .

Firstly, Atlantic incursion from the west into the southern HSA appears to have been greater in this cruise than in May 1983 because 1) the shapes of the ^{137}Cs and salinity contours in this region,

Figure 4.2.b1
Station Positions
August 1983 Cruise

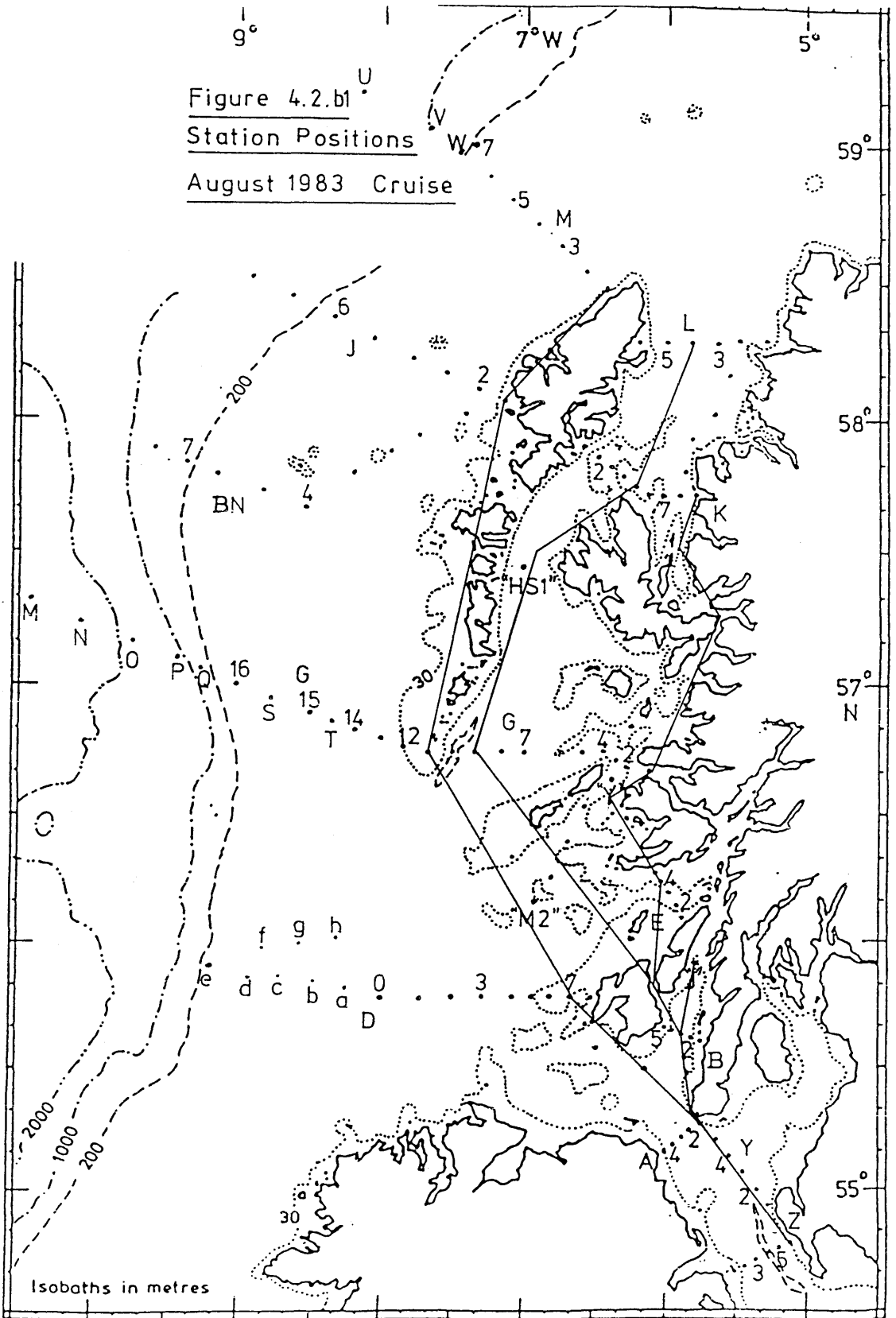


Figure 4.2.b2

Salinity Contours (‰) - August 1983 Cruise

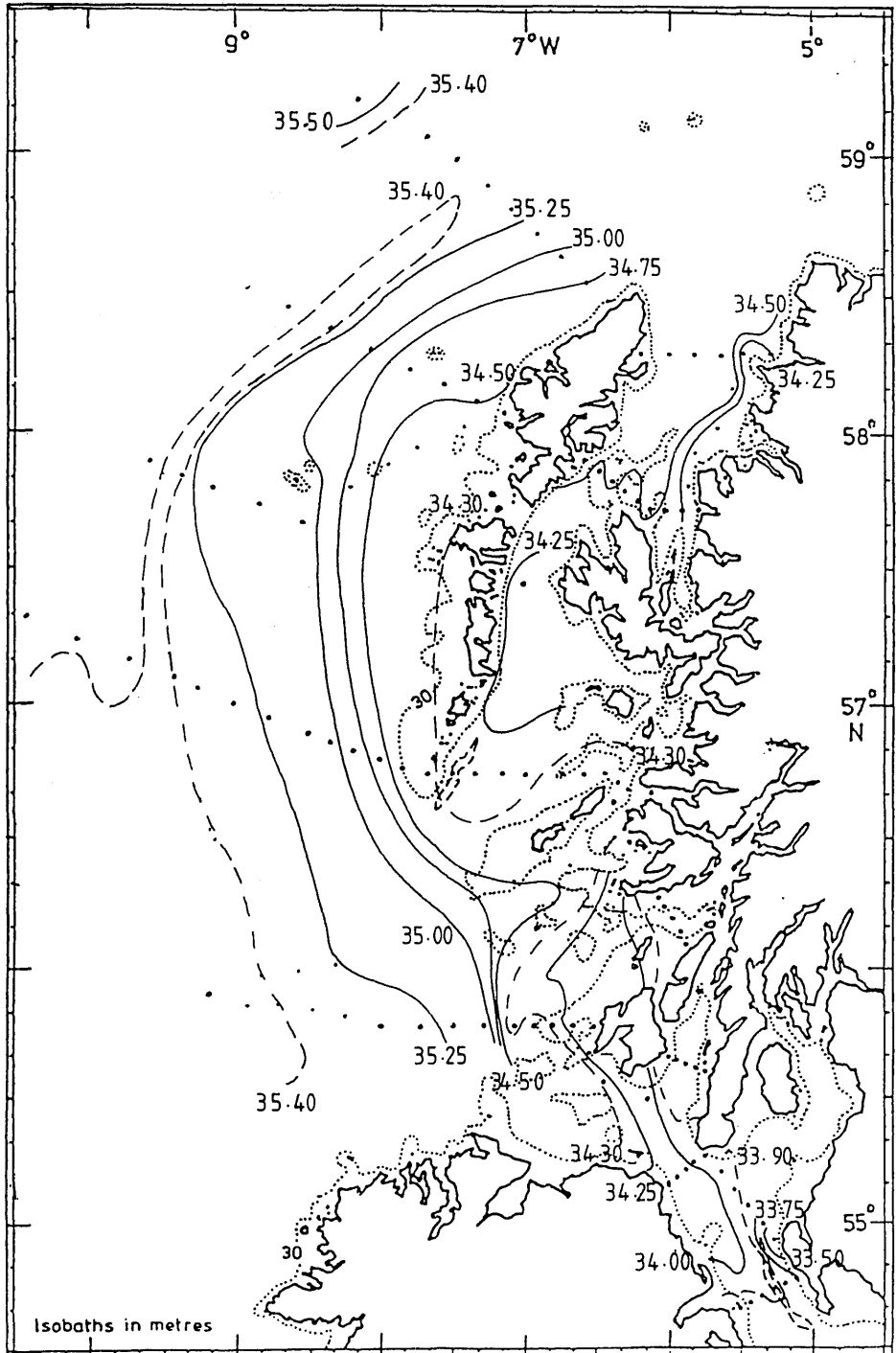
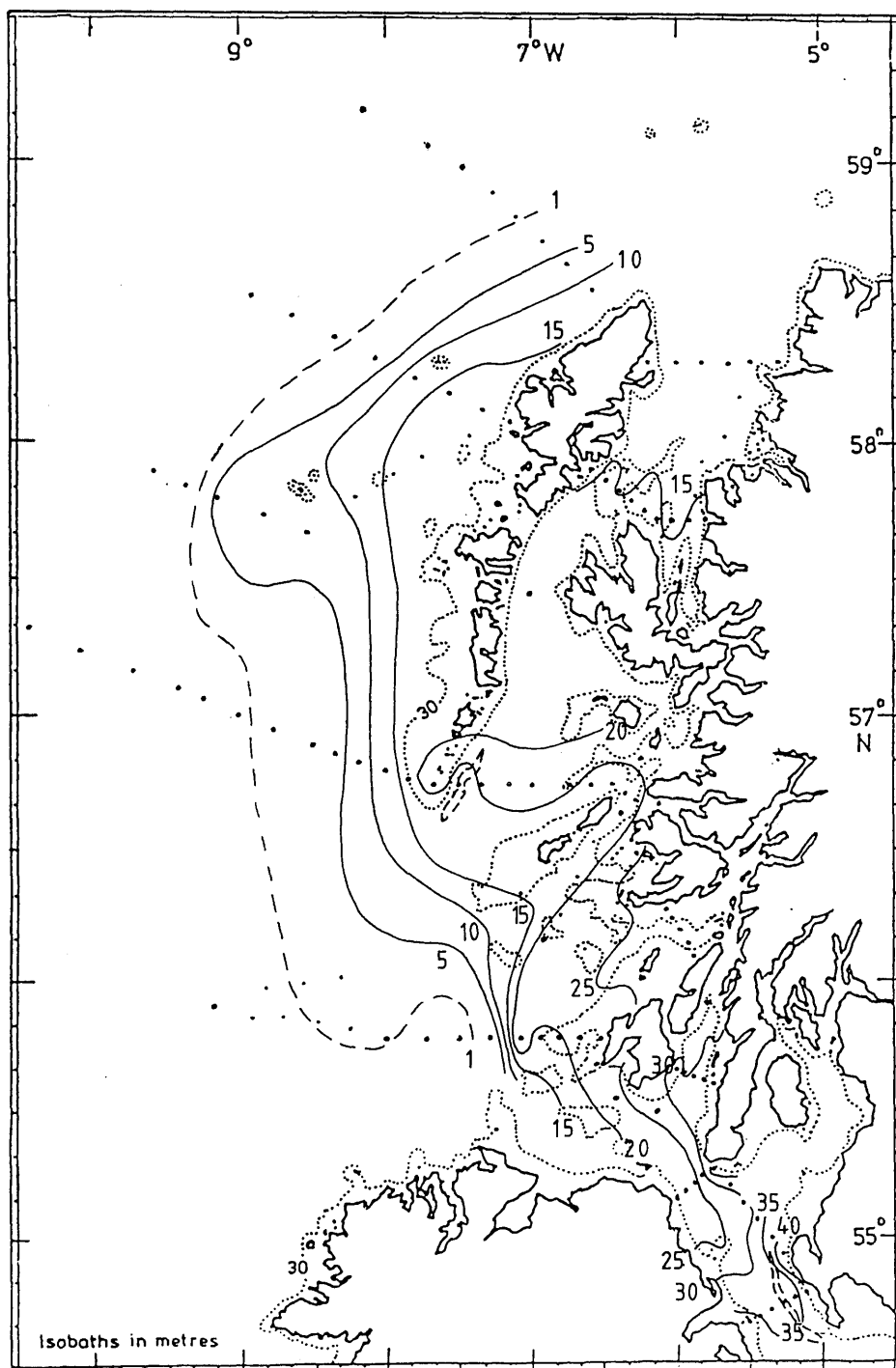


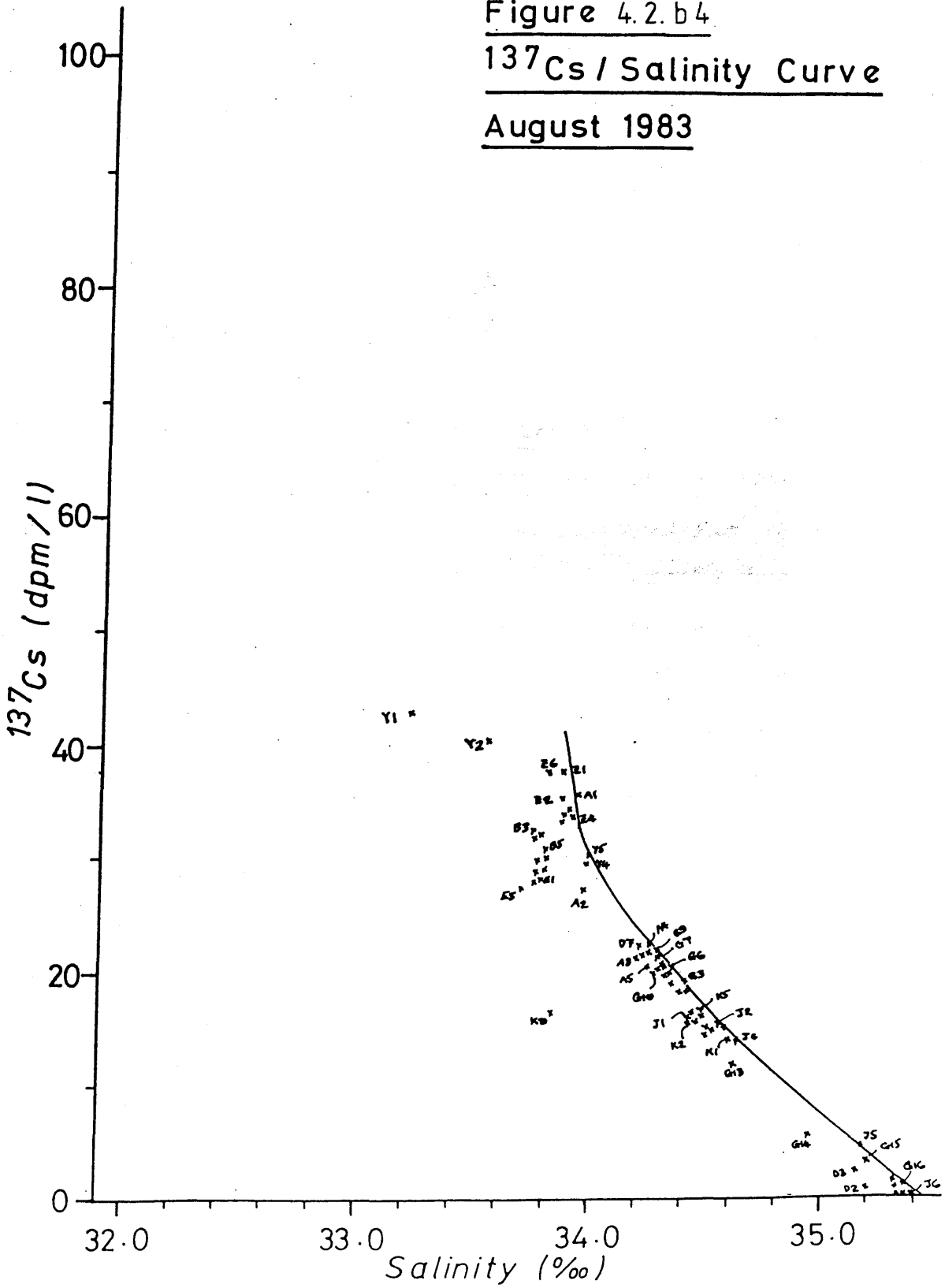
Figure 4.2.b3

 ^{137}Cs Contours (dpm/l) - August 1983 Cruise

especially between latitudes $56^{\circ}00'$ and $56^{\circ}35'N$ east of $7^{\circ}10'W$ up to $6^{\circ}30'W$, indicate more extensive Atlantic water penetration during the later cruise (August 1983), 2) salinities south of about $57^{\circ}00'N$ were found to be noticeably higher in August than in May 1983 and are accompanied by lower ^{137}Cs levels, salinities ranging from 33.80‰ to 34.25‰ and from 34.20‰ to 34.60‰ for the May 1983 and August 1983 cruises respectively in the region, 3) the Islay Front occurred further to the east, at $7^{\circ}00' - 7^{\circ}10'W$, and was more intense in the August cruise than in May when the front was observed at $7^{\circ}30' - 8^{\circ}00'W$ and 4) the radiocaesium plume appears to have been restricted more to the mainland coastline in the southern HSA during the August cruise.

Secondly, the stations with highest measured ^{137}Cs levels were found to occur not at the southeasternmost region of the North Channel but across the CSA entrance at stations Y1 and Y2. From the ^{137}Cs / salinity curve in Figure 4.2.b4 it appears that these stations had been diluted significantly by fresh water relative with stations nearby, e.g. on transect Z. This would then imply some surface outflow of CSA water into the North Channel at these stations with inflow occurring, as implied by the shape of the radiocaesium and salinity isopleths, at stations Y5 and Y4 where salinities are higher. However, stations Y1 and Y2 represent the least diluted samples of water of Irish Sea origin detected in the North Channel and appear to be "cut off" from the Irish Sea by water which has been diluted more extensively with respect to radiocaesium (than with salinity). The isolation of this fraction of water implies an interruption in northward movement of the radiocaesium plume through the North Channel. The shape of the contours in Figures 4.2.b2 and 4.2.b3 largely indicates southward movement in the North Channel, with the

Figure 4.2.b4

 ^{137}Cs / Salinity CurveAugust 1983

higher salinity, lower ^{137}Cs surface water entering the North Channel from the northwest and continuing southeastward. It seems, therefore, that we are witnessing a "blockage" of the Irish Sea / CSA water's northward flow through the North Channel by relatively high salinity water entering from the northwest. Earlier observations of the blocking of the North Channel's northward flow have been referred to by Lee (1960) who describes the North Channel's "normal" (northward) flow to have been at least partially blocked on 3 occasions during the period March 1953 - January 1954 by oceanic water from the north.

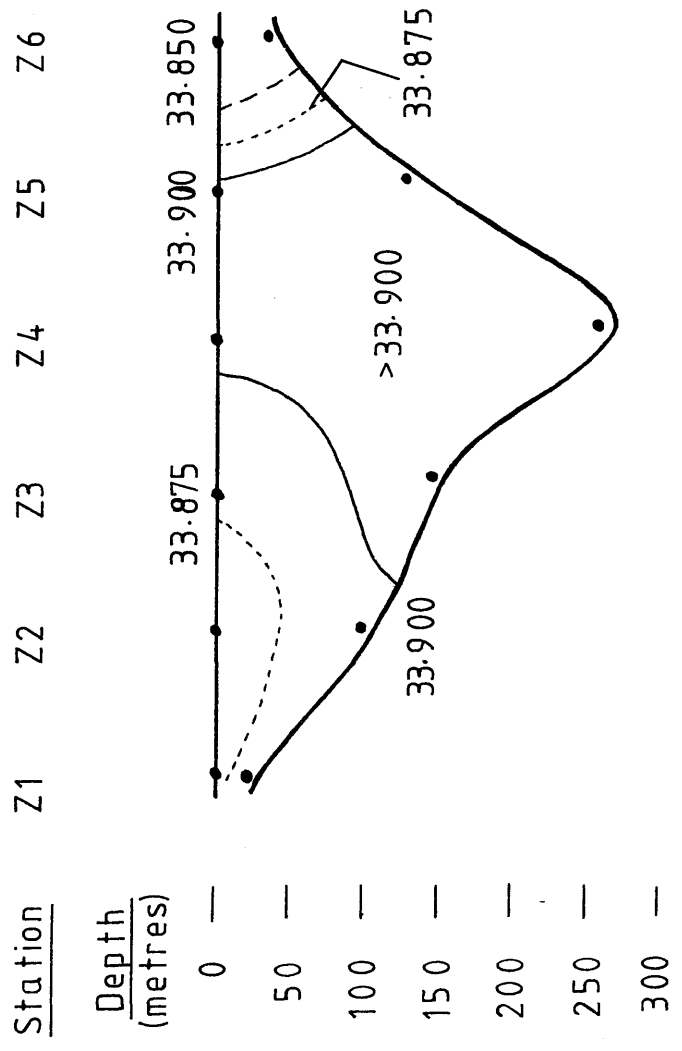
From the salinity profiles across transects Z and A (Figure 4.2.b5), it is not clear whether the North Channel's northward flow was blocked at depth as well as at the surface.

There are two plausible explanations for the observed low salinities (accompanying the high radiocaesium levels) at stations Y1 and Y2. Firstly, as suggested above, surface outflow from the CSA (water of low salinity) may have been the cause. Secondly, if the water at Y1 and Y2 represented newer water (lower radiocaesium discharge) and the rest of the surface water in the North Channel was "older" through residual mixing, then Y1 and Y2 data would plot to the left side of the ^{137}Cs / salinity curve with apparent fresh water dilution. The low salinities, may, in fact, indicate low salinity Irish Sea-derived water, isolated by the south-flowing water, of lower radiocaesium content than expected because of the decrease in recent discharge levels. However, because of the timescales involved and of the fact that for 3 months prior to the cruise discharges had been generally increasing, this is a less likely explanation than that involving enhanced CSA surface outflow. Waters at Y1 and Y2 and at stations in the North Channel are probably of similar "age" and therefore correspond to similar discharge levels (i.e. the CSA could

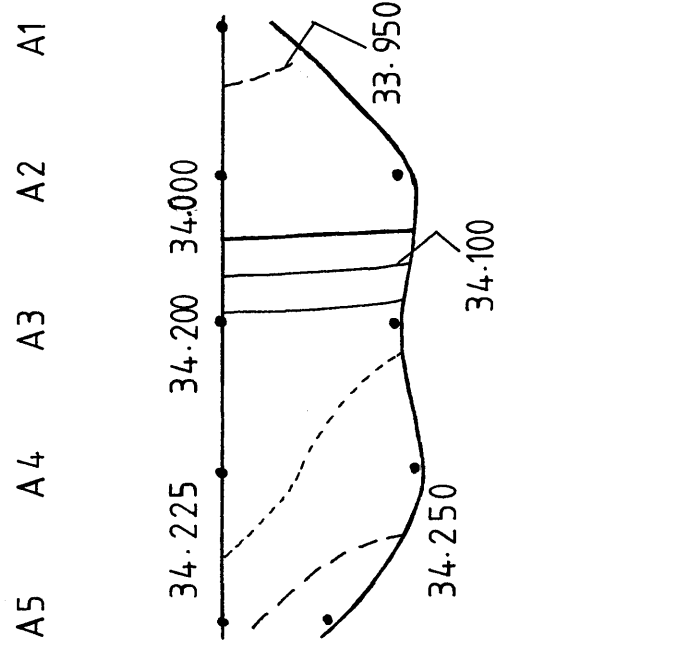
Figure 4.2.b5

Salinity Profile (‰) Across (i) Transect Z and (ii) Transect A, August 1983

(i) Transect Z



(ii) Transect A

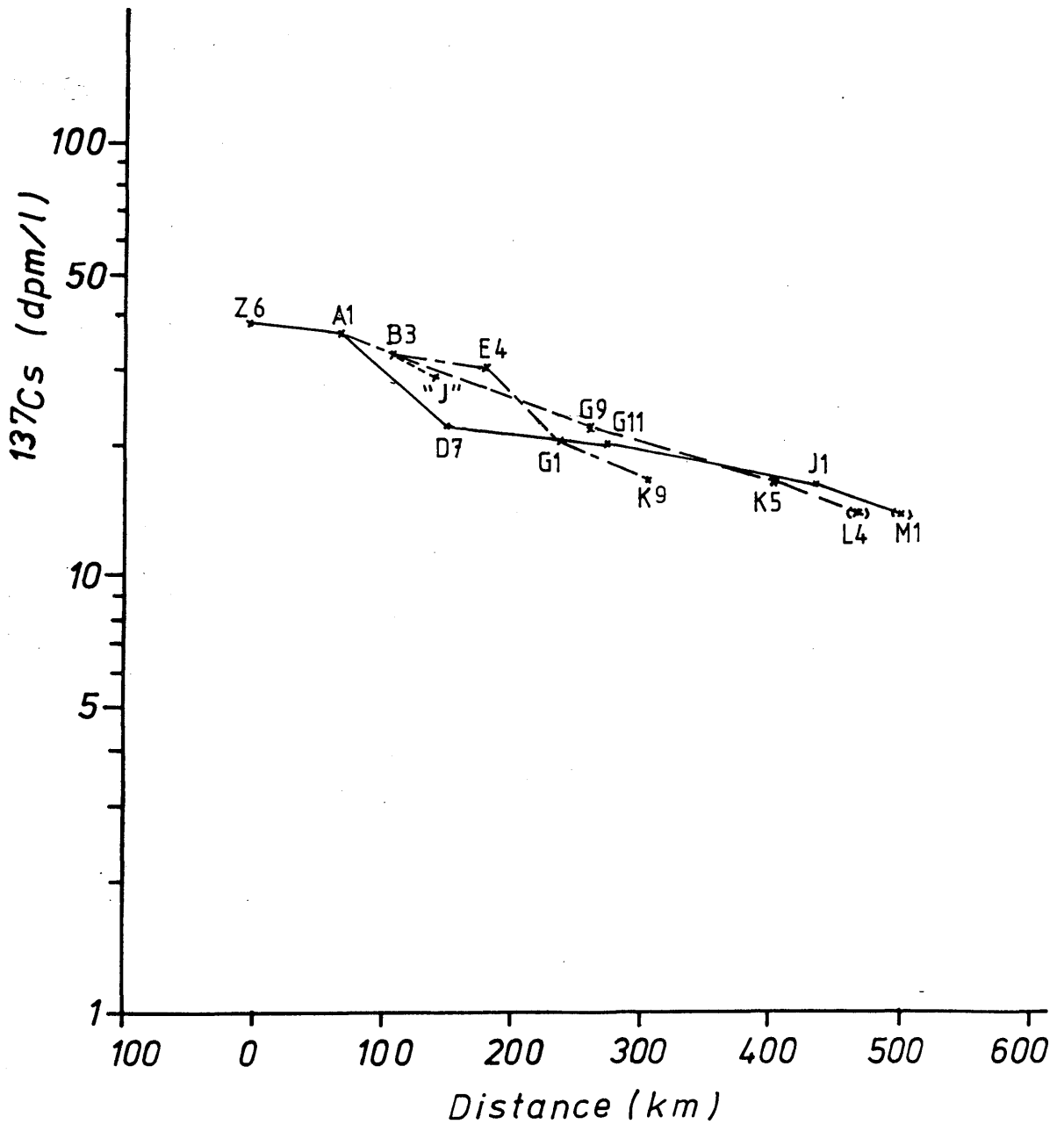


have retained this Y1 / Y2 water for a while and the south-flowing water mixed with older water). If Y1 / Y2 water was "new" then it would have relatively high radiocaesium content for its salinity and would not appear on the left hand side of the ^{137}Cs / salinity curve. If Y1/Y2 water represented water retained in the CSA then radiocaesium levels would be expected to correspond to older discharges but it is not possible to define the effect of the fresh water dilution unless actual CSA levels are known. A CSA station sampled on 25/8/83 (see Chapter 3), 13 days after the North Channel transects were collected (12/8/83), was found to have a ^{137}Cs content of 43.7 dpm/l at salinity 31.58‰. The more saline sample (33.213‰) at station Y1 had a ^{137}Cs content of only 42.6 dpm/l (corresponding to 43.7 dpm/l at 31.58‰). This would imply that the CSA sample corresponded to a higher discharge level than those in the North Channel. Indeed, ~5 months prior to the cruise (the time estimated for transit from Sellafield to the CSA, see Chapter 3) discharges were higher than during the 0.5 - 3.5 months prior to the cruise. Thus, water from stations Y1 and Y2 did not represent CSA water although the evidence suggests that it had undergone some fresh water dilution from the CSA.

A consequence of the increased Atlantic penetration into the southern HSA during this August cruise is the greater restriction of the radiocaesium plume to inner shore regions of the west coast of Scotland. This is evident from the higher ^{137}Cs levels measured east of Islay (transect B) than west of Islay (transect D). Figures 4.2.a9 and 4.2.b6 allow comparison of reduction in ^{137}Cs levels from the North Channel to either side of Islay for May and August respectively. In May 1983, the dilution was slightly greater for the eastern path around Islay than in the west since the main bulk of the plume flows in the former direction. In August 1983, dilution is observed to have

Figure 4.2. b6

^{137}Cs Along Main Path of
Plume (From North Channel)
August 1983



been less extensive along the eastern branch due to less mixing with Atlantic water whilst significant dilution occurred along the western path. Further north, dilution was still marginal in the eastern branch via transect E - Figure 4.2.b4 shows stations of transects B and E occurring very close to each other, with hardly any discernible dilution by either fresh or saline water during transit from one transect (B) to the other (E) (see also section 4.3 for dilution factors). This pattern continued until higher salinity waters approaching from the west were encountered around Mull and significant dilution ensued.

The confinement of the plume is observable, then, up to about latitude $56^{\circ}30'N$. North of this, contours show the plume spreading out in surface waters. ^{137}Cs levels directly east and west of the Outer Hebrides were approximately equal (e.g. compare transect K with stations J1-J4) whereas in May 1983 ^{137}Cs levels west of the Islands were approximately half those to the east. Atlantic influence - indicated by salinities - was similar for the two cruises north of $57^{\circ}00'N$ with slightly higher ^{137}Cs levels and lower salinities in this cruise, in particular, immediately west of N. Uist and Aird Breinish, Lewis. The generally higher ^{137}Cs levels north of $57^{\circ}00'N$ in August (relative to May) could reflect the arrival north of the "high" southern levels observed in May 1983, hence implying a transit time of about 3 months from the southern HSA to latitude $58^{\circ}00'N$.

The ^{137}Cs / salinity curve (Figure 4.2.b4) shows most points on or near the curve, with inshore samples falling to the left of the line, exhibiting more fresh water influence, e.g. transects B and E, stations K1, Y1 and Y2. Because of the partial blocking of the North Channel, the curve is disrupted across the CSA entrance and much lower ^{137}Cs levels are found in the North Channel than were observed in May

1983.

ii) Summary

1) Atlantic water influence was more marked - south of 57°N - in this cruise than in May 1983 as shown by a) the more easterly position of the Islay Front, b) generally higher salinities and lower radiocaesium levels in the southern HSA, c) high salinities and lower radiocaesium levels in the North Channel and 4) greater restriction of the coastal current, in the southern HSA, to the west coast of Scotland.

2) North of 57°N , however, radiocaesium levels were higher in this cruise than in May, perhaps marking the arrival of the earlier (May) enhanced levels in the southern HSA. If so, a water transit time, from the southern HSA to the Minches, of ~ 3 months is suggested.

3) Blockage of the "normal" northwards flow of water through the North Channel was observed at the time of the cruise and a southerly flow through the North Channel, caused by Atlantic inflow along the Northern Irish coastline from the north west, was identified.

4.2(c) January 1984

i) Results and Discussion

This cruise was not as extensive as the two cruises already discussed. Samples for radiocaesium analysis (25 in total) were collected only as far north as transect G - about latitude $56^{\circ} 50' N$ - and as far south as transect A - the northern exit of the North Channel (see Figure 4.2.c1); no sub-surface samples or CTD profiles were taken.

The most notable feature of this winter cruise is the considerable dilution of the radiocaesium plume as evidenced by the relatively high salinities and low ^{137}Cs levels - in Figures 4.2.c2 and 4.2.c3 respectively - compared to values from the previous cruises. For example, the maximum salinities found in the North Channel in August 1983 and May 1983 were 34.248‰ and 33.877‰ respectively whilst for this cruise salinities reached 34.500‰ (Appendices II.1-3) the corresponding maximum ^{137}Cs levels for the August and May 1983 cruises at transect A were 53.1 dpm/l and 35.5 dpm/l respectively compared to 25.3 dpm/l for this cruise (Appendices II.1-3). Apart from inshore regions exhibiting significant fresh water dilution (see below), high salinities and low ^{137}Cs levels prevailed throughout the area under investigation; this pattern is highlighted by the easterly position of the 34.5‰ isohaline compared to its more western positions in the previous two cruises.

The shapes of the ^{137}Cs and salinity contours indicate northward flow at transect A; thus, irrespective of the high salinities in the North Channel, there was no blocking of the northward flow of Irish Sea / CSA water through the North Channel.

Figure 4.2.c1

Station Positions - January 1984 Cruise.

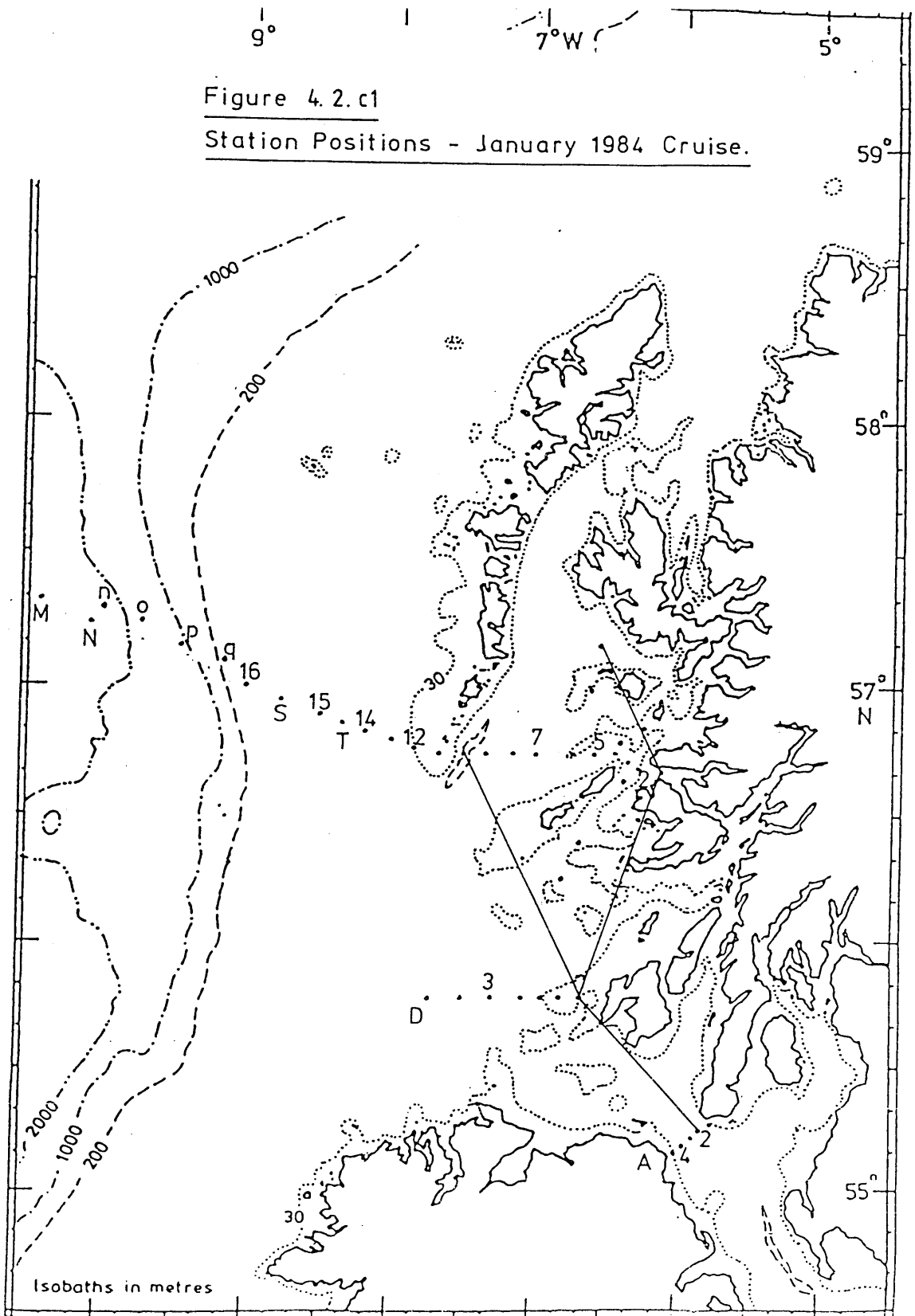


Figure 4.2.c2

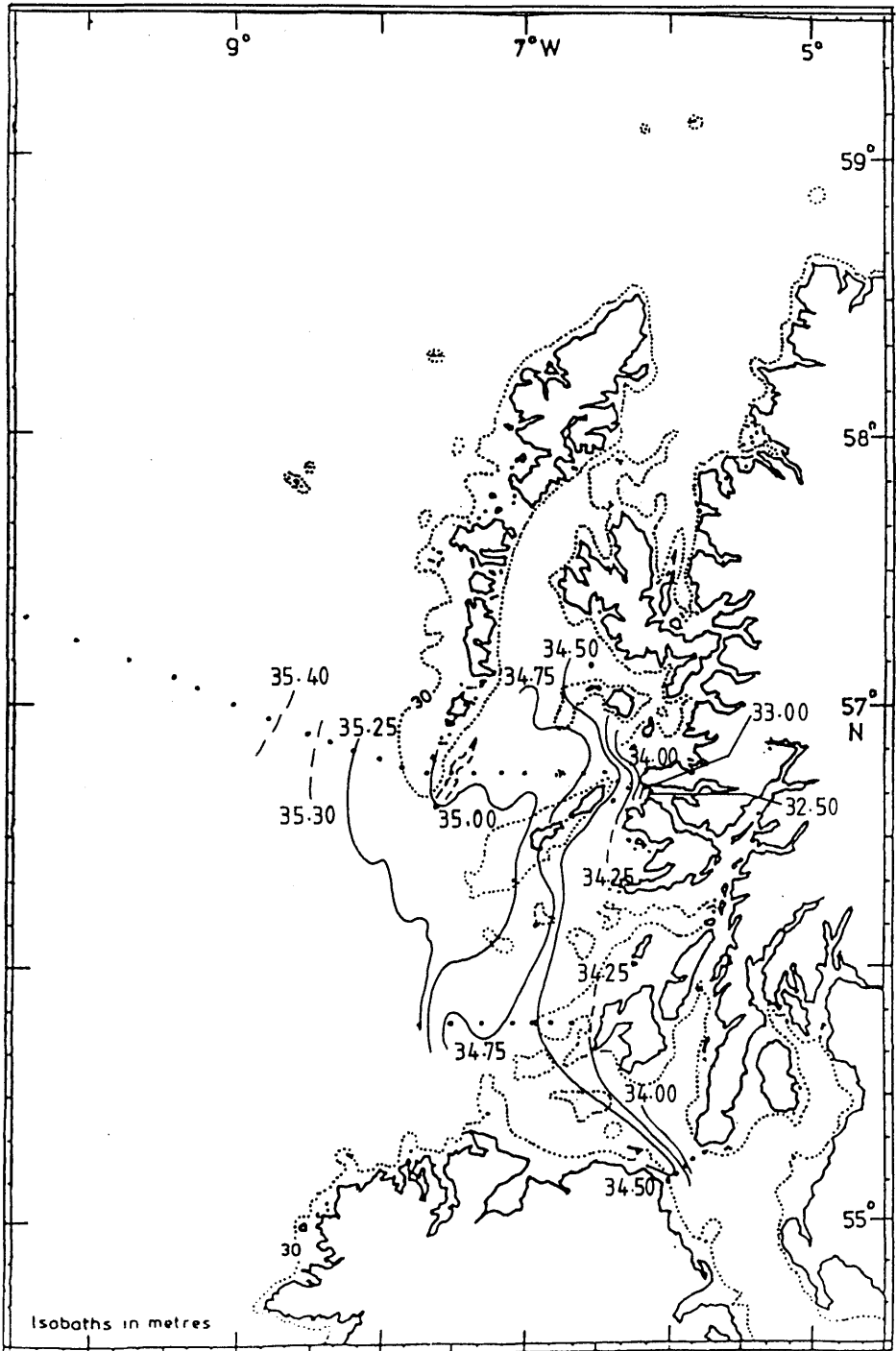
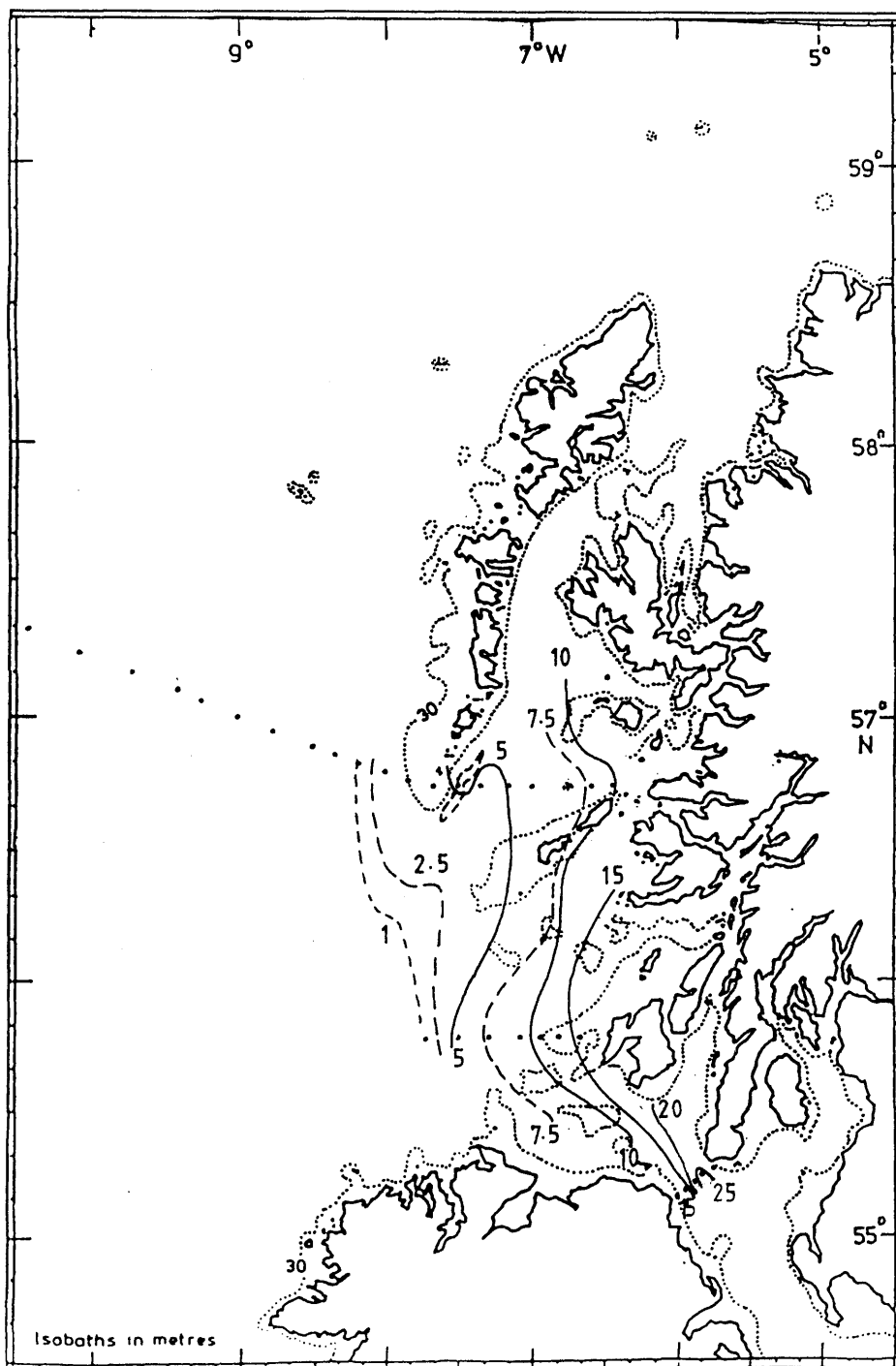
Salinity Contours (‰) - January 1984 Cruise

Figure 4.2.c3

^{137}Cs Contours (dpm/l) - January 1984 Cruise

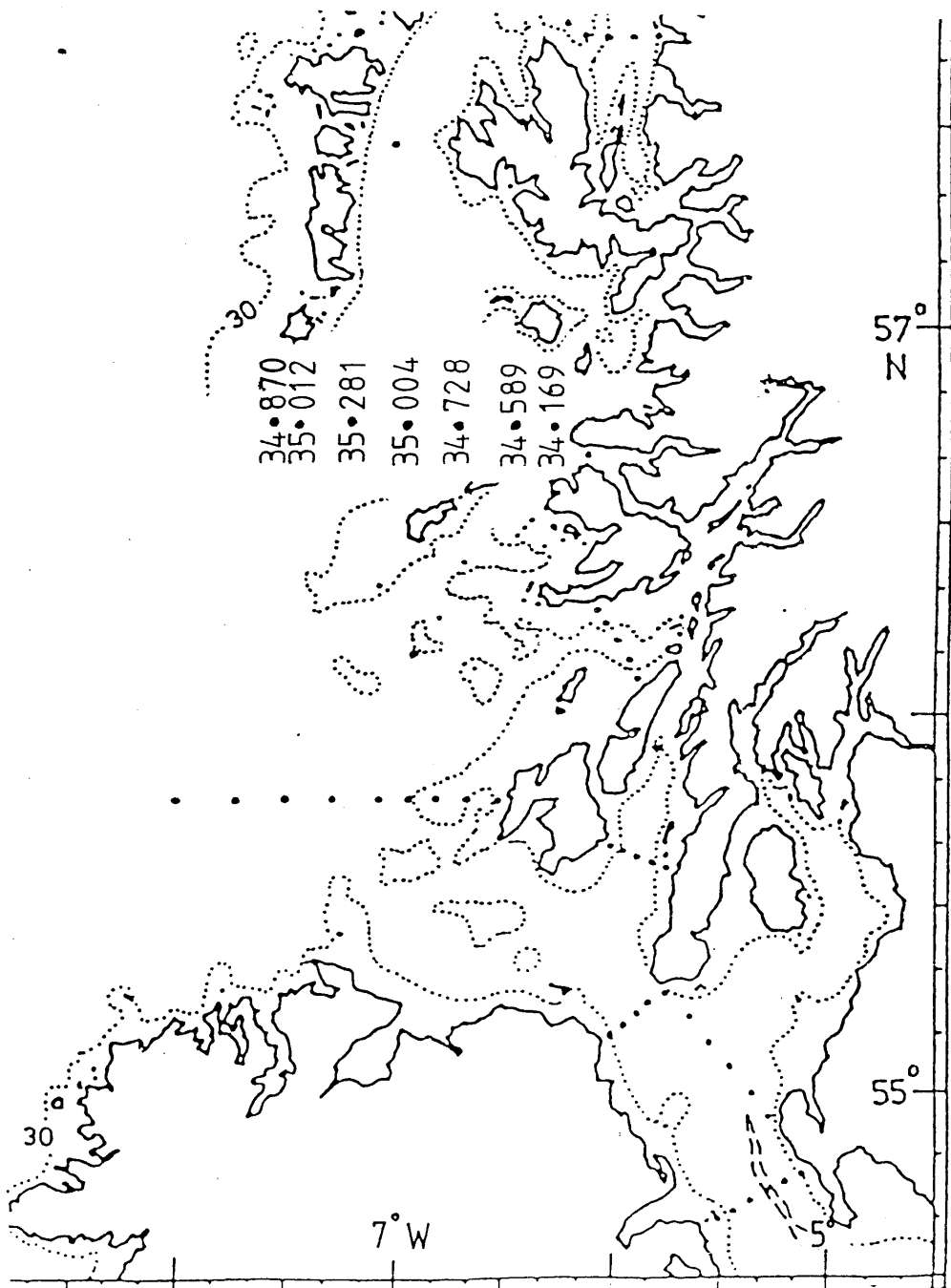


This contrasts with the August 1983 situation, when salinities were markedly lower than those of this cruise yet the flow appeared to have been obstructed. Although it is the Atlantic's incursion into the North Channel which blocks the northward flow and the extent of Atlantic influence is indicated by salinity (and radiocaesium), it is not the actual measured salinities but their distribution, i.e. the shape and pattern of the isohalines, which indicates the behaviour of Atlantic flow. Thus, although salinities were relatively high during this cruise, the Atlantic was not necessarily exerting major influence on the southern HSA and North Channel current flow at the time of the cruise.

The Islay Front can be seen to lie at a relatively western position, around $7^{\circ}30'$ - $7^{\circ}50'W$, similar to, but perhaps more intense than, the May 1983 front. This westerly positioning of the front suggests that Atlantic water penetration into the southern HSA was not noticeably stronger than in August 1983, when it was further to the east and coincident with blockage of the North Channel's northward flow.

At first, this suggestion of "weak" incursion of the Atlantic in the southern HSA seems to be paradoxical to the relatively high salinities noted throughout the area; this is analogous to the situation in the North Channel - high salinities but no strong incursion of oceanic water to block northward flow. The observed situation, therefore, could be indicative of the withdrawal of Atlantic water from the southern HSA following an earlier incursion when salinities higher and the Islay Front further to the east. Thus, the high salinity values reflect the behaviour of the Atlantic water prior to this cruise whilst the salinity distribution reflects the present behaviour of the oceanic water. Indeed, a transect from Barra

Figure 4.2.c4

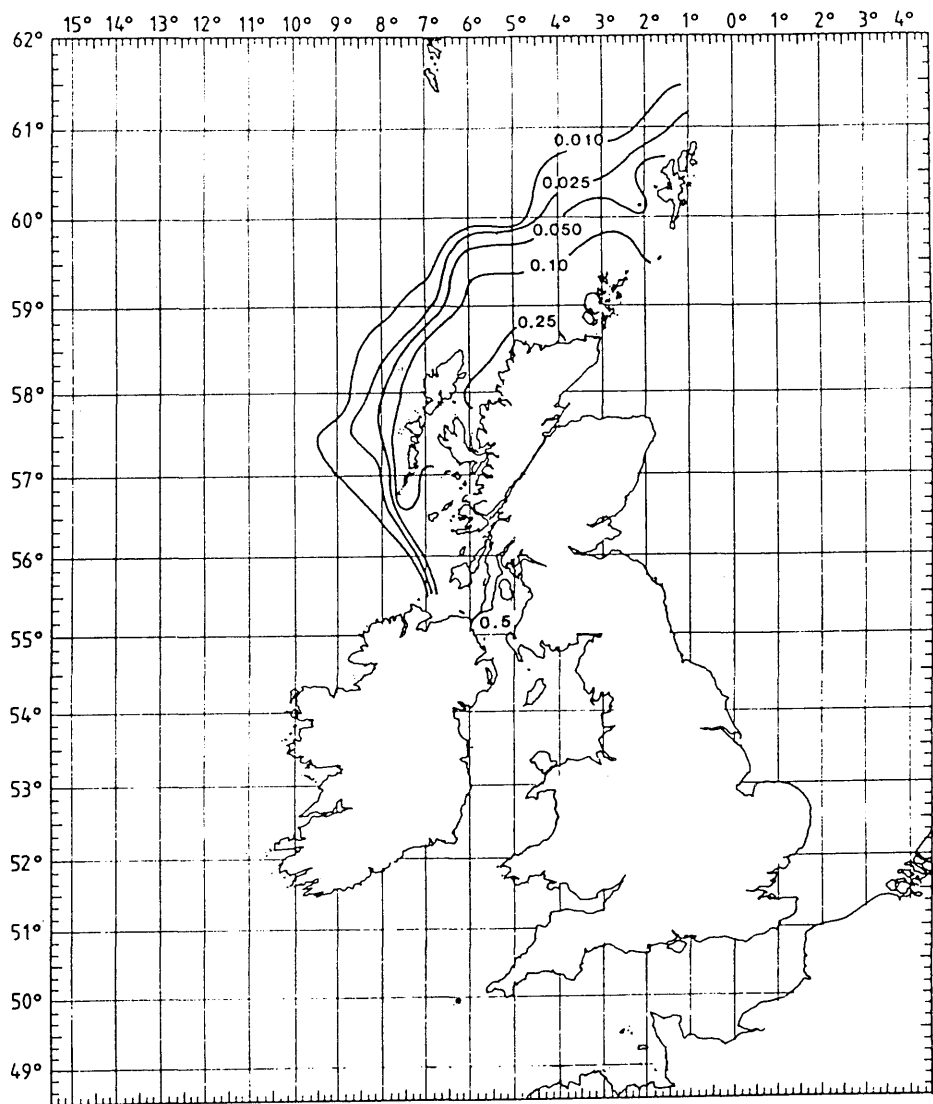
Salinities (‰) Across Transect G (17/11/83)

Head towards Coll near station G3 on 17th November 1983 was monitored for salinities by SMBA and revealed even higher salinities than those observed in this cruise (Figure 4.2.c4). The maximum salinity in the November transect was 35.281‰, by far the highest salinity measured across this transect during all the cruises. This evidence supports the suggestion that an influx of saline Atlantic water into the southern HSA had occurred prior to January 1984. At this stage, it seems appropriate to refer to a MAFF cruise in the HSA in October 1983 (Hunt, 1984, pers. comm.) which, from ^{137}Cs contours, shows the Islay Front at $6^{\circ}40' - 7^{\circ}00'W$, the most easterly position recorded for the front thus far (Figure 4.2.c5). MAFF radiocaesium data for the transect from Barra Head to near Coll are presented in Table 4.2.c1 and show an extremely low ^{137}Cs content at station G9 - where the salinity reached 35.281‰ in the November 1983 transect - and lower ^{137}Cs levels than in January 1984 at all stations except for G11 - where the salinity was only 34.870‰.

From the data thus far, then, it is likely that a strong incursion of Atlantic water into the southern HSA occurred around October 1983 and that residual saline Atlantic water was still detectable in the HSA in January 1984, though, by this time, the oceanic influence had begun to withdraw.

Although no samples were collected south of transect A during this cruise, the monthly CSA sampling programme has provided a sample coinciding with the exact time of the cruise. From the monthly ^{137}Cs levels measured in the CSA (Figure 3.2, Chapter 3), a sharp decrease is noted in early February (9/2/84) which is too sudden (on the scale of ~1 week) to have arisen from the Sellafield radiocaesium discharge trend. It could have resulted, however, from the Atlantic incursion into the HSA (described above): the incursion

Figure 4.2.c5



Concentration (Bq kg⁻¹) of caesium-137 in filtered surface water from the north-west of Scotland, October 1983 (Hunt, 1985).

Table 4.2. c1

¹³⁷Cs Levels Across Transect G, October/November 1983,
as Determined by MAFF (Hunt, 1984, pers. comm.)

<u>Station</u>	<u>¹³⁷Cs Level (dpm/l)</u>
G2	12.4
G4	8.2
G6	6.7
G7	3.2
G9	0.4
G11	5.1

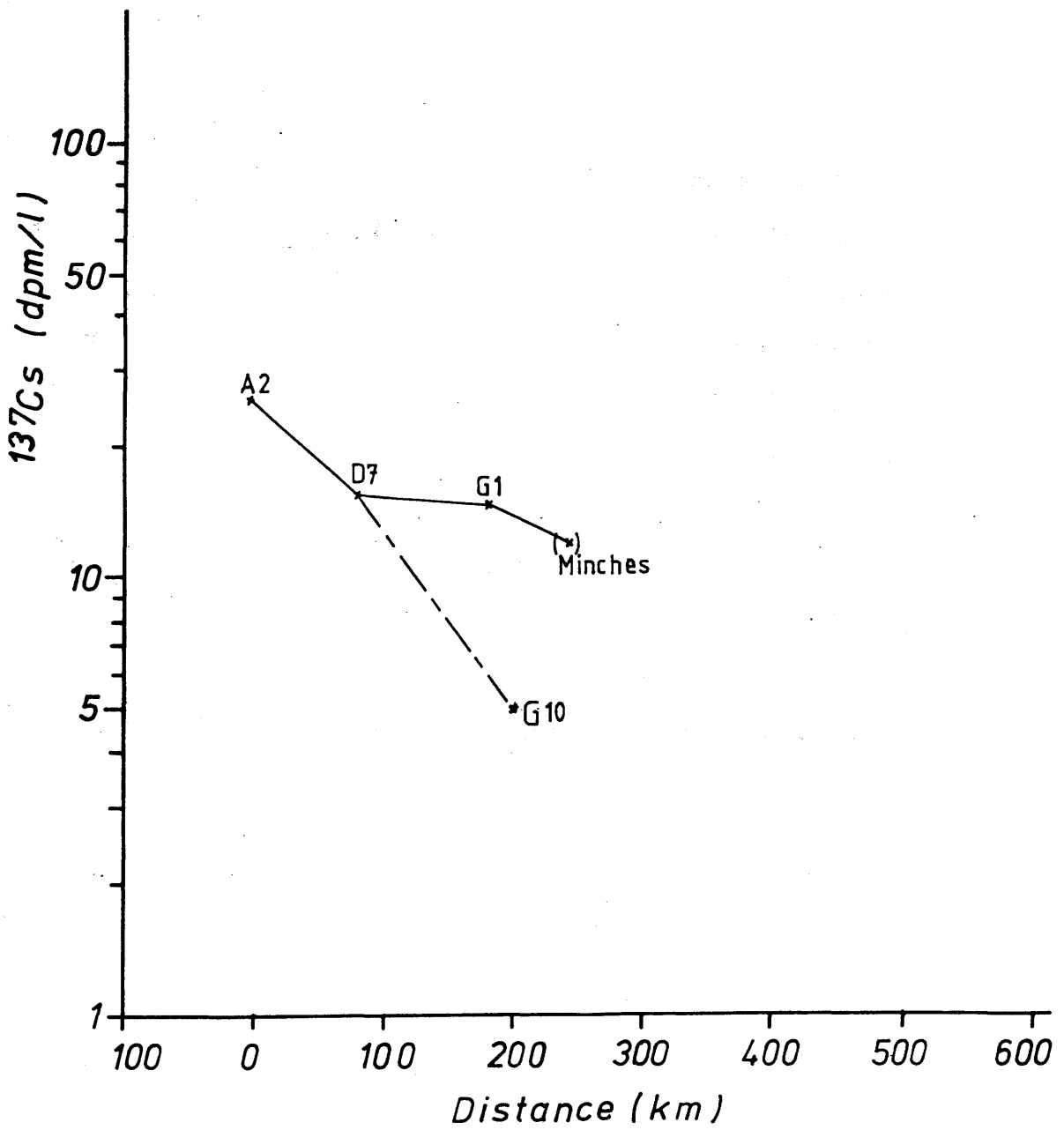
may not have influenced the region south of transect A (the North Channel) until about the time of the January 1984 cruise and appeared only for a brief period in the CSA around 9/2/84. Indeed, ^{137}Cs levels in October 1983 across the northern exit of the North Channel (30 dpm/l) were overall noticeably higher than those found in January 1984 (11.2 - 25.3 dpm/l). If the Atlantic incursion was directed towards the Little Minch area, i.e. northeastwards, as indicated in the January 1984 cruise data, then any effect on the North Channel, i.e. southeastwards to the Atlantic, would be expected to be less intense and to appear at a later stage; thus, the decrease in ^{137}Cs levels in this region may have occurred as a delayed response to the earlier decrease in the HSA.

In Figure 4.2.c6, radiocaesium levels along the path of the plume are plotted against distance (see Figure 4.2.c1 for sections concerned). ^{137}Cs levels were higher to the east than to the west of the Outer Hebrides because of the lower salinities in the former. From transect G, only G1, G2 and G3 had ^{137}Cs concentrations of >10 dpm/l and salinities of $<34.550\%$; hence the plume was very much confined to inshore regions of the west coast of Scotland at this latitude ($56^{\circ}45'\text{N}$), with ^{137}Cs levels west of Coll (≈ 7 dpm/l) being only about half the maximum levels measured (14.8 dpm/l) at the easternmost station, G1. West of the Outer Hebrides, ^{137}Cs levels were found to be below 5 dpm/l; furthermore, whereas in the previous 2 cruises the isopleths around the Islay Front region spread out extensively on reaching latitude $57^{\circ}00'\text{N}$ and occurred mostly to the west of the Outer Hebrides, they occurred further to the east in this cruise; thus the coastal current was highly restricted to inshore areas at this latitude.

The rate of dilution of the plume (Figure 4.2.c6) along the

Figure 4.2.c6

^{137}Cs Along Main Path of
Plume (From North Channel)
January 1984



western route was similar to that for the North Channel to HSA sector whereas, in the eastern branch, dilution was considerably slower. Overall, then, we see a pattern of relatively slow reduction of ^{137}Cs levels latitudinally, i.e. along the path of the plume, but faster dilution longitudinally - across the path of flow. Sections 4.3(b), (e) also deal with dilution of the radiocaesium plume during its travel.

From Figure 4.2.c7, the ^{137}Cs / salinity curve, stations A1, A2, G1 and D2 fall noticeably to the left of the curve, the rest of the stations exhibiting similar degrees of fresh water dilution and hence falling on or close to the curve. Whereas stations A1, A2 and G1 are liable to more fresh water dilution because of their inshore positions, the same cannot be said for station D2. Here, the indication is that water from the current around the northern coast of Ireland was flowing north between the Atlantic water and the Scottish coastal current water (see Figure 4.2.c2) and was of lower salinity than Atlantic water, thus appearing to have a slight fresh water dilution effect on the Irish Sea-derived water.

ii) Summary

1) Although high salinities and low radiocaesium levels prevailed throughout the southern HSA and North Channel at the time of this cruise, the salinity distribution indicates withdrawal of Atlantic influence in these region. It is therefore suggested that an earlier incursion of Atlantic water (around October / November 1983) had introduced the observed high salinities in the HSA but, at the time of this cruise, was withdrawing as evidenced by the westerly position of the Islay Front.

2) The coastal current was largely restricted to inshore regions, especially north of about 56° 30'N, with dilution of the radiocaesium plume being greater longitudinally than in the direction of the plume's travel.

3) A short, sudden drop in radiocaesium levels in the CSA is thought to have been the result of a delayed response to the Atlantic water's incursion into the southern HSA.

4) The deviation of station D2 data to the left side of the ¹³⁷Cs/salinity curve is attributed to dilution of Irish Sea-derived water by water travelling northwards via the northwestern coast of Ireland.

4.2(d) April / May 1984

i) Results and Discussion

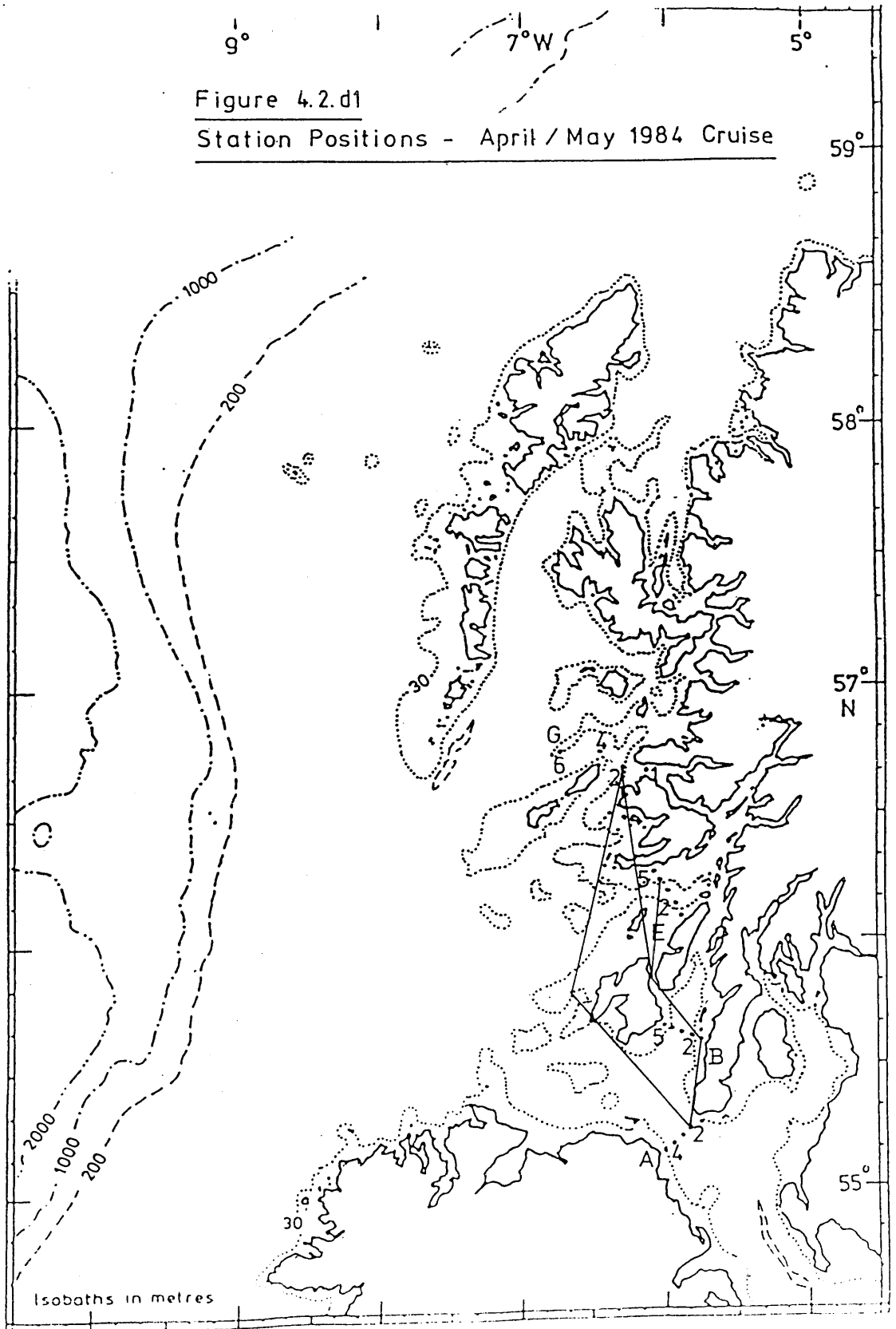
This cruise was not extensive (Figure 4.2.d1); 14 stations - transects A, E and B - were sampled for radiocaesium content analyses at Glasgow University (GU) with 11 additional samples (from stations G1, G2, G4 and G6 - 4 surface, 7 subsurface) being similarly assessed by MAFF.

Figures 4.2.d2 and 4.2.d3 show the salinity and ^{137}Cs distributions respectively for this cruise. The ^{137}Cs levels were found to have increased since January 1984 - when the radiocaesium plume had undergone considerable dilution by relatively saline waters - and the salinities to have decreased in the North Channel; transects B and E cannot be compared since they were not sampled in the earlier cruise. Figure 4.2.d4 indicates that minimal dilution of the plume occurred between the northern exit of the North Channel to transect B (across the Sound of Jura), i.e. for the branch of water travelling to the east of Islay, but this was followed by more extensive dilution en route to transect E (across the Firth of Lorn) and to transect G (north of Mull). The extent of dilution via the path to the west of Islay is unknown since data are unavailable south of transect G. However, the net dilution during water transit from the North Channel to station G2 via the west of Islay is more severe than that via the east of Islay.

Because of the limited data set here, it is not possible to generate a satisfactory ^{137}Cs / salinity curve (Figure 4.2.d5). It is not clear, for example, whether stations at transect E have undergone only fresh water dilution relative to those at transect B or whether

Figure 4.2.d1

Station Positions - April / May 1984 Cruise



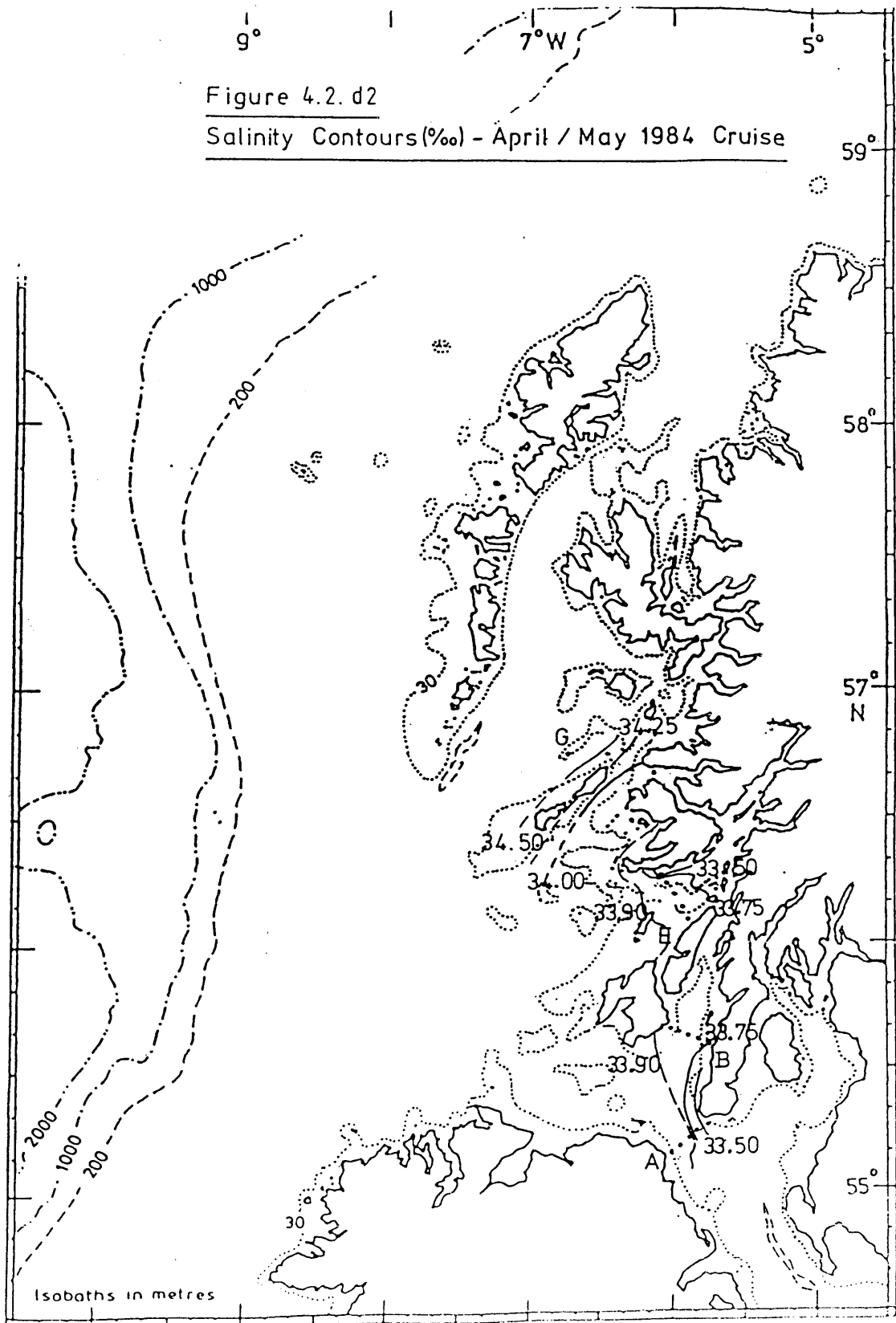


Figure 4.2.d3

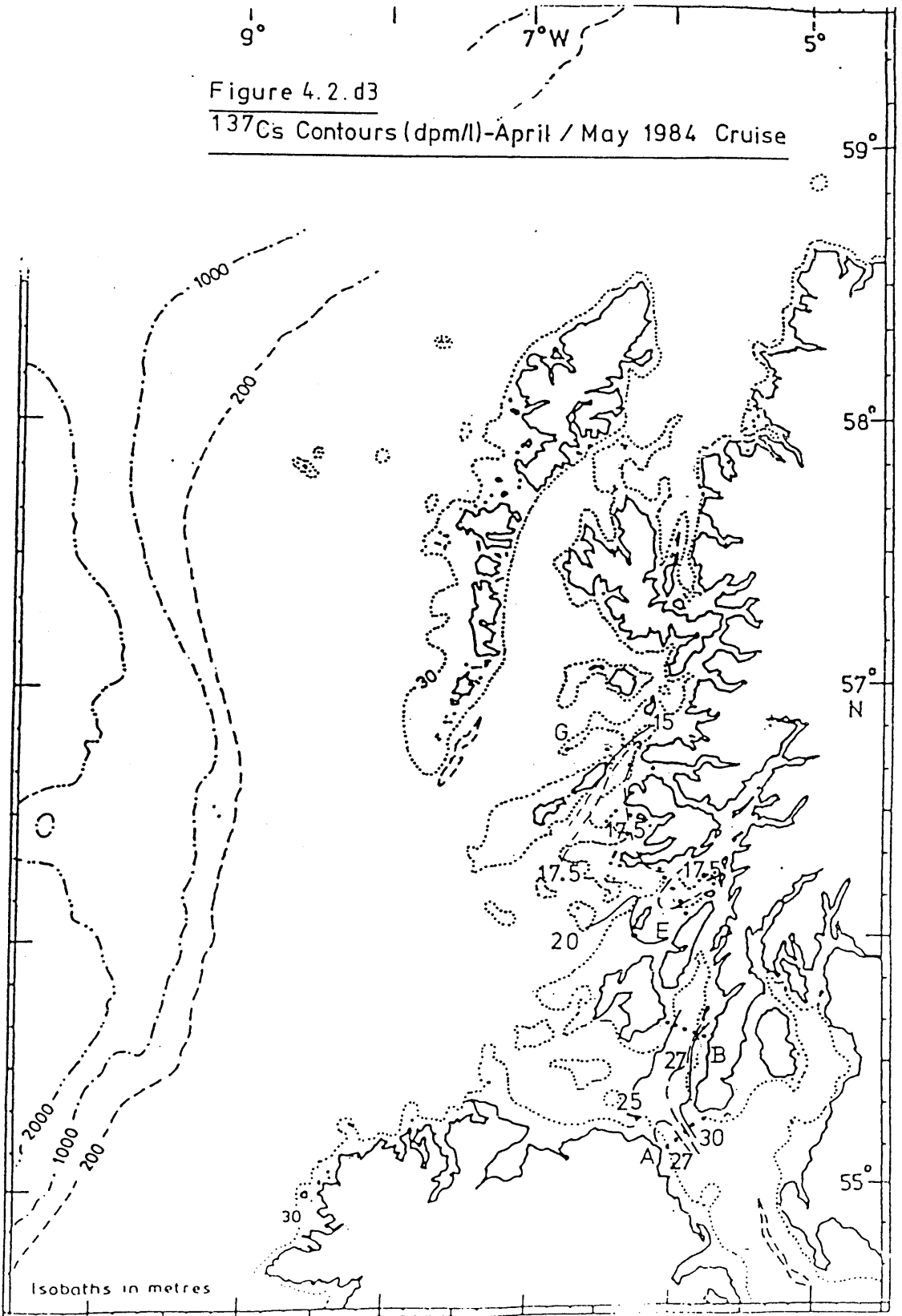
 ^{137}Cs Contours (dpm/l)-April / May 1984 Cruise

Figure 4.2.d4

^{137}Cs Along Main Path of
Plume (From North Channel)

April / May 1984

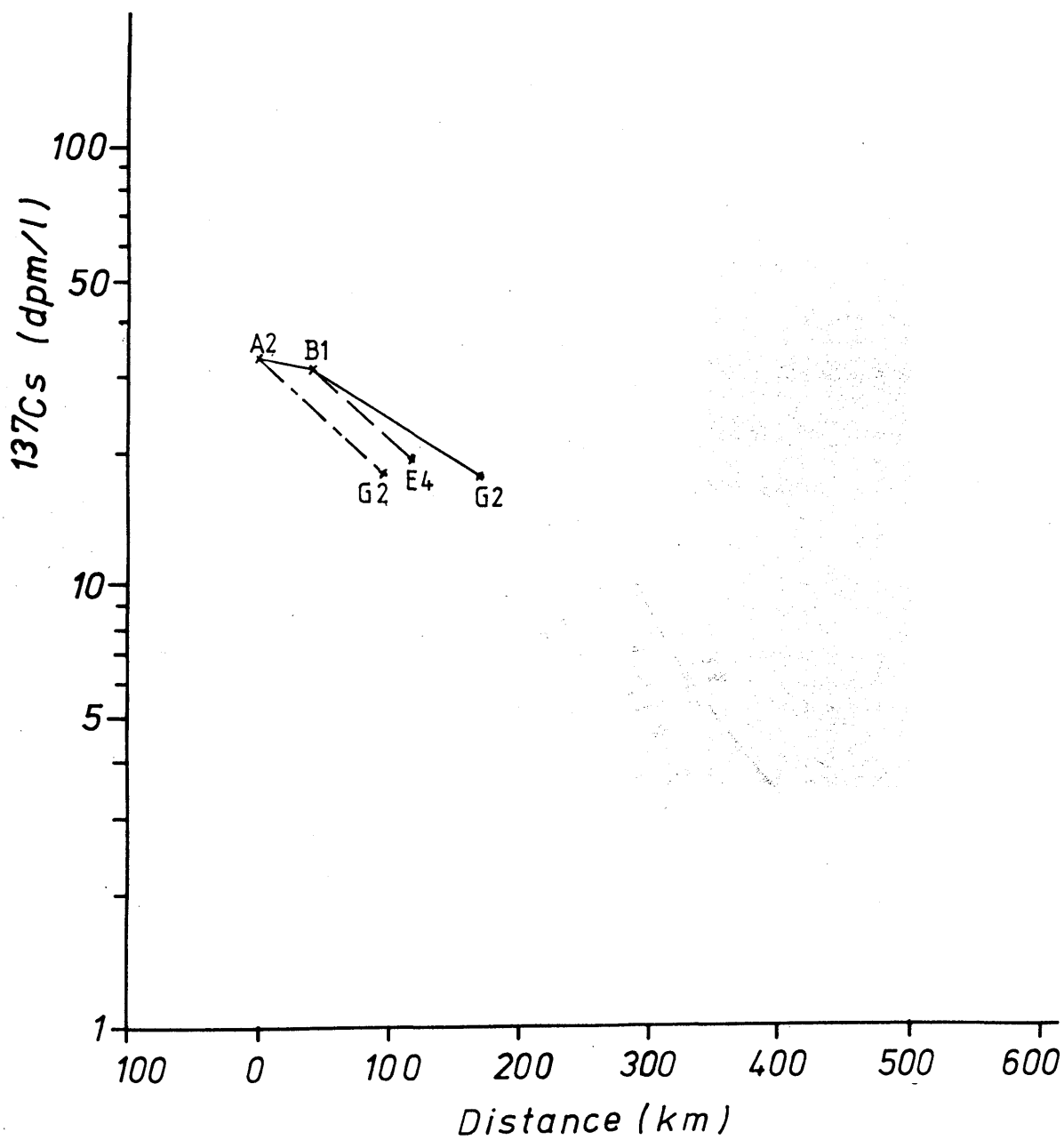
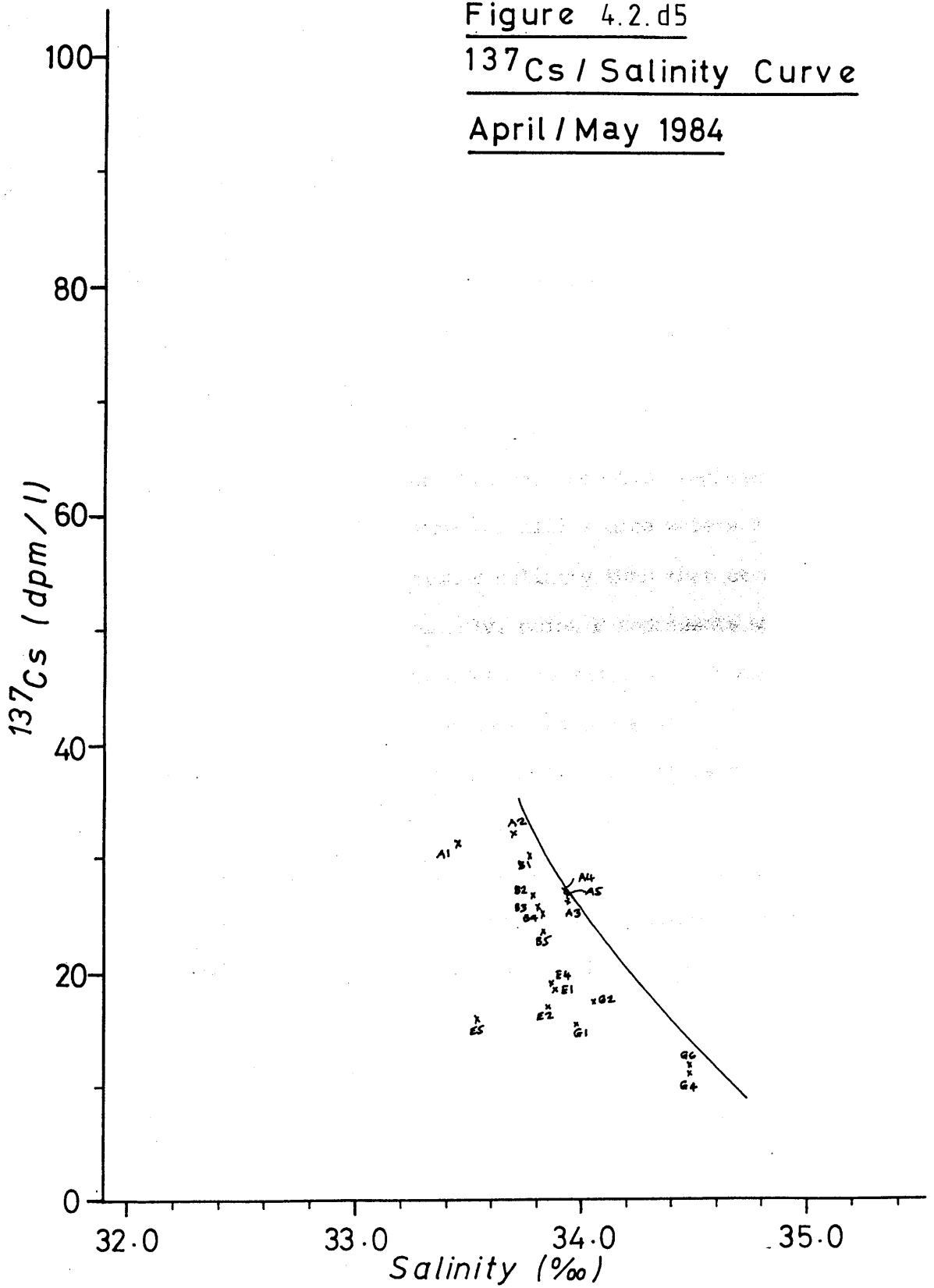


Figure 4.2.d5

 ^{137}Cs / Salinity CurveApril / May 1984

the dilution of the ^{137}Cs is due also to mixing with saline waters. However, a general pattern of dilutions can be seen with most extensive dilution at A1, G1 and across transect E.

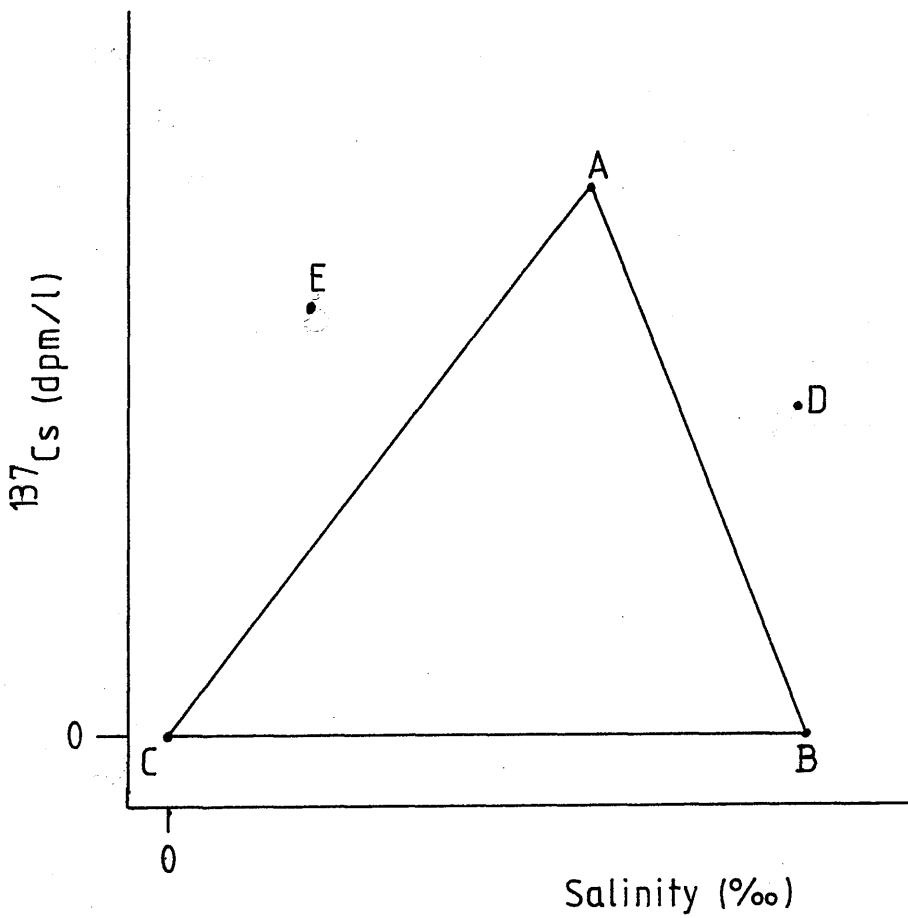
As explained in subsection 4.2(a), the 3 main source water types mixing in the area under investigation are Atlantic water (high salinity, essentially no radiocaesium), fresh water (no salinity and negligible radiocaesium) and Irish Sea-derived water (34.0‰ salinity, high radiocaesium). Any mixture of these waters in any proportion will be represented on a ^{137}Cs / salinity diagram within the triangle drawn through the 3 source points - A, B and C in Figure 4.2.d6. No water types outwith the triangle can be produced without an additional source water. Hence from Figure 4.2.d6, point D represents water produced by mixing of not only some (or all) source waters A, B and C but also with a water type of higher salinity than that at A with or without radiocaesium input; similarly, point E represents water which could have been produced by mixing with an additional water type of lower salinity (than that at A) and some radiocaesium.

Since in this system there is only one relevant source of radiocaesium (Chapter 1), water types represented by point D in Figure 4.2.d6 cannot be produced since this requires an additional input of radiocaesium and / or salt. Similarly, a low salinity source of radiocaesium does not exist to produce point E.

Instead of using the mixing triangle to mark the boundaries of the possible water types produceable from mixing of source waters, the main ^{137}Cs / salinity curve drawn through the points could be used to mark the extent of water types produced, since points falling to the right hand side of it, although still within the "triangle", have not been observed in this region of interest. Because the curve in this case is not as complete as those for other cruises (it is drawn from

Figure 4.2.d6

^{137}Cs / Salinity Plot for Mixing of
Three Water Types (A, B and C)



few data points), any deductions on its use as a marker for the boundary between "produceable" and "non-produceable" water types are made tentatively. From Figure 4.2.d5, then, it seems that water at station B1 probably did not originate from water at station A1 - which experienced fresh water dilution (probably from the CSA) - since this would have required mixing between station A1 - type water and a component whose characteristics would be represented by a point to the right hand side of station B1 along a straight line through A1 and B1. Such a point may well occur on to the right of the ^{137}Cs / salinity curve, in which case, it would appear safer to assume that B1-type water arose from water passing via station A2.

This method of deduction of possible paths for the radiocaesium plume has been employed during preparation of the plot of ^{137}Cs against distance. Defining the probable route for the coastal current in this way was relevant in cases where fresh water dilution had been significant but the ^{137}Cs level was still at the maximum value observed across that particular transect. In those cases where the water at that transect could not generate water further along the path of the coastal current then another route was chosen as the path for the radiocaesium plume.

ii) Summary

1) Because of the limited data for this cruise, it has been difficult to carry out extensive interpretation. In general, salinities were quite low in the North Channel (similar to May 1983) relative to August 1983 and January 1984; the mean ^{137}Cs level across transect A (28.9 dpm/l) of the North Channel was higher than for these two previous cruises (August 1983 - 25.3 dpm/l, January 1984 - 18.7

dpm/l). Hence Atlantic influence in the southern HSA appears to have been weak with no obvious severe restriction of the radiocaesium plume towards the mainland.

2) A method for assessing the possible routes of transport for the radiocaesium coastal current has been discussed.

4.2(e) June / July 1984

i) Results and Discussion

During this cruise 82 water samples were collected for analysis of radiocaesium (Figure 4.2.e1), 59 from the surface and 23 from depth; some samples were obtained within the Irish Sea. Radiocaesium data in addition to those from the 82 samples analysed at GU were obtained either from MAFF (Appendix II.5) or by extrapolation from known salinities (see section 4.2.a). Figures 4.2.e2 and 4.2.e3 show the surface salinity and ^{137}Cs distribution patterns respectively.

Figure 4.2.e3 shows that radiocaesium levels in the North Channel (transect A) had decreased since the previous cruise (May 1984) (whereas the CSA level (station GMT 7) was higher just prior to this cruise than during the last cruise). This difference probably reflects a 1-2 month delay time between the North Channel and the CSA, the residence half-time of water in the CSA having been estimated at ~1-2 months (McKinley et al., 1981b; Edwards, 1986, pers. comm.) If so, the lower North Channel ^{137}Cs levels for this cruise would predict a future lowering of CSA ^{137}Cs levels. From Figure 3.3 (Chapter 3) we can, in fact, recognise a significant drop in CSA levels at the end of July 1984, about 10 days after the cruise ended.

The salinity contours (Figure 4.2.e2) in conjunction with the radiocaesium data show general northward transport of ^{137}Cs in surface waters of the mid- and eastern sections of the North Channel. In the western section, however, southward movement of surface water is indicated. As noted in the cruise of August 1983, the station of maximum ^{137}Cs level occurred not at the southeasternmost position of the North Channel but in the centre of the CSA entrance at station Y3.

Figure 4.2.e1

Station Positions - June / July 1984 Cruise

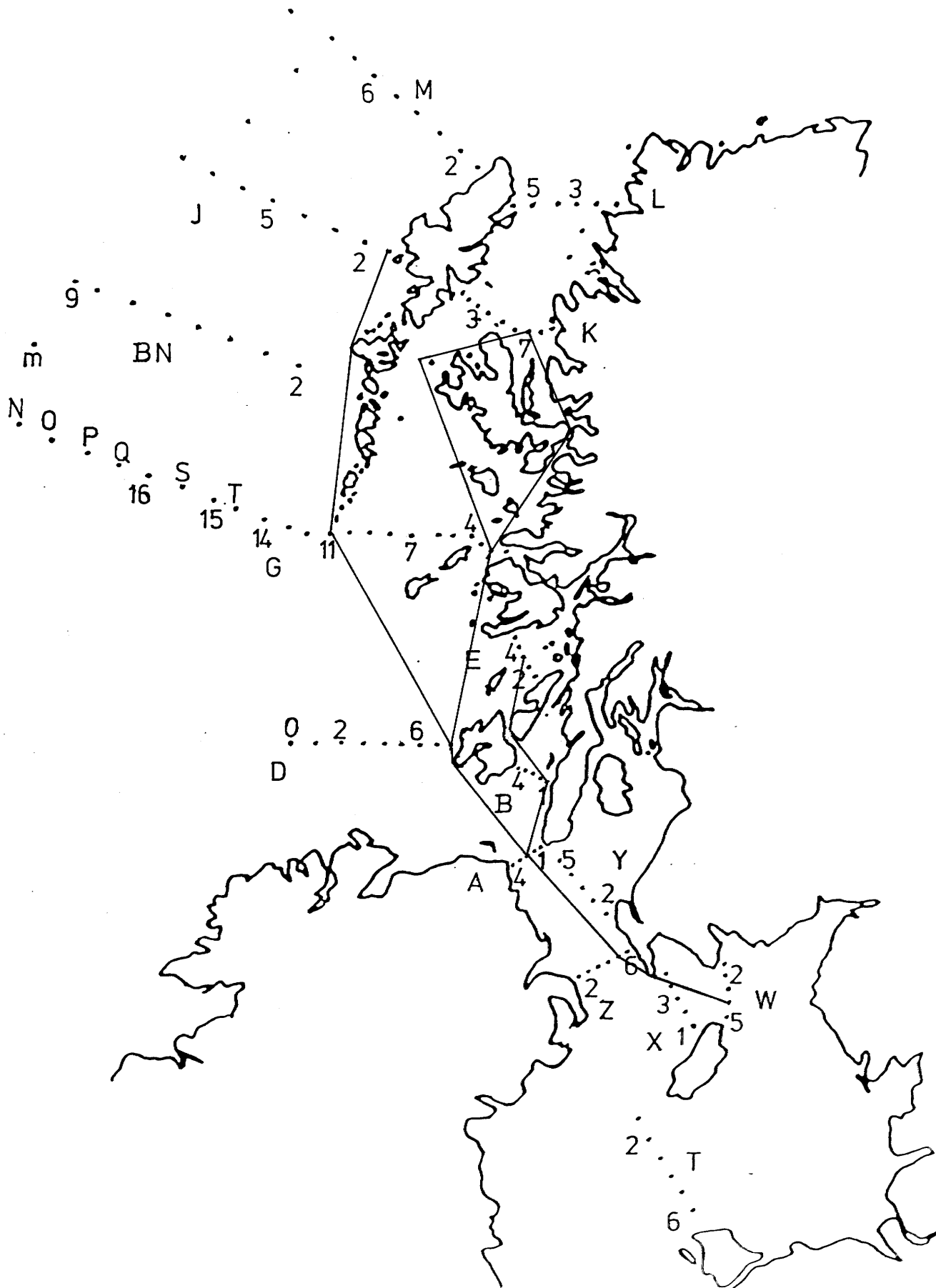


Figure 4. 2.e2

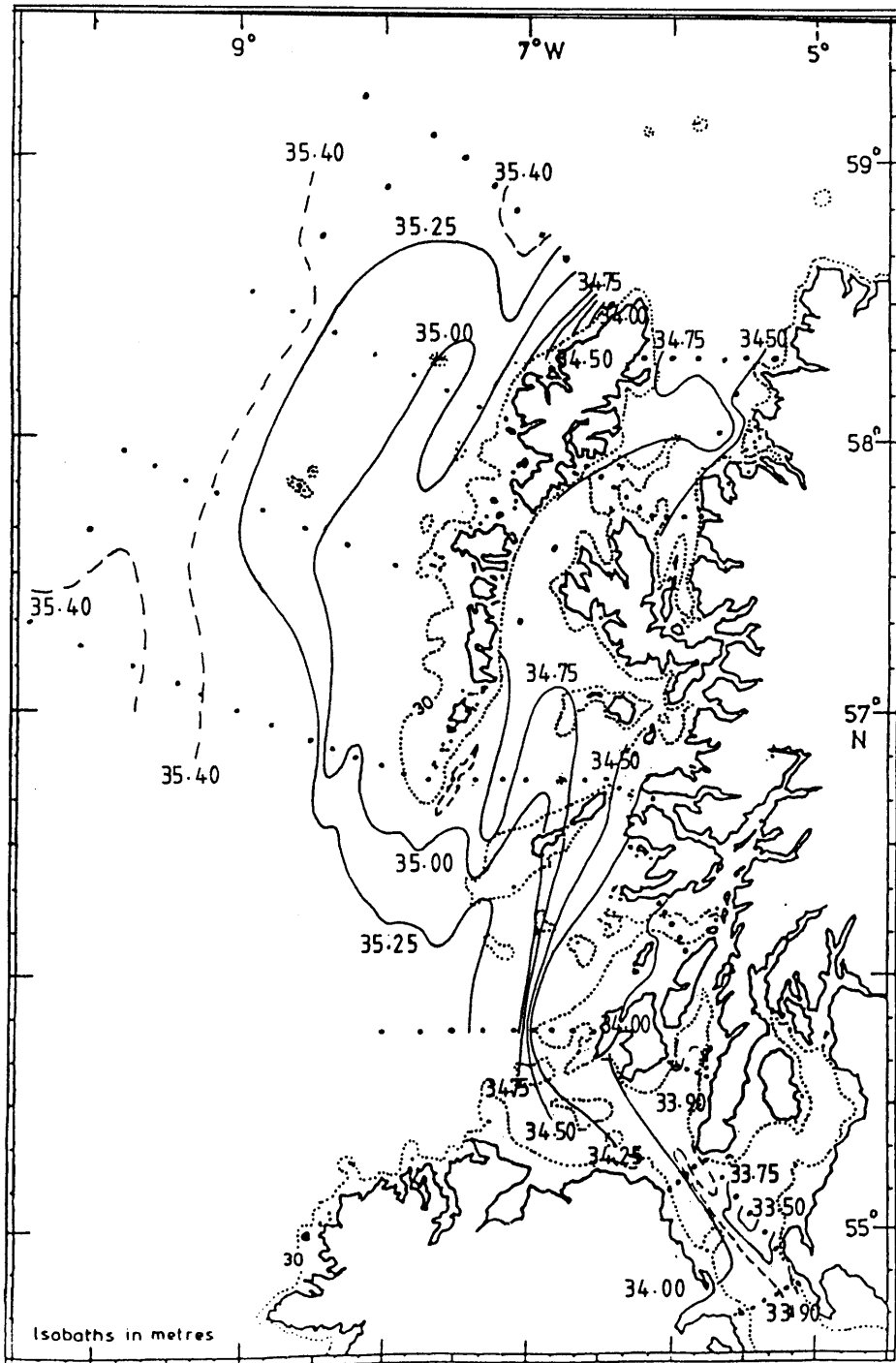
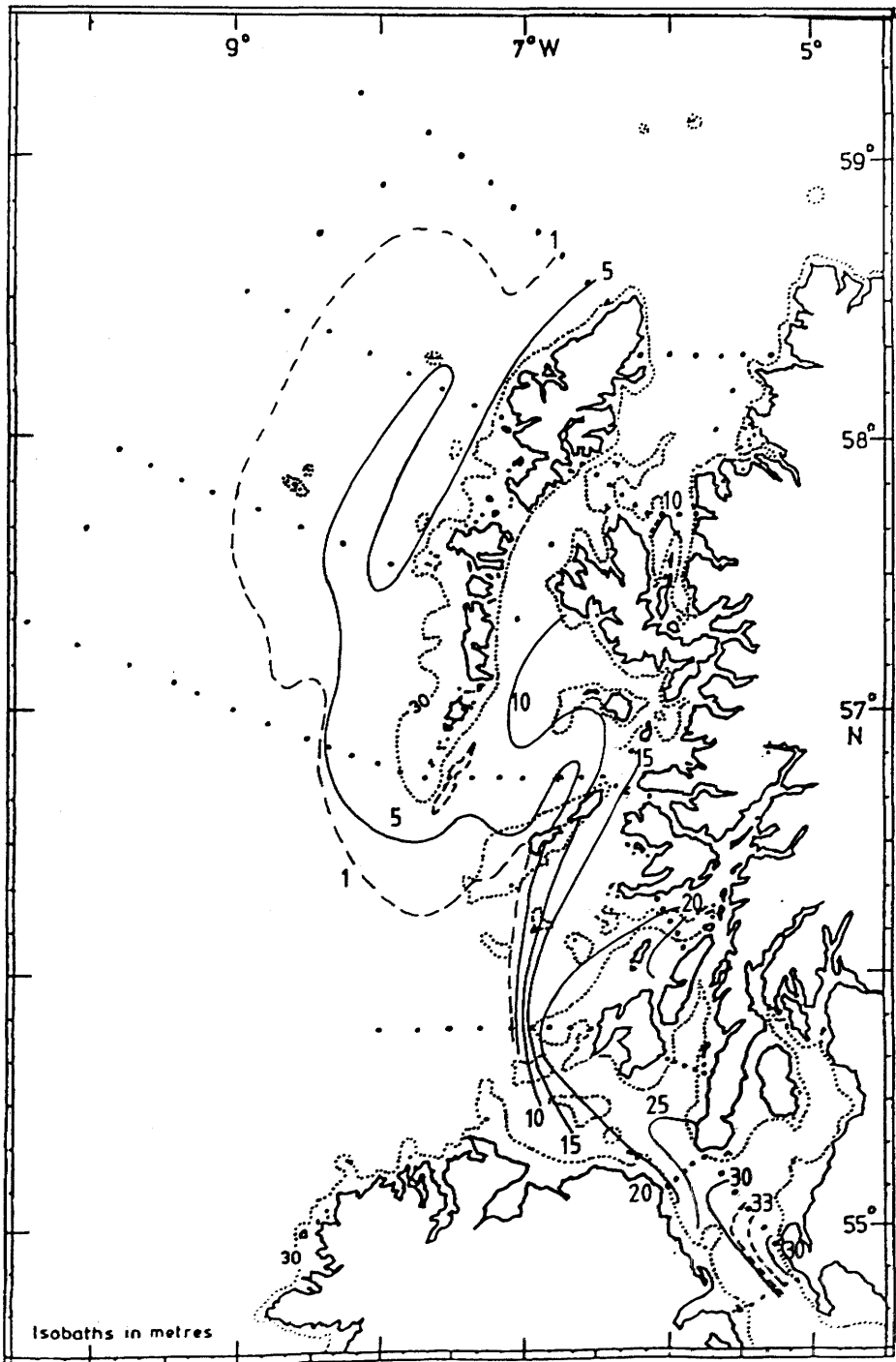
Salinity Contours (‰) - June/July 1984 Cruise

Figure 4.2. e3

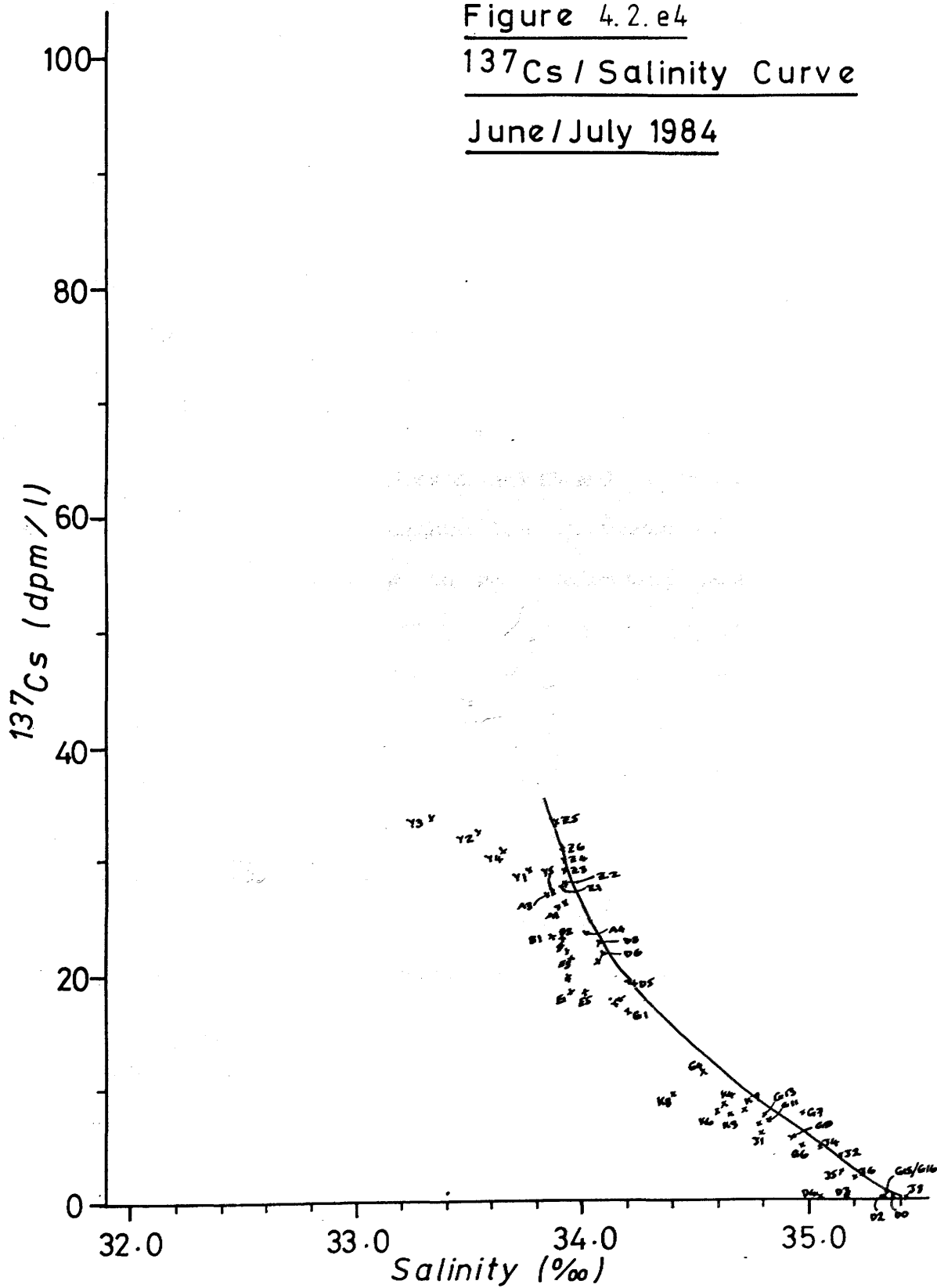
 ^{137}Cs Contours (dpm/l) - June / July 1984 Cruise

Although the difference between this maximum (33.6 ± 1.0 dpm/l) and the transect Z maximum (33.4 ± 0.5 dpm/l at station Z5) is within counting error and therefore not significant, the Y transect stations appear to have undergone fresh water dilution (they fall to the left side of the ^{137}Cs / salinity curve, (Figure 4.2.e4)) and, therefore, at salinities similar to those of transect Z ($>33.80\%$), they correspond to higher radiocaesium levels. If the low salinity was not a result of CSA runoff but represented Irish Sea water (undiluted by Atlantic water), then an interruption the northward flow in the North Channel must have occurred to have isolated this fraction of water at the entrance to the CSA. If this was the case, then stations Y2 and Y3 would actually have represented water of relatively low (i.e. recent) discharges compared to the surrounding waters in the North Channel. This is clearly not the case, i.e. water at Y2 and Y3 represent relatively high discharges, thus water at stations Y2 and Y3 seems to be "older" (higher ^{137}Cs discharge) water influenced by CSA fresh water runoff.

Further north, the radiocaesium and salinity distributions were found to be more or less uniform across the Sound of Jura, with higher radiocaesium levels here than across transect D - to the west of Islay. The Islay Front occurred at a longitude of $6^{\circ}50'W$, a relatively easterly position compared to its position in other cruises;

indeed, only the MAFF cruise of October 1983 showed such an extreme easterly position of the front. For this cruise, then, ^{137}Cs levels across the front dropped from 19.3 dpm/l to 0.5 dpm/l between stations D5 and D4, whilst the corresponding salinity change was an increase of 0.827% (from 34.237% to 35.064%). Thus Atlantic influence in the southern HSA was strong during this cruise, relatively high salinities entering the southern entrance to the Minch

Figure 4.2.e4

 ^{137}Cs / Salinity CurveJune/July 1984

(maximum of 34.994‰).

At the entrance to the Firth of Lorn, (transect E), the maximum ^{137}Cs value, 21.3 dpm/l, occurred at station E3 and was not much lower than the highest levels immediately east and west of Islay (22.5 dpm/l).

Comparison of salinities between this and the May 1984 cruise shows generally more saline water throughout the area in June / July. This trend was accompanied by lower ^{137}Cs levels across transects A and B but by higher values across transect E; Loch Etive and the CSA also exhibited higher radiocaesium levels at this time (Figure 3.5, Chapter 3). At transect G, radiocaesium levels for the two cruises were very similar between stations G1 and G5 and, although the data were limited for May 1984, slightly less confinement of the plume towards the coast is apparent in May, reflecting less Atlantic influence here at that time.

The indication thus far, then, is that the water entering the HSA via the North Channel was of lower ^{137}Cs content than older waters already present. In the CSA, at transects E and G and in Loch Etive the higher radiocaesium levels reflect older water of higher discharge and are indicative of the lag-times within the system.

Because of the confinement of the plume to the west coast during this cruise, ^{137}Cs levels entering the Little Minch were generally about twice those in water travelling along the "western branch", i.e. west of the Outer Hebrides.

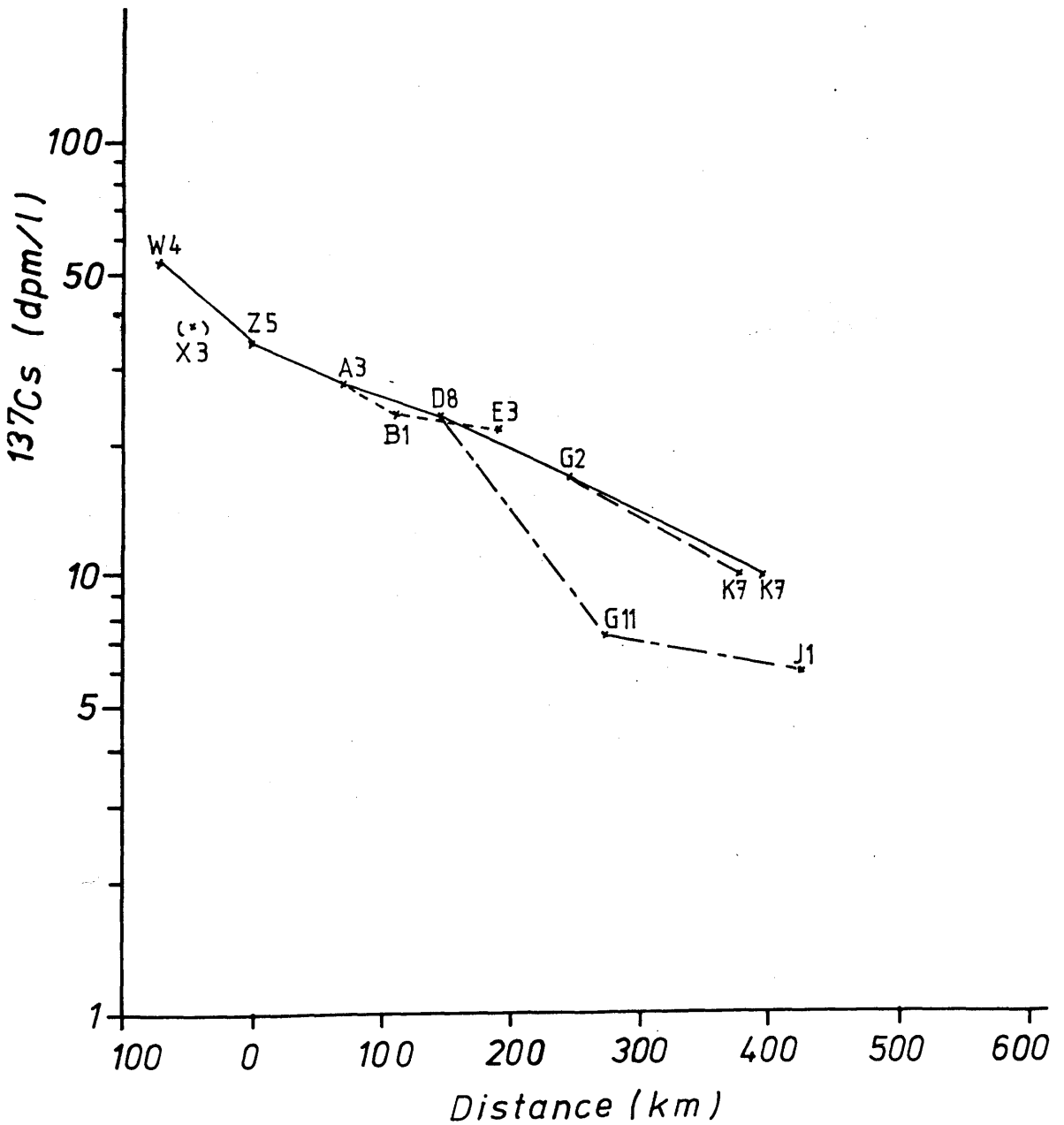
From the ^{137}Cs / salinity curve, (Figure 4.2.e4), the stations most noticeably exhibiting fresh water dilution include those specified in previous cruises, i.e. transect Y, transect E and B stations to a lesser extent and some transect A and inshore stations (e.g. K1 and K2 of The Minches). In this cruise, however, stations D3

and D4, both of which are immediately to the west of the Islay Front, also deviate. It is possible that this latter water represents slightly diluted Atlantic water from the coastal current which rounds the northwest coast of Ireland. There is, however, another explanation. It has already been stated (section 4.2.a) that for the ^{137}Cs / salinity curve to be usefully related to dilution patterns along the coastal current path and to mixing between the three source waters, the transit or flushing time of the water throughout the region must be sufficiently short that the "recently" discharged water entering the area does not lose its identity by mixing with residual ("older") water. It appears here that the lower section of the curve (<16 dpm/l) represents the more northern transects, J, K and G (i.e. older water) and that the upper section (>16 dpm/l) records more recently discharged water at the southerly stations, transects Z, A and Y. Since the Sellafield discharges in 1984 had decreased to about one third of the 1983 levels, the activity variations might be expected to be proportionally greater than actually observed. Indeed, the pattern of discharges might be expected to be recognised, to some extent, in various parts of the HSA at different times. However, mixing "en route" has reduced the variability, thus stations D3 and D4 may reflect mixing with recent discharges, as do stations D5 - D8, the North Channel and transect B stations (see above), whereas stations D0 - D2 are characteristic of mixing with the older, higher discharge waters. In this case, water at stations D3 and D4 have been diluted by saline Atlantic water sooner than water further eastwards (i.e. water which reached stations D5 - D8). This dilution could have occurred during incursion of Atlantic water into the southern HSA and would explain why stations D3 and D4 fall below the curve. However, the extent to which the latter occurs indicates that Atlantic dilution of

Figure 4.2. e5

^{137}Cs Along Main Path of
Plume (From North Channel)

June/July 1984



low discharge water may not have been the only cause and that fresh water dilution could also have played a part. This lower section of the curve is drawn mainly through the stations of the more northerly transects, J and K, the latter corresponding to higher (older) discharges. Recent low radiocaesium water entering southern areas would be expected, then, to be indicated in the next cruise (November 1984) by low levels in northerly regions: this prediction is examined on the ^{137}Cs / salinity curves for the two cruises in section 4.2(f).

Figure 4.2.e5 shows, on a log scale, measured ^{137}Cs levels against distance from transect Z of the North Channel. The greatest reduction in levels (along the main path of the plume) occurred within the Irish sea, from transect D to transect G - this being where the Atlantic water had penetrated significantly into the HSA - and from transect G to the Minches.

Data for the Irish Sea (Figures 4.2.e6 and 4.2.e7) show that the radiocaesium plume passed between the Isle of Man and Galloway, with maximum levels concentrated along the southern to central (i.e. the Isle of Man side) regions of the transects from the Isle of Man to Galloway; maximum radiocaesium levels were accompanied by minimum salinities. This suggests a direct route from Sellafield to the North Channel rather than a path following the coastline from Sellafield via the Solway Firth and to the North Channel. Levels across transect W varied between 44.1 and 50.1 dpm/l (minimum 87% of maximum value). Across transect T (Isle of Man to Anglesey) the range was 17.4 - 25.3 dpm/l (minimum 69% of maximum value), at approximately half the levels in waters passing to the north of the Isle of Man.

Figure 4.2.e6

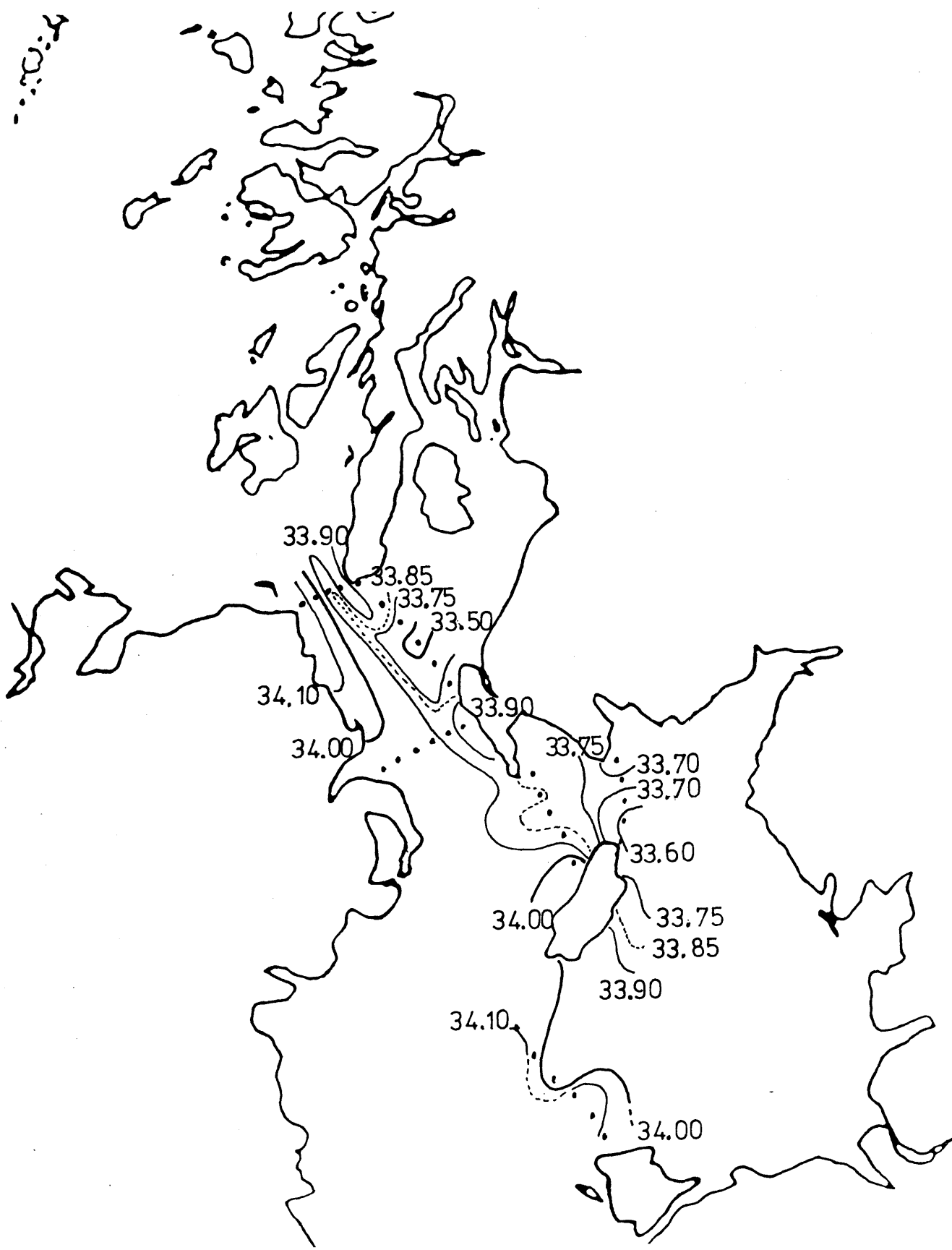
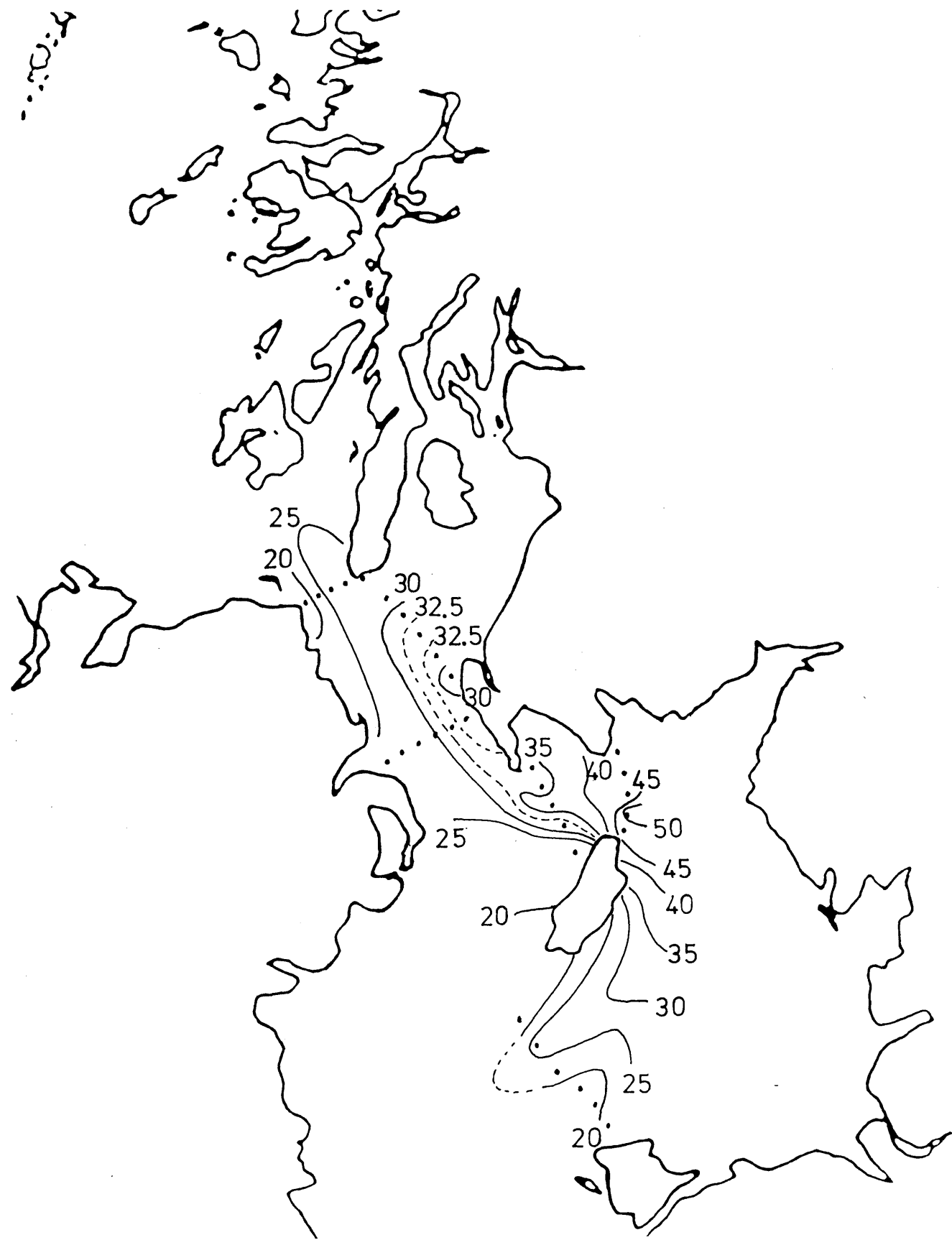
Salinity Contours(‰) - June/July 1984 Cruise[Irish Sea Section]

Figure 4.2.e7

 ^{137}Cs Contours (dpm/l) - June/July 1984 Cruise[Irish Sea Section]

ii) Summary

1) A delay of ~2 months was observed in the CSA response to the radiocaesium discharge pattern relative to the North Channel response.

2) Water of lower radiocaesium content entered the southern HSA via the North Channel during this cruise (c.f. the previous cruise (May 1984)). However, in the more northern regions (transect E, Loch Etive) and the CSA, higher radiocaesium levels were found during this cruise, indicating the presence of older water. High salinities in the HSA were encountered north from Islay and south of the entrance to the Little Minch but not to the southeast of Islay.

3) As found in the southern HSA in August 1983 and particularly in the northern HSA in January 1984, the coastal current during this cruise was partly restricted to the west coast of the mainland (c.f. the May 1983 and April / May 1984 cruises); radiocaesium levels in water travelling via the Little Minch were about twice those in water to the west of the Outer Hebrides, although, further south, levels in water passing to the east of Islay were only slightly higher than those in water passing to the west.

4) The Islay Front occurred at an easterly position similar to that in October 1983 and was marked by sharp ^{137}Cs and salinity gradients.

5) Data for stations D3 and D4, both immediately west of the Islay Front, plotted to the left of the ^{137}Cs / salinity curve and it is suggested that fresh water dilution from the coast of Northern Ireland was the probable cause. In addition, these waters may reflect more

recent discharges (of lower radiocaesium content) than at stations in transects K and J. Hence, it is suggested that water at stations D3 and D4 had been rapidly diluted by saline Atlantic water.

6) Radiocaesium levels in the Irish Sea indicate a direct path of plume travel from the Sellafield pipeline to the North Channel, in the main, bypassing the Solway Firth.

7) Radiocaesium levels in waters travelling to the south of the Isle of Man were approximately half those in northerly advecting water.

4.2(f) November 1984i) Results and Discussion

During this November cruise, 65 water samples - 50 from the surface and 15 from depth - were collected for analysis of radiocaesium content at GU, whilst additional samples for transect G stations were collected for analyses by MAFF (Figure 4.2.f1). Figures 4.2.f2 and 4.2.f3 show the isopleths of salinity and ^{137}Cs respectively. Transect D was not sampled during this cruise; hence examination of the Islay Front has not been possible. The Hebridean Shelf, west of the Outer Hebrides, was also not investigated; instead, efforts were concentrated on inshore regions and on extension southwards into the Irish Sea.

The highest ^{137}Cs level observed, 100.1 dpm/l, occurred at station W1 (near Burrow Head) in the Irish Sea with levels decreasing westwards - towards the Mull of Galloway - and southward - towards the Isle of Man (Figure 4.2.f3). Surface radiocaesium concentrations continued to be higher in the eastern sector of the plume as it travelled around the Mull of Galloway into the North Channel and then northeastward into the CSA or northwestward to exit the North Channel system. Levels up to here and as far north as $\sim 56^\circ\text{N}$ were generally higher than those for the previous cruise (June 1984), except at station GMT 7 in the CSA (Chapter 2) where older water (of lower ^{137}Cs level) was probably circulating with the newer water entering the North Channel / CSA system (see section 4.2.e). North of 56°N , however, activities were lower in this cruise, especially across transects E (Firth of Lorn) and G (entrance to the Little Minch) and west of the Outer Hebrides.

Figure 4.2.f1

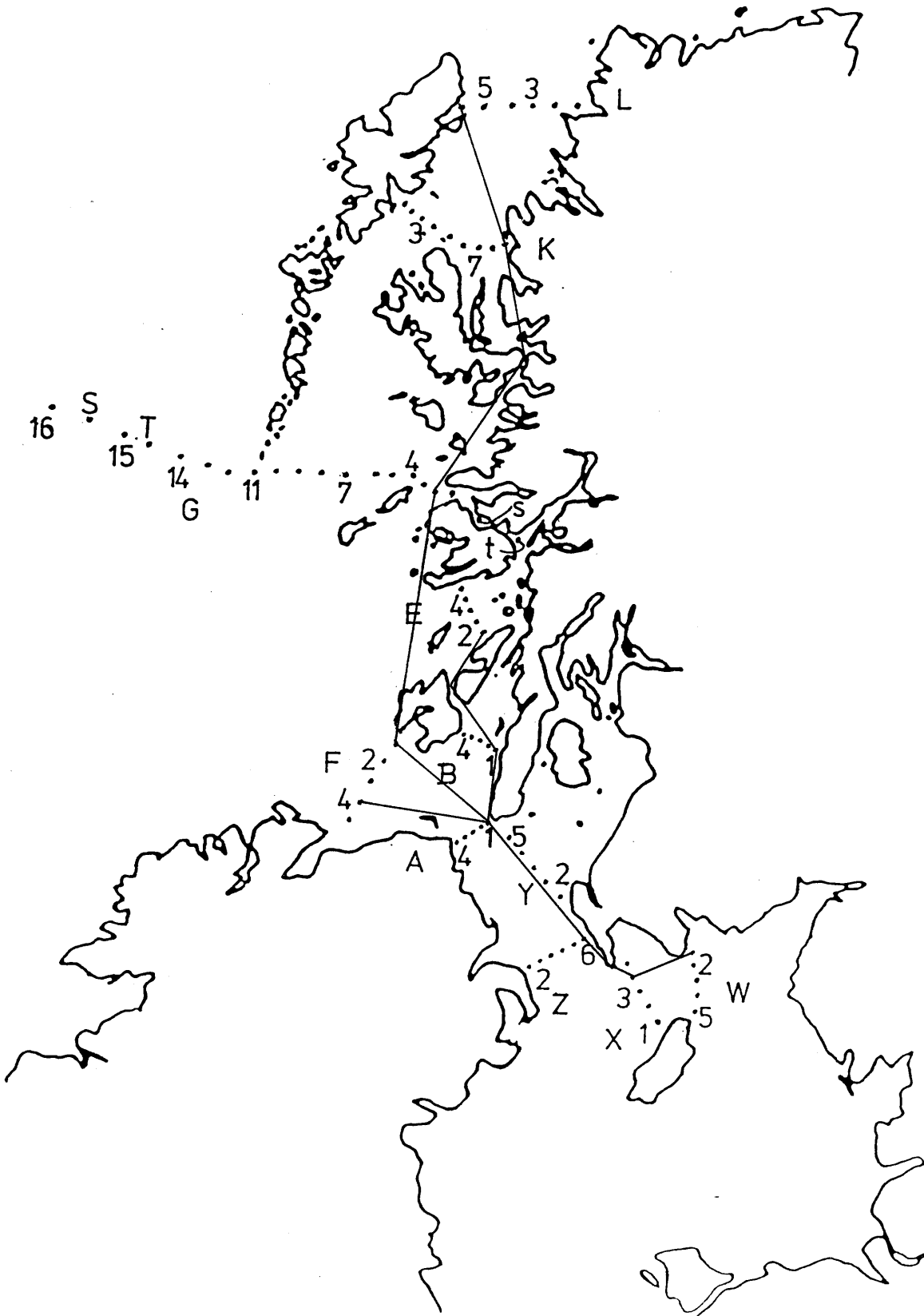
Station Positions - November 1984 Cruise

Figure 4.2.f2

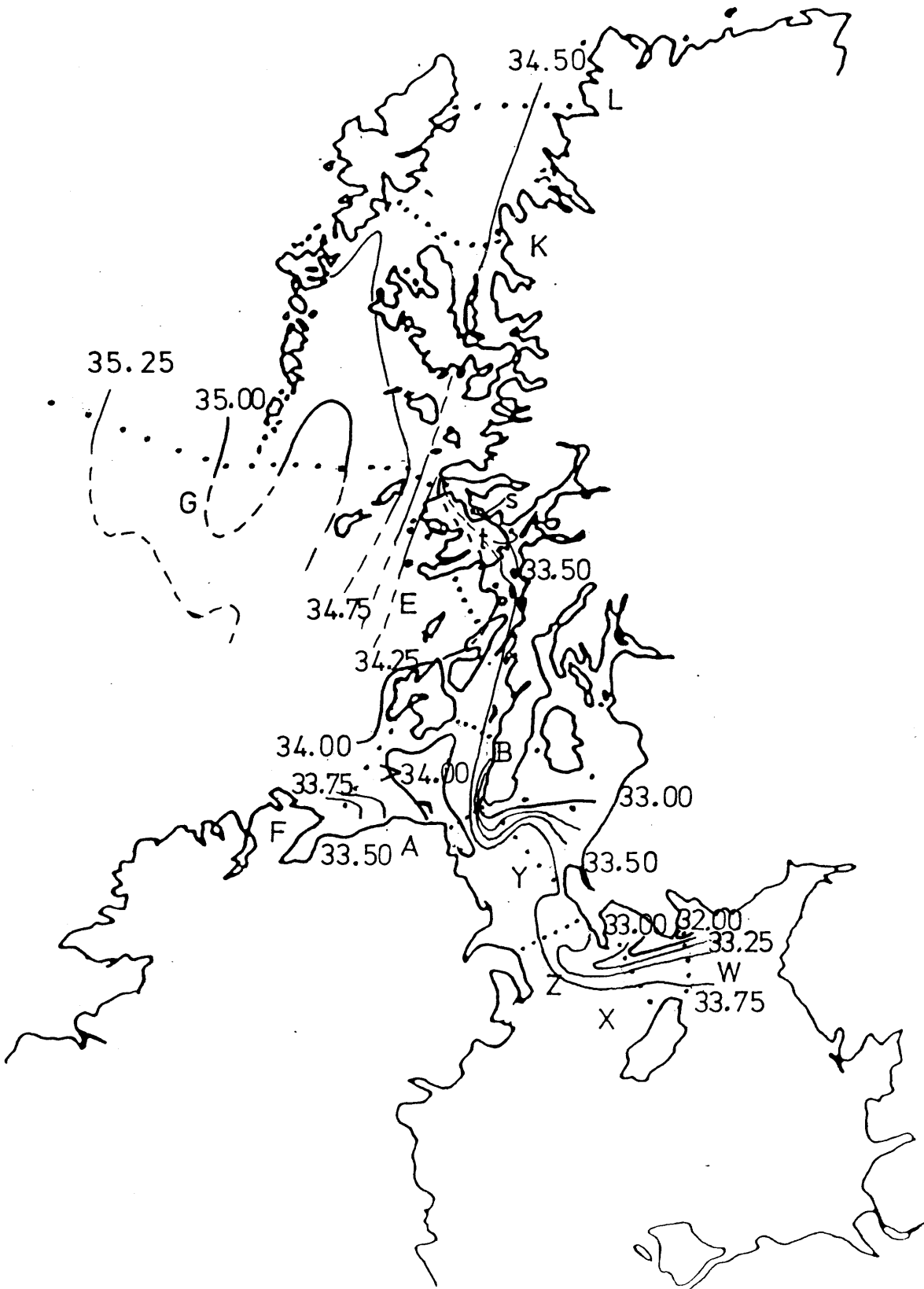
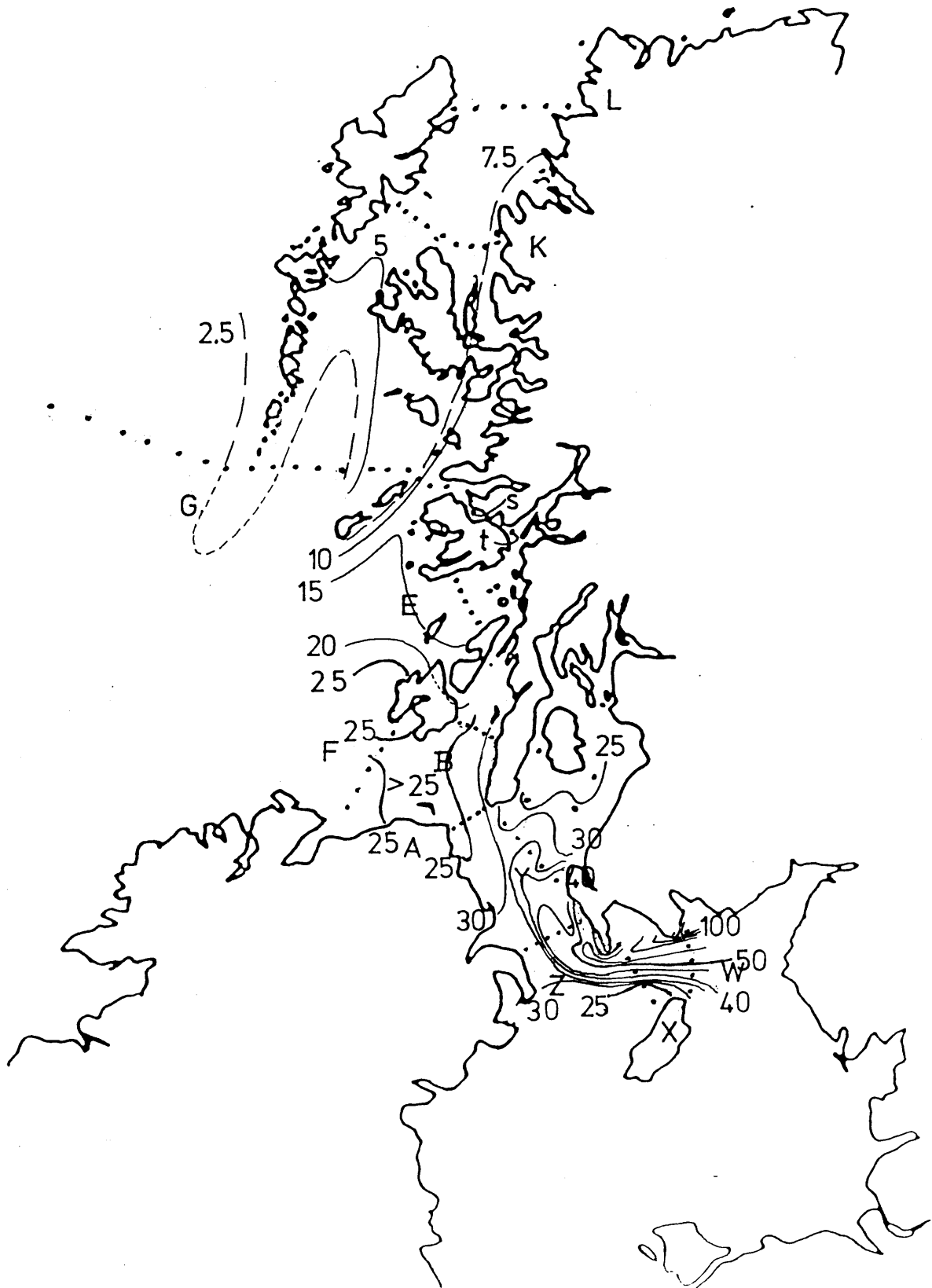
Salinity Contours (‰) - November 1984 Cruise

Figure 4.2.f3

 ^{137}Cs Contours (dpm/l)-November 1984 Cruise

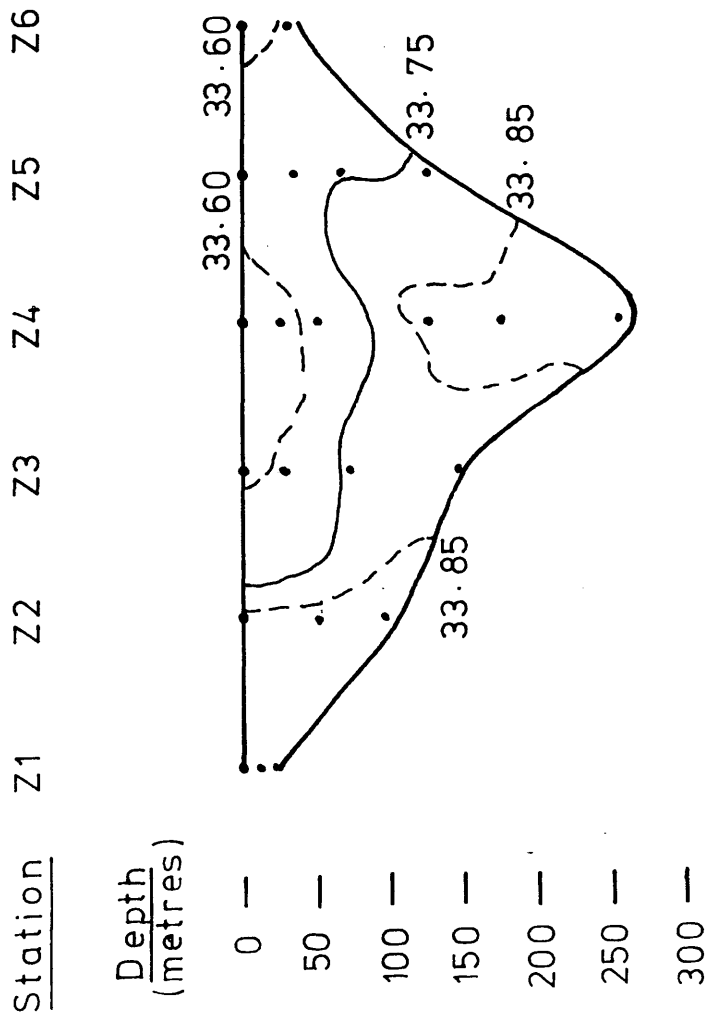
South of transect G it is not possible to define the extent of plume restriction to the coastline since samples were not taken west of Islay (transect D). However, transect F, from Rhinns Point, Islay to near Portrush, N. Ireland, shows an average of 26.7 dpm/l compared to the average of 25.6 dpm/l across transect B to the east of Islay (Sound of Jura). This relatively uniform distribution of radiocaesium levels implies that the radioactive plume to the south of Islay was thereafter not necessarily directed via the east of Islay, i.e. was not restricted to the Scottish coastline. By transect G, however, radiocaesium levels had decreased quite sharply in a westward direction from around station G6, showing lowest radiocaesium levels recorded thus far (< 5 dpm/l) for most of the entrance to the Little Minch and higher levels occurring only to the extreme east, between Coll and the mainland. This pattern, complemented by the westward increase in salinities, illustrates confinement of the surface water plume at this latitude to the Scottish coast under the influence of saline ($< 35.0\%$) Atlantic waters approaching the entrance to the Minch. For comparison, in August 1983 radiocaesium levels across transect B were about 150% of those across this transect; hence restriction of the coastal current to the mainland coastline was apparent (as it was also, particularly north of about $56^{\circ} 30'N$, in January 1984 and June 1984). In May 1983 and May 1984, the plume did not appear to be confined to the coast.

Further south, in the North Channel, salinities were generally quite low (maximum 34.110%), correlating well with the relatively high ^{137}Cs levels observed here. A portion of relatively saline surface water ($> 34.0\%$), however, appears to have been isolated between Islay and the North Channel, surrounded by lower salinity water. From Figures 4.2.f4 and 4.2.f5 - vertical profiles of salinity

Figure 4.2.f4

Salinity Profile (‰) Across (i) Transect Z and (ii) Transect A, November 1984

(i) Transect Z



(ii) Transect A

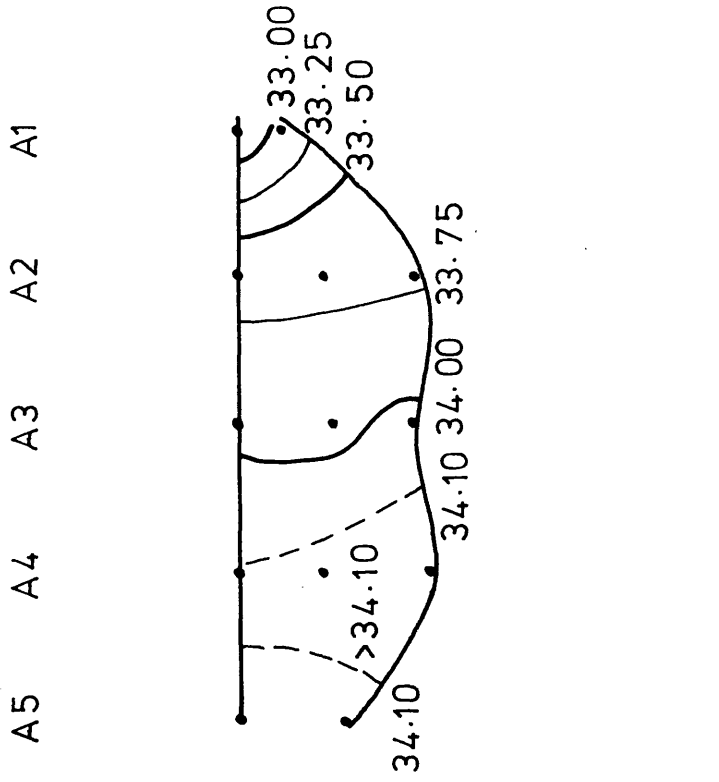
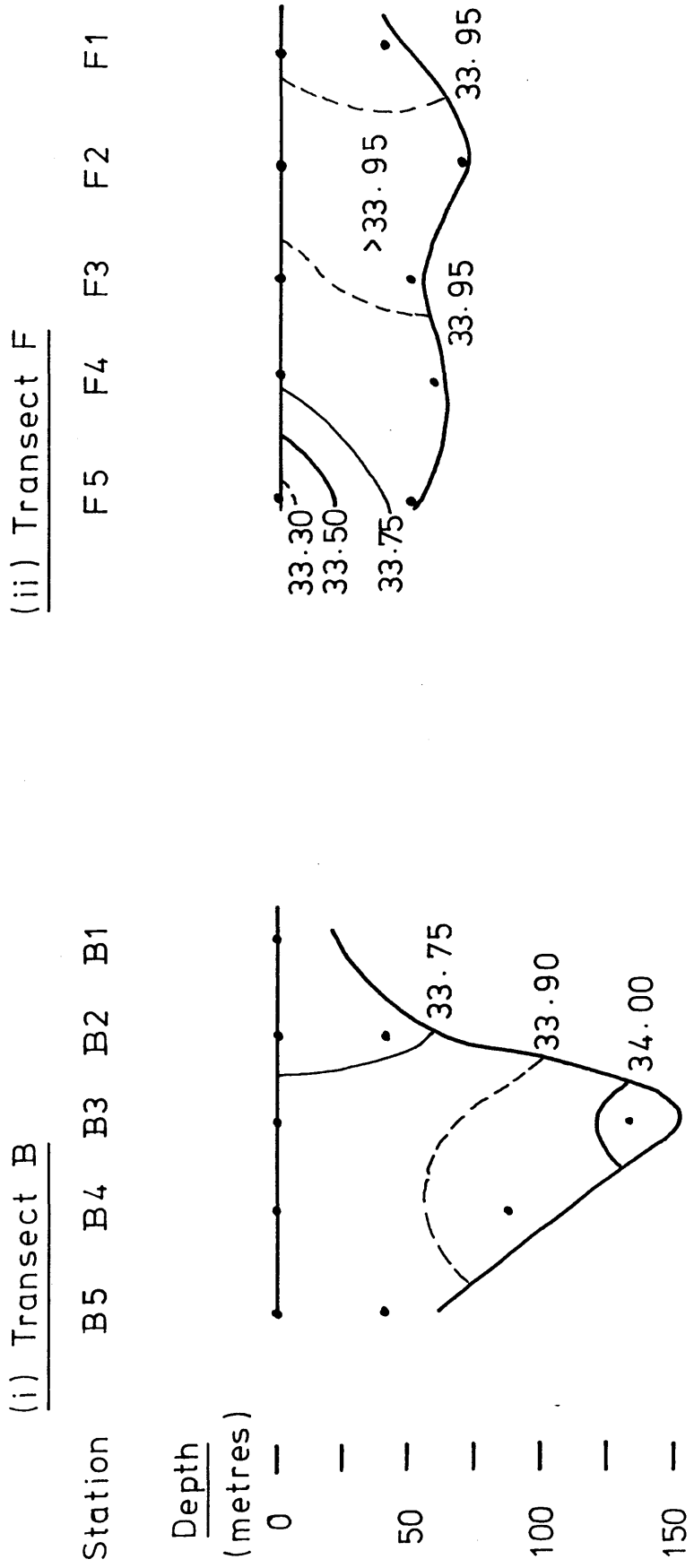


Figure 4.2.f5

Salinity Profile (‰) Across (i) Transect B and (ii) Transect F, November 1984



across transects Z and A and across B and F respectively - the maximum salinities occurring at station A4 throughout the water column confirm that isolation of this "high" salinity fraction of water also occurred at depth. Without data for stations west of transect F, at this latitude, it is difficult to determine whether the low salinities across transect F were due purely to fresh water dilution from N. Ireland runoff or whether the saline Atlantic water had withdrawn from the area. Although fresh water dilution is strongly implied for the southern station of transect F - F5 - (see ^{137}Cs / salinity curve, Figure 4.2.f6), higher salinities (>33.980‰) were measured at the central stations and hence the northern station, F1, may record water diluted by fresh water from Islay not from N. Ireland. However, if the high salinity fraction was isolated by increased fresh water at F1, it would probably have occurred mainly at the surface whereas the low salinity water at F1 was, in fact, maintained throughout the water column. Hence it seems likely that the "isolation" process was caused by Atlantic withdrawal. In support of this suggestion are the comparatively low salinities which occurred to the west of the Outer Hebrides; the maximum across transect G, at station G16, was 35.292‰ whereas in May 1983, August 1983, January 1984 and June/July 1984 the maximum salinities were 35.406‰, 35.359‰, 35.459‰ and 35.393‰ respectively.

To compare radiocaesium levels in this cruise with those of previous cruises, and bearing in mind the temporal variation in discharge levels, the degree of dilution needs to be known. It was predicted (in section 4.2.e) that comparison between ^{137}Cs / salinity curves for the November and June/July cruises would reveal the low radiocaesium levels found in the southern HSA in June/July 1984 appearing in more northern regions in this November cruise. The two

Figure 4.2.f6

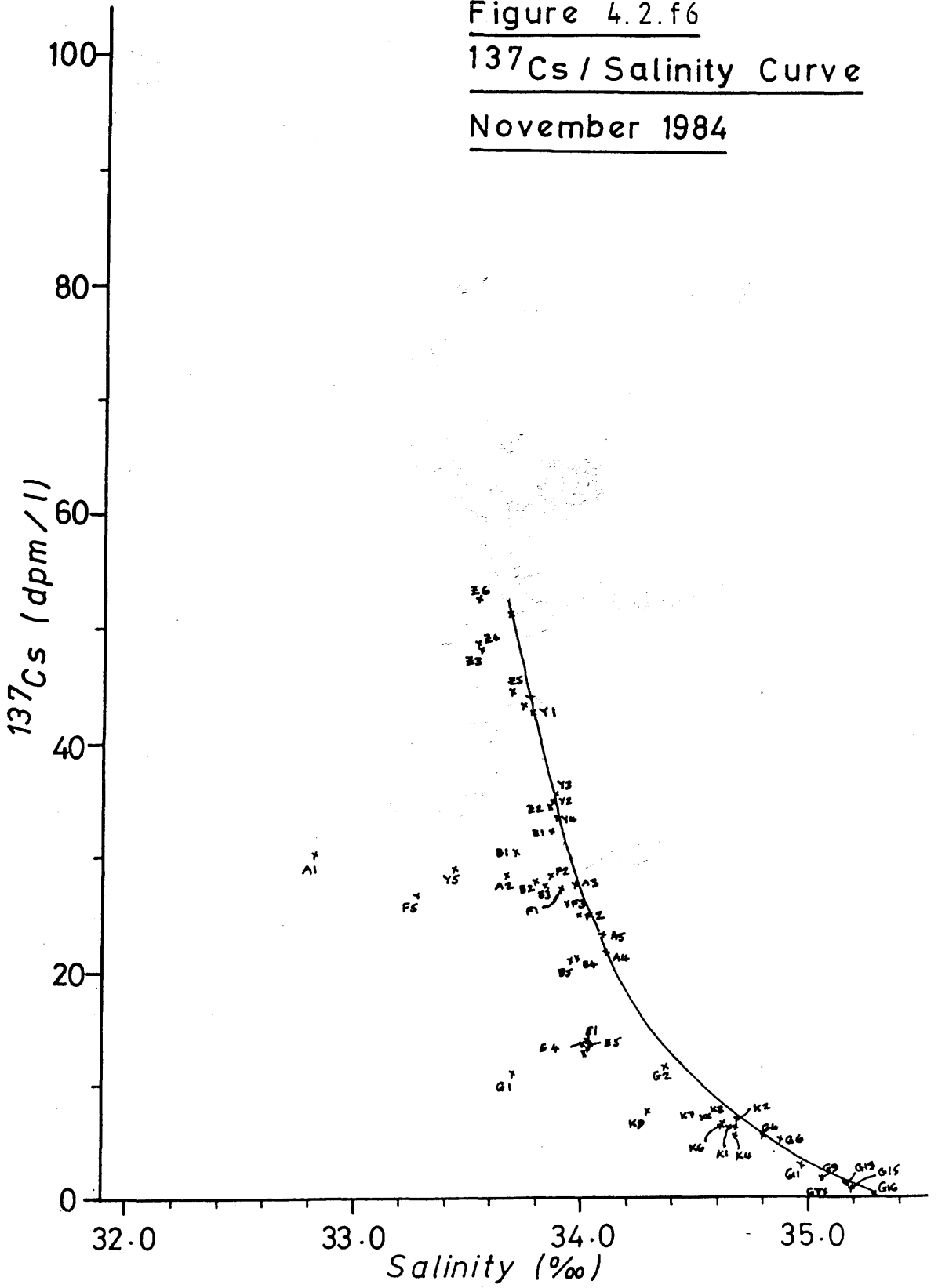
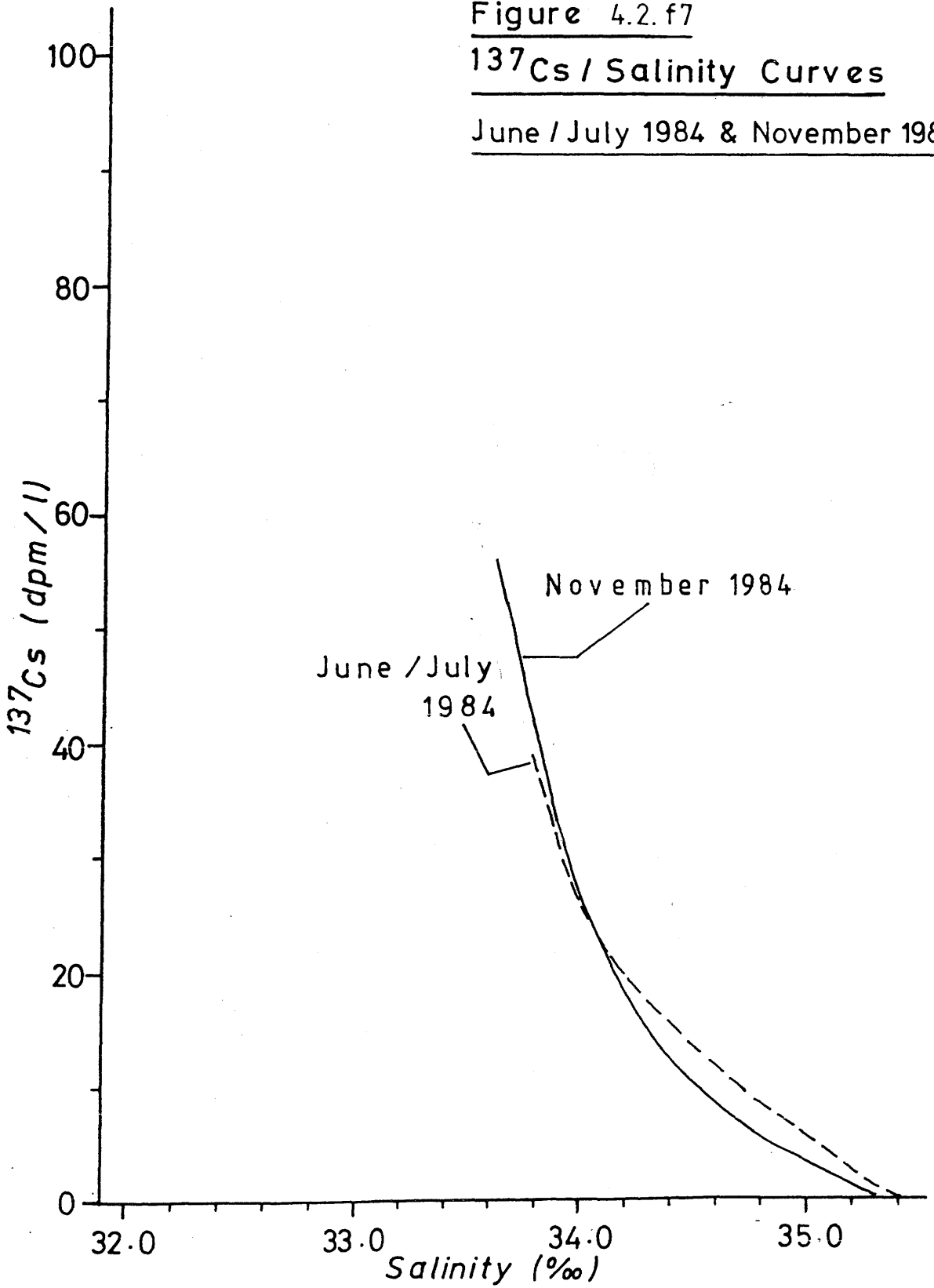
 ^{137}Cs / Salinity CurveNovember 1984

Figure 4.2.f7

 ^{137}Cs / Salinity CurvesJune / July 1984 & November 1984

curves (Figure 4.2.f7) confirm that this, in fact, occurred: the lower section (< 20 dpm/l, $< 34.15\%$) of November's curve - representing transects K and G - shows lower radiocaesium levels than the corresponding section for the June/July cruise. By contrast, the section of the June/July curve corresponding to the southern HSA (> 20 dpm/l, $< 34.15\%$) falls below that of the November plot, i.e. exhibits lower radiocaesium levels. It is not possible to state with total certainty, however, whether the later low radiocaesium levels in the northern regions were a reflection of the earlier low activities in the more southern regions or whether they were caused by increased fresh water dilution. However, a time series of such data - comprising radiocaesium levels at a variety of sites throughout the study period - can provide more detailed assessment of radiocaesium trends and lag-times between sites and this treatment is applied in section 4.3.

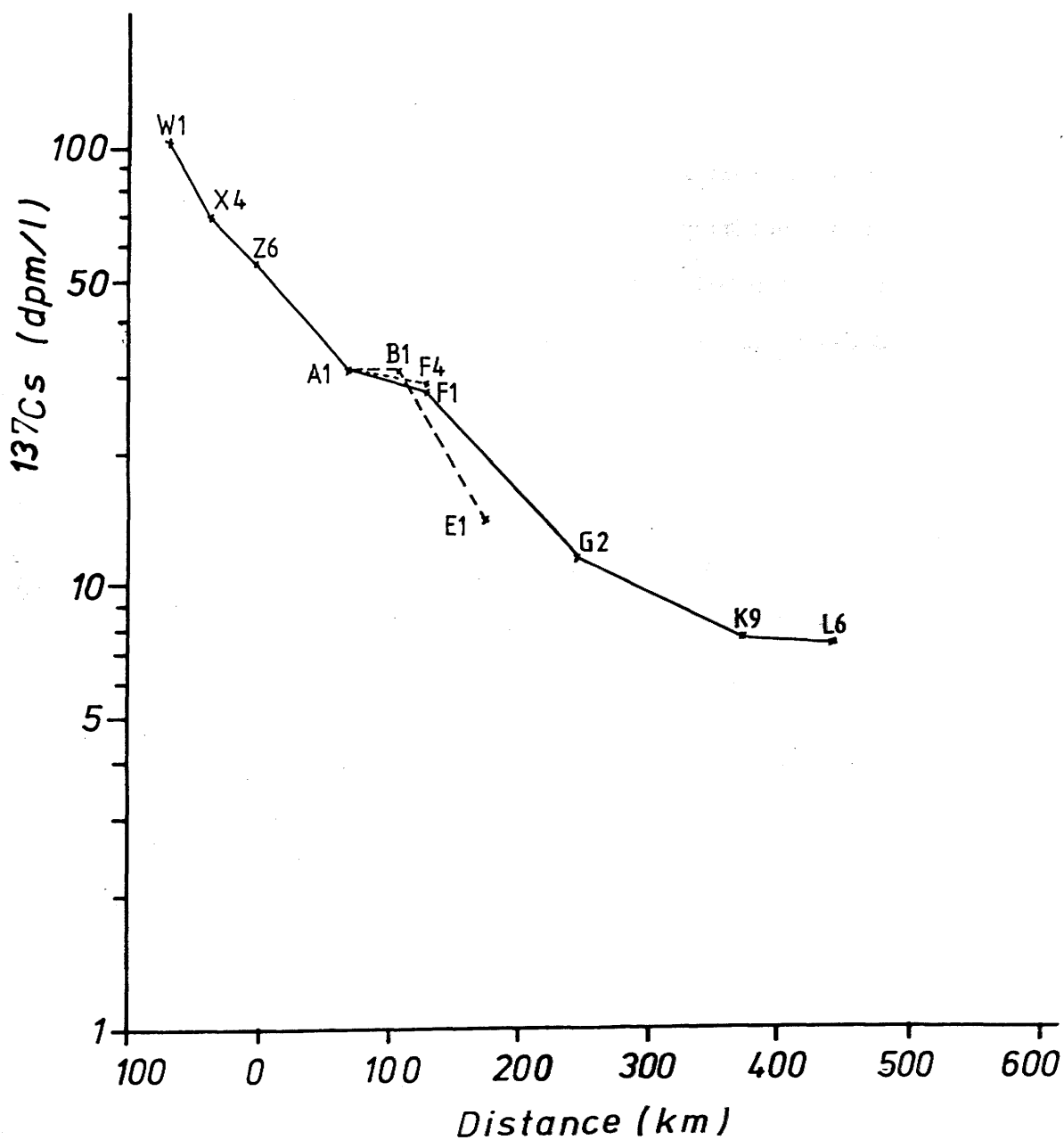
From Figure 4.2.f8, it is clear that the proportional decrease in radiocaesium levels with distance was not linear during this cruise. The sharpest decrease occurred in the Irish Sea and North Channel areas whilst between transect A and the southern and eastern HSA the change in radiocaesium levels was much less severe. North of here, significant decrease in radiocaesium levels was apparent towards transect G (entrance to The Minches) but in The Minches the decrease was minimal. This emphasises the relatively low dilution of the plume in the southern HSA - as noted above and attributed to limited exchange between Irish Sea / CSA and Atlantic waters - and the somewhat higher dilution (by Atlantic water) in the northern HSA towards the approaches to the Minches.

Maximum radiocaesium levels in the Irish Sea (Figure 4.3.f3) were approximately double those of June/July 1984. The accompanying lower salinities indicate less dilution by Atlantic water during the

Figure 4.2.f8

^{137}Cs Along Main Path of
Plume (From North Channel)

November 1984



November cruise. The higher radiocaesium levels later were probably also a reflection of the peak in discharges in September and October 1984 (see Figure 3.3, Chapter 3). Comparison of ^{137}Cs / salinity curves for the two cruises indicates higher (salinity normalised) ^{137}Cs levels in the North Channel area (i.e. maximum levels on the curve) during the November cruise. From Figures 4.2.f2 and 4.2.f3 (salinity and radiocaesium contours respectively), the radiocaesium plume in the Irish Sea appears to have followed the coastline quite closely; levels on the plume's mainland side indicate travel quite close to the coast possibly because of Atlantic water incursion from the St. George's Channel.

These results contrast with the findings from the previous cruise in that the latter 1) did not show significant differences in radiocaesium levels across transects and 2) indicated a more direct transport path for the plume from Sellafield to the North Channel.

ii) Summary

1) Restriction of the coastal current was observed for the area at the entrance to the Minches (across transect G) but, in the southern HSA, radiocaesium levels were quite uniform within the areas investigated.

2) Isolation of saline (>34.0‰), low radiocaesium water occurred between Islay and the coast of N.Ireland throughout the water column. It is suggested that the cause was not fresh water dilution from N. Ireland (although this was observed at the southernmost station of transect F, F5) but was withdrawal of Atlantic water from the HSA. Atlantic withdrawal was also indicated by low salinities to the west

of the Outer Hebrides (with a maximum across transect G, at station G16, of only 35.292‰ compared with 35.359 - 35.459 ‰ for the rest of the cruises (for which data are available)).

3) Comparison of ^{137}Cs / salinity curves for this and the June/July 1984 cruises shows that the northern transects in November 1984 exhibit the low radiocaesium levels found in summer 1984 at the southern transects; however, it is not yet clear whether the low ^{137}Cs levels in this cruise reflect an advective time-lag or are the results of increased fresh water dilution.

4) Radiocaesium levels in the Irish Sea were twice those of the previous cruise; a peak in radiocaesium discharges in September / October 1984 is suggested as the main cause. In the June / July 1984 cruise, a direct path of travel from Sellafield to the North Channel was indicated whereas, in this cruise, the plume appears to have travelled closer to the Dumfries and Galloway coast, probably restricted to the coastline by penetration of Atlantic water from the St. George's Channel.

4.2(g) February 1985

Samples for radiocaesium analyses at GU were collected from one transect only (transect Z), whilst, for analyses by MAFF, samples from transect G were collected; both transects had samples taken from mid- and bottom depths. The results are discussed in THE sections which follow, with reference to 1) deep stations and 2) the variation of radiocaesium levels across each transect with time.

4.2(h) May 1982

i) Results and Discussion

Collection of samples during this cruise was carried out by UCNW (University College of North Wales). Consequently different station positions were involved relative to those for all other cruises (Figure 4.2.h1). A total of 48 water samples were analysed for radiocaesium content and the results are presented as ^{137}Cs contours in Figure 4.2.h3; the corresponding salinity data are shown in Figure 4.2.h2.

Any comparisons of results for this cruise with those for the other cruises are made tentatively since the different grid of station positions could give rise to inconsistencies and ambiguities, e.g. across the northern North Channel exit a gradient of ^{137}Cs levels has been observed during most cruises; thus, it is not clear whether the one North Channel ^{137}Cs level (44.6 dpm/l) obtained during this cruise (station 51) was closer, say, to the average or to the maximum value entering the HSA. A CSA sample taken 10 days prior to this cruise was found to contain 68.8 dpm/l at salinity 32.17‰, which implies that 44.6 dpm/l may be too low to have represented maximum ^{137}Cs levels passing through the northern North Channel exit.

The ^{137}Cs / salinity curve (Figure 4.2.h4) for this cruise shows 2 stations falling significantly to the left of the curve (stations 51 and 18). Water at the former could have undergone fresh water dilution from Loch Foyle (N. Ireland) but the latter occurs in the midst of the Islay Front and suggests a component of somewhat fresher Atlantic water from the coastal current which rounds the west and northwest coasts of Ireland.

Figure 4.2.h1

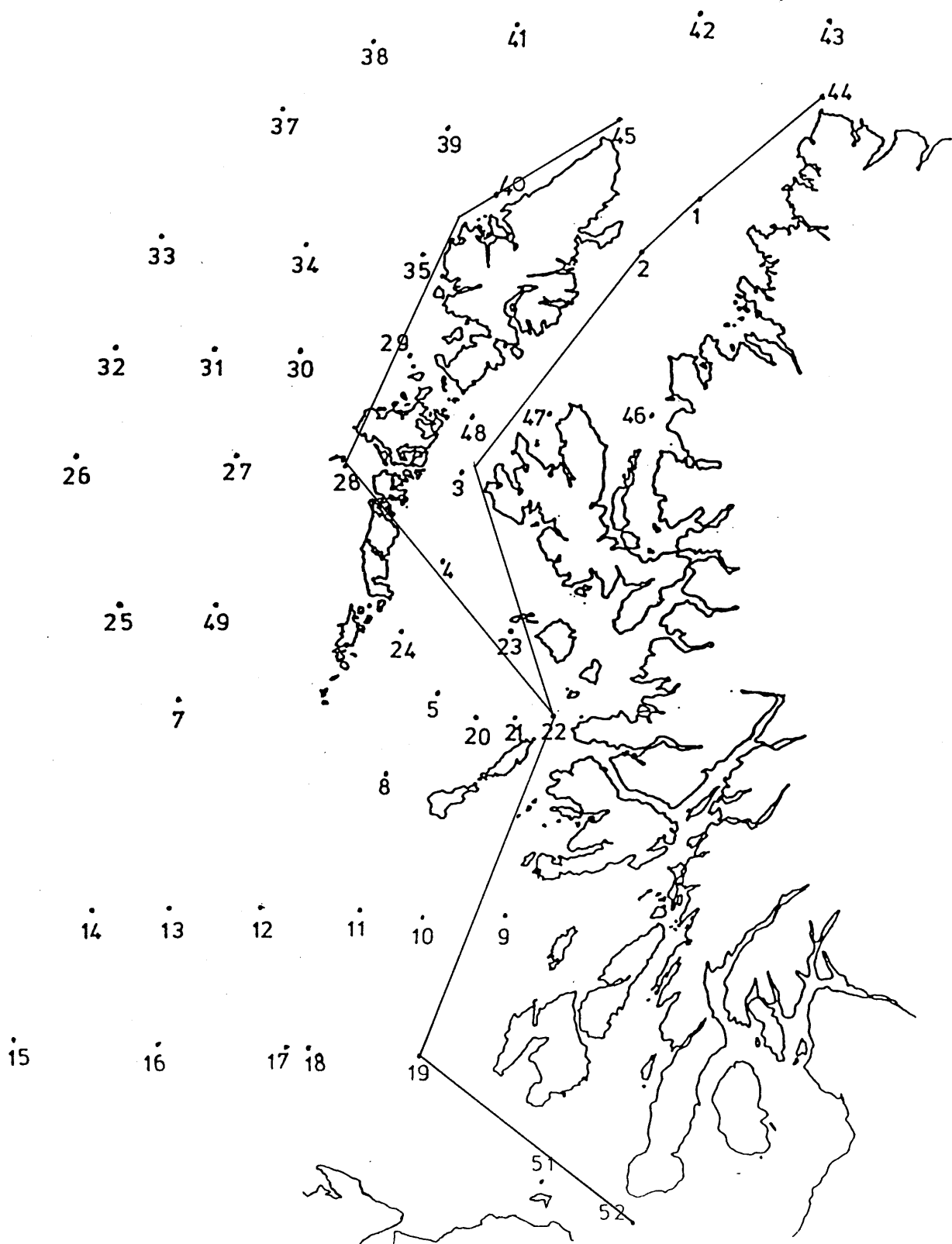
Station Positions - May 1982 Cruise.

Figure 4.2.h2

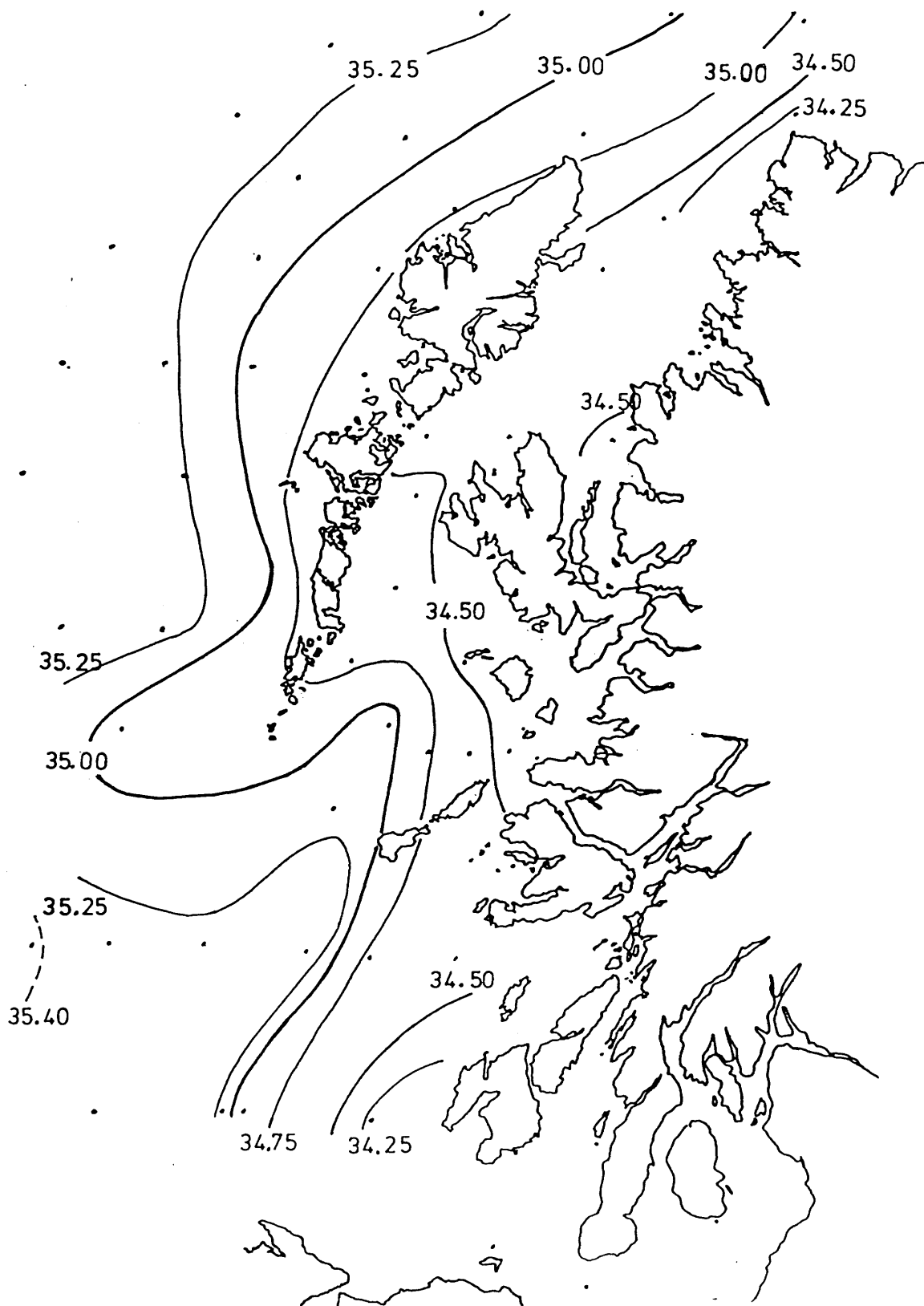
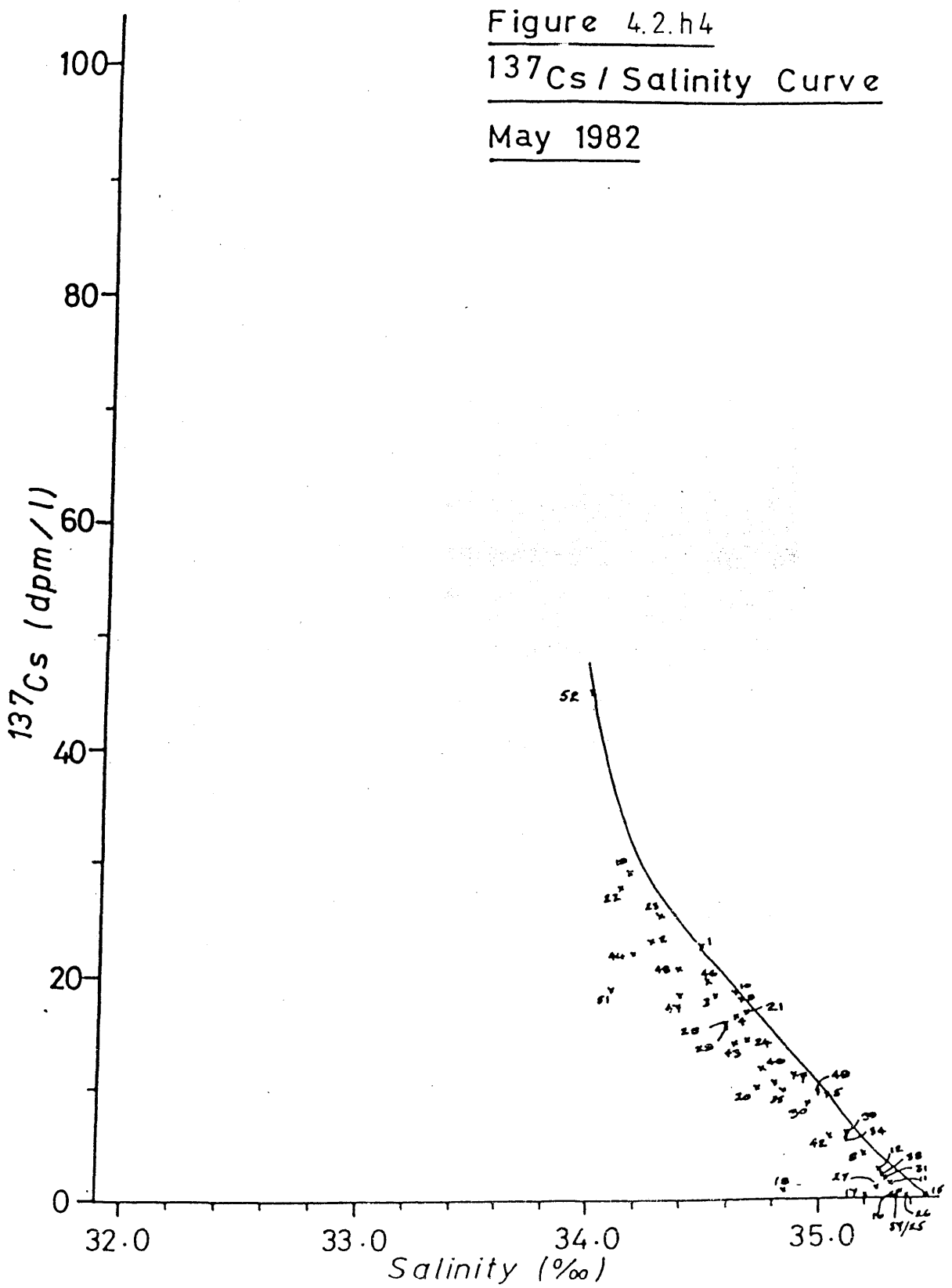
Salinity Contours (‰) - May 1982 Cruise

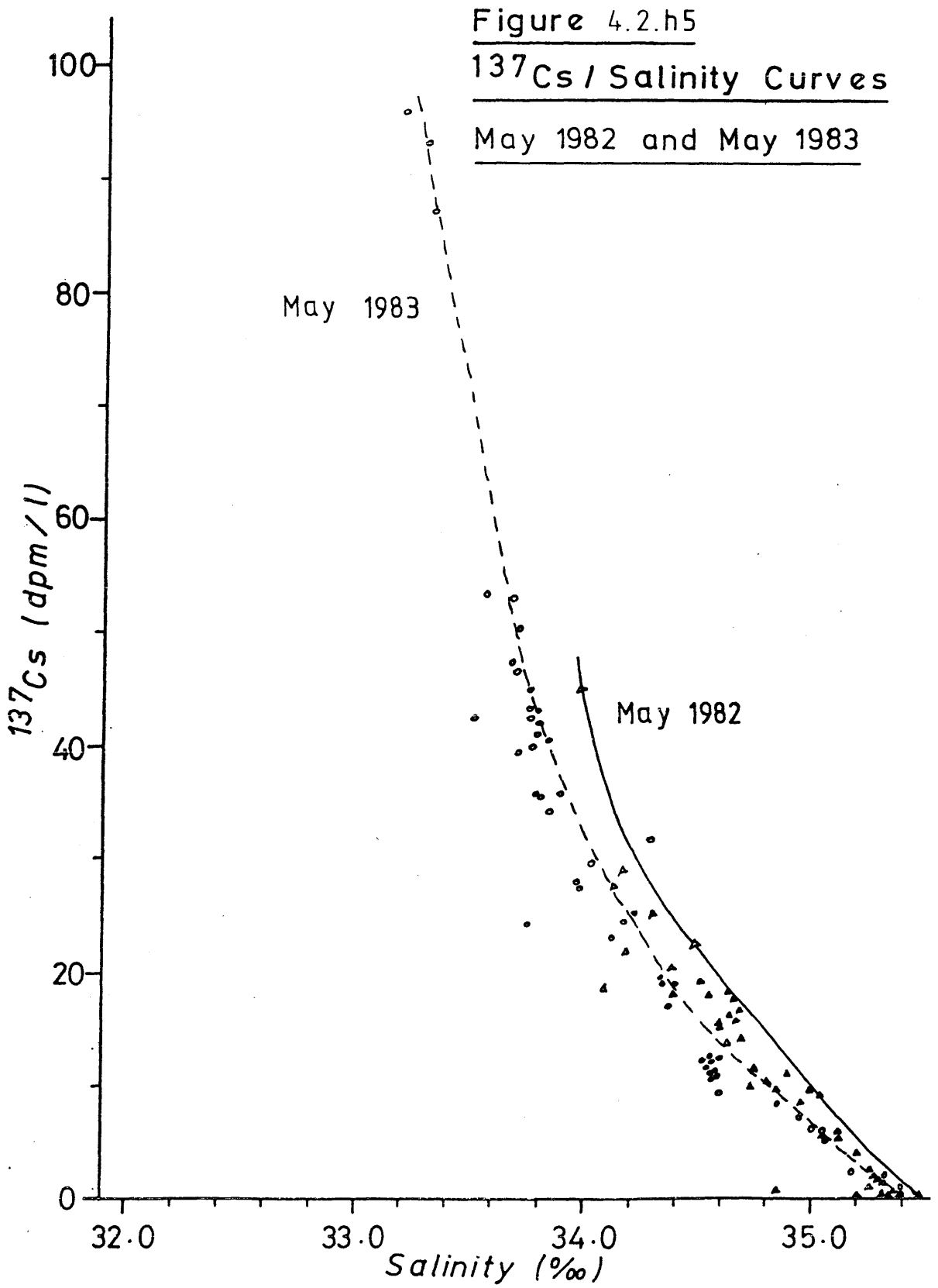
Figure 4.2.h3

 ^{137}Cs Contours (dpm/l) - May 1982 Cruise



A general comparison of the data from this cruise with those of May 1983 shows lower radiocaesium levels in the southern HSA in this 1982 cruise but higher levels further north, in the Minches, where ^{137}Cs levels were in the range 17-22 dpm/l during this cruise and in the range 15-20 dpm/l in the 1983 cruise. In the southern HSA, salinities were generally higher during this cruise than in most subsequent cruises, implying that, the Irish Sea / CSA water was largely confined to undersampled inshore regions where the maximum ^{137}Cs levels might have been found. Supporting evidence comes from the Loch Etive sample, collected 3 weeks before the cruise, which gave a relatively high ^{137}Cs content level of 32.39 dpm/l (at salinity 24.12‰), the corresponding level for May 1983 being only 17.7 dpm/l (at salinity 27.469‰). It is therefore implied that the observed generally low levels in May 1982 were largely due to dilution by saline, low ^{137}Cs Atlantic water and not to variations in Sellafield discharges. To investigate the possible effect which variations in Sellafield discharges have exerted on the levels reaching the HSA, it is necessary to examine the temporal discharge record. That is, to understand whether observed increases and decreases relate, at least partially, to the pattern of discharges, it is necessary to compare temporal trends and to assess whether a correlation and lag-time exist between Sellafield and the southern HSA data (see section 4.3). However, since the monthly CSA ^{137}Cs trend has already been shown to reflect reasonably the time-lagged discharge record (Chapter 3), then it could be used to represent the HSA source water: a lag-time from the CSA to the HSA would thus be adequate for our purposes if the two data sets (CSA and HSA) are correlated.

In order to determine whether radiocaesium levels in this cruise, when normalised with respect to salinity, were genuinely higher than



those in May 1983 (i.e. whether they corresponded to higher Sellafield discharges than those of May 1983), the ^{137}Cs / salinity curves for the two cruises should be compared and Figure 4.2 h5 presents the two curves. In fact, the 1982 curve exhibits approximately 1.5 times the ^{137}Cs levels of 1983 for the same salinities (1.25 - 1.40 times for southern regions, 1.60 - 1.70 times for northern regions).

Thus, although discharged ^{137}Cs levels were higher for the earlier cruise (May 1982), the prevailing flow patterns (and subsequent extent of dilution by saline waters) ultimately controlled whether ^{137}Cs levels were restricted to inshore areas or reached western regions, as far as or beyond the Outer Hebrides.

Salinities within The Minches were not particularly high, being similar to the range for other cruises (approximately 34.4 - 34.6 ‰). The accompanying higher ^{137}Cs levels therefore, support the concept that the contemporary lower southern ^{137}Cs levels were caused by dilution by saline waters.

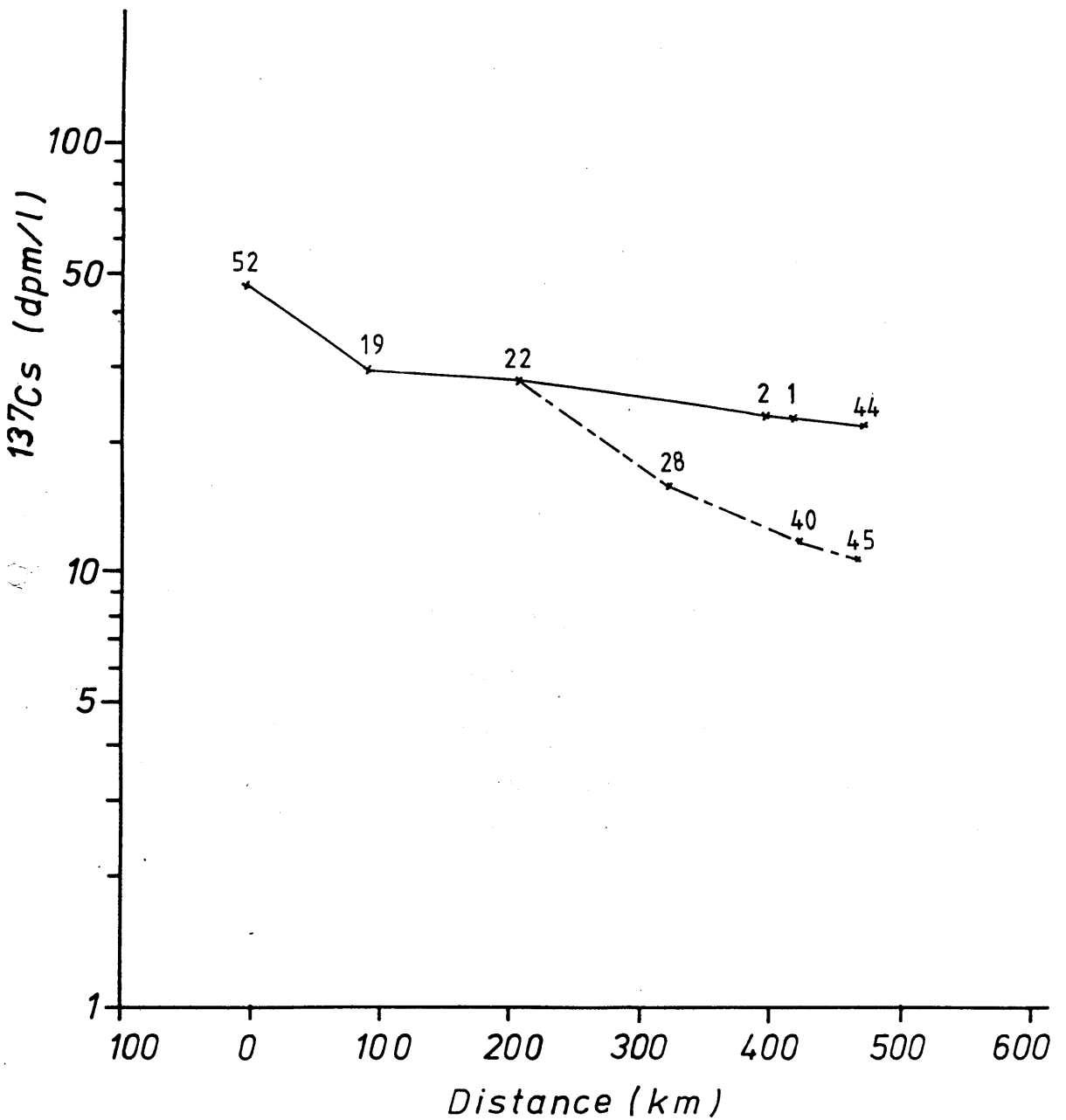
To the west of the Outer Hebrides, ^{137}Cs and salinity contours are similar to those for August 1983 and June 1984, indicating slow northward dilution and with isopleths following the shape of the coastline. This pattern contrasts with the May 1983 situation, when spreading of the plume extended far to the west at $\sim 57^{\circ}00'\text{N}$ so that high ^{137}Cs levels (>30 dpm/l) reached the west of the Outer Hebrides before saline Atlantic water to the west (and north) began to dilute the plume. From the shape of the 35.00‰ isohaline south west of Barra, it can be seen that Atlantic water just to the north had penetrated quite sharply eastward towards the west of the Outer Hebrides and had left a relatively undiluted patch of water ($<35.00\%$) there, south west of Barra.

The graph of ^{137}Cs levels against distance from the North

Figure 4.2.h6

^{137}Cs Along Main Path of
Plume (From North Channel)

May 1982



Channel, (Figure 4.2.h6) shows that greatest dilution occurred 1) from the North Channel to the west of Islay and 2) from Station 22 to Station 28, i.e. across the tongue of saline, Atlantic water which was penetrating, from west of the Outer Hebrides towards the entrance to The Minches. Overall, then, greater dilution of the plume occurred in the western branch, the eastern current clearly retaining its higher radiocaesium levels during travel through the Minches; north of Skye, it can be seen to have concentrated along a path running through the centre of The Minch.

ii) Summary

1) Unlike the results for May 1983 which did not show positive incursion of Atlantic water into the southern HSA or into the Minches, the ^{137}Cs and salinity isopleths of this May 1982 cruise indicate quite a strong influence of Atlantic water in southern regions - similar to those of January and June 1984.

2) By extrapolating the ^{137}Cs / salinity curves for both cruises, it is found that normalised ^{137}Cs levels in the earlier cruise were about 150% those of May 1984 despite the fact that the actual measured radiocaesium levels were lower in the 1982 cruise; the evidence shows that the coastal plume was restricted to inshore areas in the southern HSA and that dilution by Atlantic water was the main cause of the observed low radiocaesium distribution here.

3) In the Minches, salinities were "normal" for that area and ^{137}Cs levels were quite high.

4) A relatively undiluted (low salinity) patch of water was found south west of Barra, probably resulting from advance of Atlantic water around it.

5) Two stations, identified by the ^{137}Cs /salinity plot, were notably fresh. Fresh water dilution from N. Ireland is suggested as the cause at one station, whilst, the other, a component of water from the Irish coastal current is probable.

6) Reductions in radiocaesium levels along the main paths of the plume were found to be greatest 1) from the North Channel to the west of Islay and 2) from station 22 to station 28 along the the west of the Outer Hebrides.

4.3 Time Trends

4.3(a) Introduction

Advection, rates of mixing and dilution of radiocaesium-labelled water "en route" to a specific region affect when, and how much of, the originally discharged activity arrives there. By sampling a particular station regularly for radiocaesium levels (an Eulerian approach) and comparing the observed temporal pattern with the discharge trend from Sellafield (e.g. Chapter 3, Figure 3.2), it is possible to estimate a water transit time between the two sites. Subsection 4.3(e) deals with such matching of temporal radiocaesium trends at various transects.

When considering changes in radiocaesium levels with time across a transect, it should be borne in mind that the resulting patterns or trends in the data are a reflection of two main contributing factors, namely the ^{137}Cs discharge levels and the water flow and mixing regimes. On a short timescale of weeks / months, both are constantly changing and thus the resulting picture is quite complex. For example, a change in current velocity may cause a change in transit time between two sites - as found for Sellafield to CSA transport before and after 1981 (McKay, 1985). However, such changes, if in the short term (i.e. days or weeks), are not likely to have any lasting effects and, in averaging transit times and current velocities (as in matching of temporal trends between various positions to estimate lag-times - see subsection 4.3(e)), they are eliminated.

From spatial radiocaesium distribution patterns from individual cruises, only the net effect, at one point in time, of all the processes can be seen; thus comparison with earlier and later cruise

data can provide a more detailed temporal picture. In section 4.2, each set of cruise data was assessed individually, whilst, in this section, the 8 cruises are examined simultaneously, comparing various features and property distribution patterns with time. Discussions include the use of data on current velocities and wind speeds. Because of the decrease in radiocaesium discharge levels and the subsequent increase in associated errors on the $^{134}\text{Cs} : ^{137}\text{Cs}$ ratios, the value of the latter during this is very limited here.

4.3(b) Dilution Factors

Table 4.3.1 presents dilution factors of radiocaesium levels, from transect A to various regions throughout the HSA, for each cruise. Variations between the cruises are largely the result of changing water flow conditions, e.g. the 60 times dilution at St. Kilda in the MAFF October 1983 cruise would have been largely due to increased Atlantic water incursion on this part of the shelf. The last column in Table 4.3.1 presents the mean dilution factor calculated for each site; for areas as far north as Coll - within the main coastal plume - they are ≤ 2 . On reaching Skye and to the east of the Butt of Lewis, mean dilutions are ~ 3 whilst to Barra Head and then to the west of the Outer Hebrides, St. Kilda, they are ~ 5 and ~ 10 respectively (the latter excluding the exceptional 60 times dilution of October 1983).

Overall, then, dilutions along the main path of the plume are low along the west coast of Scotland with levels in the Minches of ~ 3 times lower than the highest levels leaving the northern exit of the North Channel. The branch of the plume flowing to the west of the Outer Hebrides, however, encounters greater dilution. These results

Table 4.3.1

Dilution Factors of Radiocaesium Levels Between the North Channel - Transect A - and Various Sites

Site	May 1983	August 1983	October* 1983	January 1984	April/May 1984	June/July 1984	November 1984	May 1982	Mean Dilution Factor
Transect B	1.1	1.1	N.D.	N.D.	N.D.	1.18	1.0	N.D.	1.1 ± 0.1
Transect D	1.2	1.6	2.0	1.6	1.1	1.19	1.07	1.4	1.4 ± 0.3
Transect E	1.5	1.2	1.5	N.D.	N.D.	1.3	2.2	1.3	1.5 ± 0.3
Coll	2.0	1.8	3.0	1.7	1.7	1.6	1.6	1.65	1.9 ± 0.4
Barra Head (east)	1.8	1.7	4.0	5.0	1.8	4.2	12.2	4.5	4.4 ± 3.2
Barra Head (west)	1.8	1.8	4.3	7.1	N.D.	4.2	8.7	3.7	4.5 ± 2.4
Skye (north west)	4.3	2.3	2.4	N.D.	N.D.	3.0	4.5	2.2	3.1 ± 0.9
Skye (north)	4.3	2.2	2.4	N.D.	N.D.	3.1	4.0	2.4	3.1 ± 0.8
Butt of Lewis (east)	4.8	(2.7)	2.4	N.D.	N.D.	3.6	4.1	2.0	3.3 ± 1.0
Butt of Lewis (west)	7.6	(2.7)	3.0	N.D.	N.D.	5.4	N.D.	4.5	4.6 ± 1.8
St. Kilda	17.7	4.4	60.0	N.D.	N.D.	7.7	N.D.	9.0	19.8 ± 20.6 9.7 ± 4.9 ‡

() = Estimated from salinities

‡ = Excluding October 1983 data

N.D. = No data available

* = MAFF cruise

are in good agreement with those of Mauchline (1980) who estimated dilution factors of 2-5 between the North Channel and Cape Wrath and Livingston et al. (1982b) who found dilutions of 3 times between Irish Sea outflow and North Sea inflow.

Dilution factors obtained from Ea values are discussed in subsection 4.2(e).

4.3(c) ^{137}Cs / Salinity Curves

In order to compare the ^{137}Cs / salinity curves in the context of assessing variations in flow dynamics between each cruise, it might be considered necessary to alter the vertical (radiocaesium) scale of each graph, from the common to an individual scale, so that all the maximum radiocaesium levels - at approximately the same station for each cruise - overlap. This process might then allow comparison between curve shapes and eliminate, to some degree, the changes in observed radiocaesium levels due to variations in discharge. Variations in curve shape, however, would then be largely attributable to fresh water influence throughout the system and so would not provide information on changes in flow conditions. The most convenient way to compare the curves, therefore, is to consider each transect individually as a function of time.

There are sufficient data to plot 4 transects, Z, A, B and G (Figures 4.3.1-4); results from the cruise of May 1981 by McKay et al. (1986) are also included. The later cruise data appear further down the vertical scale because of the lower radiocaesium discharges influencing them. This difference in position along the radiocaesium axis with time appears to be more pronounced for transects closer to the discharge point, i.e. for Z and A relative to B, which in turn is

Figure 4.3.1

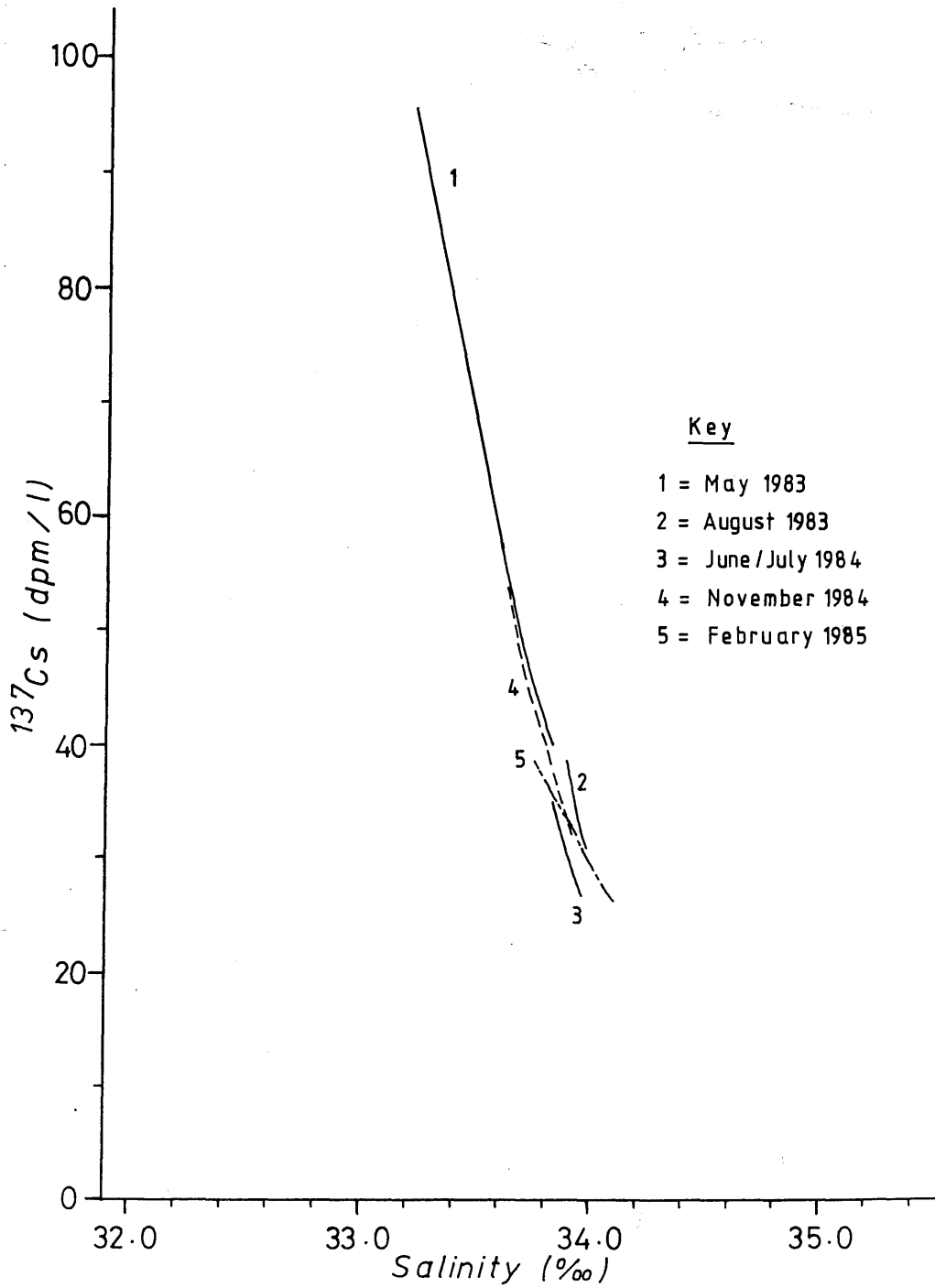
 ^{137}Cs / Salinity Curves for Transect Z

Figure 4.3.2

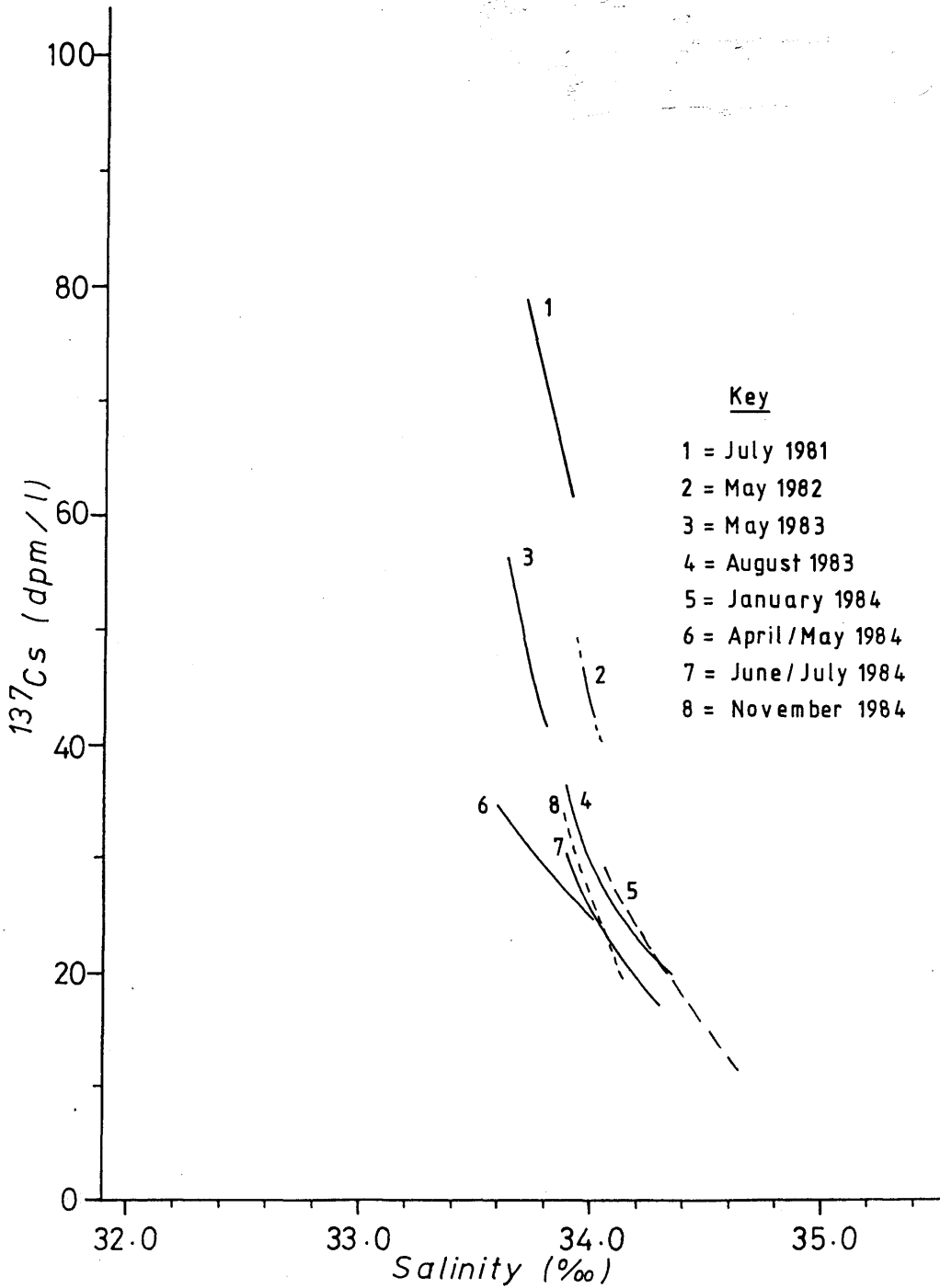
 ^{137}Cs / Salinity Curves for Transect A

Figure 4.3.3

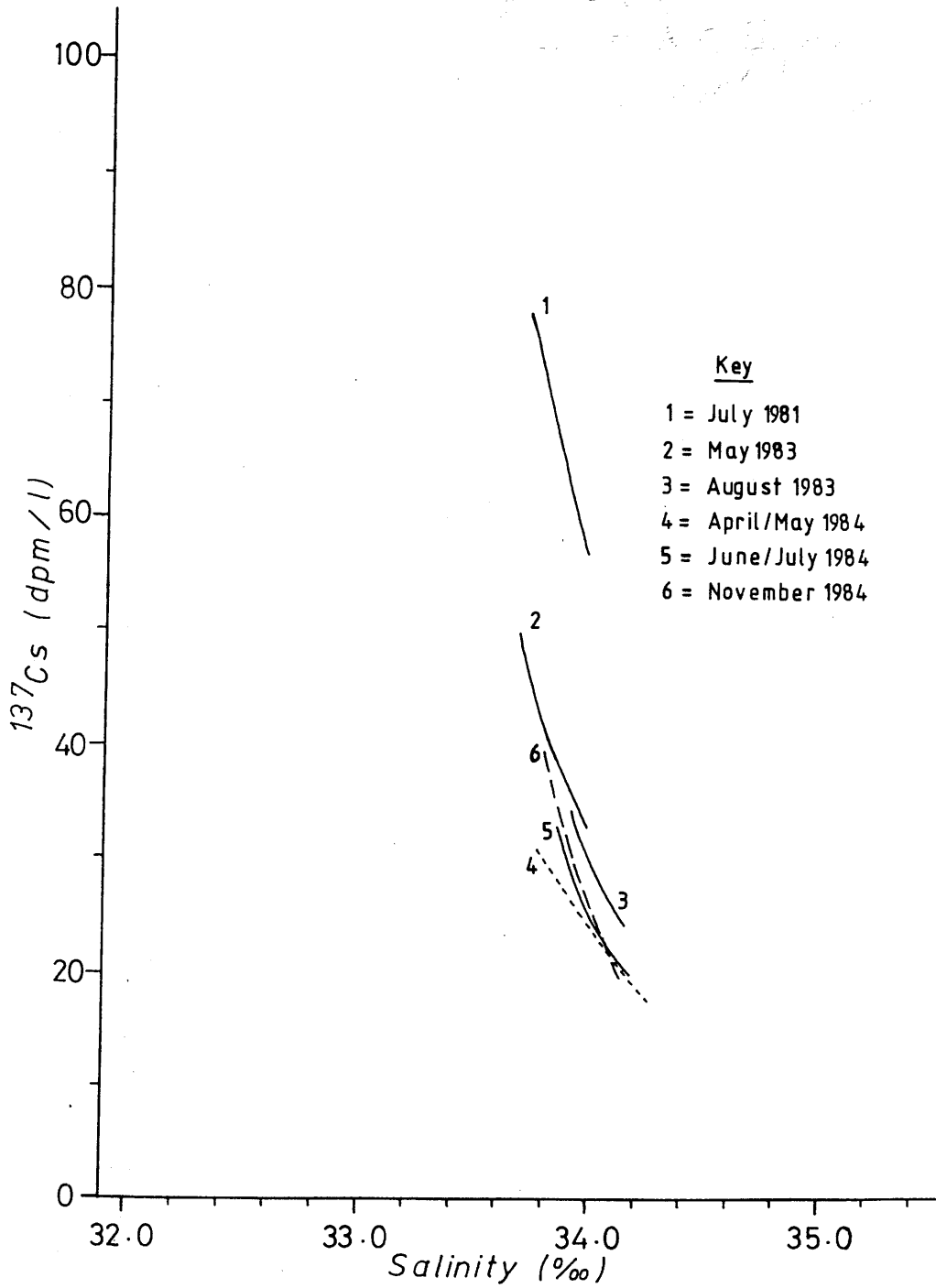
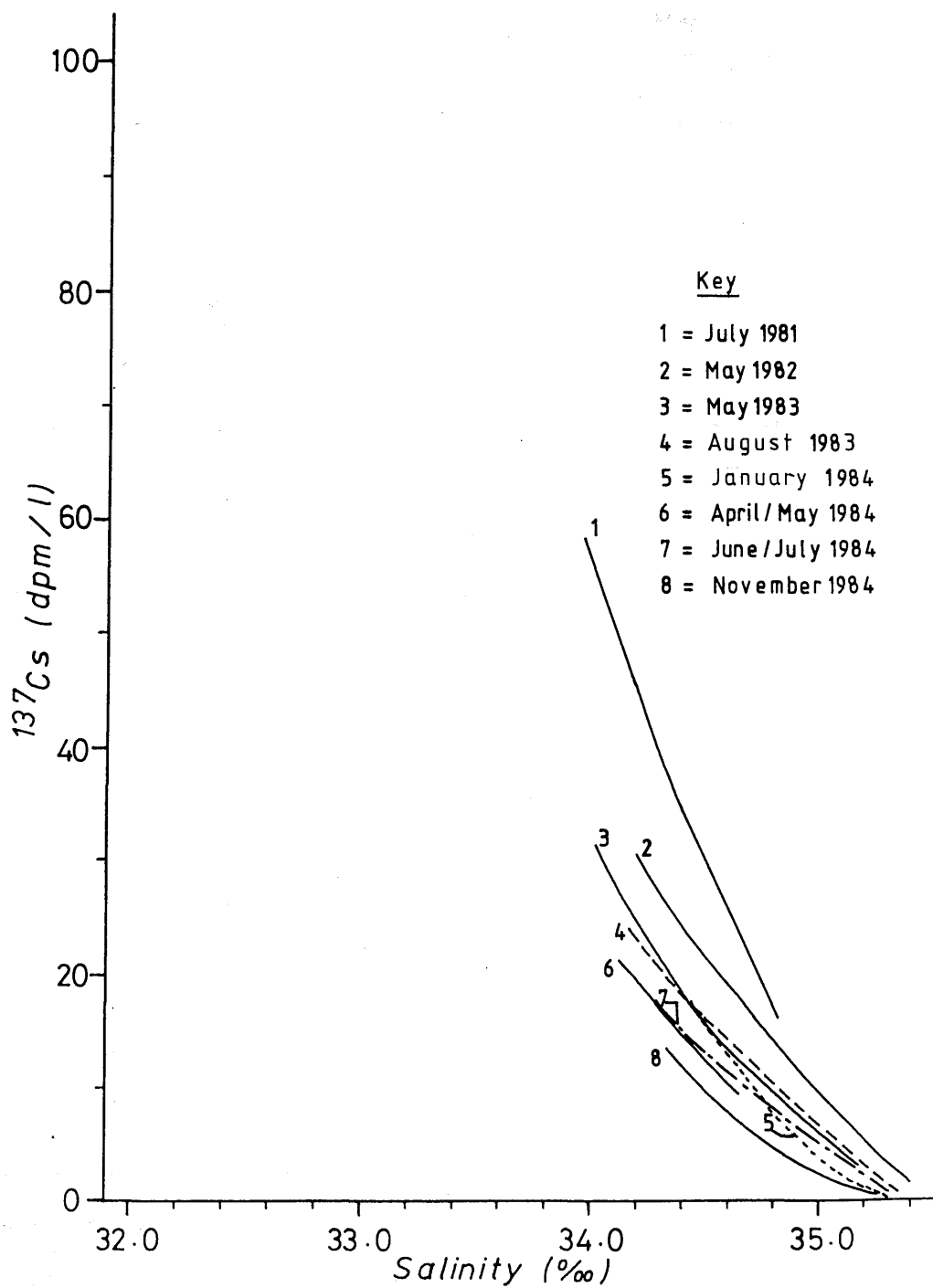
 ^{137}Cs /Salinity Curves for Transect B

Figure 4.3.4

 ^{137}Cs / Salinity Curves for Transect G

more pronounced than for G. There are two possible explanations for this trend, namely: i) in the case of proportionately equal changes in levels near and far from the discharge point (where levels are relatively high and low respectively), the linear radiocaesium scale used would give the impression that change in levels was greater near the discharge point; a log scale would, however, clearly show proportionately equal change in the two regions and ii) the closer to the point of discharge, the less overall dampening of the discharge record (from water residence / mixing) can be expected to have occurred; thus, the effect of increases and decreases in discharges would be more pronounced. With regard to the latter explanation, it is worth referring to Figures 4.3.7 and 4.3.8 (discussed in subsection 4.3(e)) which show temporal variations in radiocaesium levels at each transect. Also plotted on a linear scale, these data reveal a greater range in radiocaesium levels for the transects nearer the source than for those farther afield. However, when considering the range / differences as a proportion of the actual levels, then, apart from transect Z, there is little difference between transects. This implies that some water mixing / residence is occurring between transects Z and A, i.e. within the North Channel / CSA system, but very little occurs north of here, along the main path of the plume, at least as far as the Minches.

More accurate interpretation would require application of water lag-times between the various transects (see subsection 4.3(e)) to account for variations in discharges with time at each transect. In this study, however, the errors arising from estimates of lag-times create even greater errors in attempting to account for variations in discharges with time. With more accurate estimates of lag-times there is certainly scope for more thorough interpretation of data in this

¹³⁷Cs

Salinity

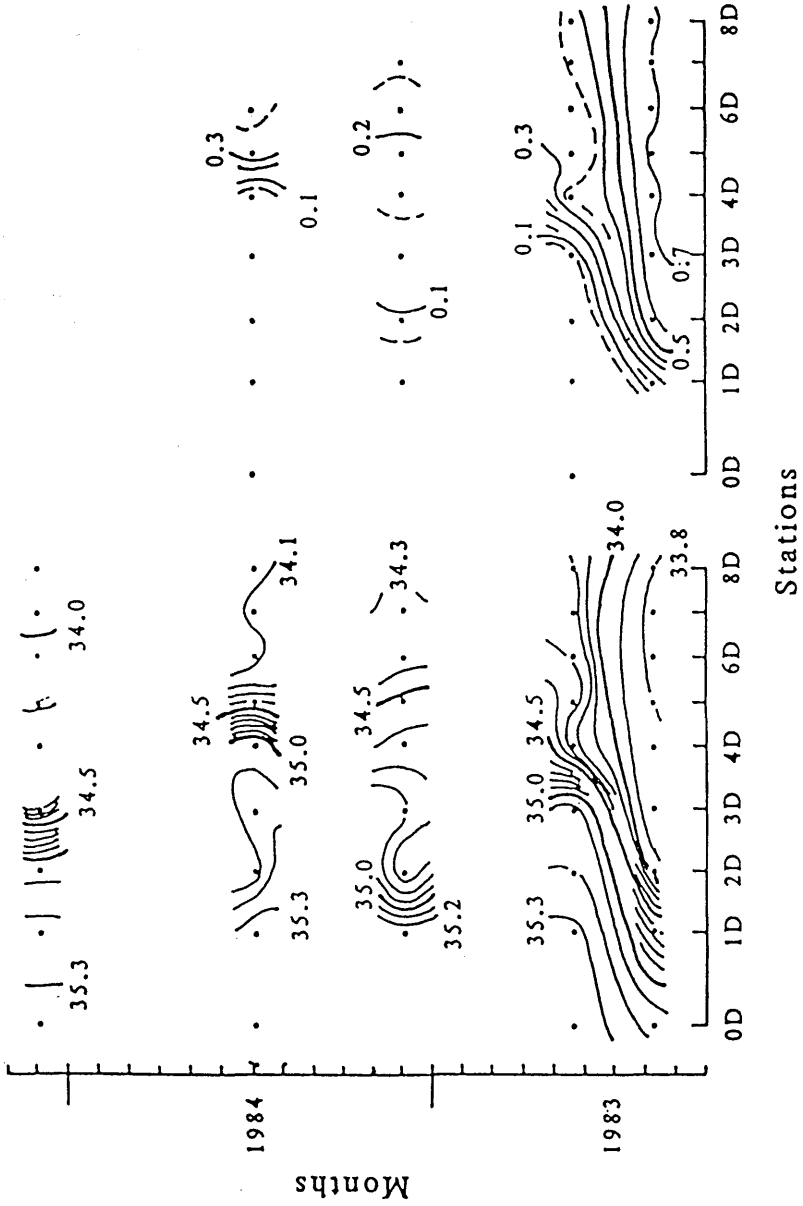


Figure 4.3.5 Isopleths of ¹³⁷Cs (Bq/l) and salinity (x 10³) against time for

section D, west of Islay

form or plotted on either a log vertical scale or with the latter scaled so that the maximum radiocaesium levels for each transect coincide (in order to obtain "proportional" differences).

4.3(d) The Islay Front

The Islay Front is a notable feature marking the convergence of Irish Sea / CSA water with Atlantic water in the southern HSA (see 4.2 (a)(i)); some attention has been focused here on defining its "behaviour".

The position and intensity of the Islay Front have been found to vary slightly between each cruise. In order to qualify these variations (using both radiocaesium and salinity observations), Figure 4.3.5 (^{137}Cs and salinity contours across the front for each cruise) has been used to deduce salinity and ^{137}Cs gradients across the front. This was performed by taking the change in salinity / ^{137}Cs across the span of the front and dividing by the distance of the latter. In some cases, the radiocaesium change across the front was derived from known salinity data by extrapolation using the corresponding ^{137}Cs / salinity curve (see subsection 4.2(a)). For the purpose of these calculations, the distances were obtained from the longitudinal coordinates of the actual station positions - presented in Table 4.3.2. Table 4.3.3 shows the results for the intensity of the front each cruise using both salinity and ^{137}Cs wherever possible. In attempting to understand the significance of the gradient across the front in terms of water flow, comparisons have been made with measurements of current velocities.

The current velocity record from the Tiree passage (provided by Ellett of SMBA - see Chapter 2, Figure 2.3) is shown in Figure 4.3.6

Table 4.3.2

Span of Islay Front Along Transect D (55°46'N)

Cruise	Span of Front (Longitudinal Degrees)	Salinity Change Across Front (‰)	¹³⁷ Cs Change Across Front (dpml ⁻¹)
July 1981	8.5'	6	8
May 1982	50.0'	10	5.6
May 1983	20.5'	10	4.1
August 1983	12.0'	8	5.3
*October 1983	15.0'	N.D.	5
January 1984	12.0'	5	4
June/July 1984	7.5'	7	9.5
February 1985	12.5'	8	N.D.

* = MAFF cruise

N.D. = No data available

Table 4.3.3

Intensity of Islay Front (Salinity and ^{137}Cs Gradients)
and Tiree Current Speeds (arbitrary units)

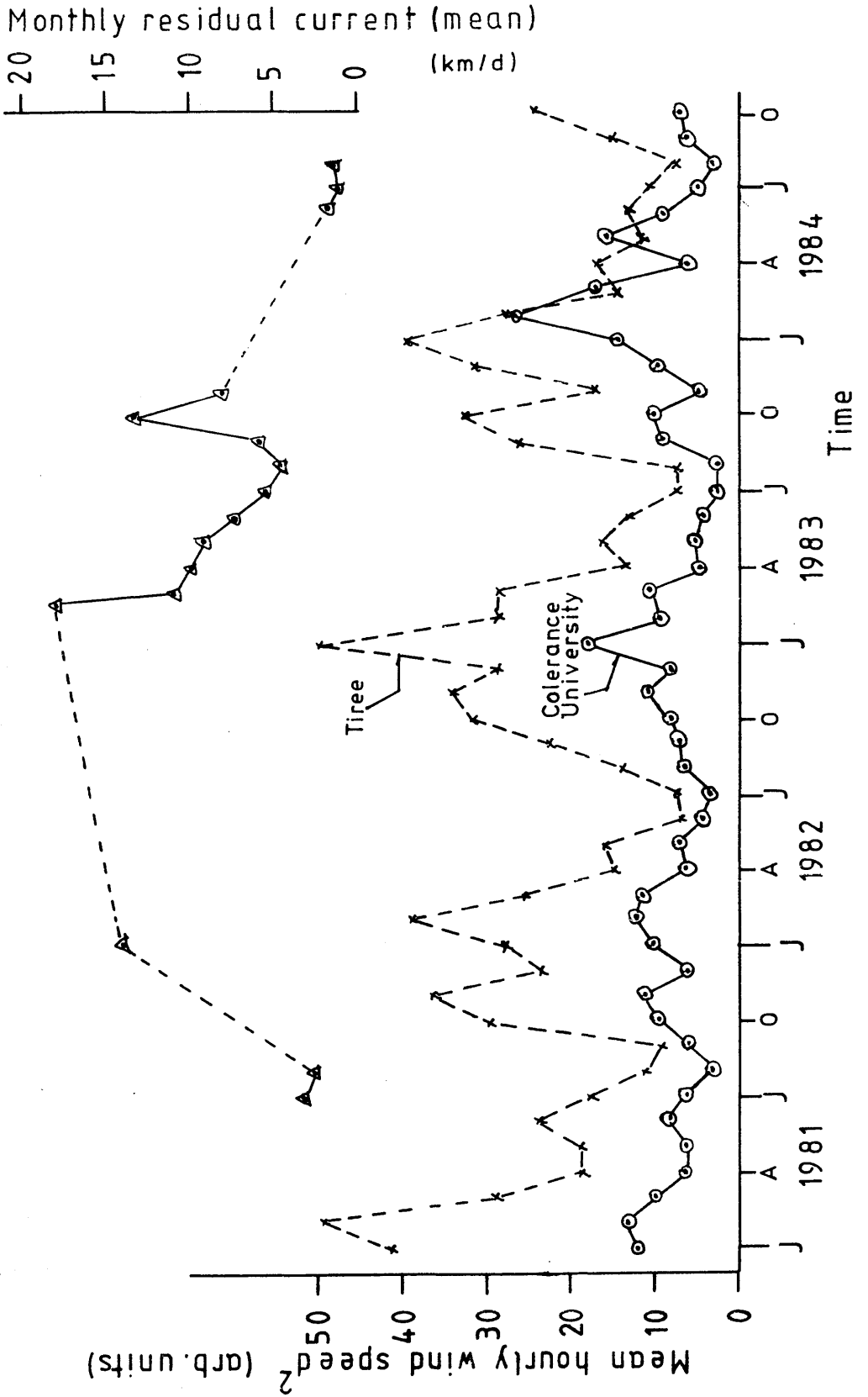
Cruise	Salinity gradient across front	^{137}Cs gradient across front	Tiree current speeds (kmdy^{-1})
July 1981	0.71	0.94	2.6
May 1982	0.18	0.11	5.6 in HSA ‡
May 1983	0.49	0.20	9.5
August 1983	0.67	0.44	5.5
*October 1983	N.D.	0.33	11.5
January 1984	0.42	0.33	Fast winds (see Figure 4.36)
June/July 1984	0.93	1.27	1.7
February 1985	0.64	N.D.	N.D.

* = MAFF cruise

‡ = Source of data = Hill (1983) (pers. comm)

N.D. = No data available

Figure 4.3.6 Current Speed at Tiree and Colerance² at Tiree and Colerance



and, in Table 4.3.3, the data (where available) are presented alongside the measurements of gradient intensity; data of the Tiree current velocities are supplemented by estimates / other measurements as indicated. Although the available current velocity data are not direct measurements from the region of the front, they can, for our purposes, be assumed indicative of generally weak or strong currents in the southern HSA - see correlation between Tiree and Colerance University (N. Ireland) wind speeds, (Figure 4.3.6). From Table 4.3.3, then, good inverse correlation can be seen between the front's intensity and the current velocities nearby. For May 1982, May 1983, October 1983 and January 1984, relatively fast currents (> 6 km day⁻¹) have been measured or, in the case of January 1984, estimated; for July 1981 (McKay et al., 1986) and June 1984 the currents were comparatively slow (< 4 km day⁻¹); for August 1983 a "moderate" current (≈ 5.5 km day⁻¹) was measured. Thus, the times of fastest and slowest currents have been found to correspond to times of weakest and strongest gradients respectively. This could be explained in the following manner. If two water masses meet and there is very little energy within the system (at the surface or throughout the water column) to provide strong mixing, then a strong gradient may form between the two. In a high energy system, however, the situation will create a weaker gradient, providing a less prominent boundary. It follows, then, that fast currents would be expected to prevent formation of a strong gradient whereas weaker currents would allow gradient development.

Having considered the changing intensity of the front, its shift in position east to west is examined. Figure 4.3.5 (transect D with time) shows the change in the front's position with time for the 7 cruises from May 1983 to January 1985 for which data are available. In

May 1983, then, the front was relatively weak (Table 4.3.3), current velocities measured at Tiree were relatively high and the front was positioned approximately between longitudes $7^{\circ}30'W$ and $7^{\circ}55'W$. From Figure 4.3.5 it can clearly be seen that this was a comparatively western position for the front. By August 1983, the front had shifted to a more eastern position, approximately $7^{\circ}00' - 7^{\circ}10'W$, and appeared stronger (Table 4.3.3), coinciding with slower Tiree current speeds which began to increase again with time until October 1983 when the MAFF cruise shows the front at its most eastern position yet, at about $6^{\circ}40' - 7^{\circ}00'W$, where it exists as a "weak" gradient (associated with fast currents at Tiree). A subsequent decrease in wind speeds (Figure 4.3.6) was accompanied by the recession / withdrawal of the front westwards and, in January 1984, it was observed at about $7^{\circ}30' - 7^{\circ}50'W$, (still) of relatively weak intensity and high current velocity (as estimated from records of strong winds) (see Figure 4.3.6). In June 1984, the front had shifted across to about $6^{\circ}55' - 7^{\circ}00'W$ where it was observed as a strong gradient accompanied by much slower currents (1.7km day^{-1}). There appears to be no simple relationship between current velocity and front position, although, with more detailed information on current directions (particularly along transect D), some correlation may be established, e.g. fast-moving Atlantic waters pushing into the HSA might shift the front to a more eastern position, whilst slow-moving Atlantic waters could allow (or be followed by) withdrawal of these waters from the HSA and cause the front to shift to the west. Also, there could be some correlation between positioning of the front and seasonal wind pattern, e.g. more eastern positions were observed in the summer months (August 1983, October 1983 and June 1984) and may have been the result of strong earlier winds / currents. Future investigations of short-term water

flow variations in the HSA would, no doubt, be helped by more detailed studies of the Islay Front and its behaviour.

4.3(e) Environmental Appearance (Ea) Factors Derived From Matching of Radiocaesium Time-Trends

By matching of radiocaesium time trends it has been possible to estimate transit times between various regions throughout the area of interest. In total, comparisons were made of 11 time-trends including the ^{137}Cs discharge record from Sellafield and the monthly ^{137}Cs levels measured in the CSA and Loch Etive (Figures 3.2 and 3.3, Chapter 3). The remaining 7 trends were those of transects Z, A, B, E, D, G and K. The maximum ^{137}Cs level found across each transect was used since only one value was required for each point in time. Figures 4.3.7-8 show the variation in levels with time for each of the 7 transects. By matching the trends and using the lag-times from Sellafield to the CSA and from Sellafield to Loch Etive, as derived in Chapter 3, lag-times were obtained from Sellafield to each region and are presented in Table 4.3.4.

From these lag-times, values for the environmental appearance (Ea) factor (see Chapter 3) were calculated. For every transect, a range of lag-times was obtained hence a range of Ea values was calculated.

The CSA Ea's show a notable increase after November 1983 (Chapter 3) with values almost reaching 0.800 and averaging at about 0.470 for 1984 whereas the average was less than half of this (~0.206) for 1983, 0.184 in 1982 and 0.220 in 1981. The sudden increase in Ea's was found to coincide with the sharp decrease in ^{137}Cs discharge levels and thus to reflect the amount of time required for the CSA to "register" the

Figure 4.3.7
Temporal Trend of ^{137}Cs Levels at Transects Z, A and D

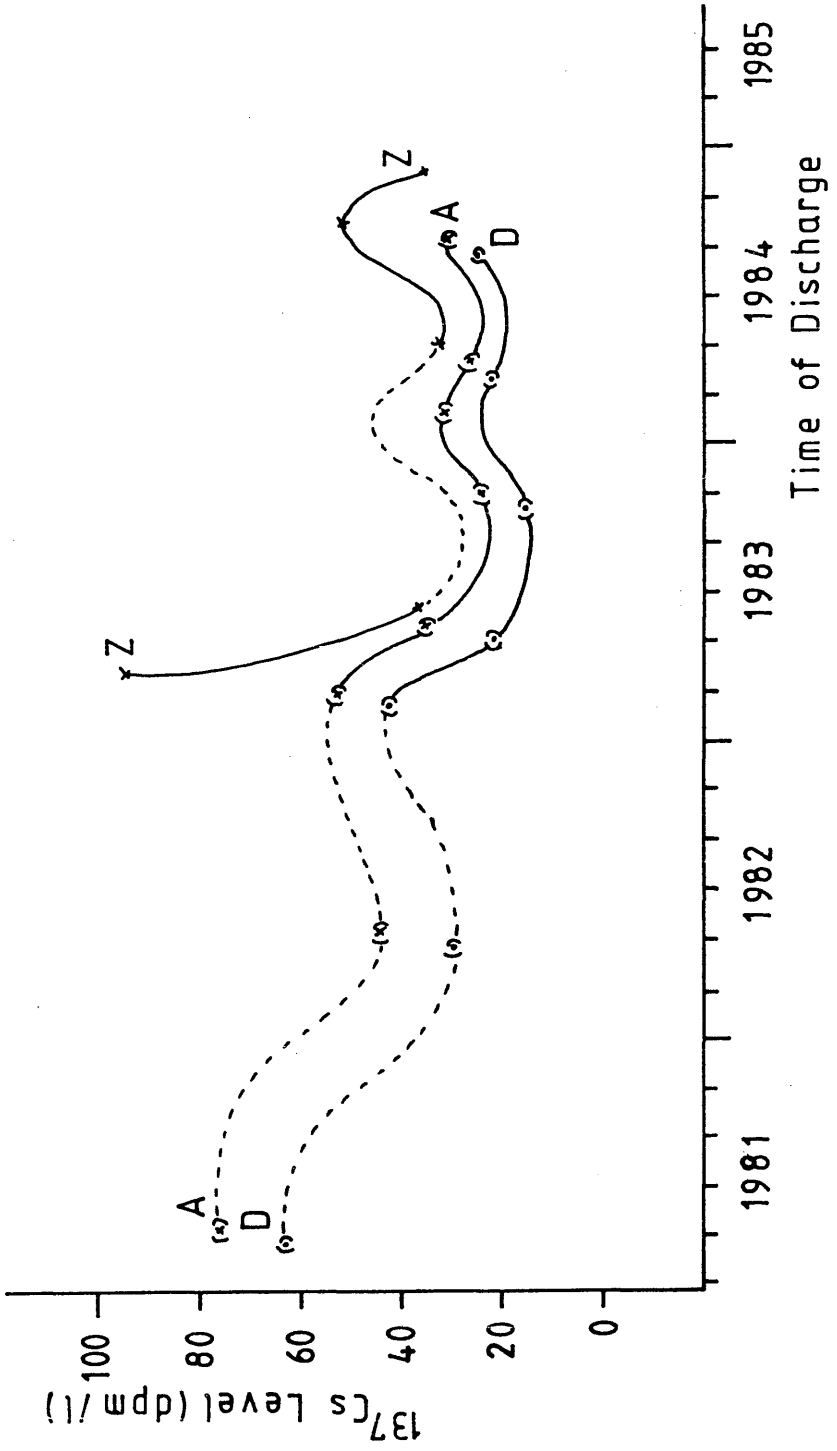


Figure 4.3.8
Temporal Trend of ^{137}Cs Levels at Transects B, E, G and K

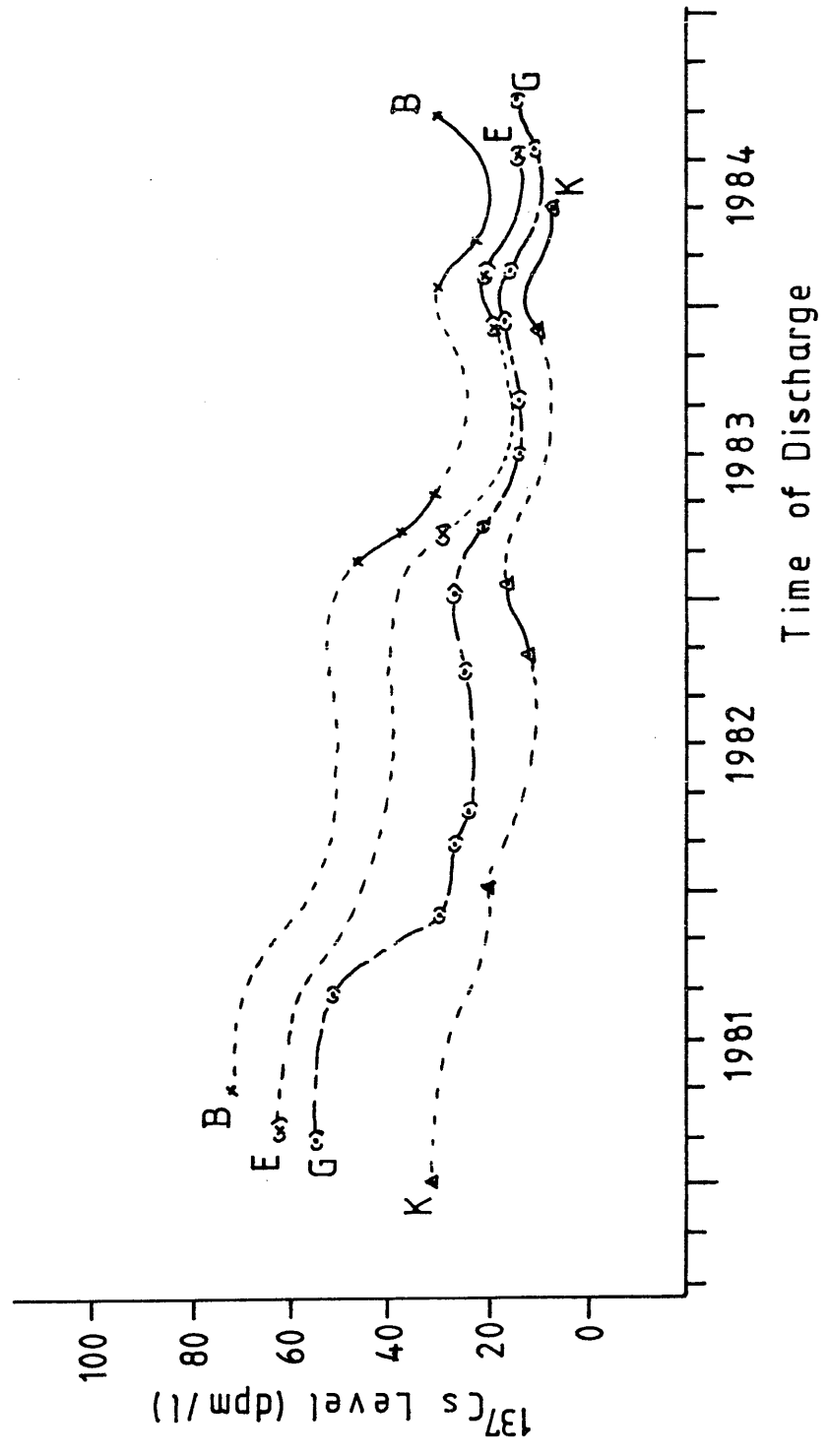


Table 4.3.4Transit Times From Sellafield to Various Transects

<u>Transect</u>	<u>Transit Time (months)</u>
Z	1.4 \pm 1.0
A	2.3 \pm 1.0
B	2.9 \pm 0.6
D	3.2 \pm 0.8
G	4.4 \pm 0.7
E	4.7 \pm 0.8
K	6.7 \pm 1.0

significant change in discharges. This delay in the CSA's recognition of the change in discharge levels was attributed to water residence / mixing between Sellafield and the CSA.

Furthermore, the fact that it has been possible to match up the 7 radiocaesium time trends (Figures 4.3.7,8) indicates that water mixing could not have been sufficiently thorough, along the main path of the plume, to disrupt the general radiocaesium pattern with time. Since a match between these 7 trends and those of the CSA, Loch Etive and the Sellafield discharges is also achievable (see Figures 3.2 and 3.3, Chapter 3), the conclusion drawn is that, although some mixing is detectable within the Irish Sea section (see above), the general radiocaesium discharge pattern with time is recognisably retained in sea water levels as far as the Minches ("transect K). If thorough mixing had occurred at any stage along the path of the plume then retention of the Sellafield discharge record would not be expected throughout the plume's journey. The main discrepancy between the Sellafield discharge record and the North Channel and HSA trends occurs at the time of the July - September 1983 discharges. This increase in discharges has been recorded fairly consistently as a trough in other trends. From the CSA trend, however, a peak, interrupted by a sharp, sudden drop in February 1984, is evident. This drop has earlier (Chapter 3) been attributed to the significant dilution of HSA waters by low-radiocaesium Atlantic waters, as observed from the January 1984 cruise data. Such dilution by saline waters from the Atlantic would, therefore, explain why the trough is apparent in transects A, D and G whilst it took longer to appear, and was less obvious, in the CSA. Therefore, although the Sellafield discharge pattern can, with an adequately long record, be recognised, the effects of the Atlantic behaviour are superimposed on the record

Table 4.3.5

Environmental Appearance (Ea) Factors for Various Transects for Corresponding Lag Times
from Sellafield (see Table 4.3.4) ($\text{Bq l}^{-1}/\text{TBq day}^{-1}$)

	<u>Month of Discharge</u>		<u>Transect</u>						
	Z	A	B	D	G	E	K		
<u>1982</u>									
Feb.	N.D.	N.D.	0.175	0.094	0.080	N.D.	N.D.	N.D.	
Mar.	N.D.	0.147	N.D.	N.D.	0.079	N.D.	N.D.	N.D.	
Sept.	N.D.	N.D.	N.D.	N.D.	N.D.	N.D.	N.D.	N.D.	
Oct.	N.D.	N.D.	N.D.	N.D.	N.D.	N.D.	N.D.	N.D.	
Nov.	N.D.	N.D.	N.D.	N.D.	N.D.	N.D.	N.D.	0.033	
Dec.	N.D.	N.D.	N.D.	N.D.	N.D.	N.D.	N.D.	N.D.	
<u>1983</u>									
Jan.	N.D.	N.D.	N.D.	N.D.	0.103	N.D.	N.D.	N.D.	
Feb.	N.D.	N.D.	N.D.	0.161	N.D.	N.D.	N.D.	0.061	
Mar.	N.D.	0.191	N.D.	N.D.	N.D.	0.107	N.D.	N.D.	
Apr.	N.D.	N.D.	N.D.	N.D.	0.114	N.D.	N.D.	N.D.	
May	0.243*	N.D.	0.213	0.146	N.D.	N.D.	N.D.	N.D.	
Jun.	0.180	0.171	N.D.	N.D.	0.070	N.D.	N.D.	N.D.	
Jul.	N.D.	N.D.	N.D.	N.D.	N.D.	N.D.	N.D.	N.D.	
Aug.	N.D.	N.D.	N.D.	N.D.	N.D.	N.D.	N.D.	N.D.	
Sep.	N.D.	N.D.	N.D.	N.D.	0.060	N.D.	N.D.	N.D.	
Oct.	N.D.	N.D.	N.D.	0.085	N.D.	N.D.	N.D.	N.D.	
Nov.	N.D.	0.245	N.D.	N.D.	N.D.	N.D.	N.D.	N.D.	
Dec.	N.D.	N.D.	N.D.	N.D.	0.274	0.297	0.156	0.156	

Table 4.3.5 cont.'d

Environmental Appearance (Ea) Factors for Various Transects for Corresponding Lag Times from Sellafield (see Table 4.3.4) ($\text{Bq l}^{-1}/\text{TBq day}^{-1}$)

Month of Discharge	Transect											
	Z	A	B	D	G	E	K					
<u>1984</u>												
Jan.	N.D.	N.D.	N.D.	N.D.	N.D.	N.D.	N.D.	N.D.	N.D.	N.D.	N.D.	N.D.
Feb.	N.D.	0.450	0.360	N.D.	0.230	0.297	N.D.	N.D.	N.D.	N.D.	N.D.	N.D.
Mar.	N.D.	N.D.	0.515	0.501	N.D.	N.D.	N.D.	N.D.	N.D.	N.D.	N.D.	N.D.
Apr.	N.D.	0.600	N.D.	N.D.	N.D.	N.D.	N.D.	N.D.	N.D.	N.D.	N.D.	N.D.
May	0.557	N.D.	N.D.	N.D.	N.D.	N.D.	N.D.	N.D.	N.D.	N.D.	0.127	N.D.
Jun.	N.D.	N.D.	N.D.	N.D.	N.D.	N.D.	N.D.	N.D.	N.D.	N.D.	N.D.	N.D.
Jul.	N.D.	N.D.	N.D.	N.D.	0.259	0.265	N.D.	N.D.	N.D.	N.D.	N.D.	N.D.
Aug.	N.D.	N.D.	N.D.	0.385	N.D.	N.D.	N.D.	N.D.	N.D.	N.D.	N.D.	N.D.
Sept.	N.D.	N.D.	0.300	N.D.	N.D.	N.D.	N.D.	N.D.	N.D.	N.D.	N.D.	N.D.
Oct.	0.502	0.350*	N.D.	N.D.	N.D.	N.D.	N.D.	N.D.	N.D.	N.D.	N.D.	N.D.
Nov.	N.D.	N.D.	N.D.	N.D.	N.D.	N.D.	N.D.	N.D.	N.D.	N.D.	N.D.	N.D.
Dec.	0.555	N.D.	N.D.	N.D.	N.D.	N.D.	N.D.	N.D.	N.D.	N.D.	N.D.	N.D.
<u>1985</u>												
Jan.	N.D.	N.D.	N.D.	N.D.	N.D.	N.D.	N.D.	N.D.	N.D.	N.D.	N.D.	N.D.

N.D. = No data available

* = ^{137}Cs level corrected for fresh water dilution using ^{137}Cs salinity curve

as are the effects of water residence, e.g. in the Irish Sea.

Table 4.3.5 shows the E_a values for the mean lag-time for each transect whilst E_a 's for the range of lag-times are presented in Appendices III.3 - III.9. As discussed in Chapter 3 (section 3.1), a series of E_a 's can give an indication of dilution factors between two sites besides giving a measure of the extent of water residence. The greater the residence time, the longer lasting the effect of old discharge levels on recent discharges and, thus, the more pronounced the smoothing / dampening effect on the radiocaesium discharge record. Table 4.3.6 presents the dilutions from transect A, thus allowing comparison with the dilution factors obtained from spatial radiocaesium distributions (Table 4.3.1), as discussed in subsection 4.3(b). There is good agreement between the two methods, with dilutions along the path of the main radiocaesium plume remaining quite low, i.e. 2-3 times for the approaches to the Little Minch. Across the path of the plume, dilution factors obtained from E_a values indicate ~4.5 times dilution by Barra Head.

From Table 4.3.5, the increase in E_a value after the November 1983 discharge is apparent for each transect (Z, A, B, D, G, E and K) and, in certain cases (transects A, B and D), there are sufficient data to show the subsequent drop in E_a 's approximately after the April 1984 discharge.

As might be expected, the E_a 's generally decrease northwards, i.e. with increasing distance from the point of radiocaesium discharge, but it is interesting to note that the CSA (Table 3.1, Chapter 3) has higher E_a 's and a longer transit time than have transects B, D, G and E and transect E has generally higher E_a 's and a longer transit time than has transect G. In the first case, this could be explained by mixing of the plume with low-radiocaesium Atlantic

Table 4.3.6

Dilution Factors of ^{137}Cs Between the North Channel (Transect A) and Various Transects,
as Derived from Respective E_a values

<u>Transect</u>	<u>B</u>	<u>D</u>	<u>E</u>	<u>G</u>
Dilution Factor	1.06 (Feb. '84)	1.53 (Mar. '82)	1.79 (Mar. '83)	1.84 (Mar. '82)
(Month of Discharge)	1.17 (Apr. '84)	1.23 (Mar. '83)	1.52 (Feb. '84)	2.44 (Jun. '83)
	1.09 (Sep. '84)	1.20 (Apr. '84)		1.96 (Feb. '84)
Mean Dilution Factor (σ_n)	1.11 (\pm 0.05)	1.32 (\pm 0.15)	1.66 (\pm 0.14)	2.08 (\pm 0.26)

waters "en route" to transects B, D, G and E; hence dilution is marked, regardless of the transit time. For the CSA, however, a higher proportion of the radiocaesium plume waters has mixed with "moderate-radiocaesium" waters within the CSA, i.e. in a more restricted / isolated area; thus, dilution is not so marked. A similar explanation could be applied to the second case; transect G, being closer to the Atlantic water, is more exposed to lower radiocaesium levels than is transect E; thus, dilution is more marked than in the latter, again, regardless of the transit times involved.

From Table 4.3.6, it seems that, once the radiocaesium plume exits the North Channel, there is limited water residence since the ratio of Ea's between Transect A and each transect has remained more or less constant. Although the data used in deducing this are few, they are consistent. In order to qualify the above suggestion with additional data, Ea ratios of Seascale to Transect A and of Seascale to Transect G have been considered and are presented in Table 4.3.7. Variation in the ratio of Ea's of two sites with time indicates the influence of water residence between the two sites and, as can be seen from Table 4.3.7, the decrease in dilution factor (ratio of Ea's) between Seascale and Transect A (~ 0.5), after the November 1983 discharge, is very similar to that between Seascale and Transect G. Therefore, between Transects A and G, there would appear to be very little variation and any water residence between Sellafield and the HSA (e.g. transect G) would thus appear to have occurred almost entirely within the Irish Sea. The dilution factor from Seascale to Transect A was found to be ~ 22 before (and ~ 12 after) the November 1983 discharge, whilst, correspondingly, from Seascale to Transect G, it was ~ 45 (and ~ 20). These data indicate that greater dilution has occurred within the Irish Sea (\sim twentyfold) than along the west coast

Table 4.3.7

Dilution Factors of Radiocaesium Between Seascale
and Transect A and Seascale and Transect G

() = Dilution factor normalised to that for March 1982 discharge

Month of Discharge	Seascale to Transect A	Seascale to Transect G
<u>1982</u>		
Jan.	N.D.	38.9 (0.97)
Feb.	N.D.	N.D.
Mar.	21.8 (1.00)	40.1 (1.00)
Sep.	N.D.	50.5 (1.26)
<u>1983</u>		
Jan.	N.D.	36.5 (0.91)
Feb.	N.D.	N.D.
Mar.	20.2 (0.93)	N.D.
Apr.	N.D.	65.8 (1.64)
May	N.D.	N.D.
Jun.	22.9 (1.05)	55.0 (1.39)
Sep.	N.D.	47.1 (1.18)
Oct.	N.D.	N.D.
Nov.	24.1 (1.11)	N.D.
Dec.	N.D.	15.2 (0.38)
<u>1984</u>		
Feb.	10.2 (0.47)	19.9 (0.50)
Mar.	N.D.	N.D.
Apr.	15.4 (0.71)	N.D.
Jul.	N.D.	23.9 (0.60)
Oct.	9.03 (0.41)	N.D.

N.D. = No data available

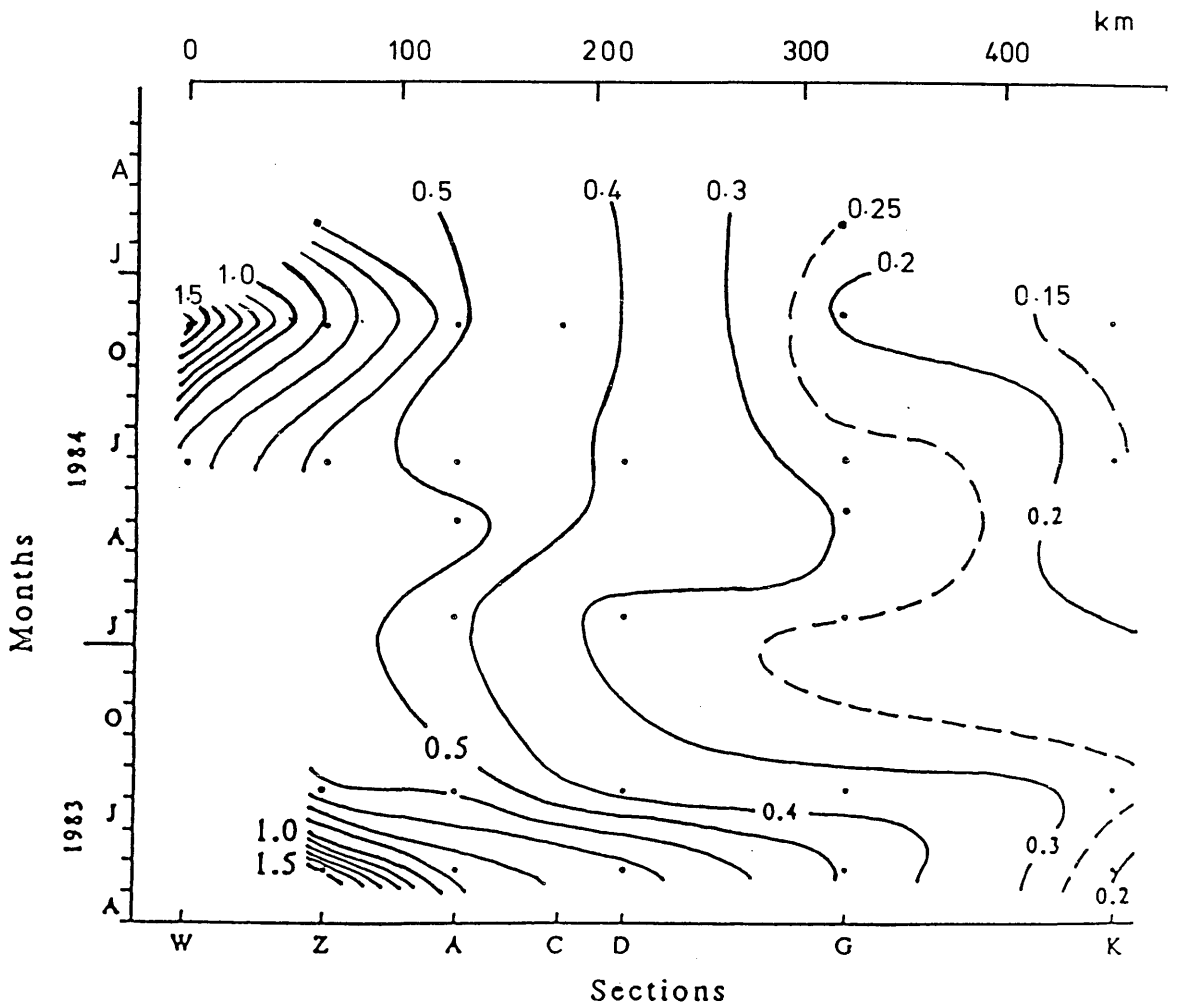
of Scotland (~twofold).

Monthly data from a series of stations would allow further investigation of variations in E_a 's and assessment of the degrees of mixing occurring in the various regions.

4.3(f) Overall Radiocaesium Variations with Time

An overall view of radiocaesium changes with time throughout the area is presented in Figure 4.3.9. A brief explanation of this figure is as follows. From bottom to top is the time scale and from left to right the distance, along the main path of the plume, from transect W (in the Irish Sea) as far as transect K (the Minches). The maximum radiocaesium level across each transect has been used for each cruise and ^{137}Cs contours subsequently drawn to show the general change in radiocaesium levels with time throughout the area. The isopleths, therefore, show highest radiocaesium concentrations occurring in the Irish Sea, with levels decreasing with increasing distance from the source point (i.e. from left to right) and with time (i.e. from bottom to top). Superimposed on this general trend are short-term (~2-6 months) variations in Sellafield radiocaesium discharge levels and also variations in Atlantic water behaviour. For example, the relatively high levels throughout the area during the May 1983 cruise are attributable both to the relatively high discharge levels ~2-5 months prior to the cruise and to the relatively low influence of Atlantic water in the area at the time of the cruise (subsection 4.2(a)) whilst the much lower levels in the August 1983 and January 1984 cruises are mainly attributable to the strong influx of Atlantic waters into the area, particularly around September / October 1983 (see subsection 4.2(c)).

Figure 4.3.9



Isopleths of ^{137}Cs peak values (Bq/l) on the sampling sections against time, 1983-85

When a change in levels affects the entire area under study at the same time then the cause was probably a change in Atlantic water behaviour (e.g. the decreased radiocaesium levels in January 1984 due to increased dilution by Atlantic waters). When an increase or decrease is observed at different times at different places, however, the cause is more likely to be changes in the Sellafield discharges which appear in areas near the source point earlier than they do in areas remote from the source point. For example, the increase in Irish Sea and North Channel radiocaesium levels in November 1984 do not appear north of about transect D until the February 1985 cruise when the increase is observed at transect G. This, therefore, must be a result of increased discharge levels in September / October 1984 with the increase being detected at progressive stages of the plume's path with time. The relatively high levels observed at transect K in the August 1983 cruise - as a result of the earlier (May 1983), relatively high levels - were probably a result both of low dilution by Atlantic waters due to weak Atlantic influx in the southern HSA and of relatively high discharges around February 1983 appearing as relatively high radiocaesium levels in the southern HSA and in the Minches (transect K) in May 1983 and August 1983 respectively.

4.3(g) Summary and Conclusions

Dilution factors obtained using two independent methods indicate a relatively low rate of dilution ("two-threefold) of the main radiocaesium plume along the west Scottish coast, i.e. from the northern exit of the North Channel to the Minches. Data obtained from one of these two methods - from E_a values - indicate correspondingly greater ("twentyfold) dilution within the Irish Sea.

^{137}Cs /salinity plots for individual transects with time reflect the general temporal decrease in radiocaesium discharges. For transects nearer the discharge point, "apparent" greater variation in radiocaesium levels with time than for those of transects farther from the discharge point have been, in the main, attributed to the linear radiocaesium scale used.

Comparison of radiocaesium time-trends at each transect has shown that only between the North Channel's southern and northern transects was there any noticeable difference in proportional variations in radiocaesium levels. This indicates that some mixing occurs within this region (North Channel / CSA) but almost none occurs beyond here, during the main plume's path along the west coast of Scotland, as far as the Minches.

Matching of radiocaesium time trends at various sites in the HSA and nearby waters has allowed estimation of transit times between these sites. Such partial preservation of the Sellafield discharge record in radiocaesium levels along the path of the plume as far as The Minches (transect K) indicates that there was no thorough mixing of these waters at any stage of the plume's journey. Thus, although some mixing occurs within the Irish Sea, a fraction of the Sellafield discharged material, travelling mainly in the surface waters of the coastal current, arrives in the Minches having, overall, undergone relatively little mixing.

From comparison of E_a values at various sites, it appears that most of the water residence undergone between Sellafield and the transects along the west coast of Scotland had been incurred within the northeastern Irish Sea.

Higher E_a 's accompanied by longer transit times for some areas (e.g. the CSA) than others (e.g. transects B and G) have been

attributed, in the case of the latter, to greater dilution by "low-radiocaesium" waters along a more direct route and, in the former context, to longer residence / mixing with "moderate-radiocaesium" waters, in the case of the CSA, because of (some degree of) isolation of the area from low-radiocaesium waters, e.g. Atlantic water.

Observation of the behaviour of the Islay Front has revealed that, during the period studied, the front is accompanied by slow currents when it is strong (i.e. the ^{137}Cs /salinity gradient across the front is sharp) and by fast currents when it is weak. The current velocities were measured at Tiree and were found to correlate well with wind speeds, measured both at Tiree and N. Ireland, and, thus, were assumed to reflect conditions near / at the Islay Front.

Since the front marks the boundary between Atlantic and Irish Sea / CSA waters, its east - west movements may be related to Atlantic water incursions into the HSA, influenced / controlled by the wind regime.

Presentation of maximum radiocaesium levels at each transect from each cruise has provided an overall record of temporal variations of radiocaesium levels throughout the area. This picture illustrates earlier explanations for the causes of the radiocaesium variations (i.e. changes in Atlantic water behaviour and in Sellafield discharge levels).

4.4 Deep Samples

a) Introduction

To date, measurements of radiocaesium levels at depth in waters of the British Isles have been concentrated largely in the Irish Sea and North Channel and have been carried out almost exclusively by MAFF (e.g. Preston et al., 1972; Jefferies et al., 1973, 1982) during their regular sampling schedules.

Within the Irish Sea, the above workers found little stratification of radiocaesium in the water column except in the immediate vicinity of discharge - with surface levels twice the bottom values - and in the deep channel area between the Irish coast, the Isle of Man and Anglesey - surface levels here are about 1.5 times those at depth. In the latter case, radiocaesium concentration was found to be inversely proportional to salinity (bottom waters being the more saline); in the former case, it was assumed that fresh water effluent had not been completely mixed. The Clyde and Minch were found to be well mixed (May 1972) but, west of Tiree off Barra Head and midway between the Butt of Lewis and Cape Wrath (in July 1972), bottom radiocaesium levels were only half those at the surface. The North Channel was found to be generally well-mixed.

Livingston and Bowen (1977) collected 3 subsurface samples from one station in the Minch and found the radiocaesium content of the deepest sample (10 metres from the bottom) to be >75% of the surface value and ~72% of the maximum measured level, the latter being at 30 metres. Other workers (McKinley, 1979; McKay, 1983) have investigated subsurface radiocaesium levels in the more isolated systems of Scottish sea lochs.

As described earlier, modelling the circulation of these ¹³⁷Cs-rich coastal waters has been attempted on various scales and has involved a range of assumptions re the vertical distribution of radiocaesium in the water column (Wilson, 1974; McKinley et al., 1981b; McKay and Baxter, 1985a; Prandle, 1984; McKay et al., 1986). Prandle assumed a homogenous water column for the Irish Sea, HSA, coastal waters along west and north Scotland and North Sea. He concluded that the cause of the breakdown of agreement between the modelled and observed radiocaesium levels after 1976 originated within the Irish Sea and he suggested the use of a more detailed three dimensional model. McKay and Baxter (1985a) and McKinley et al. (1981b) assumed a homogenous water column for the Clyde Sea Area as did Wilson (1974) for the Irish Sea, whilst McKay et al. (1986) proposed that, in summer, advective changes of radioactivity on the scale of 1-2 months in the HSA were in the "surface mixed layer" (i.e. above the halocline) and that below the halocline, changes in levels were negligible during this period. Somewhere between the two extremes, a) total homogeneity and b) total confinement to surface waters, lies the true picture. To improve our knowledge of the latter, actual "field" / observed data, i.e. subsurface, as well as surface radiocaesium levels, are required. It is with this aim in mind that the following results are presented and discussed.

The data are first considered in chronological cruise order since different stations were sampled at depth during each cruise. In subsection 4.4(b), the five cruises, August 1983, April/May 1984, June 1984, November 1984 and January 1985 respectively, are dealt with first. Then the topic of radiocaesium flow through the North Channel is discussed. Subsection 4.4(c) provides a summary and conclusion to this section.

b) Results and Discussion

(i) August 1983

Five deep samples were collected from a total of 4 stations - G7, J2, J3 and K3 - during this cruise; the results are presented in Appendix II.2b and Table 4.4.1. The two samples from below the Atlantic / Irish Sea halocline* (G7-137 metres, near the sea bed and J2-90 metres) were the two of significantly reduced radiocaesium levels (<10% and 55% respectively) relative to surface values. For the "above-halocline" samples or those from a well-mixed water column, the subsurface radiocaesium levels were found to be 80% of the surface values.

To examine whether the relationship between subsurface radiocaesium and salinity levels is comparable with that for surface waters, the subsurface data were plotted on the ^{137}Cs / salinity curve. In Figure 4.4.1, these points fall on, or very close to, the curve, indicating that subsurface waters do, indeed, carry the same relationship signal between the two properties as do surface waters. If this finding holds generally, extrapolations data for deep water radiocaesium levels could be generated from known salinities. However, more supporting data are necessary.

* determined by the salinity increase between the surface and each sample depth, e.g. a salinity increase of >0.150‰ at 50 metres (relative to surface salinity) would imply that 50 metres was below the "halocline".

Table 4.4.1Results of Deep Samples, August 1983

Station	Depth (metres)	^{137}Cs (dpm l^{-1})	$\frac{^{137}\text{Cs}}{^{137}\text{Cs}-0m}$ * (%)	Salinity (‰)	ΔS † (‰)
G7	136	2.0	9.5	35.228	1.050
J2	50	14.5	94	34.627	0.085
J2	90	8.4	55	34.926	0.384
J3	40	12.7	84	34.694	0.108
K3	60	14.6	99	34.549	0.008

* $^{137}\text{Cs}-0m = ^{137}\text{Cs}$ Level

† $\Delta S = \text{Salinity} - \text{Surface salinity}$

Figure 4.4.1

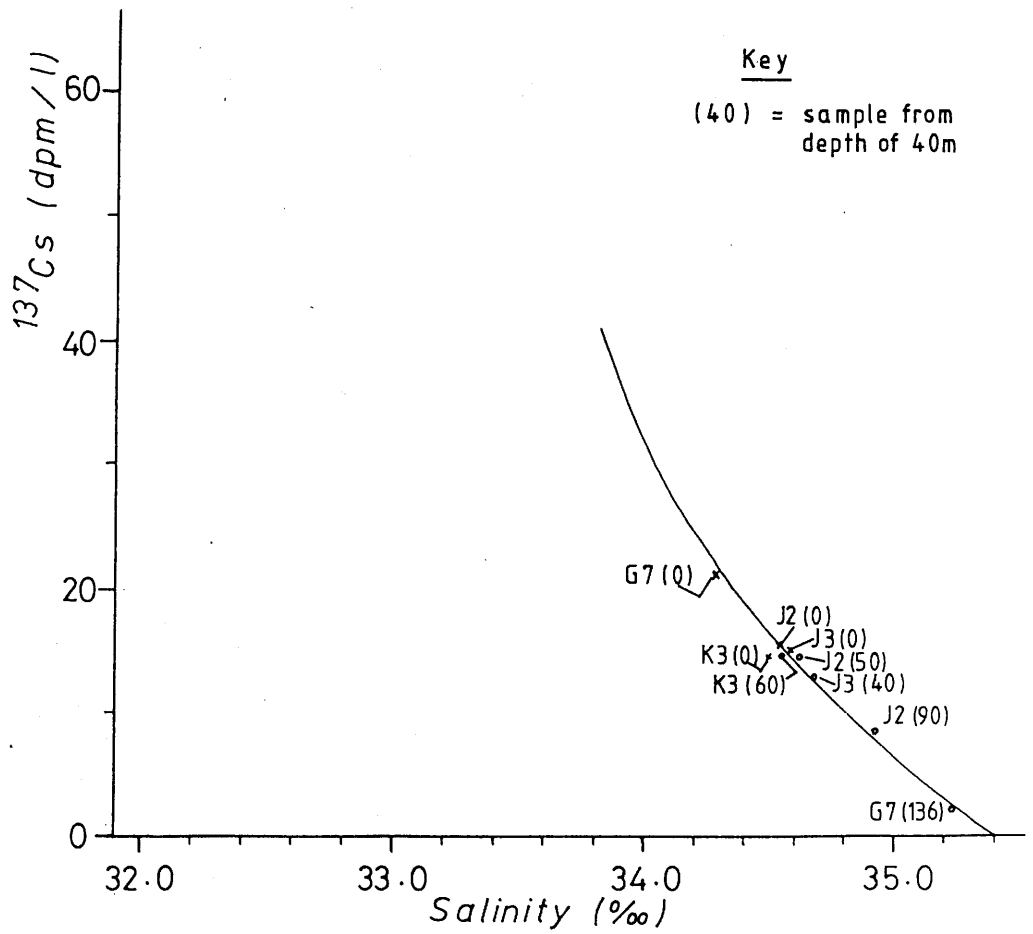
 ^{137}Cs / Salinity Curve - August 1983

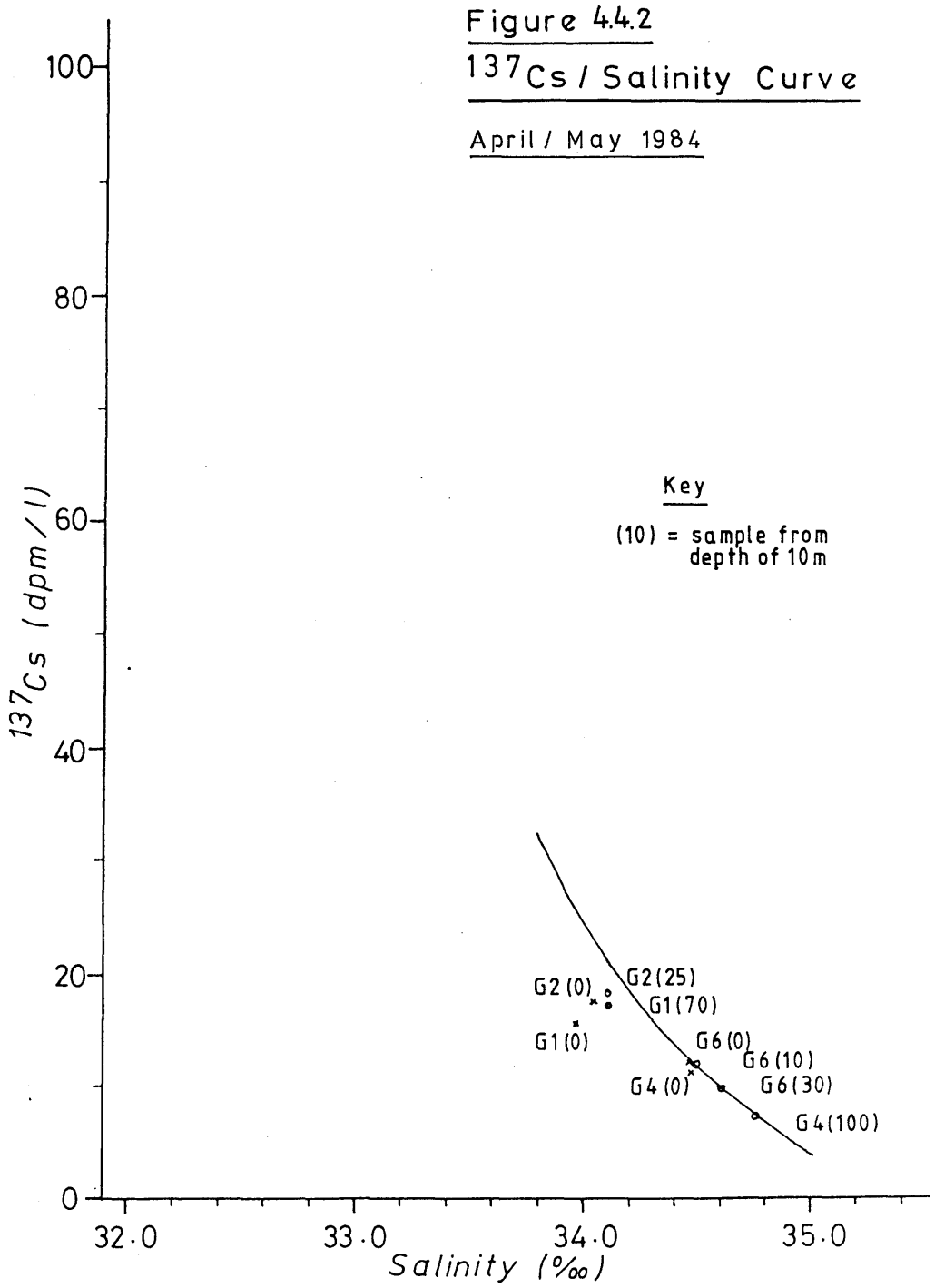
Table 4.4.2Results of Deep Samples, April/May 1984

Station	Depth (metres)	^{137}Cs (dpm l ⁻¹)	$\frac{^{137}\text{Cs}}{^{137}\text{Cs-0m}^*}$ (%)	Salinity (‰)	ΔS † (‰)
G1	10	17.6	114	N.M.	N.M.
G1	30	17.0	110	N.M.	N.M.
G1	70	17.0	110	34.124	0.135
G2	25	18.1	103	34.139	0.071
G4	75	9.8	87	N.M.	N.M.
G4	100	7.2	64	34.775	0.225
G6	10	11.9	100	34.512	0.009
G6	30	9.8	82	34.619	0.116

* $^{137}\text{Cs-0m} = ^{137}\text{Cs}$ level at surface

† $\Delta S = \text{Salinity} - \text{surface salinity}$

NM = Not measured



(ii) April / May 1984

Only 8 deep samples from transect G - analysed by MAFF - were collected during this cruise (Appendix II.4b). The two inshore stations, G1 and G2, showed slightly higher radiocaesium at depth than at the surface; this can be attributed to surface fresh water dilution (see Table 4.4.2) - as indicated by the greater deviation to the left hand side of the ^{137}Cs / salinity curve by surface G1 and G2 samples than by corresponding deeper samples (Figure 4.4.2). The other 2 stations, G4 and G6, exhibited decreased radiocaesium levels at depth as follows; at G4-100 metres, a 1.6 times reduction to 64% of the surface value and, at G6-30 metres, a 1.2 times reduction to 83% of the surface value. Both were accompanied by salinity increases at depth, 0.275‰ at G4 and 0.116‰ at G6 (Table 4.4.2). Again, it is the sample from below the "halocline" (G4-100 metres) which showed the greatest reduction (relative to surface values) in radiocaesium content.

(iii) June / July 1984

From this summer cruise, 23 deep samples were analysed by GU and an additional 17 by MAFF; the data are presented in Appendix II.5b and Table 4.4.3. Figure 4.4.3 shows the sample data presented on the ^{137}Cs / salinity curve; most fall very close to the curve.

Beginning at transect W in the Irish Sea, two stations were sampled at 55 metres - about 10 metres above the sea bed. Their radiocaesium levels were >90% of the respective surface levels, whilst salinity data showed a <0.05‰ change throughout the water column; this illustrates a well-mixed column. However, the horizontal

Table 4.4.3Results of Deep Samples, June/July 1984

Station	Depth (metres)	^{137}Cs (dpm l ⁻¹)	$^{137}\text{Cs}/^{137}\text{Cs-0m}^*$ (%)	Salinity (‰)	ΔS † (‰)
A2	50	24.8	95	33.940	0.017
A2	100	23.3	89	34.045	0.122
A4	100	18.8	80	34.221	0.138
B2	30	21.5	94	33.915	0.008
B2	60	23.3	101	33.917	0.010
B4	50	21.3	96	33.903	0.005
B4	112	24.2	109	33.907	0.009
D2	40	0.5	167	33.050	-0.285
D4	40	1.8	360	35.011	-0.053
D7	40	20.7	99	34.125	0.005
E3	80	19.0	89	33.982	0.025
G1	25	15.0	91	34.237	0.025
G1	55	15.0	91	34.263	0.051
G2	20	16.5	100	34.305	-0.004
G2	40	16.5	100	34.302	-0.007
G4	30	10.3	91	34.620	0.049
G4	75	6.7	59	34.920	0.349
G6	30	5.6	119	34.994	0.000
G7	60	7.7	100	35.020	0.040
G7	130	0.8	10.4	35.321	0.341

cont.'d

Table 4.4.3 cont.'d

Results of Deep Samples, June/July 1984

Station	Depth (metres)	^{137}Cs (dpm l ⁻¹)	$^{137}\text{Cs}/^{137}\text{Cs-0m}^*$ (%)	Salinity (‰)	ΔS^\ddagger (‰)
G9	75	0.04	0.7	35.390	0.458
G9	150	0.1	1.8	35.413	0.481
G11	30	7.2	100	34.828	0.003
G11	60	6.7	15	34.892	0.067
G13	40	5.1	71	34.970	0.152
G13	100	2.2	31	35.200	0.382
G15	100	0.4	100	35.369	0.016
G16	125	0.1	33	35.420	0.027
J2	40	4.0	93	35.100	-0.045
J2	60	3.8	88	35.065	-0.800
J2	80	3.8	88	35.077	-0.068
K2	100	7.8	96	34.738	0.017
W2	55	39.2	91	33.732	0.020
W4	55	46.3	92	33.561	-0.006
Y2	40	28.6	89	33.857	0.319
Y4	60	28.4	93	33.838	0.184
Z2	50	25.7	93	33.95	0.03
Z2	100	26.3	95	33.937	0.019
Z4	100	25.1	84	33.98	0.06
Z4	200	22.7	76	34.00	0.08

* $^{137}\text{Cs} - 0\text{m} = ^{137}\text{Cs}$ level at surface

† $\Delta S = \text{Salinity} - \text{surface salinity}$

Figure 4.4.3
 ^{137}Cs / Salinity Curve
June / July 1984

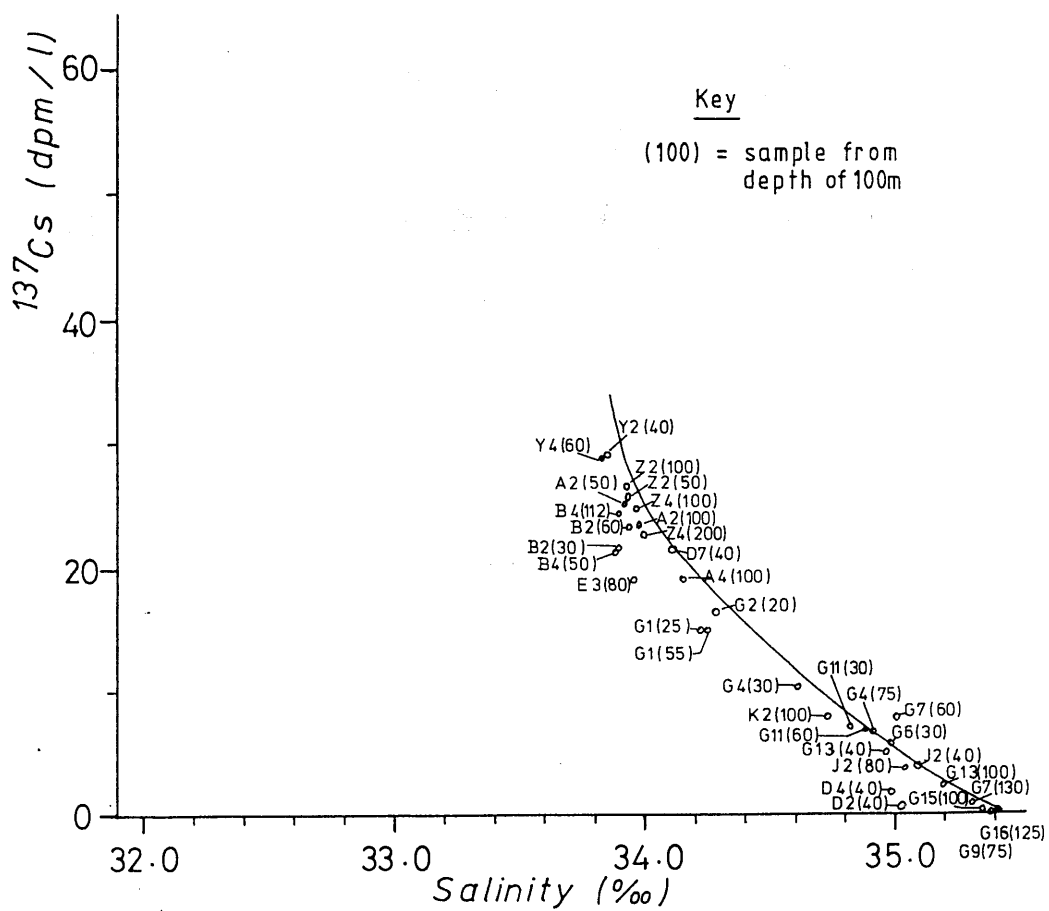
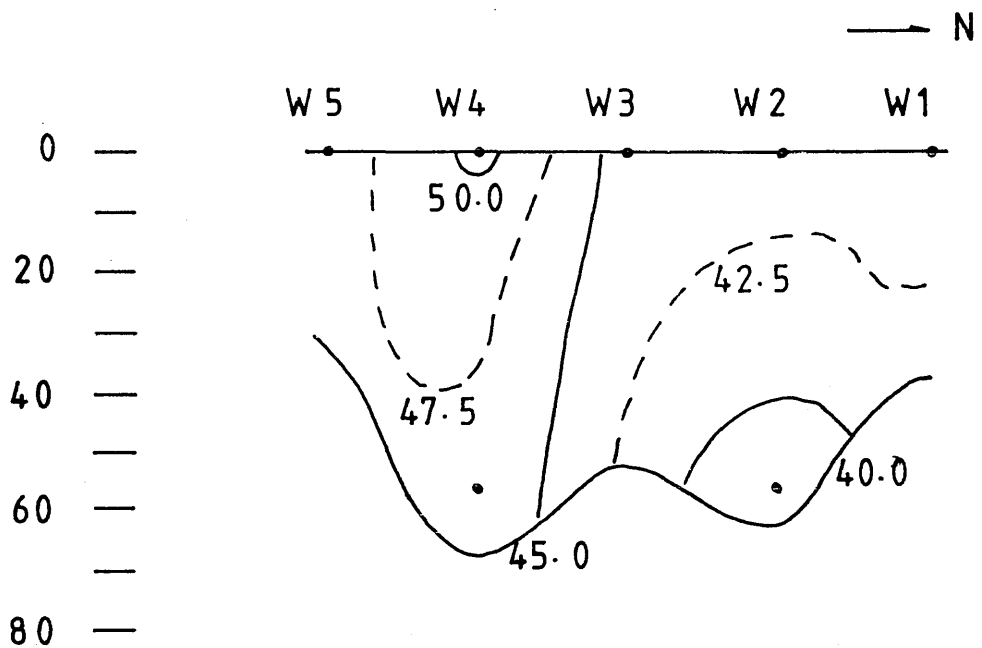


Figure 4.4.4

^{137}Cs Profile Across Transect W (Irish Sea), June / July 1984 (dpm/l)



distribution (Figure 4.4.4 - radiocaesium profile across Transect W) shows higher levels (46 - 51 dpm l⁻¹) at the southern end than (39 - 44 dpm l⁻¹) at the northern end, thus revealing non-homogeneity across the transect and suggesting dilution by fresh water from the Solway Firth.

At transect Z - southern transect of the North Channel - a more significant decrease in subsurface radiocaesium levels was apparent on the east side (~1.2 times reduction to <85% of surface value at 100 metres) than on the west (~1.1 times reduction to >90% of surface value at 100 metres); highest salinities accompanied the lowest radiocaesium levels.

At transect Y - across the CSA entrance - the southern station, Y2, showed slightly greater reduction in radiocaesium levels down the water column (89% of surface level at 40 metres) than the northern and more homogenous station, Y4 (93% of surface level at 60 metres).

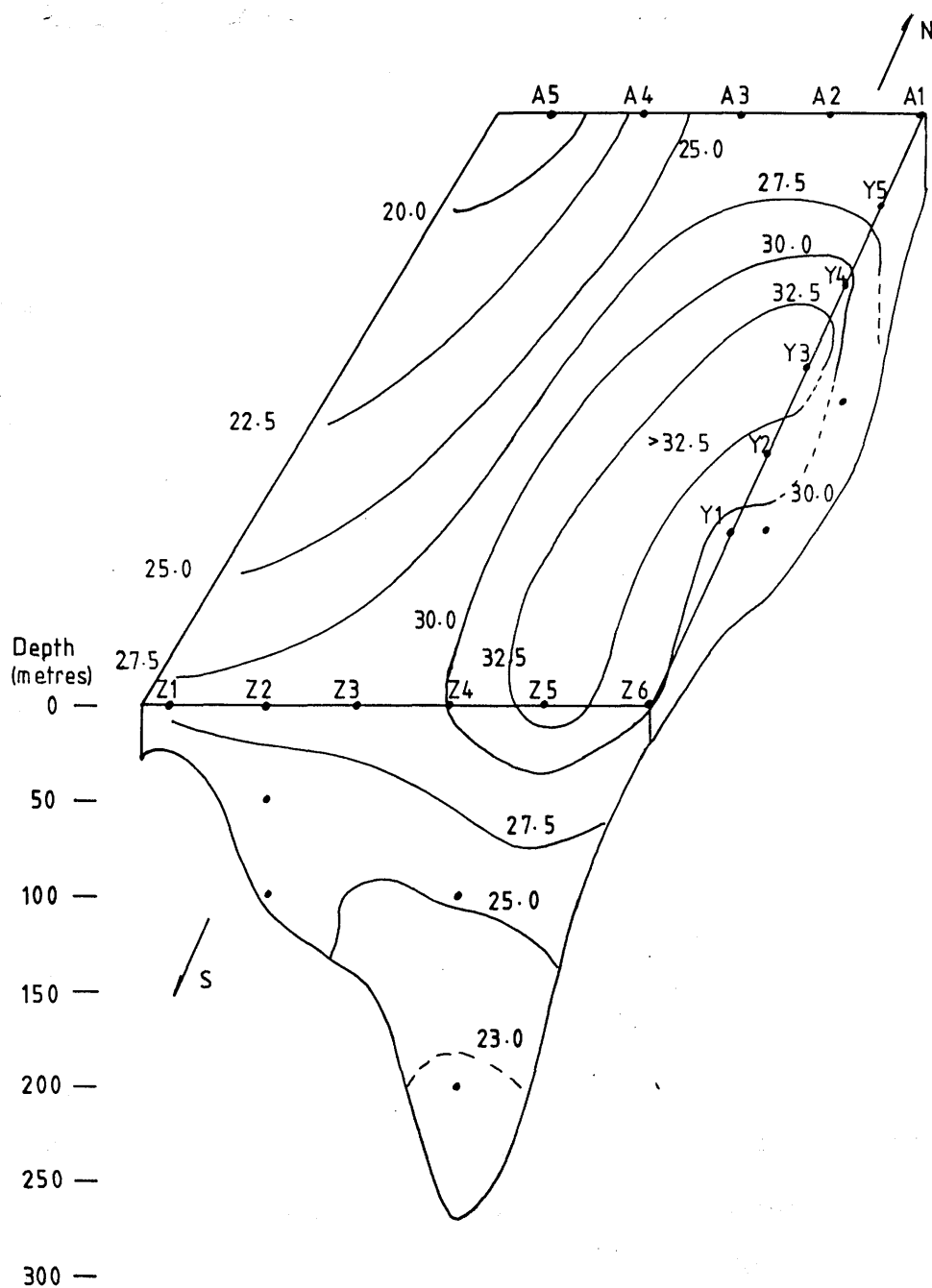
At the northern North Channel transect, transect A, there was significantly greater reduction in radiocaesium levels at depth on the west side (1.25 times reduction, 80% of surface level at 100 metres) than on the east (1.12 times reduction, ~90% of surface level at 100 metres). This can be attributed to the greater dilution by saline waters on the west where southward flowing water from the Atlantic enters the North Channel via the Irish coast.

Figure 4.4.5 is a three-dimensional representation of radiocaesium in the North Channel and clearly illustrates the high-radiocaesium surface layer flowing from the Irish Sea, via the North Channel (where it "hugs" the Galloway coastline), into the CSA (northeastwards) and HSA (northwards).

Across Islay to the Mull of Kintyre (transect B) stations B2 and B4 show reduced radiocaesium levels at mid-depth and increased levels

Figure 4.4.5

Three - dimensional ^{137}Cs Distribution in the North Channel, June / July 1984 (dpm/l)



at the bottom (relative to surface values), not small enough to be attributed to counting errors. On the ^{137}Cs / salinity diagram (Figure 4.4.3), the 4 points corresponding to these subsurface samples fall to the left hand side of the curve (as do those for the surface samples), thus reflecting fresh water dilution. The latter is slightly more pronounced in the mid-depth samples than in the bottom and surface samples but, since these mid-depth salinities were extrapolated from CTD profiles (Figure 4.4.6), some error ($\pm 0.05\%$) exists in these values. From the temperature traces (Figure 4.4.6), there is some consistency here, in the occurrence of a small abrupt decrease at around mid-depth at stations B2 and B4. Increased radiocaesium levels and salinities at depth indicate surface fresh water dilution; however, it is not clear why, at mid-depth, the radiocaesium levels are lower than surface and bottom levels when the salinities show a general increase with depth. The surface waters may represent fresh water outflow from the Sound of Jura, whilst the bottom waters represent northward-flowing Irish Sea / CSA water not so influenced by fresh water and therefore containing more radiocaesium than surface waters. The observed sharp change at mid-depth at each station may mark the boundary between surface and bottom waters as a result of fresh water emerging from a relatively shallow region and entering deeper waters.

Across transect D (immediately west of Islay towards the Atlantic), 3 deep samples (from 3 stations) were collected from 40 metres. Two of them exhibited higher radiocaesium levels and lower salinities than surface values, as illustrated in Figure 4.4.7. The saline, low-radiocaesium Atlantic water from the west is present in the surface layer, with colder, slightly fresher Atlantic water beneath. Only for August 1983 is there data showing similar vertical

Figure 4.4.6

Salinity / Temperature Profiles for Stations (i) B2 and (ii) B4, June / July 1984

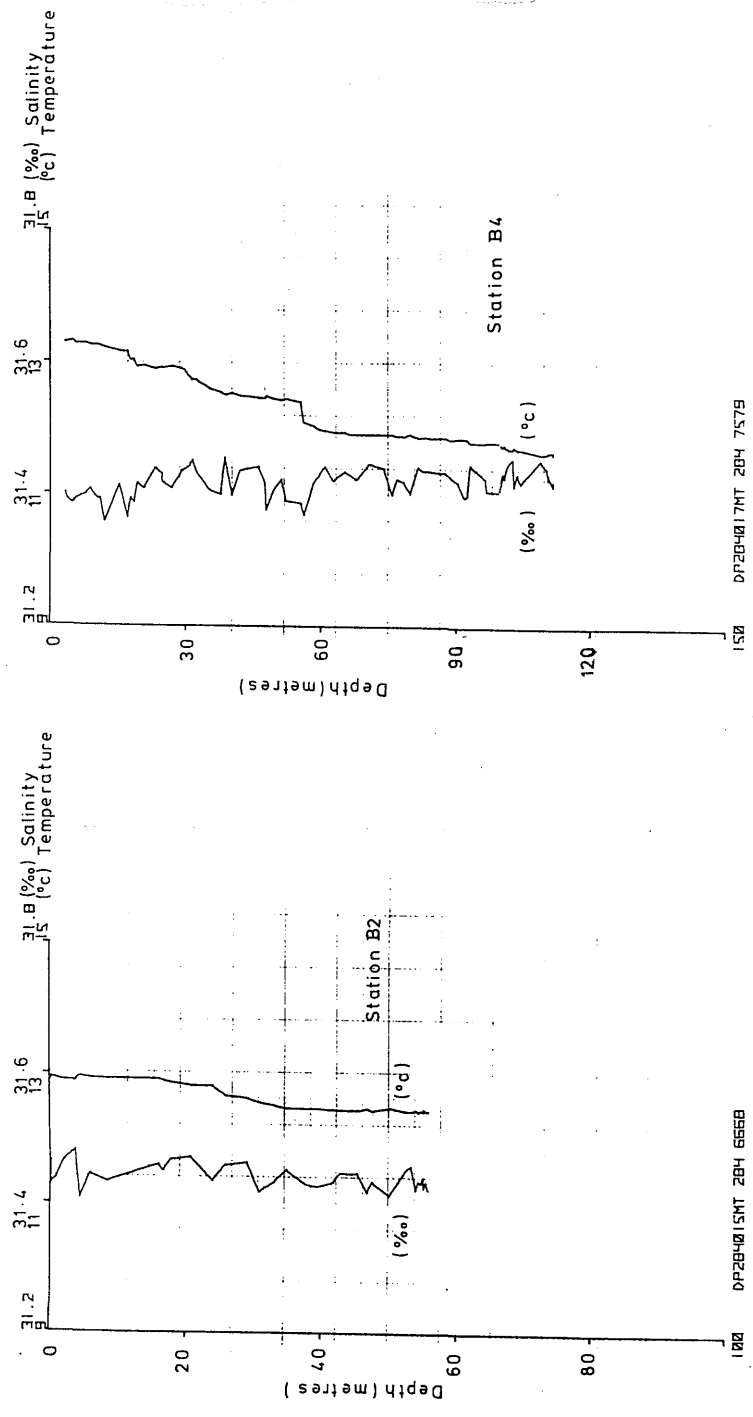
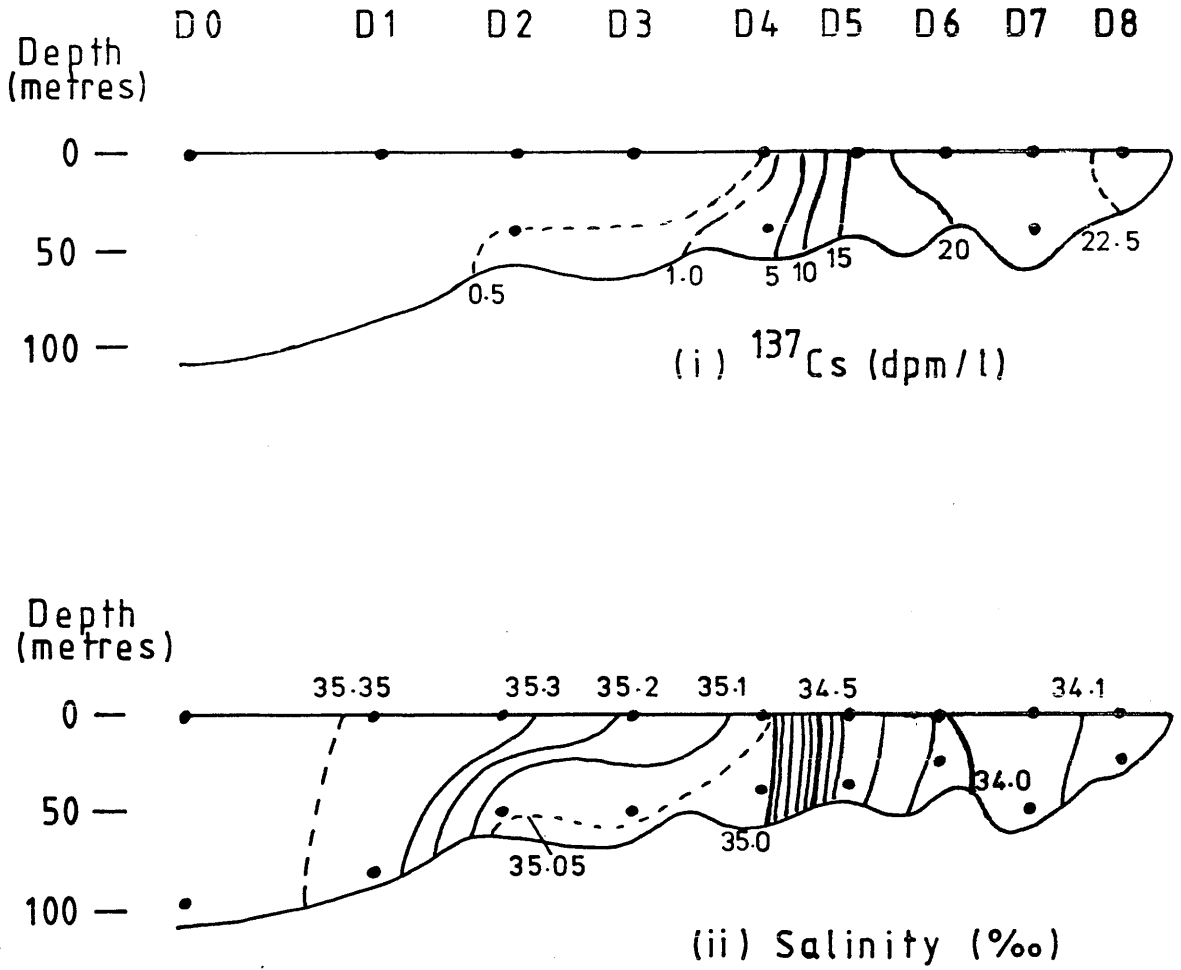


Figure 4.4.7

Profiles of Transect D, June / July 1984, for (i) ^{137}Cs and (ii) Salinity



distribution of Atlantic water in the HSA (see Figures 4.4.7,8); there were no relevant data for the cruises January 1984, April / May 1984 and November 1984, but May 1983 and February 1985 results show greater extension of Atlantic water into the HSA at depth than at the surface. Thus, the indication is that either there was withdrawal of bottom (Atlantic) waters in the HSA (presumably followed by withdrawal of surface waters) or that wind stress was responsible for an incursion of surface Atlantic waters into the region - possibly followed by similar movement of bottom waters.

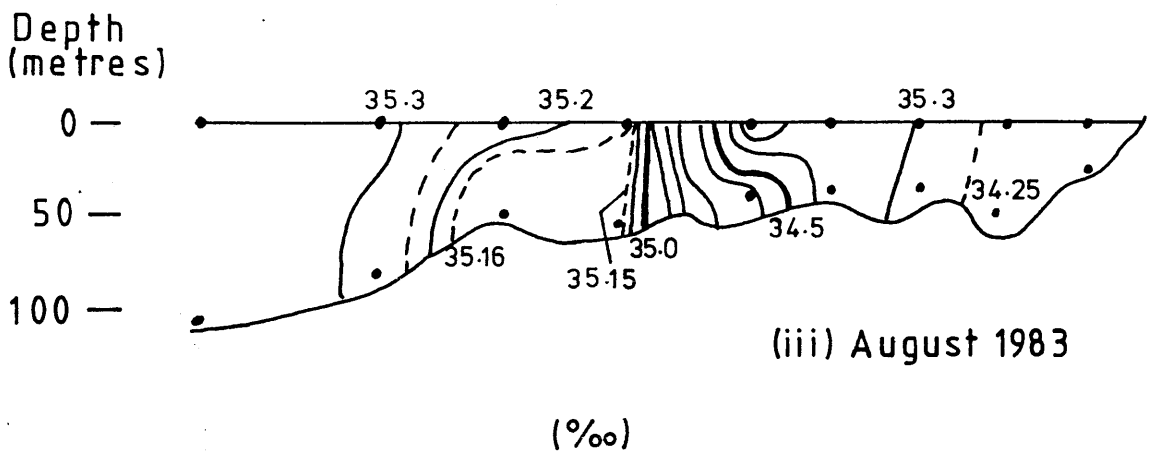
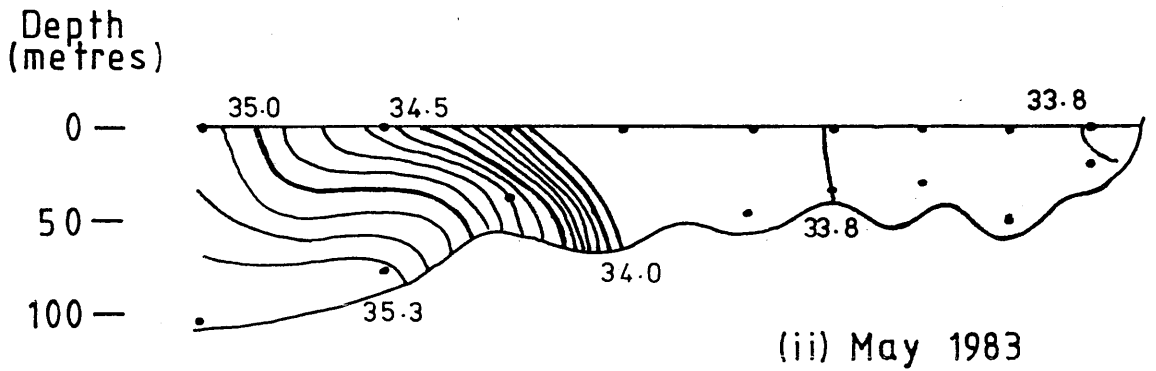
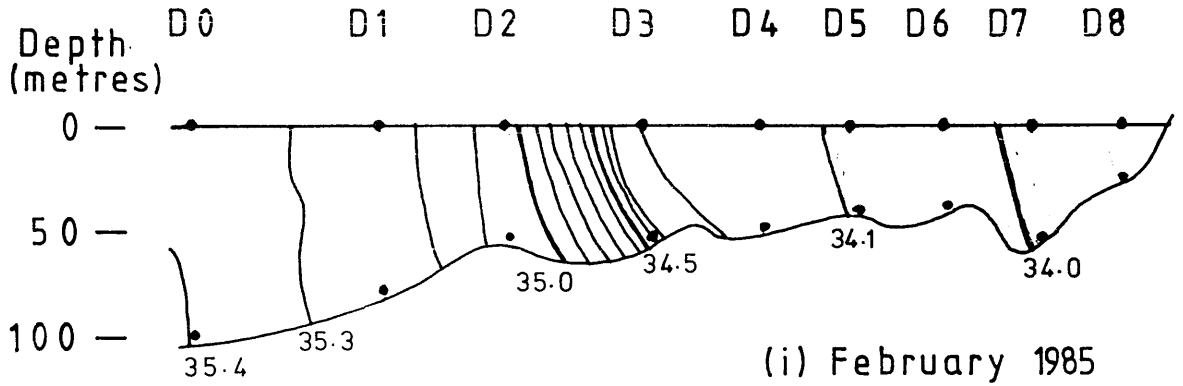
The occurrence of the deep samples at stations D2 and D4 on the left hand side of the ^{137}Cs / salinity curve suggests, as described in section 4.2(e), that i) a section of transect D (from D4 westwards) was influenced significantly by fresh water (presumably from N. Ireland) and / or ii) with recent low discharges and, since the bottom half of this curve represents older water of the northern transects (which correspond to older, higher ^{137}Cs discharges), then stations D2 and D4 reflect recent (low) discharges which have been diluted relatively quickly by Atlantic water from the west thus; in comparison to, say, samples from transect J, they appear to have low ^{137}Cs levels for their salinities (and / or low salinities for their radiocaesium levels).

At transect E (across the entrance to the Firth of Lorn), the near-bottom sample's radiocaesium level was $\sim 90\%$ of the corresponding surface level and its salinity was only 0.025‰ higher than that at the surface, thus indicating a well-mixed column.

Across transect G (across the entrance to the Minches and westwards from Barra Head), almost all the deep samples exhibit reduced radiocaesium levels and increased salinities relative to the surface samples; the exception is station G6 where greater (1.18

Figure 4.4.8

Salinity Profiles Across Transect D for
 (i) February 1985, (ii) May 1983 and (iii) August 1983



times) radiocaesium than at the surface was found at 30 metres (12 metres from the sea bed) whilst salinity showed no change at depth. Again, samples from below the "halocline" (rather than from above it) exhibit greatest reductions in radiocaesium levels relative to surface levels, e.g. compare G4-30 metres to G4-75 metres, G7-60 metres to G7-130 metres, G9-75 metres and G9-150 metres to G9-0 metres and G13 -40 metres to G15-100 metres.

Water at station K2 (The Little Minch) was well-mixed with only a small decrease (1.04 times) in near-bottom radiocaesium content to 96% of the surface level.

At station J2 (west of the Outer Hebrides), a decrease in radiocaesium levels down the water column (to 88% of the surface level at 80 metres) was accompanied by a decrease (0.068%) in salinity. Thus intrusion of Atlantic water in this region is indicated at depth, possibly from the north west (see Figure 4.2.e3).

(iv) November 1984

During this cruise, 15 deep samples were collected from 11 stations (5 transects) for analysis at GU, whilst transect G was, again, analysed by MAFF. The results are presented in Appendix II.6b and Table 4.4.4 and Figure 4.4.9 shows the data represented on the ^{137}Cs / salinity curve.

For the three Irish Sea samples, decreased radiocaesium levels and increased salinities in the near-bottom samples have been observed, e.g. the X4-55 metres sample contained only 44% of the surface radiocaesium level and was of higher (0.800%) salinity than at the surface. This clearly illustrates non-homogeneity within the Irish Sea (see Figure 4.4.10 - radiocaesium profiles across transects

Table 4.4.4Results of Deep Samples, November 1984

Station	Depth (metres)	^{137}Cs (dpm l ⁻¹)	$^{137}\text{Cs}/^{137}\text{Cs-0m}^*$ (%)	Salinity (‰)	ΔS^\ddagger (‰)
A2	120	27.6	97	33.749	0.090
A4	125	23.5	109	34.124	0.014
G1	60	10.7	98	34.221	0.529
G1	130	10.2	94	34.260	0.568
G2	30	11.3	97	34.356	-0.004
G4	80	5.8	106	34.776	-0.003
G6	25	4.9	93	34.864	0.085
G7	65	0.3	75	35.078	0.005
G7	130	0.4	100	35.082	0.009
G9	70	0.5	29	35.097	0.049
G9	145	0.6	35	35.132	0.084
G11	25	2.6	93	34.988	0.026
G11	50	2.5	89	34.992	0.030
G15	120	0.4	57	35.241	0.050
G16	125	0.1	111	35.365	0.073
K2	100	5.9	87	34.693	0.003
K8	140	6.8	97	34.561	0.000
W2	40	63.1	96	33.556	0.219
W4	30	33.9	78	33.780	0.041
X4	55	30.2	44	33.906	0.798

cont. 'd

Table 4.4.4 cont.'d

Results of Deep Samples, November 1984

Station	Depth (metres)	^{137}Cs (dpm l ⁻¹)	$^{137}\text{Cs}/^{137}\text{Cs-Om}^*$ (%)	Salinity (‰)	ΔS^\dagger (‰)
Z2	49	33.3	97	33.859	0.000
Z2	98	33.8	98	33.859	0.000
Z3	70	41.9	87	33.753	0.200
Z3	140	36.0	75	33.839	0.286
Z4	130	37.5	77	33.852	0.308
Z4	260	34.3	70	33.855	0.311
Z5	60	41.6	94	33.750	0.063
Z5	120	38.5	87	33.775	0.088

* $^{137}\text{Cs-Om} = ^{137}\text{Cs}$ level at surface

† $\Delta S = \text{Salinity} - \text{surface salinity}$

Figure 4.4.9

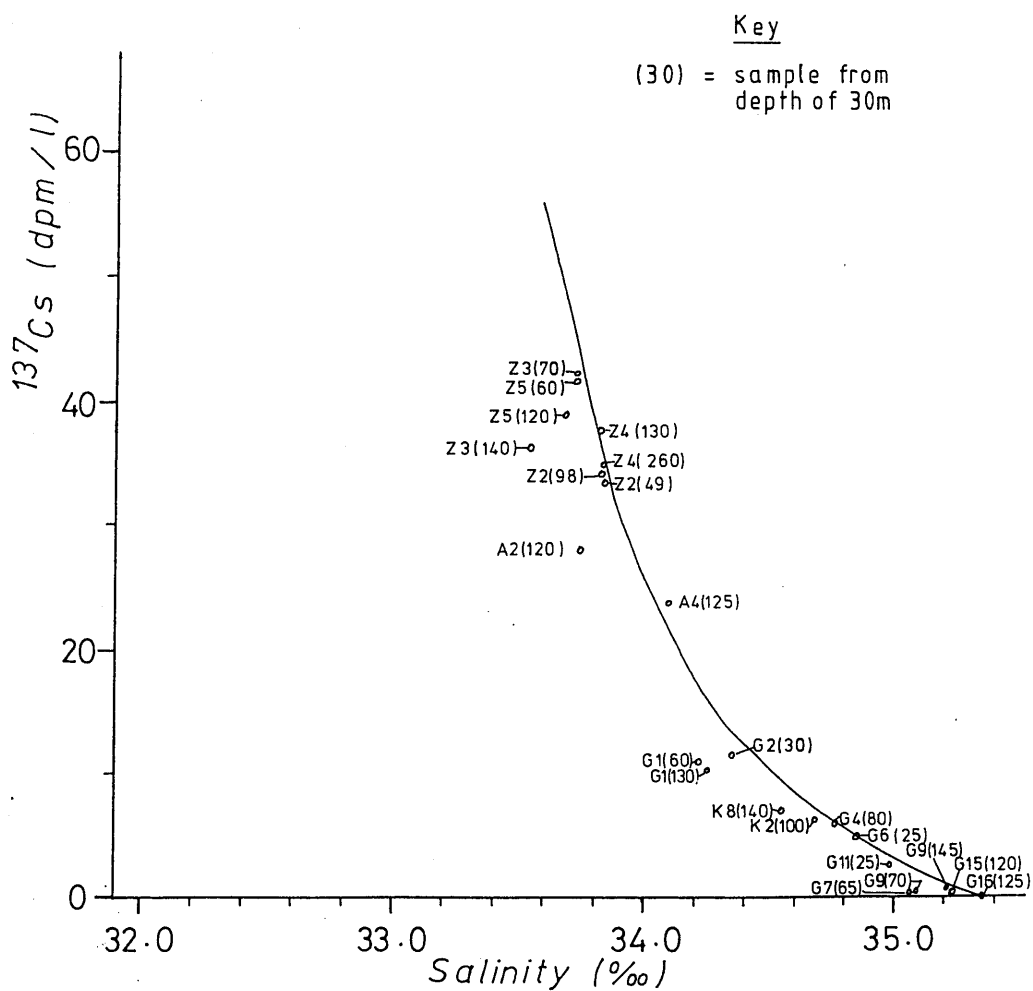
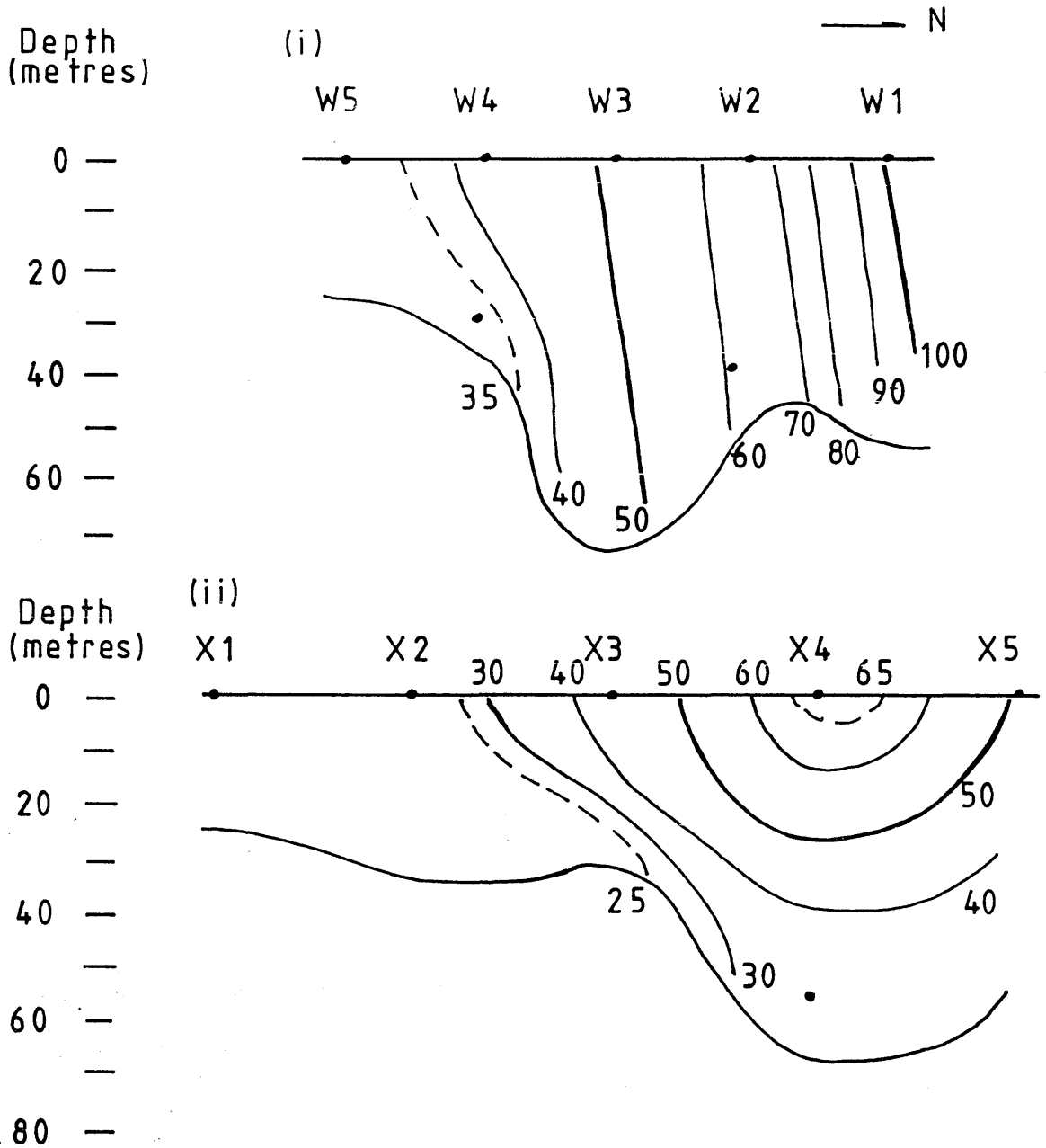
 ^{137}Cs / Salinity Curve - November 1984

Figure 4.4.10

^{137}Cs Profiles Across (i) Transect W and (ii) Transect X (Irish Sea), November 1984 (dpm/l)



X and W) and retention of high radiocaesium levels in surface waters, as suggested in Chapters 3 and 4.

In the North Channel, most stations showed decreased radiocaesium levels accompanied by higher salinities at depth. At station A4, however, a slight increase in radiocaesium and salinity values, relative to surface values, was found at 120 metres, possibly due to some surface fresh water dilution from the CSA. The other stations varied in their degree of reduction in radiocaesium content at depth (relative to surface levels), the greatest decrease occurring at 260 metres at station Z4 (the deepest station), corresponding to a >1.4 times reduction to 70% of the surface value.

For transect G, most stations had reduced radiocaesium levels at depth; where levels increased at depth (G4, G7 and G16), the apparent increase is only slight and is probably within analytical error (assuming MAFF errors are similar to GU errors). Salinities increased at depth for all but stations G2 and G4, the latter decreasing by only 0.003‰ and the former by 0.004‰, thus exhibiting an essentially homogenous water column. Only G9 and G15 show reductions in deep radiocaesium levels to <70% of their surface values - the former to ~30% and the latter to <60% - but, in both cases, radiocaesium content was very low (e.g. surface values were <2 dpm/l) and associated errors are thus proportionately high.

The two stations in The Minches (K2 and K8) indicate a generally well-mixed water column, with bottom radiocaesium levels of >85% of surface values.

(v) February 1985

Only samples from two transects, transect Z of the North Channel

Table 4.4.5

Results of Deep Samples, February 1985

Station	Depth (metres)	^{137}Cs (dpm l^{-1})	$^{137}\text{Cs}/^{137}\text{Cs-0m}^*$ (%)	Salinity (‰)	ΔS^\dagger (‰)
G1	30	14.4	96	N.M.	N.M.
G1	60	13.6	90	34.267	0.443
G4	50	10.1	85	N.M.	N.M.
G4	105	6.1	56	34.789	0.350
G6	20	10.1	105	N.M.	N.M.
G6	40	8.4	88	34.661	0.132
G7	50	7.1	94	N.M.	N.M.
G7	130	4.3	57	35.138	0.350
G9	75	1.3	34	N.M.	N.M.
G9	150	0.8	21	35.246	0.285
G11	50	6.0	108	34.872	-0.003
G13	50	4.2	102	N.M.	N.M.
G13	85	3.6	86	35.075	0.097
G15	110	0.56	28	35.338	0.221
G16	120	0.25	139	35.398	-0.009
Z2	50	26.7	95	34.020	0.061
Z2	85	19.6	70	34.269	0.310
Z3	75	16.5	63	34.385	0.320
Z3	150	15.2	58	34.428	0.363
Z4	100	13.7	43	34.422	0.479
Z4	185	13.2	42	34.459	0.516
Z5	70	23.6	66	33.960	0.166
Z5	140	30.2	84	34.223	0.429

* $^{137}\text{Cs-0m} = ^{137}\text{Cs}$ level at surface

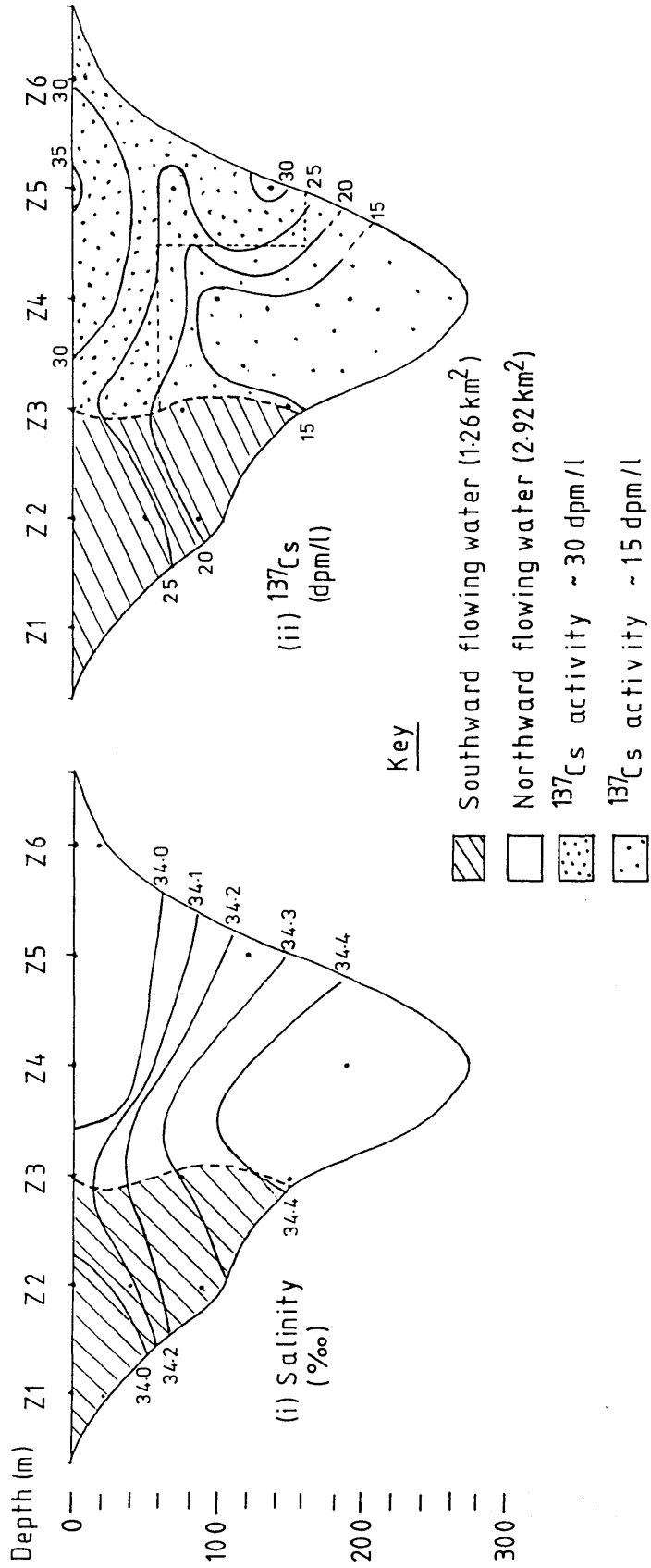
† $\Delta S = \text{Salinity} - \text{surface salinity}$

and transect G (analysed by MAFF), were collected for this cruise (Appendix II.7b, Table 4.4.5).

Across transect Z, the most significant decrease in radiocaesium levels occurred at station Z4 - the deepest station - with a ~ 2.4 times reduction to $\sim 40\%$ of the surface value occurring by 100 metres and being maintained to 185 metres (Table 4.4.5). For the next station to the west, Z3, reduction in radiocaesium level at depth (1.7 times to 58% surface value at 150 metres) was greater than that (1.2 times reduction to 84% surface value at 140 metres) for the station to the east of Z4, Z5; at mid-depth, however, there was a 1.5 times reduction (to 66% surface value) at Z5. Greater influence of saline, low radiocaesium water along the west side (than along the east) of this transect at depth, persisting upwards toward the east (mid-depth by Z5), can be seen in Figure 4.4.11. Radiocaesium levels in the bottom half of the water column were generally $\sim 40-65\%$ surface values. For purposes of budgeting the radiocaesium flux through the North Channel, then, this reduction at depth is obviously significant. Thus, where previously it was assumed that either the water column was homogenous with regard to radiocaesium or that all the radiocaesium was contained in the surface waters, it is clear now that details of subsurface samples are important.

Across transect G, only 2 stations, G11 and G16, showed slightly increased radiocaesium levels and decreased salinities at depth compared to the surface. The remaining stations exhibited lowered radiocaesium levels and increases in salinities with increased depth, the most significant radiocaesium decrease occurring at station G9-150 metres as a 4.8 times reduction to $\sim 20\%$ surface value. The reduction of bottom radiocaesium levels varied, with samples from deeper than ~ 70 metres (as far west as G9) exhibiting quite significant decreases

Figure 4.4.11
 Salinity and ^{137}Cs Profiles Across Transect Z, February 1985



in radiocaesium (e.g. G4-105 metres, G7-130 metres, G9-75 and -150 metres). These samples also record significant increases in salinity relative to surface values (i.e. they are from below the halocline - the "barrier" between Atlantic and coastal water); thus the influence of Atlantic water dilution is, again, very apparent.

(vi) Estimated Radiocaesium Fluxes Through the North Channel

In the past, various attempts have been made to quantify water flow through the North Channel, e.g. Bowden (1955), Craig (1959), McKinley et al. (1981a), Jefferies et al. (1982), Prandle (1984), McKay et al. (1986). Most of these estimates have not, however, taken into account two-directional flow and none have considered reduced subsurface radiocaesium levels (relative to surface levels) in their calculations.

Radiocaesium flux through the North Channel has been calculated from known radiocaesium content across a section of the North Channel (transect A) and known transit time (mean net transit time) of radiocaesium for the Sellafield to CSA journey (McKay and Baxter, 1985a). However, there are two important assumptions involved, as follows.

Firstly, the transit time (from this study, 4.8 months) obtained from matching of radiocaesium time trends (Chapter 3) is taken to represent the mean time required for the radiocaesium from Sellafield to appear in the CSA. However, diffusion also plays a part in dispersing the radiocaesium; thus the time taken for the water to travel this distance could be longer, i.e. the water transit time is underestimated (or the mean velocity is overestimated). In addition, underestimation of water transit time may arise because the transit of

radiocaesium is probably mostly via surface waters and deeper waters may have slower velocities. Conversely (and most importantly), since the transit time represents a 3-year mean flow velocity for the Sellafeld - CSA journey (and thus is more consistent than current meter data taken, say, from one station in the North Channel covering a period of a few months when the direction of flow might be periodically reversed), then it most probably underestimates North Channel flow speeds since the latter are expected to be faster than those within the CSA and the Irish Sea.

Secondly, all the water across the North Channel section is assumed to be travelling in the same direction, as well as at the same speed. Across the North Channel, however, although it is generally accepted that there is net northward flow through the North Channel, current velocities are constantly changing in this system; southward flow of water along the Irish coast has often been recorded (e.g. Proudman, 1939; Howarth, 1982), observed (e.g. Craig and Slinn, 1957; Lee, 1960; Barnes and Goodley, 1961; Ramster and Hill, 1969) or computed (e.g. Harvey and Buchan, 1963; Hunter, 1972) and, throughout the cruises of this study, such southward flow has been apparent. Thus, in assuming mass northward transport for the entire transect, northward flux is overestimated.

To avoid underestimation of the northward flow velocity through the North Channel by averaging the speed for the entire Sellafeld-CSA journey, lag-times from Sellafeld to transects Z and A of the North Channel (estimated by matching radiocaesium time-trends - Table 4.3.4, Chapter 4) can be used to provide a more particular estimate for the North Channel area. Between the 2 transects is a difference of 0.9 months lag-time and a distance of $\sqrt{72}$ km, thus a mean net northward velocity is estimated at 2.7 km day⁻¹. This figure is well within the

range of computed, 0.5 - 13.0 km day⁻¹ (e.g. Knudsen, 1907; Bowden, 1950; Craig, 1959; Harvey and Buchan, 1963; Hunter, 1972; Jefferies et al., 1982; McKay and Baxter, 1985a) and measured, 0.9 - 10.0 km day⁻¹ (e.g. Harvey and Buchan, 1963; Howarth, 1982) velocities reported by other workers. However, because the associated error for this estimate is high (>100%, see Table 4.3.4), the mean Sellafeld-CSA velocity, 1.7 km day⁻¹, which has an associated error of ~6%, is also used and comparison between these velocities is possible.

From the salinity and radiocaesium contours across transect Z, an attempt has been made to distinguish between the north- and southward flowing fractions of water (Figures 4.4.11-13). Thus the above current speed (2.7 km day⁻¹) may be applied to the north flowing fraction.

In order to calculate the amount of northward flowing radiocaesium, however, it has been necessary to take into account the reduction of radiocaesium levels at depth; thus calculations have been possible for cruises June / July 1984, November 1984 and February 1985, for which subsurface radiocaesium levels for transect Z are available.

For the cruise of June / July 1984, then, 3.38 km² corresponds to northward flowing water; of this, 1.15 km² (upper layers) and 2.24 km² (lower layers) represent water of radiocaesium activities 30 dpm l⁻¹ and 25 dpm l⁻¹ respectively (Figure 4.4.12). Using the 2.7 km day⁻¹ mean velocity of northward transport (see above), then the water volume fluxes across the upper and lower sections correspond to 3.1 km³ day⁻¹ (3.1 x 10¹² l day⁻¹) and 6.0 km³ day⁻¹ (6.0 x 10¹² l day⁻¹) respectively. Applying the corresponding radiocaesium concentrations to these two sections, a total northward radiocaesium flux through the North Channel at the time of this cruise is estimated at ~2.45 x 10¹⁴ dpm day⁻¹ whilst the corresponding water flux is estimated at 9.1 km³

Figure 4.4.12
 Salinity and ^{137}Cs Profiles Across Transect Z, June / July 1984

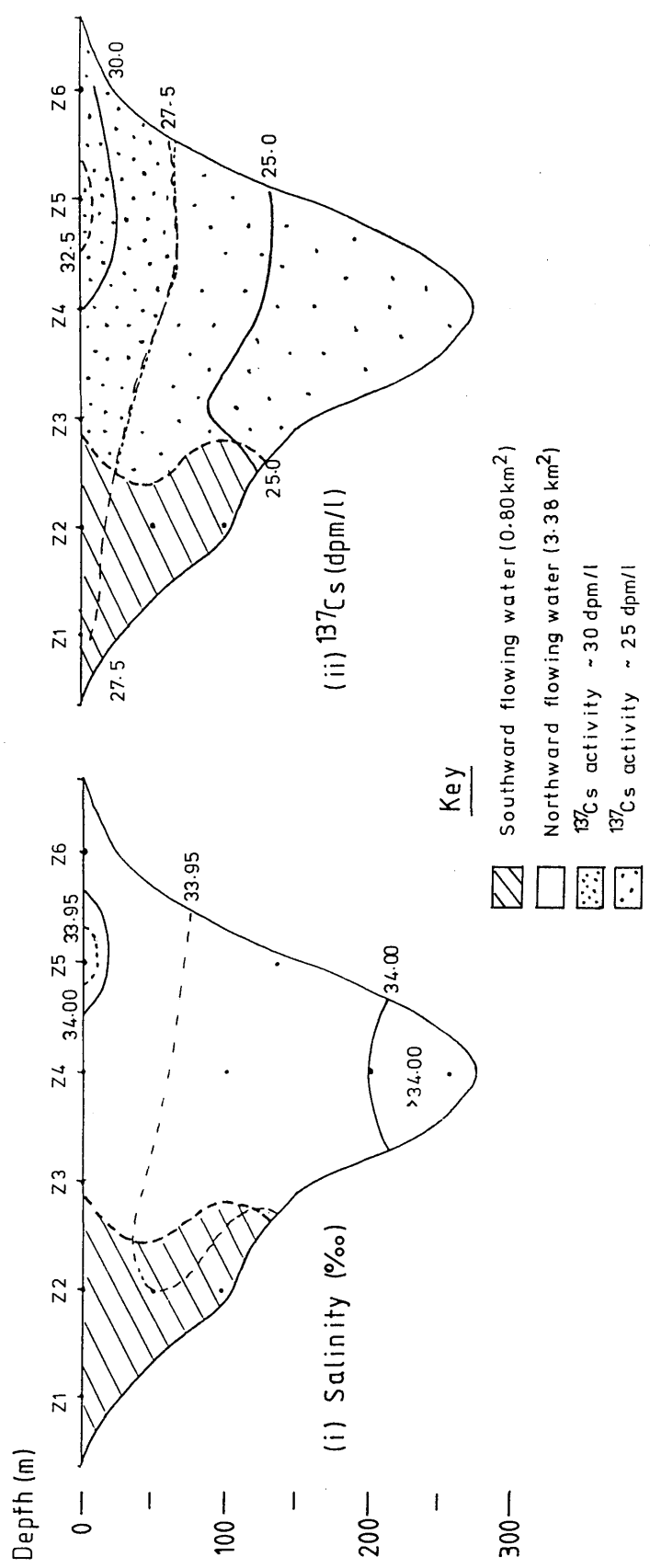
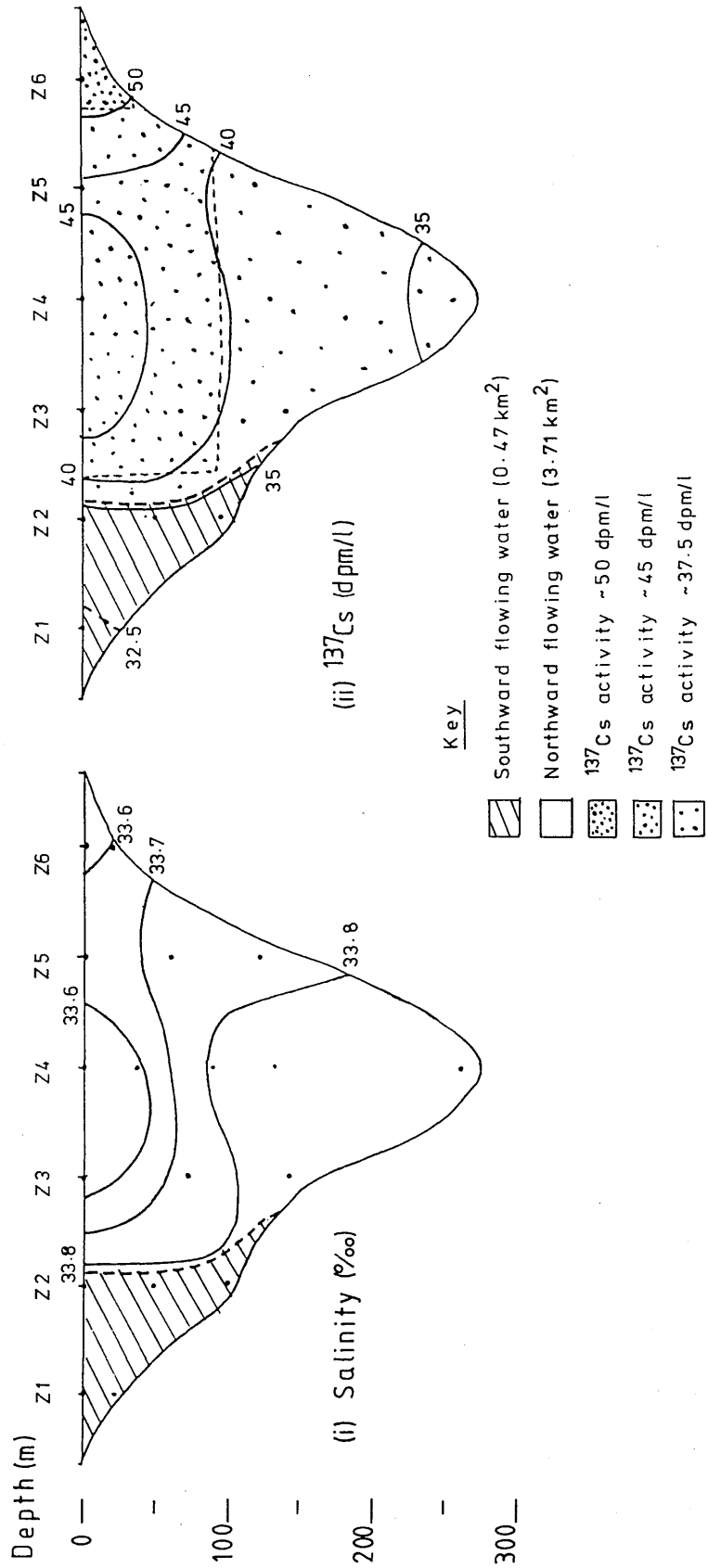


Figure 4.4.13
 Salinity and ^{137}Cs Profiles Across Transect Z, November 1984



day⁻¹ (Table 4.4.6).

Similarly, the radiocaesium fluxes northward through the North Channel for the November 1984 and February 1985 cruises are estimated at 4.13 and 1.83×10^{14} dpm day⁻¹ respectively, whilst the corresponding water flows are estimated at 10.0 and 7.9 km³ day⁻¹ respectively (Table 4.4.6 and Figures 4.4.11, 13).

It must be borne in mind, however, that current velocities in the North Channel have so far been observed to be very variable. Thus, although the current velocity used for these calculations is well within actual measurements made by other workers, the latter vary quite substantially and allow for at least a twofold increase (or decrease) in the above calculations pending a twofold increase (or decrease) in the estimated mean velocity used (see above). Radiocaesium and water fluxes calculated using a current velocity of 1.7 km day⁻¹ are presented in Table 4.4.6; they are ~0.6 of the values calculated using the faster velocity.

In spite of having accounted for southward flowing water in the North Channel, the water fluxes obtained are relatively high when compared to other estimates. Table 4.4.7 allows comparison of results obtained during this study with those obtained by other workers. Agreement is best for the values calculated using the 1.7 km day⁻¹ velocity rather than for those calculated with the 2.7 km day⁻¹ velocity.

The net radiocaesium flux through the channel is, however, not known since the southward flowing portion of water could be returning some of the radiocaesium back into the Irish Sea and the speed at which the southward flowing water travels is not known. Return of the radioactive material may be initiated within the North Channel, at its northern exit (transect A), between Islay and transect A or between

Table 4.4.6

Estimated Radiocaesium and Water Fluxes Through the North Channel
 using 2.7 km day^{-1} (1.7 km day^{-1}) current velocity

Time of Cruise	Radiocaesium Flux (dpm day^{-1})	Water Volume Flux ($\text{km}^3 \text{ day}^{-1}$)
June/July 1984	2.47×10^{14} (1.56×10^{14})	9.1 (5.8)
November 1984	4.13×10^{14} (2.60×10^{14})	10.0 (6.3)
February 1985	1.83×10^{14} (1.15×10^{14})	7.9 (5.0)

Values in parenthesis correspond to the 1.7 km day^{-1} current velocity.

Table 4.4.7Estimates of Northward Water Flux Through the North Channel

<u>Northward Water Flux (km³ day⁻¹)</u>	<u>Original Source</u>
2.2	Bowden (1950)
5.0	Craig (1959)
4.0	Wilson (1974)
5.0	Jefferies et al. (1982)
5.2	Prandle (1984)
4.0	McKay et al. (1986)
5.7 *	Present study
9.0 †	Present study

* at flow of 1.7 km day⁻¹

† at flow of 2.7 km day⁻¹

Islay and N.Ireland.

c) Summary and Conclusions

The most significant reductions in radiocaesium levels at depth occur below the "halocline", attributable to dilution by Atlantic waters. At the surface, however, the plume of Sellafield discharge continues along its journey encountering noticeably less dilution. The most uniformly vertically mixed region is probably The Minches; elsewhere, some reduction in radiocaesium levels at depth is observed.

Data from the North Channel and Irish Sea indicate the transport of a plume of relatively undiluted water from the northern Irish Sea northwards via the eastern side of the North Channel into the HSA where the plume encounters Atlantic water. During its travel northward through the HSA, although being progressively diluted by Atlantic waters, the plume retains its characteristics (relatively high radiocaesium content) at the surface and, to a lesser extent, at depth. In shallow areas, little reduction in radiocaesium levels at depth is noted whereas in deeper areas or at stations near convergence of Atlantic and Irish Sea / CSA waters, the reduction can be more than 10 times, i.e. deep radiocaesium levels may be 10% surface levels.

These results support the concept, suggested in Chapters 3 and 4, of a plume of surface water in the north east Irish Sea travelling, via the surface through the North Channel, into the HSA and along the Scottish coast, encountering relatively little mixing en route, whereas, at depth, greater dilution by Atlantic waters occurs.

Atlantic incursion into the HSA, west of the Islay Front, across transect D ($55^{\circ}45'N$), is noted to have occurred at the surface rather than at depth on two occasions. This may have been due to surface

influx as a result of wind stress. Elsewhere, Atlantic influence was found to be greater at depth.

Estimates of northward radiocaesium and water fluxes through the North Channel have been obtained for three of the cruises. Subsurface radiocaesium levels have been found to be important to such estimates, since significant reductions in radiocaesium levels at depth (relative to surface levels) can occur. North and south flowing fractions of water in the North Channel have been distinguished and calculations of ^{137}Cs / water fluxes relate to the north flowing fraction only. Two values for mean current velocity were used, both in good agreement with other workers' estimates and / or measurements. Water fluxes estimated using the 1.7 km day⁻¹ velocity, however, were in better agreement with other reported values than were those obtained using the 2.7 km day⁻¹ velocity. The former and latter values lie in the ranges 5.0 - 6.3 km³ day⁻¹ and 7.9 - 10.0 km³ day⁻¹ respectively.

4.5 Summary and Conclusions

Various forms of data presentation have been used throughout this work, e.g. radiocaesium and salinity spatial distributions, ^{137}Cs / salinity and ^{137}Cs / distance plots, temporal (surface) radiocaesium trends at one point in space, across one transect or at a number of transects and standardisation of radiocaesium levels with respect to discharged levels, i.e. Environmental Appearance (Ea) factor values. From each method, different aspects of water behaviour have been investigated and characterised.

From surface radiocaesium and salinity spatial distributions in the HSA and surrounding waters, various patterns of water behaviour have been recognised.

For example, variation in intensity of Atlantic incursions into the southern HSA appears to determine the degree of confinement of the radiocaesium plume to the Scottish coast, e.g. in May 1983 and April / May 1984, there was relatively little or very weak Atlantic incursion in the HSA and this was consequently accompanied by relatively little restriction of the plume to the Scottish mainland. On the other hand, in May 1982, August 1983 and June / July 1984, Atlantic influence in the HSA was stronger and the restriction of the coastal current to the mainland was more pronounced. Degree of coastal restriction of the plume seems to affect the fraction of Irish Sea - derived coastal water passing via the west (as opposed to the east) of the Outer Hebrides, north of $\sim 56^{\circ}40'\text{N}$. Actual observed radiocaesium levels are largely controlled by the salinities present and hence by the extent of dilution by Atlantic waters; in the case of near coastal regions, however, fresh water dilution can be important. Despite the obvious,

anticipated relationship between high salinities / low radiocaesium levels and strong Atlantic influence, it has been found that high salinities do not necessarily correspond to a current Atlantic influx into the HSA: they may, in fact, be recording an earlier incursion and a current withdrawal of oceanic waters, e.g. January 1984 (subsection 4.2(c)). Rather than actual observed radiocaesium levels (or salinities), a better indication of Atlantic behaviour is provided by the radiocaesium (/salinity) distribution as deduced from ^{137}Cs (/salinity) contours. For example, the position of the Islay Front was found to be a good indicator of the extent of Atlantic influence in the southern HSA.

A relationship between the Islay Front intensity (gradient across the front) and current velocities at Tiree was noted, i.e. fast currents accompanied weak radiocaesium and salinity gradients across the front (e.g. May 1982, May 1983 and October 1983), whereas slow currents accompanied strong gradients (e.g. June / July 1984). The Tiree current velocities showed positive correlation with Tiree wind speeds.

Spatial water property distributions have also revealed that, in the North Channel, the northward movement of Irish Sea / CSA water was blocked, presumably by southward moving oceanic water along the coast of N.Ireland during the August 1983 cruise (subsection 4.2(b)).

The ^{137}Cs / salinity curve allows estimation of the extent of fresh water and saline Atlantic water dilution of the radiocaesium plume during its travel. From this, it follows that the response of various areas under consideration to the Sellafield discharge pattern or to strong or weak dilution by Atlantic water can, to some degree, be recognised. Delay in the CSA's response (compared with the North Channel's) to the discharge pattern was noted in the June / July 1984

cruise (subsection 4.2(e)). Relatively low radiocaesium water entered the southern HSA via the North Channel in June / July 1984 whilst the northern regions and the CSA contained higher radiocaesium levels corresponding to older discharges. In November 1984, water at the northern transects appeared to reflect these earlier (June / July 1984), low radiocaesium levels found at more southern transects in the previous cruise (subsection 4.3(f)). Similarly, relatively high radiocaesium levels in The Minches in August 1983 are suggested to represent the earlier (May 1983) relatively high levels in the southern HSA. This correlation implies a water transit time between the southern HSA (around transect D) to The Minches (around transect K) of ~3-4 months, in good agreement with the estimated lag-time noted from radiocaesium time-trends (Table 4.3.4, subsection 4.3(e), see below) of 3.5 (+/- 1.8) months from transect D to transect K.

From the ^{137}Cs / distance plots, the extent of reduction in radiocaesium levels in the radiocaesium plume along its path of travel can be studied. By plotting radiocaesium values on a log scale, the reductions are considered proportionally; hence comparisons between regions and cruises are possible.

It has been found that mixing is not sufficiently intense to eliminate the detailed Sellafield - discharged radiocaesium history in the radiocaesium levels of surface waters along the main path of the radioactive plume. Thus, matching radiocaesium time-trends at various transects has allowed estimates of lag-times / transit times between stations to be derived. These lag-times were then used to obtain E_a factor values for radiocaesium at each transect at particular times. Comparison of E_a values between sites provides a quantitative assessment of corresponding radiocaesium dilution. Comparison of E_a variations with time between transects has revealed information on the

relative importance of water residence / mixing in the various regions, e.g. water residence, in order of decreasing importance, has been observed to occur to the following extents; Irish Sea > North Channel / CSA > Scottish coastal current (HSA).

Mean dilution factors of the radiocaesium plume during travel through the HSA were calculated using observed radiocaesium levels at various points in space and time and also from E_a values, i.e. by relating the observed data to their corresponding discharges. Both methods indicate a low rate of dilution along the main path of the plume off the west Scottish coast (i.e. ~two - threefold from the North Channel to The Minches), whereas, from E_a values, dilution within the Irish Sea was found to be much greater (i.e. ~twentyfold from near-Sellafield to the North Channel). This trend is probably related to the greater influence of water residence / mixing in the Irish Sea than along the west Scottish coast.

From the data in the Irish Sea obtained during two of the cruises (June / July 1984 and November 1984), the September / October 1984 peak in discharges can be recognised from the increased radiocaesium levels in the later cruise relative to the former.

Maximum surface radiocaesium levels at each transect as a function of time provide an overall picture of temporal variations in radiocaesium levels throughout the area and thus help to illustrate the effects, with time and distance, both of Atlantic water influence and of variations in Sellafield discharge levels.

From investigations of radiocaesium levels at depth, it has been found that subsurface samples from below the halocline exhibit marked reductions in radiocaesium levels relative to surface values, in many cases, to < 10% surface values. Such extensive reduction in radiocaesium levels is attributed to dilution by Atlantic waters. On

two occasions, Atlantic incursion in the HSA at $\sim 55^{\circ}45'N$ (west of the Islay Front) was found to be stronger at the surface than at depth. The most vertically mixed region was found to be The Minches.

Subsurface radiocaesium levels have also revealed that a fraction of Sellafield discharge, probably retained largely in surface waters within the Irish Sea, is transported - via the eastern side of the North Channel - northwards along the west Scottish coast without extensive mixing. The resultant partial preservation of the Sellafield radiocaesium discharge record in these surface waters would explain why (as described above) temporal trends of radiocaesium at various transects could be recognised and hence estimates of lag-times between the transects obtained. This evidence supports the suggestion (Chapter 3) that relatively unmixed surface Irish Sea waters carry discharged material from Sellafield to the Clyde, whilst most of the Irish Sea region is well-mixed. However, even with this surface flow of Sellafield material, throughout the plume's journey as far north as The Minches, it is within the Irish Sea that the most extensive mixing has been found to occur (as shown by dilution factors, E_a values and radiocaesium time-trends).

North and south flowing fractions of North Channel water have been differentiated and mean current velocities (obtained from matching radiocaesium time-trends, Chapters 3 and 4) have been applied to the north-flowing fraction. Thus, northward water fluxes through the North Channel of $5.0 - 10.0 \text{ km}^3\text{day}^{-1}$ (between June / July 1984 and February 1985) have been estimated. Using subsurface radiocaesium levels, corresponding radiocaesium fluxes of $1.2 - 4.2 \times 10^{14} \text{ dpm day}^{-1}$ have been defined. Southward and thus net northward flow is unknown.

Detailed (monthly) time-trends at each transect throughout the

HSA would provide improved estimates of lag-times between these sites, thereby providing more accurate mean transit velocities. The latter could be used to calculate radiocaesium and / or water fluxes through the various transects "en route".

CHAPTER 5

Seaweeds

5.1 Introduction

Seaweeds have been consumed by man for many years although in more recent years consumption has decreased. Algae from the Outer Hebrides are still harvested and sent to alginate factories where they are turned into alginates for use in a variety of foods, pharmaceuticals, cosmetics and other commercial products. Various seaweeds are also collected by locals for use in e.g. soups and stews in N.Ireland, the west coast of Scotland and the Ayrshire coast (Johnston, 1983, pers. comm.). Laverbread is made from the "red" seaweed, Porphyra, and is eaten mostly in South Wales. Other seaweeds such as Dulse are quite commonly eaten in Ireland and the use of seaweeds as fertilizers has been widespread for some years; indeed, it is still used today in some areas of the U.K. - Isle of Man (I.O.M.) (Walton, 1983, pers. comm.), Outer Hebrides (Buchanan, 1983, pers. comm.), N.Ireland (Johnston, 1983, pers. comm.) and the Channel Islands (Cross and Day, 1981).

There are two main reasons for an interest in radioactivity levels in seaweeds from the west coast of Britain. First, there is concern about the environmental radiological impact of discharged Sellafield radioactivity returning to man directly - via consumption of seaweeds - or indirectly - via use of algae for agricultural

purposes. In the former context, although harvesting of Porphyra from the Sellafield vicinity is assumed to have ceased for the moment, continued monitoring is still regarded as necessary by MAFF in case harvesting resumes in future (Hunt, 1985). It is also possible that existing consumption of other algal species may generate significant but as yet unquantified exposures to man. In the latter context, it is possible that, in areas where seaweeds are used as soil fertilisers, radioactivity may transfer back to man via consumption of the locally produced foodstuffs grown on the seaweed - fertilised soil (Cross and Day, 1981).

Secondly, although radioactive discharges from Sellafield are now generally decreasing from year to year, they are still sufficiently high to be detected in the marine environment and in particular in organisms which concentrate the radionuclides from already measurable levels in the seawater. Information on the transport processes of the radionuclides in the marine environment could be deduced from the levels found in seaweeds and so help to improve our understanding of their behaviour in marine systems. On this subject, Hunt (1985) has emphasised the importance of Porphyra as an indicator and the use of seaweeds in general to trace radionuclides in the environment because of their ability to concentrate radionuclides from seawater (see Table 1.5).

Radiological assessments on U.K. seaweeds are performed regularly by MAFF (e.g. Hunt, 1985) and BNFL (e.g. BNFL, 1985). Tracer applications, in which radionuclide trends in time and space are assessed, are more sparsely documented. Cross and Day (1981) analysed samples of the bladder wrack, Fucus vesiculosus, collected from the Channel Islands and analysed for alpha-emitting nuclides. From the uniform ratio of plutonium and americium levels to natural alpha

Table 5.1 Artificial Radioactivity in Seaweeds Collected on 3/4 January 1983,
Counted on Ge(Li) Detector - units in mBq/g dry weight.

<u>SITE</u>	<u>137 Cs</u>	<u>134 Cs</u>	<u>106 Ru</u>	<u>95 Nb</u>	<u>95 Zr</u>	<u>60 Co</u>	<u>110m Ag</u>
Ravenglass	2.40E 03 +9.36E 01	1.00E 02 +5.88E 00	1.27E 03 +6.92E 01	6.92E 02 +2.01E 01	5.99E 02 +1.25E 01	5.25E 01 +2.76E 00	1.39E 01 +4.63E 00
Sellafield	2.37E 03 +9.25E 01	1.12E 02 +5.99E 00	8.81E 02 +6.07E 01	4.14E 02 +2.75E 01	5.37E 02 +1.95E 01	5.00E 01 +2.69E 00	1.33E 01 +4.51E 00
St. Bees	1.42E 03 +5.55E 01	6.29E 01 +3.89E 00	6.29E 02 +3.52E 01	3.43E 02 +2.39E 01	3.70E 02 +1.44E 01	N.D.	N.D.
Annan	5.66E 02 +2.46E 01	1.84E 01 +1.64E 00	N.D.	3.35E 01 +4.00E 00	N.D.	N.D.	N.D.
Balcary Bay	6.73E 02 +2.65E 01	2.61E 01 +1.94E 00	1.14E 02 +1.62E 01	6.96E 01 +7.47E 00	8.51E 01 4.96E 00	9.36E 00 1.78E 00	N.D.
Sandhead	1.54E 02 +7.10E 00	5.74E 00 +1.03E 00	4.92E 01 +1.30E 01	2.39E 01 +3.57E 00	N.D.	N.D.	N.D.
Ballantrae	1.29E 02 +5.62E 00	3.92E 00 +6.85E-01	4.48E 01 +1.37E 01	7.77E 00 +2.42E 00	N.D.	N.D.	N.D.
Turnberry	1.62E 02 +7.44E 00	5.44E 00 +8.18E-01	N.D.	N.D.	N.D.	N.D.	N.D.
Saltcoats	1.38E 02 +5.92E 00	5.29E 00 +8.66E-01	N.D.	N.D.	N.D.	N.D.	N.D.
Gourock	8.36E 01 +4.40E 00	N.D.	N.D.	N.D.	N.D.	N.D.	N.D.
Loch Fyne	9.21E 01 +4.48E 00	N.D.	N.D.	N.D.	N.D.	N.D.	N.D.

Table 5.1. continued

SITE	^{144}Ce	^{154}Eu	^{54}Mn	^{103}Ru	^{125}Sb	^{155}Eu
Ravenglass	8.66E 01 +1.29E 01	2.96E 01 +3.26E 00	2.00E 00 +2.00E-01	1.48E 01 +4.26E 00	2.68E 01 +6.99E 00	2.84E 01 +5.74E 00
Sellafield	7.55E 01 +1.15E 01	1.52E 01 +2.82E 00	N.D.	N.D.	N.D.	N.D.
St. Bees	N.D.	N.D.	N.D.	N.D.	N.D.	N.D.
Annan	N.D.	N.D.	N.D.	N.D.	N.D.	N.D.
Balcary Bay	N.D.	N.D.	N.D.	N.D.	N.D.	N.D.
Sandhead	N.D.	N.D.	N.D.	N.D.	N.D.	N.D.
Ballantrae	N.D.	N.D.	N.D.	N.D.	N.D.	N.D.
Turnberry	N.D.	N.D.	N.D.	N.D.	N.D.	N.D.
Saltcoats	N.D.	N.D.	N.D.	N.D.	N.D.	N.D.
Gourock	N.D.	N.D.	N.D.	N.D.	N.D.	N.D.
Loch Fyne	N.D.	N.D.	N.D.	N.D.	N.D.	N.D.

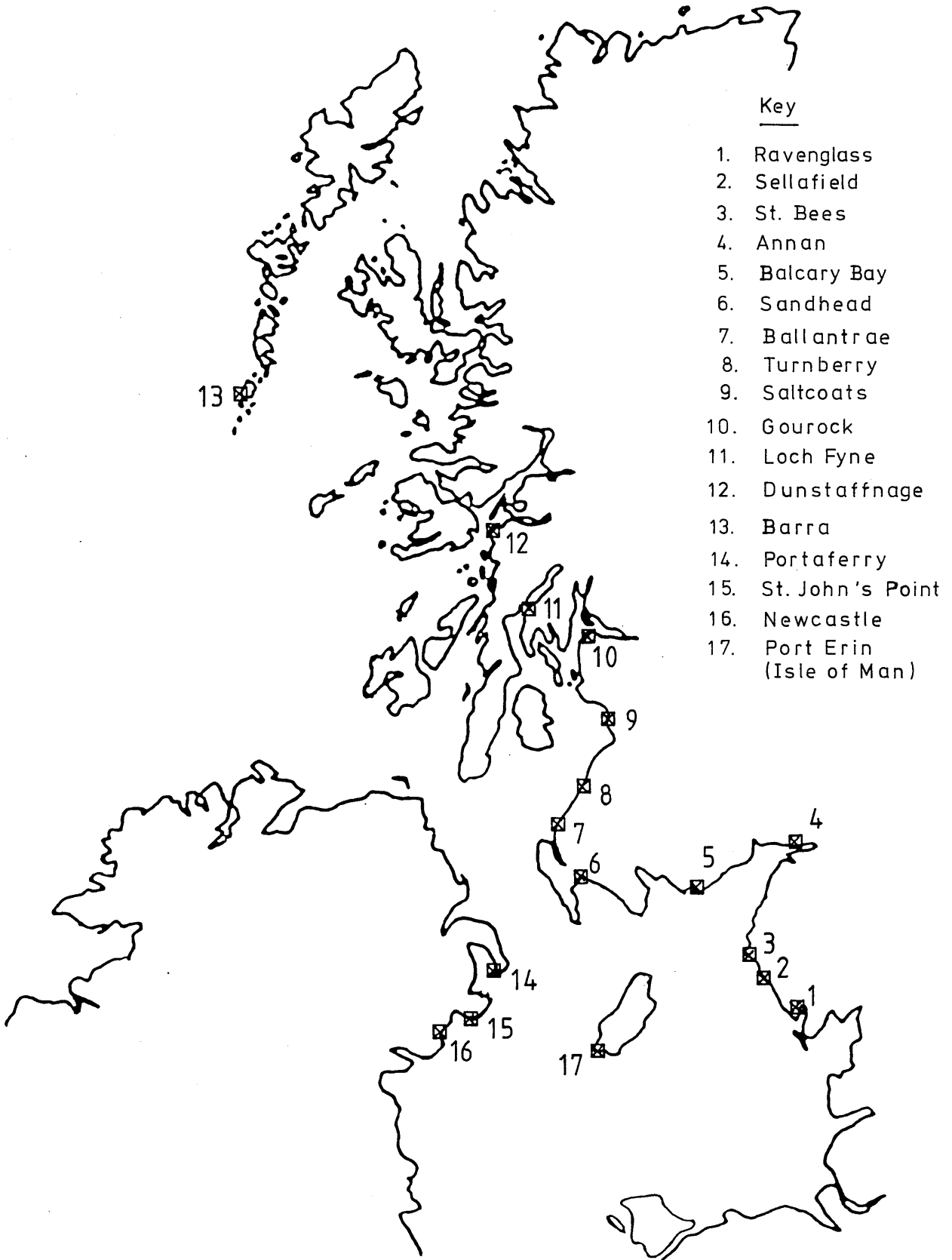
N.D. = Not Detected

activities it was concluded that the waters surrounding the Channel Islands are well mixed. The source of the radioactivity in this case was attributed to the nuclear fuel reprocessing plant at Cap de la Hague. Work by Thompson et al. (1982) also on the alga F. vesiculosus, collected from Cumbria and the Isle of Man, involved analyses of both alpha and gamma activities and used these as markers of ambient seawater concentrations. Differences in the environmental behaviour of the various radionuclides were observed, particularly regarding their relative degrees of conservative behaviour. Hallstadius et al. (1986) used plutonium and americium levels of seaweeds from north and north west Britain and from Ireland to obtain estimates of residence and removal times of these elements in Scottish and nearby waters.

During this project, preliminary studies have been carried out on a set of Fucus seaweed samples collected from the north west coast of Britain (Figure 5.1) on 3,4 January 1983; these involved assessment of gamma-emitting nuclide activities in the seaweeds. Fucus seaweed samples were also taken from Barra, Outer Hebrides, N. Ireland, I.O.M., Dunstaffnage (near Oban, Argyll), Sellafield and Ravensglass (the latter two being repeated sites) and were similarly assayed. In parallel with these studies, gamma-analyses were performed on samples of four alginate products - Ester B, Alginic acid H/FD, DMF and GMB - and on three edible seaweed health food products - Irish Moss, Irish Dulse and Arame Sea Vegetable. Complementary work was carried out by measuring the levels of gamma-emitting radionuclides in soils and grasses fertilised with seaweeds and comparing the results to those from soils and grasses not fertilised with seaweeds.

All sampled sites are shown in Figure 5.1 and the dates of sampling are as follows:

Figure 5.1

Sampling Sites for Seaweed, Grass and Soil Samples

west coast samplesJanuary 1983
Barra and IOMJune 1983
DunstaffnageAugust 1983
Sellafield and	
Ravenglass (repeated)November 1983
N.IrelandApril 1984

Besides gamma analyses of the seaweeds collected in January 1983, measurements of their alpha - emitting Pu isotope activities were carried out.

5.2 Radiological Investigations

Results of the gamma-radioactivity levels found in the Fucus seaweeds from the north west coast of Britain are presented in Table 5.1 in mBq/g dry weight (for conversion to wet weight analysis, see Appendix III.1). For the most radioactive sample, i.e. from Ravenglass, an estimated potential dose of 0.31mSv to locals has been calculated, assuming a critical group consumption rate of 11kg/yr (Clokier, 1986, pers. comm.). This corresponds to a committed effective dose equivalent of 6.24% of the ICRP - recommended annual dose limit (ALI) for members of the public of 5mSv (see below). Of this, 4.33% is contributed by the Pu alpha-emitting nuclides and 1.05% by the radiocaesium nuclides (see Table 5.10 for actual levels). These results were obtained by calculating, for each radionuclide, the annual intake as a fraction of the permissible annual intake (ALI). For comparison, analysis by BNFL of Porphyra collected from Sellafield gave an estimated potential dose equivalent to 5.5% ALI whilst MAFF's

measurements give an actual intake by laverbread consumers in South Wales of $<0.1\%$ ALI (Hunt, 1985). The ICRP-recommended ALI is now 1mSv (ICRP, 1985) for long-term exposure (see section 1.3, Chapter 1).

Negligible levels of both natural and artificial radionuclides were found in the four U.K. alginate products but the country of origin of the seaweeds used in making the alginates was not known. Likely candidates overseas are Japan, Falkland Islands, South Africa and Tasmania. Although no detectable levels were found in the three seaweed health food products, seaweed eaten in Ireland by locals may be expected to be active to some extent since it is not taken to be packaged and then sold; hence, short-lived radioactivity may still be present in the seaweed when eaten by locals whereas in packaged goods radioactive decay will have significantly decreased their activities. Nevertheless, even levels measured in fresh, shoreline seaweeds from N.Ireland would result in below 0.4% of the ICRP - recommended annual dose limit of 5mSv (see Table 5.2 for actual levels). The seaweeds and other environmental samples from Barra and the Isle of Man also showed very low - in some cases below detectable - levels of radioactivity (Tables 5.3 and 5.4). The main object here was to examine the possibilities of radionuclide transfer through the food chain, i.e. via the use of seaweeds as fertilizers on soils on which vegetation is grown. In the two cases studied here, any transfer of radionuclides from the seaweeds, via the seaweed-fertilised soil, to the vegetation was not sufficient for detection. The results are presented in Tables 5.3 and 5.4. For the Isle of Man samples, radiocaesium was present in the fresh seaweed, the fertilised soil and the two unfertilised soils but not in the grass samples. The levels in the fertilised and unfertilised soils were not significantly different. No radiocaesium was detected in the fresh Barra seaweed or in the grasses, whilst

Table 5.2

Gamma - Emitting Radionuclides Found in Seaweeds From
Dunstaffnage and Northern Ireland - units in mBq/g dry weight.

<u>SITE</u>	<u>^{137}Cs</u>	<u>^{40}K</u>	<u>$^{137}\text{Cs}/^{40}\text{K}$</u>
<u>Dunstaffnage</u>			
1. Pelvetia canaliculata	3.96E 01 +4.14E 00	5.00E 02 +5.96E 01	7.92E-02
2. Fucus spiralis	7.03E 01 +4.40E 00	6.96E 02 +6.07E 01	1.01E-01
3. Ascophyllum nodosum	3.43E 01 +1.52E 00	3.85E 02 +2.85E 01	8.91E-02
<u>Northern Ireland</u>			
<u>Portaferry</u>			
1. Fucus vesiculosus	1.03E 02 +5.85E 00	9.21E 02 +6.22E 01	1.11E-01
2. Fucus serratus	1.41E 02 +7.81E 00	1.39E 03 +7.62E 01	1.02E-01
<u>St. John's Point</u>	7.51E 01 +4.40E 00	8.10E 02 +6.22E 01	9.27E-02
<u>Newcastle</u>	7.18E 01 +4.44E 00	9.21E 02 +6.40E 01	7.80E-02

Table 5.3

Gamma - Emitting Radionuclides Found in Environmental
Samples From the Isle of Man - units in mBq/g dry weight.

<u>Sample</u>	<u>^{137}Cs</u>	<u>^{40}K</u>	<u>$^{137}\text{Cs}/^{40}\text{K}$</u>
Fresh Seaweed	4.00E 01 <u>+3.11E 00</u>	5.85E 02 <u>+5.37E 01</u>	6.84E-02
Fertilised Soil	1.55E 01 <u>+2.54E 00</u>	3.74E 02 <u>+5.14E 01</u>	4.14E-02
Unfertilised Soil(1)	2.81E 01 <u>+2.95E 00</u>	4.59E 02 <u>+5.51E 01</u>	6.12E-02
Unfertilised Soil(2)	1.39E 01 <u>+1.85E 00</u>	3.21E 02 <u>+3.96E 01</u>	4.33E-02
Fertilised Grass	N.D.	N.D.	N.A.
Unfertilised Grass	N.D.	N.D.	N.D.

N.D. = Not Detected

N.A. = Not Applicable

Table 5.4

Gamma - Emitting Radionuclides Found in Environmental
Samples from Barra, Outer Hebrides - units in mBq/g dry weight.

<u>Sample</u>	<u>^{137}Cs</u>	<u>^{40}K</u>	<u>$^{137}\text{Cs}/^{40}\text{K}$</u>
Fresh Seaweed	N.D.	1.92E 02 <u>+5.62E 01</u>	N.A.
Dried Seaweed	9.40E 00 <u>+1.55E 00</u>	3.03E 00 <u>+3.37E-01</u>	3.10E 00
Fertilised Soil	3.70E 01 <u>+3.26E 00</u>	2.85E 02 <u>+5.77E 01</u>	1.30E-01
Unfertilised Soil	1.65E 01 <u>+2.44E 00</u>	1.96E 02 <u>+6.29E 01</u>	8.42E-02
Fertilised Grass	N.D.	1.07E 03 <u>+4.55E 01</u>	N.A.
Unfertilised Grass	N.D.	8.18E 02 <u>+9.00E-01</u>	N.A.

N.D. = Not Detected

N.A. = Not Applicable

ratios of radiocaesium to the naturally occurring ^{40}K were highest in the dried seaweed, next highest in the fertilised soil with the lowest measurable value occurring in the unfertilised soil. There is clearly insufficient and inconsistent data here to attempt to obtain nuclide transfer factors from the seaweeds to the grasses. Indeed, some of the measured radioactivity (e.g. in unfertilised soil) may have been due to fallout rather than to Sellafield discharge. However, in the two areas chosen for this study the radioactivity levels in the sea water - and consequently in the seaweeds - were not particularly high: in the case of Barra the site is quite far from the source of radioactivity and even radiocaesium was undetected in the fresh seaweed (Figure 5.2) whilst Port Erin in the Isle of Man is situated on the southern extreme of the island where sea water radiocaesium levels are considerably lower than, say, in sea water around the northern and eastern end of the island (see Figure 4.2.e7, Chapter 4). Figure 5.3 shows that, of all the fresh seaweeds analysed, the two lowest radiocaesium levels found correspond to these two sites. There is still scope, therefore, for further investigations of this type in, say, N.Ireland - where normalised radiocaesium levels in seaweeds were 1.5 - 2 times higher than those from the Isle of Man and where seaweeds are known to be used as fertilisers (Johnston, 1986, pers. comm.) - or Dumfries and Galloway - where relatively high radioactivity levels in seaweeds were found during this study (Figure 5.3) and where concern has been expressed by the Soil Association (Eastmond, 1985) with regard to the use of radioactive seaweeds as soil fertilisers.

The radiological aspects of this work, then, suggest that, in general, there is negligible exposure to radioactivity via either consumption of seaweeds or the less direct use of seaweeds or their

Figure 5.2

^{137}Cs Activity of Seaweeds (mBq g^{-1})

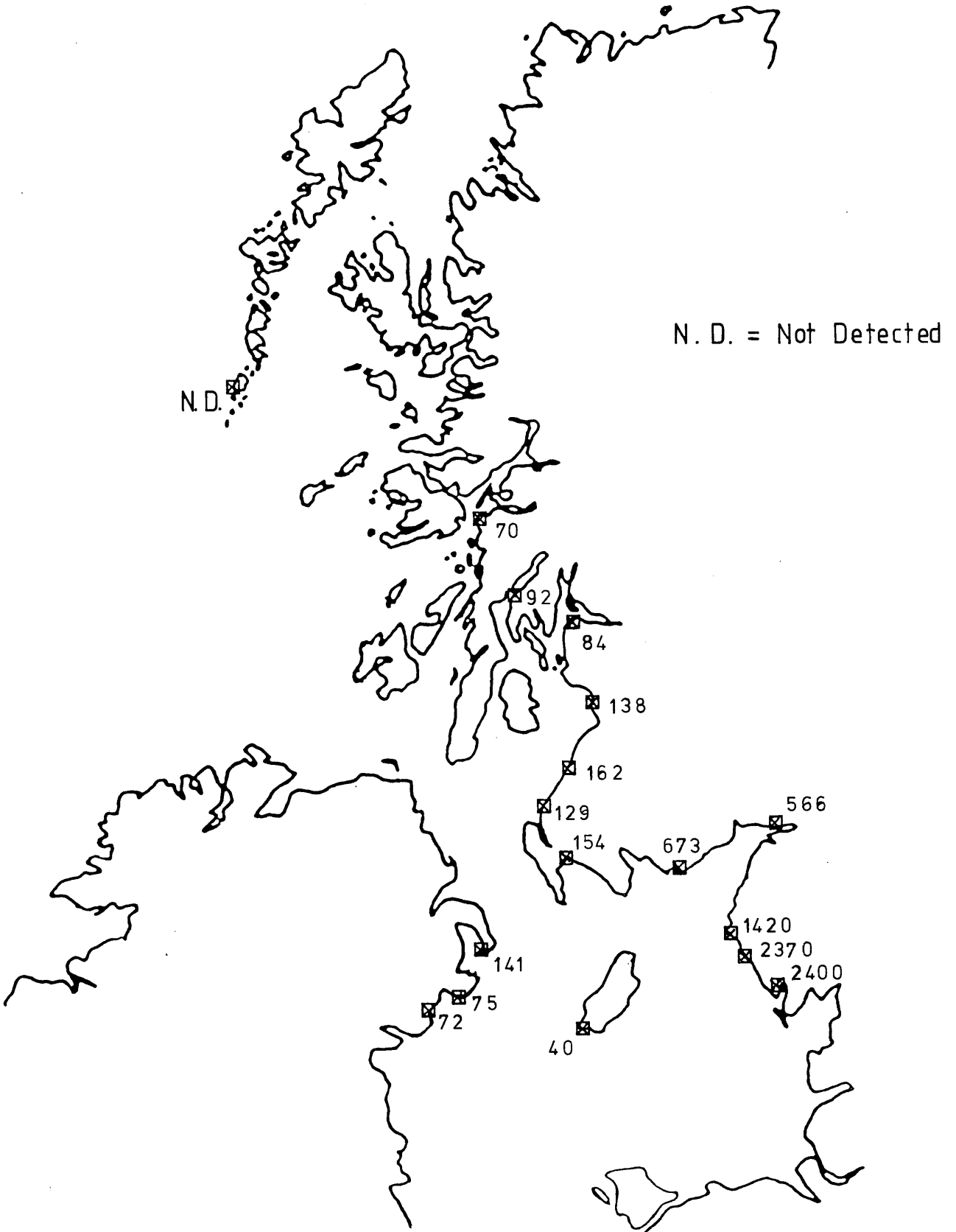
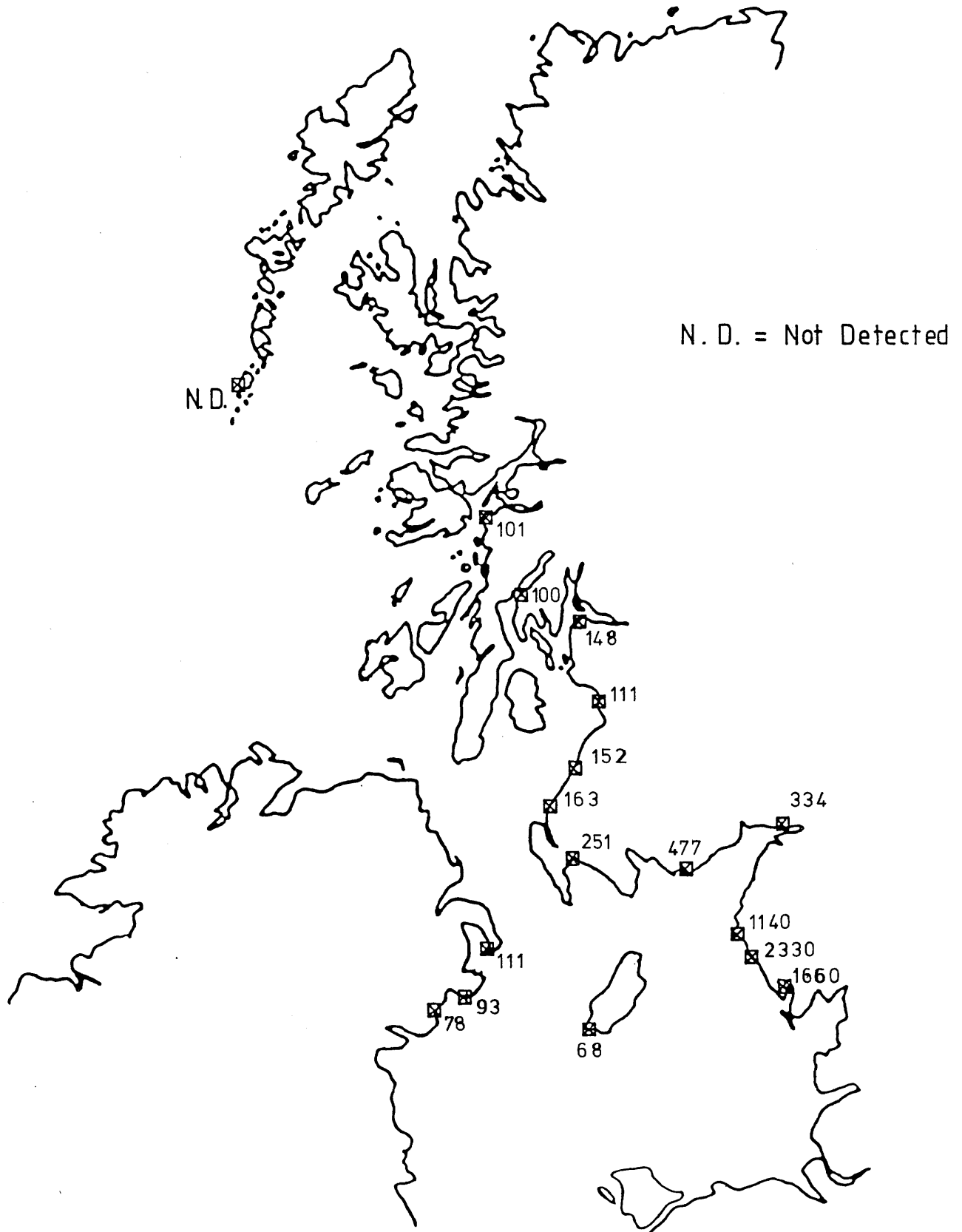


Figure 5.3

Normalised ^{137}Cs Levels in Seaweeds ($\frac{^{137}\text{Cs}}{^{40}\text{K}} \times 10^3$)



products. This finding is in agreement with those of MAFF (Hunt, 1985) and BNFL (1984). If seaweed from Ravensglass, however, were to be consumed by locals in the quantities which Porphyra has been known to be consumed, then exposures of ~6.2% of the ICRP-recommended annual dose limit of 5mSv to members of the general public could result.

5.3 Tracer Applications of Seaweeds

a) Gamma-emitting Nuclides

Apart from the natural ^{40}K nuclide, only ^{137}Cs was consistently detected. At Sellafield-remote sites most other radionuclides either had decayed or had been removed from the water column.

Figure 5.2 shows the spatial trend of ^{137}Cs levels for the west coast seaweeds and also the Dunstaffnage, N. Ireland, I.O.M and "repeated" Sellafield and Ravensglass samples. Since the sampling times at the different sites varied, it is intended to discuss only the west coast samples (all of which were collected on 3,4 /1/83) in any detail and to refer to the additional sites/samples for comparison.

The occurrence of radionuclides far from the source point depends on 1) their physico-chemical behaviour in the marine environment, 2) the amount discharged from the Sellafield pipeline, 3) dilution "en route" by lower activity water (including fresh water) and 4) the radioactive half-life of each nuclide. It must be borne in mind, then, that the results in this form do not allow determination of which of these parameters dominates in producing the observed distributions.

In Table 5.5 the reduction factors for the radionuclide levels between sites (i.e. reduction in radionuclide levels between the site of maximum level - Sellafield or Ravensglass - and each of the sites)

Table 5.5.

Reduction Factors* For Most Abundant
Radionuclides in Seaweeds.

<u>SITE</u>	<u>^{137}Cs</u>	<u>^{134}Cs</u>	<u>^{95}Nb</u>	<u>^{95}Zr</u>	<u>^{106}Ru</u>	<u>^{60}Co</u>
Ravenglass	1.0	1.1	1.0	1.0	1.0	1.0
Sellafield	1.0	1.0	1.7	1.1	1.4	1.1
St. Bees	1.7	1.8	2.0	1.6	2.0	1.7
Annan	4.2	6.1	20.7	N.D.	N.D.	N.D.
Balcary Bay	3.6	4.3	10.0	7.0	11.2	5.6
Sandhead	15.6	19.5	28.9	N.D.	25.8	N.D.
Ballantrae	18.6	28.5	89.1	N.D.	28.4	N.D.
Turnberry	14.9	20.5	N.D.	N.D.	N.D.	N.D.
Saltcoats	17.4	21.1	N.D.	N.D.	N.D.	N.D.
Gourock	28.7	N.D.	N.D.	N.D.	N.D.	N.D.
Loch Fyne	26.1	N.D.	N.D.	N.D.	N.D.	N.D.

*Reduction in levels as compared to site of maximum level.

are presented. From these results it can be seen that ^{137}Cs was reduced ~ 20 -fold between Sellafield and Ballantrae and ~ 30 times to Gourock, whereas ^{134}Cs appears to have been diluted ~ 30 times by Ballantrae and was below detection beyond Saltcoats. This apparent fractionation can be explained by the significantly shorter half-life (2.06 years) of ^{134}Cs compared to that of ^{137}Cs (30.17 years). A half-life of about 2 years is short enough to reduce the ^{134}Cs activity significantly by radioactive decay in such a system (see below). Corresponding reductions for ^{95}Nb and ^{106}Ru are 90 and 28 times respectively, both nuclides having relatively short half-lives (35 and 367 days respectively).

To assess the degree to which radioactive decay influences the reduction factor, it is necessary to correct for decay and, clearly, for this purpose the time elapsed since discharge must be known. The latter may be deduced by comparing $^{134}\text{Cs} : ^{137}\text{Cs}$ ratios between sites. Since this ratio decays with a half-life of 2.2 years, then observations of the rate at which the ratios decrease allows evaluation of the time elapsed between any two sites on condition that 1) the ratio of these isotopes in the discharge has been relatively constant for some time ($\sim 1 - 2$ years) and 2) the levels detected represent "recently" discharged water, not a mixture of older waters residing in the area, i.e. there should be a short transit / residence time of water passing through the area. The former condition is met since the discharge activity ratios for the 3 years prior to sampling and for the year of sampling were as follows:

<u>Year</u>	<u>$^{134}\text{Cs}/^{137}\text{Cs}$</u>
1980	0.080
1981	0.071
1982	0.068
1983	0.074

For the year 1983, then, at sites around the North Channel, about one year should be allowed for transit (McKinley et al., 1981b; Jefferies et al., 1982; McKay and Baxter, 1985a). Hence the 1982 discharges should be applicable here and the initial ratio 0.068 was therefore chosen. Since this is the lowest mean annual ratio it provides a lower limit on the estimated transit times. With regard to the second condition (analogous to the requirements for the validity of the ^{137}Cs / salinity curve - see Chapter 4, section 4.2(a)) estimates of residence time of water in the north eastern Irish Sea range between 12 and 20 months (McKinley et al., 1981b; Jefferies et al., 1982; McKay and Baxter, 1985a). Therefore it is to be expected that some degree of mixing of recently discharged water with residual water does occur within the Irish Sea. However, because of the relatively constant mean annual discharge ratios (1981 - 1983), this could create little problem, although any deviation will induce an overestimate of transit time.

The apparent transit times between sites were calculated using the observed ^{134}Cs : ^{137}Cs ratios, the 2.2 year half - life and the first order decay law; the results are presented in Table 5.6. It is interesting to note that Annan shows a longer transit time from Sellafield than the two sites, Balcary Bay and Sandhead, despite the latter two sites being further away from Sellafield. This in turn implies a more rapid and direct route for the main radioactive plume of water travelling from Sellafield to Balcary Bay and Sandhead relative to that from Sellafield to Annan. The apparent long transit

Table 5.6

Transit Times From Sellafield Pipeline
Calculated From Decay of $^{134}\text{Cs}/^{137}\text{Cs}$ Ratio.

<u>Site</u>	<u>Transit Time (years)</u>
Sellafield	1.49
Ravenglass	1.17
St. Bees	1.36
Annan	2.35
Balcary Bay	1.78
Sandhead	1.90
Ballantrae	2.56
Turnberry	2.24
Saltcoats	1.82

times (>1 year) to even the nearest sites from the pipeline are probably a reflection of mixing of newly discharged water with older water near the point of discharge which would bring about a decrease in the initial $^{134}\text{Cs} : ^{137}\text{Cs}$ ratio.

Having obtained these apparent transit time values, it was then possible also to correct actual measured levels of ^{134}Cs for radioactive decay (Table 5.7) and hence to recalculate ^{134}Cs reduction factors. The revised factor for dilution between Sellafield and Ballantrae is 18.4 (for ^{137}Cs this is 18.6) and thus excellent agreement is obtained. It was not feasible, however, to treat other radionuclides (e.g. ^{95}Zr , ^{106}Ru) in the same manner since they have different transit times from those of radiocaesium because of their different degrees of non-conservative behaviour. Radiocaesium is assumed to exhibit conservative behaviour and thus its transit time is assumed to reflect that of the water itself.

Thus far the data have not been corrected for the effects of freshwater dilution since the emphasis has been on ratios of isotopes and these are unlikely to change with variations in fresh water dilution. However, to compare sensibly the absolute levels of any one particular radionuclide between seaweeds it is necessary to "normalise" all the data since the extent of fresh water dilution is likely to vary between sites. The only natural radionuclide detected in significant levels is ^{40}K which is present in the oceans - for water of salinity 35‰ - at a level of ~ 12 Bq/l and comprises >90% of the total natural radioactivity in the world's oceans (Burton, 1975). Since the ^{40}K concentration in fresh water is negligible relative to that in sea water (0.5% of the latter) then all radionuclide levels could be normalised for fresh water dilution by expressing each radionuclide activity relative to that of ^{40}K (Appendix III.2). This

Table 5.7

^{134}Cs Activities Corrected for Radioactive Decay
(mBq/g) and Corresponding $^{134}\text{Cs} : ^{137}\text{Cs}$ Ratios

<u>Site</u>	<u>^{134}Cs</u>	<u>$^{134}\text{Cs} : ^{137}\text{Cs}$</u>
Ravenglass	160	0.067
Sellafield	162	0.068
St. Bees	97	0.068
Annan	39	0.069
Balcary Bay	46	0.068
Sandhead	10.4	0.068
Ballantrae	8.8	0.068
Turnberry	11.0	0.068
Saltcoats	9.4	0.068

normalisation is valid on the assumption that ^{40}K is taken up by all seaweeds to the same extent relative to other radionuclides. This compensation for fresh water dilution of seaweeds is analogous to the correction applied to sea water samples (Chapter 3) by relating measured ^{137}Cs levels to salinity. It is clearly not sensible to discuss the salinity of seaweed but the ^{40}K levels are an indication of the total potassium levels in the ambient water and hence of the total salinity. The "normalised" data (Table 5.8) thus have the effects of variable fresh water dilution removed and thus the spatial / temporal trends are caused primarily by factors such as the quantities discharged, radioactive decay, removal from the water column and / or dilution by saline, low-activity sea water. The last factor will influence all radionuclides in solution similarly and the first can be quantitatively accounted for. The remaining two processes, however, control the relative reductions in radionuclide levels in sea water during transit from Sellafield.

Figure 5.3 shows the spatial distribution of the "normalised" ^{137}Cs data (Table 5.13) whilst Figure 5.4 presents the "normalised" results (Table 5.14) for the major radionuclides against distance from Sellafield. The patterns of behaviour deduced from these data can be summarised as follows:

- 1) ^{137}Cs was detected in the seaweeds furthest from Sellafield and thus, of all the nuclides measured, it persists for longest in the radioactive plume travelling northwards along the west coast of Britain. This observation confirms our assumptions about its conservative behaviour, as evidenced by its low reduction factors at each site compared with those of other radionuclides (see Table 5.5).

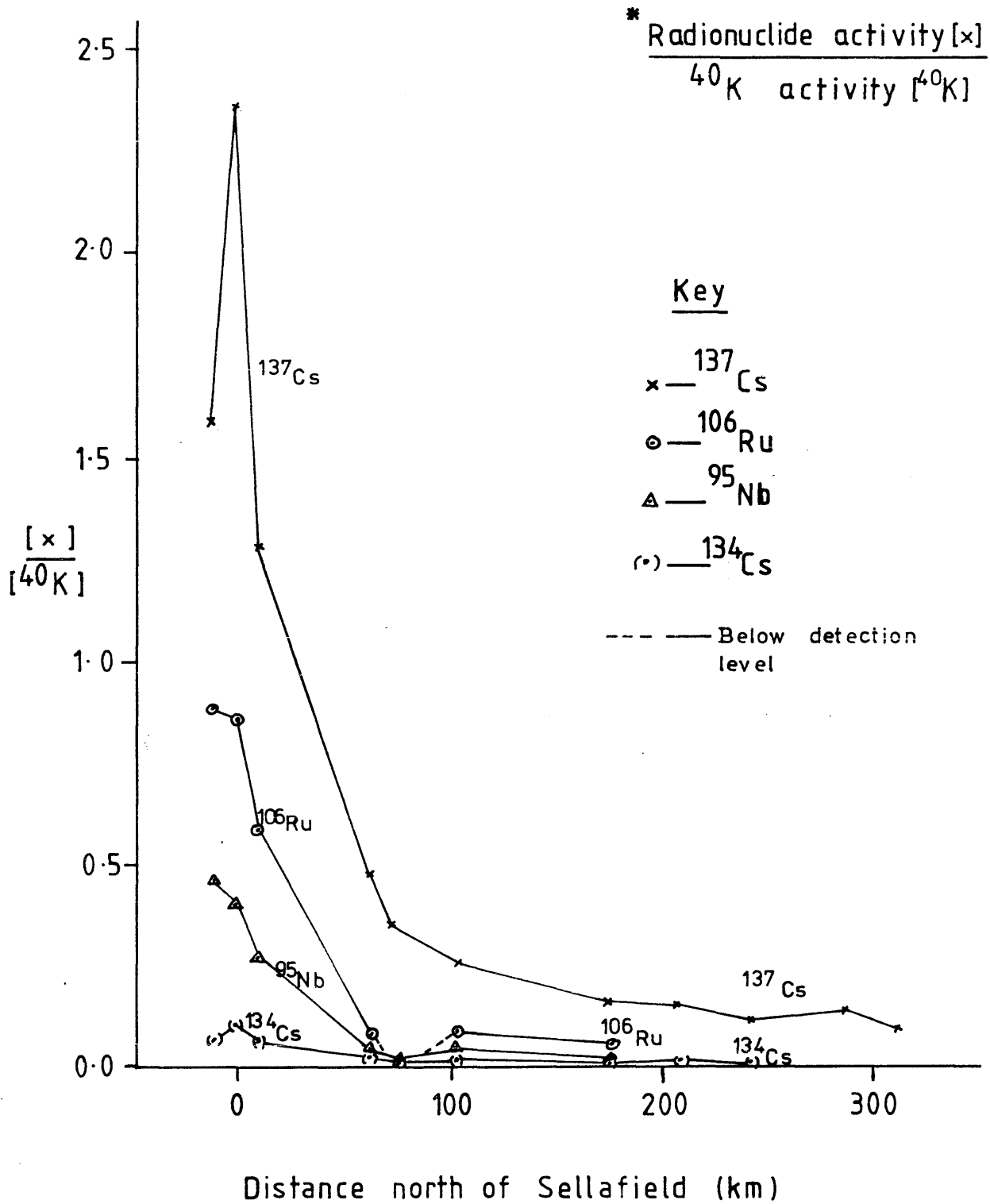
Table 5.8

Data From Table 5.1 Normalised with Respect to ^{40}K .

<u>SITE</u>	$\frac{^{137}\text{Cs}}{^{134}\text{Cs}}$	$\frac{^{106}\text{Ru}}{^{95}\text{Nb}}$	$\frac{^{95}\text{Zr}}{^{60}\text{Co}}$	$\frac{^{110m}\text{Ag}}{^{110m}\text{Ag}}$
Ravenglass	1.66E 00 +9.23E-02	8.79E-01 +5.92E-02	4.15E-01 +1.85E-02	9.61E-03 +1.45E-03
Sellafield	2.33E 00 +1.43E-01	8.65E-01 +4.12E-02	5.27E-01 +3.15E-02	1.30E-02 +4.47E-03
St. Bees	1.14E 00 +6.57E-02	5.05E-01 +3.54E-02	2.97E-01 +1.70E-02	N.D.
Annan	3.34E-01 +1.75E-02	N.D.	N.D.	N.D.
Balcary Bay	4.77E-01 +2.63E-02	8.05E-02 +1.18E-02	6.03E-02 +4.21E-03	N.D.
Sandhead	2.51E-01 +1.16E-02	8.06E-02 +2.19E-02	N.D.	N.D.
Ballantrae	1.63E-01 +1.15E-02	5.65E-02 +1.75E-02	N.D.	N.D.
Turnberry	1.52E-01 +9.73E-03	N.D.	N.D.	N.D.
Saltcoats	1.11E-01 +6.50E-03	N.D.	N.D.	N.D.
Gourock	1.48E-01 +1.52E-02	N.D.	N.D.	N.D.
Loch Fyne	9.96E-02 +6.61E-03	N.D.	N.D.	N.D.

Figure 5.4

Normalised* Radioactivity Levels in Seaweeds
Against Distance from Sellafield



- 2) Short-lived radionuclides, ^{95}Zr , ^{60}Co and ^{54}Mn , were not detected beyond Balcary Bay whilst other short-lived nuclides, ^{95}Nb and ^{106}Ru were detected as far as Annan and Ballantrae respectively. This observation can be partly attributed to the greater discharges of the latter. Nevertheless, the rapid decrease in these nuclides reflects their particle - reactive, non - conservative behaviour.
- 3) At Annan - although of similar distance from Sellafield as Balcary Bay - the seaweed ^{137}Cs content was found to be 84% of that found in the Balcary Bay sample. After "normalisation", the Annan seaweed shows only 70% of the ^{137}Cs activity of the Balcary Bay sample. The most obvious explanation is that the plume of radioactive water travelling from Sellafield finds a more direct route to Balcary Bay and to some degree bypasses the extreme reaches of the Solway Firth near Annan instead of following the coastline directly. Previous hydrographic studies of this region have indicated westward, seaward movement of surface water in the Solway Firth and eastward, upstream movement of bottom water (Perkins et al., 1964; Ramster and Hill, 1969). This pattern would therefore support the findings here that the plume bypasses the upstream regions of the Solway Firth, probably remaining largely in surface waters (see section 4.2 (e), Chapter 4).
- 4) Figure 5.4 - radionuclide levels against distance from Sellafield - shows the benefits of normalising the observed data to ^{40}K and provides an overall picture of distribution patterns along the

plume's path. One clear example of improvement of the results through normalisation can be seen by comparing the ^{137}Cs levels in the seaweeds from Turnberry and Ballantrae. Before normalising, the Turnberry seaweeds, although from farther north than Ballantrae, had the higher ^{137}Cs level but after normalisation they show correspondingly lower uptake.

- 5) Comparison between Sandhead and Annan ^{137}Cs levels shows that the Sandhead activity was 27% that of the Annan sample. Normalised levels, however, suggest that the Sandhead sample would have taken up 75% as much ^{137}Cs as the Annan sample from similar salinity water. In Figure 5.4, the relationship between radionuclide levels and distance from Sellafield is represented: from the radiocaesium data the low Annan levels are not as obvious as they are from the ruthenium and niobium data. The low Annan levels can be partly attributed to the relatively long transit time for the radionuclides to reach Annan, i.e. time for the radioactivity to undergo physical decay. However, there is insufficient data to determine whether this relatively long residence time can account fully for the observed drop in radionuclide levels at Annan; comparison of transit times (Table 5.6) and reductions in normalised levels (Figure 5.4, Table 5.14) from Sellafield to Annan and from Sellafield to Ballantrae shows proportionally greater reduction of ^{106}Ru levels in the water at Annan than at Ballantrae but less reduction of ^{95}Nb at Annan than at Ballantrae. If it were not possible to explain the low Annan levels solely from the transit times then another process must be active. A possible explanation could be that the removal of radionuclides from the water column by particulates was

greater in the shallower regions of the Solway Firth such as around Annan, since particle resuspension and sediment/water interactions are likely to be enhanced. Such an increase in the removal rates of the radionuclides would clearly be more pronounced for nuclides with high K_d 's than for those of low K_d 's and hence radiocaesium would not be expected to best illustrate such an increase in scavenging of the radionuclides from the water column. This is discussed further in section 5.3(b) with respect to the plutonium data.

In effect, normalising the data eliminates one of the variables (fresh water dilution) and leaves only the degree of radionuclide removal from the water column and of dilution by saline, low activity sea water as the two processes affecting the radionuclide distribution pattern. However, assuming radiocaesium to be perfectly conservative, its normalised values (Table 5.8, Figure 5.3) reflect dilution of the radioactive plume of water, i.e. dilution of the soluble phase. The reduction factors for normalised radiocaesium are presented in Table 5.13 and show up to 10 times reduction along the Cumbrian and Ayrshire coast of the Irish Sea region, up to 23 times reduction outwith the Irish Sea as far north as Oban, between 21 and 30 times for the three N. Ireland samples and 34 times on the south of the Isle of Man (Figure 5.3, Table 5.13). Along the path of the radioactive plume, radiocaesium can be seen to undergo greatest reduction within the Irish Sea (see Figure 5.8); this is discussed further in sections 5.3(b) and 5.4.

Assuming radiocaesium to reflect the dilution of the radioactive plume, then, the relationship between any nuclide, x , and radiocaesium should reveal the degree of removal of x from the water column (see

Table 5.9
Levels of Most Abundant Radionuclides in Seaweeds, Standardised with Respect to ^{137}Cs Levels

<u>SITE</u>	$\frac{^{134}\text{Cs} (*)}{^{137}\text{Cs}}$	$\frac{^{106}\text{Ru}}{^{137}\text{Cs}}$	$\frac{^{95}\text{Nb}}{^{137}\text{Cs}}$	$\frac{^{95}\text{Zr}}{^{137}\text{Cs}}$	$\frac{^{60}\text{Co}}{^{137}\text{Cs}}$
Ravenglass	4.18E-02	5.29E-01	2.88E-01	2.50E-01	2.19E-02
Sellafield	4.71E-02	3.71E-01	1.75E-01	2.26E-01	2.11E-02
St. Bees	4.43E-02	4.43E-01	2.41E-01	2.60E-01	2.14E-02
Annan	3.24E-02	N.D.	5.91E-02	N.D.	N.D.
Balcary Bay	3.88E-02	1.69E-01	1.03E-01	1.26E-01	1.39E-02
Sandhead	3.74E-02	3.21E-01	1.56E-01	N.D.	N.D.
Ballantrae	3.04E-02	3.47E-01	6.02E-02	N.D.	N.D.
Turnberry	3.36E-02	N.D.	N.D.	N.D.	N.D.
Saltcoats	3.83E-02	N.D.	N.D.	N.D.	N.D.

(*) see Table 5.7 for decay-corrected ^{134}Cs .

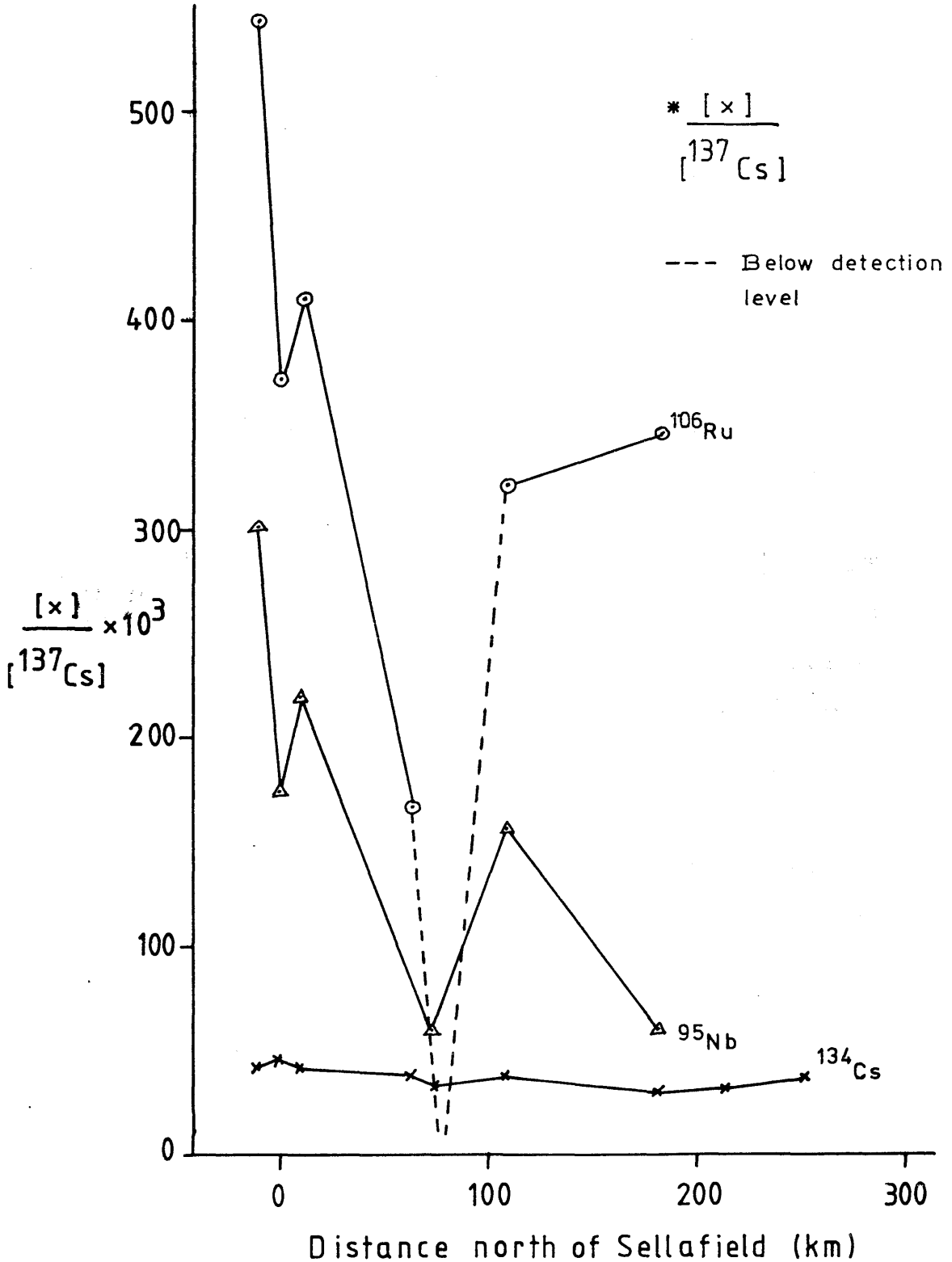
below). In practice, even radiocaesium is not perfectly conservative - some loss occurs during transit - and thus the estimated degree of removal of x will represent a lower limit (i.e. maximum limit on residence time). In Table 5.9 the $x : {}^{137}\text{Cs}$ ratios at each site are listed and can be seen to decrease generally with increasing distance from Sellafield. Only for the decay - corrected ${}^{134}\text{Cs}$ data (Table 5.7) does the ratio remain constant. Figure 5.5 illustrates how the ratios vary with distance from Sellafield for the three main nuclides and even with non-decay-corrected ${}^{134}\text{Cs}$ data the ratio is remarkably constant with distance relative to those for ${}^{106}\text{Ru}$ and ${}^{95}\text{Nb}$. This observation confirms that, whereas ${}^{134}\text{Cs}$ behaves as conservatively as ${}^{137}\text{Cs}$, ${}^{106}\text{Ru}$ and ${}^{95}\text{Nb}$ exhibit less conservative behaviour and are therefore being sequestered faster than ${}^{137}\text{Cs}$ from the water column.

If it were possible to apply decay-corrections to all the radionuclides measured (lag times between sites would thus be required) then ratios of each nuclide to, say, ${}^{106}\text{Ru}$ or ${}^{95}\text{Nb}$ would reveal more detail on how the radionuclides rank with regards to conservative behaviour.

The reduction factors have been calculated by comparing the level of radionuclide "x" at a site to that at the site where the maximum level of "x" occurred. The latter, for many nuclides, was the Ravensglass Estuary - Pu, Ru, Nb, Eu, Mn and Sb - some were not detected in the Sellafield sample. Thompson et al. (1982) reported radionuclide levels in F. vesiculosus from Braystones (near Ravensglass) and Drigg (near Sellafield) with maximum radiocaesium, Am and Pu(alpha) normalised levels occurring at the first site and maximum Ru, Ce, Zr and Nb occurring at Drigg. Comparison of the latter data with those of this project reveal that in both cases maximum radiocaesium levels occur at or near Sellafield and maximum Ru and Nb

Figure 5.5

Radionuclide Levels in Seaweeds - [x] - Standardised Against $^{137}\text{Cs}^*$ Plotted Against Distance from Sellafield



occur at/near Ravensglass; the sites of maximum Ce, Pu and Zr levels, however, are not consistent. Further comparisons cannot be made with data provided by MAFF, since these do not account for fresh water dilution but a set of seaweeds collected in November 1983 are available for comparison. These showed maximum radiocaesium and Co normalised levels in the Sellafield seaweed and maximum Ru, Pu, Nb, Eu, Mn and Sb in the Ravensglass seaweed. Overall, then, only the maximum radiocaesium (and Co although this was not detected by Thompson et al.) occurred consistently at the Sellafield site and maximum Ru at Ravensglass. The discrepancies described are presumed to have arisen as a consequence of variations in discharge levels and / or changes in physical marine processes (i.e. water and sediment movements).

b) Plutonium (alpha-emitting) Nuclides

Results of the alpha-emitting plutonium isotope analyses of seaweeds are presented in Table 5.10 and their spatial distribution shown in Figure 5.6. As expected, levels generally decreased with increasing distance from Sellafield but the overall highest levels were found in the Ravensglass Estuary. Reduction factors, as shown in Table 5.11, have been calculated relative to the Ravensglass Estuary results and show very similar values for $^{239/240}\text{Pu}$ and ^{238}Pu at all sites as a result of more or less constant $^{238}\text{Pu} : ^{239/240}\text{Pu}$ discharge ratios (Table 5.10).

As found for many of the gamma-emitting nuclides, the Annan sample showed low radionuclide activities. For the Pu nuclides the reduction factor (relative to Ravensglass) exceeded 20 and in normalising the data the low Annan level is accentuated by a reduction

Table 5.10

Pu Activities Found in Seaweeds (mBq/g dry weight)

SITE	^{238}Pu	$^{239/240}\text{Pu}$	$\frac{^{238}\text{Pu}}{^{239/240}\text{Pu}}$
Ravenglass	1.11E 02 $\pm 2.59\text{E } 00$	4.51E 02 $\pm 5.19\text{E } 00$	2.47E-01 $\pm 6.70\text{E } -03$
Sellafield	5.95E 01 $\pm 1.92\text{E } 00$	2.50E 02 $\pm 3.95\text{E } 00$	2.38E-01 $\pm 6.60\text{E } -03$
St. Bees	2.86E 01 $\pm 1.90\text{E } 00$	1.20E 02 $\pm 5.96\text{E } 00$	2.38E-01 $\pm 1.98\text{E } -02$
Annan	4.31E 00 $\pm 7.70\text{E } -02$	1.97E 01 $\pm 2.13\text{E } -01$	2.19E-01 $\pm 4.60\text{E } -03$
Balcary Bay	1.40E 01 $\pm 2.18\text{E } -01$	5.88E 01 $\pm 4.07\text{E } -01$	2.37E-01 $\pm 3.50\text{E } -03$
Sandhead	6.07E 00 $\pm 1.85\text{E } -01$	2.73E 01 $\pm 3.96\text{E } -01$	2.22E-01 $\pm 7.00\text{E } -03$
Ballantrae	4.88E 00 $\pm 9.40\text{E } -02$	2.21E 01 $\pm 2.01\text{E } -01$	2.21E-01 $\pm 4.70\text{E } -03$
Turnberry	1.01E 00 $\pm 2.47\text{E } -02$	4.36E 00 $\pm 5.10\text{E } -02$	2.32E-01 $\pm 6.30\text{E } -03$
Saltcoats	7.99E-01 $\pm 7.31\text{E } -02$	3.40E 00 $\pm 2.48\text{E } -01$	2.35E-01 $\pm 2.75\text{E } -02$
Gourock	1.98E 00 $\pm 5.90\text{E } -02$	8.44E 00 $\pm 1.22\text{E } -01$	2.34E-01 $\pm 7.80\text{E } -03$
Loch Fyne	5.34E-01 $\pm 3.02\text{E } -02$	2.38E 00 $\pm 6.40\text{E } -02$	2.25E-01 $\pm 1.40\text{E } -02$

Table 5.11

Reduction Factors For Pu Activities in Seaweeds
in Relation to Activities for the Ravensglass Sample

<u>SITE</u>	<u>^{238}Pu</u>	<u>$^{239/240}\text{Pu}$</u>
Ravenglass	1.0	1.0
Sellafield	1.9	1.8
St. Bees	3.9	3.8
Annan	25.8	22.9
Balcary Bay	7.9	7.7
Sandhead	18.3	16.5
Ballantrae	22.8	20.4
Turnberry	109.9	103.4
Saltcoats	138.9	132.7
Gourock	56.1	53.4
Loch Fyne	207.9	189.5

Table 5.12

Pu Activities in Seaweeds Normalised with Respect to ^{40}K .

<u>SITE</u>	<u>^{238}Pu</u>	<u>$^{239/240}\text{Pu}$</u>
Ravenglass	7.73E-02	3.13E-01
Sellafield	5.83E-02	2.45E-01
St. Bees	2.31E-02	9.68E-02
Annan	2.55E-03	1.17E-02
Balcary Bay	9.93E-03	4.17E-02
Sandhead	9.94E-03	4.47E-02
Ballantrae	6.16E-03	2.79E-02
Turnberry	9.53E-04	4.11E-03
Saltcoats	6.44E-04	2.74E-03
Gourock	3.52E-03	1.50E-02
Loch Fyne	5.77E-04	2.57E-03

Table 5.13

Reduction Factors* For Cs and Pu Nuclides in Seaweeds
with Activities Normalised with Respect to ^{40}K .

<u>SITE</u>	<u>^{137}Cs</u>	<u>^{134}Cs</u>	<u>$^{239/240}\text{Pu}$</u>	<u>^{238}Pu</u>
Ravenglass	1.4	1.6	1.0	1.0
Sellafield	1.0	1.0	1.3	1.3
St. Bees	2.0	2.2	3.2	3.4
Annan	7.0	10.1	26.9	30.3
Balcary Bay	4.9	5.9	7.5	7.8
Sandhead	9.3	11.6	7.0	7.8
Ballantrae	14.3	22.0	11.2	12.6
Turnberry	15.3	21.3	76.2	81.1
Saltcoats	21.0	25.7	114.2	120.0
Gourock	15.7	N.D.	20.9	22.0
Loch Fyne	23.4	N.D.	121.7	134.0

*Reduction in activities compared to activities in
Ravenglass (for Pu nuclides) or Sellafield (Cs nuclides)
seaweed.

factor value in excess of 25 (Table 5.13); the corresponding reduction for radiocaesium is <10. Following the earlier suggestion that the long transit time of water to Annan may not be able, alone, to account for the observed low radionuclide levels at Annan (5.3.a(5)), it is worth comparing the Annan plutonium and radiocaesium reduction factors to those for Ballantrae - for which the water transit time from Sellafield is similar to that to Annan (~2.5 years). The Pu reduction factors to Ballantrae are less than half those to Annan whereas the Cs ones to Ballantrae are double those to Annan (Table 5.13). These results support the idea that, in the shallow regions of the Solway Firth, non-conservative nuclides are removed from the water column to a greater degree because of the higher sediment/water interactions.

By Loch Fyne the reduction factor was ~200 whereas the corresponding value for ^{137}Cs was only ~26; hence Pu appears to have been removed from the water column ~7.7 times faster than radiocaesium. However, in normalising the Pu data with respect to ^{40}K levels (Table 5.12 and Figure 5.7), the reduction factor for Pu in Loch Fyne seaweed becomes only ~120 - because of the low ^{40}K content of the Loch Fyne seaweed compared with that of the Ravensglass sample - whilst the corresponding reduction factor for ^{137}Cs is ~23 (Table 5.13). This, then, indicates (on average throughout transit) approximately 5 times faster removal of Pu than radiocaesium (Table 5.16) assuming constant uptake factors of plutonium and radiocaesium relative to ^{40}K . In normalising the Pu data, the maximum levels were still those of the Ravensglass seaweed (Table 5.12).

From Figure 5.8 the ^{137}Cs levels can be seen to be reduced at a slower rate (with distance from Sellafield) after the North Channel than before. A similar pattern, although less clear, is seen for the normalised Pu (alpha) levels. This trend can be compared also to the

Figure 5.7

Normalised $^{239, 240}\text{Pu}$ Levels in Seaweeds

$$\left(\frac{^{239, 240}\text{Pu}}{40\text{K}} \times 10^3 \right)$$

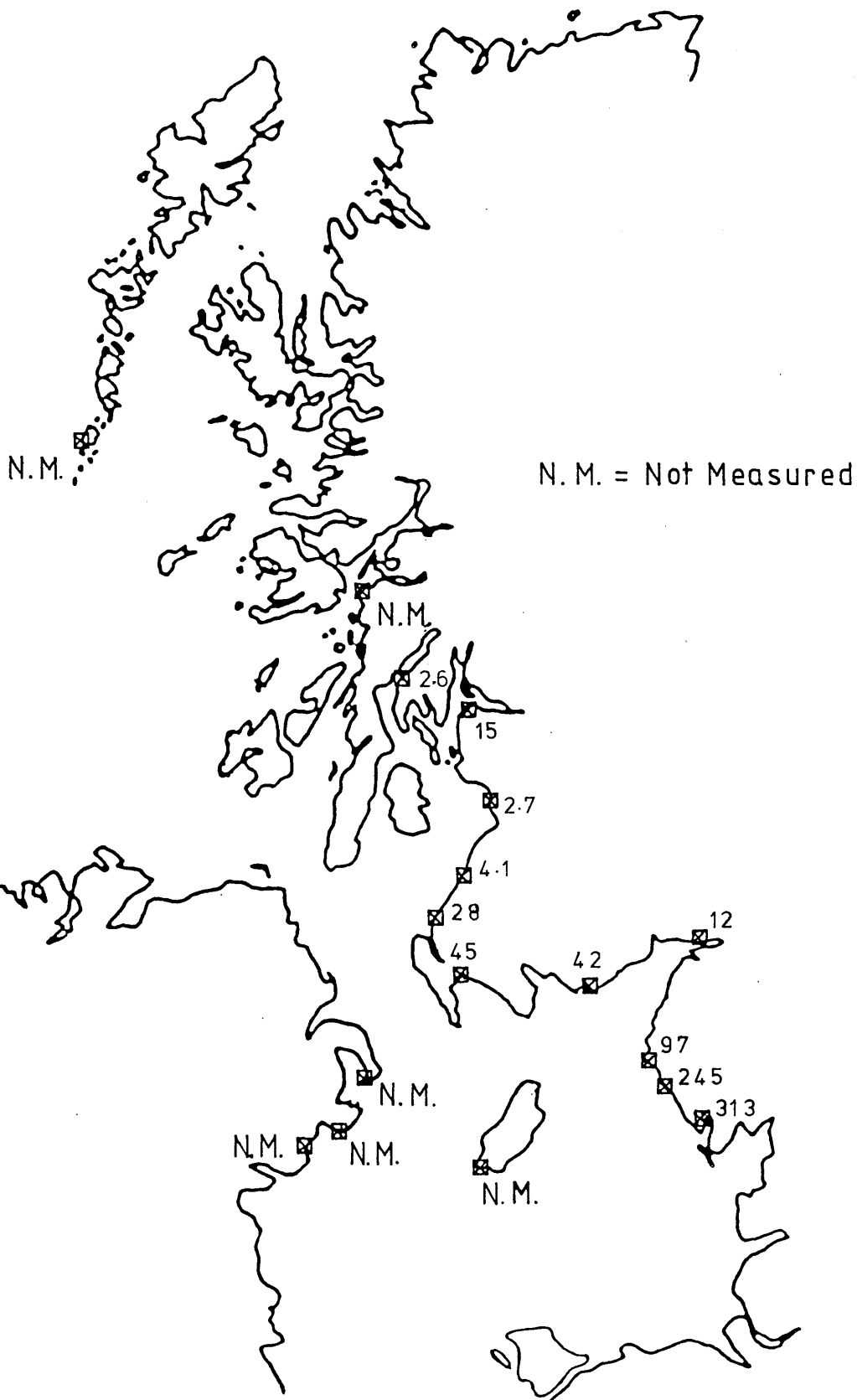
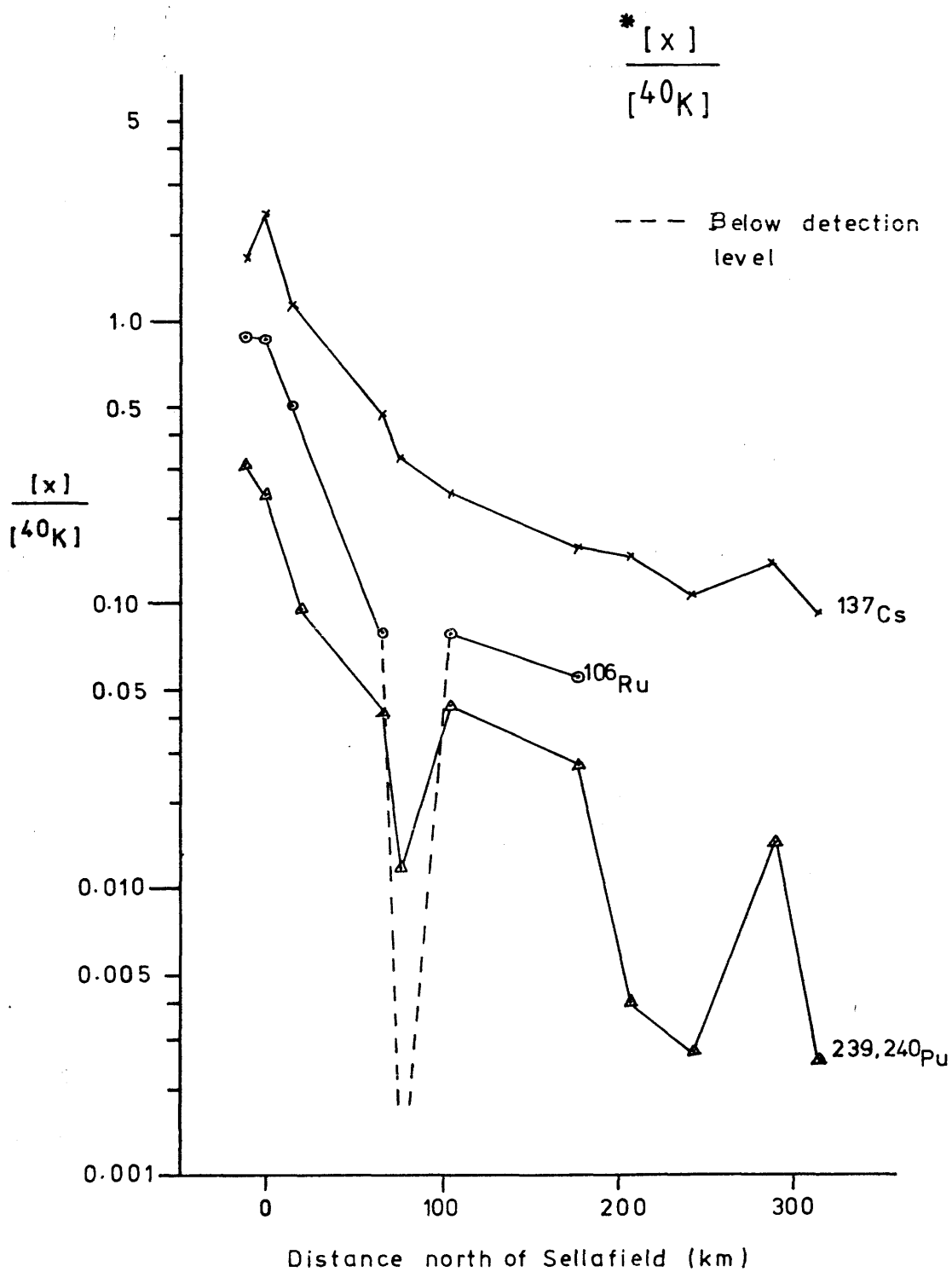


Figure 5.8

Normalised Radionuclide Levels* - [x] -
Against Distance from Sellafield



radiocaesium / distance diagrams in Chapter 4 showing greater decreases of radiocaesium for various sections of the plume in which increased dilution by saline, low-activity waters was occurring, e.g. the North Channel (see Figure 4.2.a8). It is likely that the trends are explained by proportionally greater dilution of the radioactivity immediately after introduction of the radioactive discharge into the Irish Sea and by the relatively long residence time of the water in the northern Irish Sea relative to that along the west Scottish coastal zone. There is, of course, the additional contribution by differential removal of the radionuclides from the water column which is undoubtedly occurring to some extent and is reflected in the measured levels. To establish the relative behaviours of radiocaesium and plutonium, a plot of $^{239/240}\text{Pu} : ^{137}\text{Cs}$ has been prepared (Figure 5.9 see also Table 5.15). The general decrease in ratio with increasing distance from Sellafield reflects the greater removal of Pu from the water column relative to radiocaesium and confirms the findings described above from the reduction factors of normalised radiocaesium and Pu. For the other radionuclides (Table 5.9), the relationship to radiocaesium has not been explored because of the limited data available, partly through rapid decay and / or low discharges from Sellafield.

5.4 Half - distances, Residence Times and Concentration Factors

From Figure 5.8 it is possible to derive the rates of reduction of radionuclide levels in the water column with distance along the radioactive plume for various regions of the plume. From the observed rate of reduction the half-distance - the distance over which the concentration is halved - ($d_{1/2}$) can then be obtained.

Table 5.14

Reduction Factors* For ^{106}Ru , ^{95}Zr , ^{95}Nb and ^{60}Co Nuclides
in Seaweeds with Activities Normalised with Respect to ^{40}K .

<u>SITE</u>	<u>^{106}Ru</u>	<u>^{95}Zr</u>	<u>^{95}Nb</u>	<u>^{60}Co</u>
Ravenglass	1.0	1.3	1.0	1.4
Sellafield	1.0	1.0	1.2	1.0
St. Bees	1.7	1.8	1.7	2.0
Annan	N.D.	N.D.	24.1	N.D.
Balcary Bay	10.9	8.7	9.6	7.4
Sandhead	10.9	N.D.	12.1	N.D.
Ballantrae	15.6	N.D.	48.3	N.D.
Turnberry	N.D.	N.D.	N.D.	N.D.
Saltcoats	N.D.	N.D.	N.D.	N.D.
Gourock	N.D.	N.D.	N.D.	N.D.
Loch Fyne	N.D.	N.D.	N.D.	N.D.

*Reduction in activities compared to activities
in Sellafield (for ^{95}Zr and ^{60}Co) or Ravenglass
(for ^{100}Ru and ^{95}Nb) seaweed.

Table 5.15

Pu Activities in Seaweeds Standardised
With Respect to ^{137}Cs Levels.

<u>SITE</u>	<u>^{238}Pu</u>	<u>$^{239/240}\text{Pu}$</u>
Ravenglass	4.64E-02	1.88E-01
Sellafield	2.51E-02	1.05E-01
St. Bees	2.01E-02	8.45E-02
Annan	7.61E-03	3.48E-02
Balcary Bay	2.08E-02	8.74E-02
Sandhead	3.95E-02	1.78E-01
Ballantrae	3.78E-02	1.71E-01
Turnberry	6.26E-03	2.70E-02
Saltcoats	5.79E-03	2.46E-02
Gourock	2.36E-02	1.01E-01
Loch Fyne	5.81E-03	2.58E-02

Table 5.16

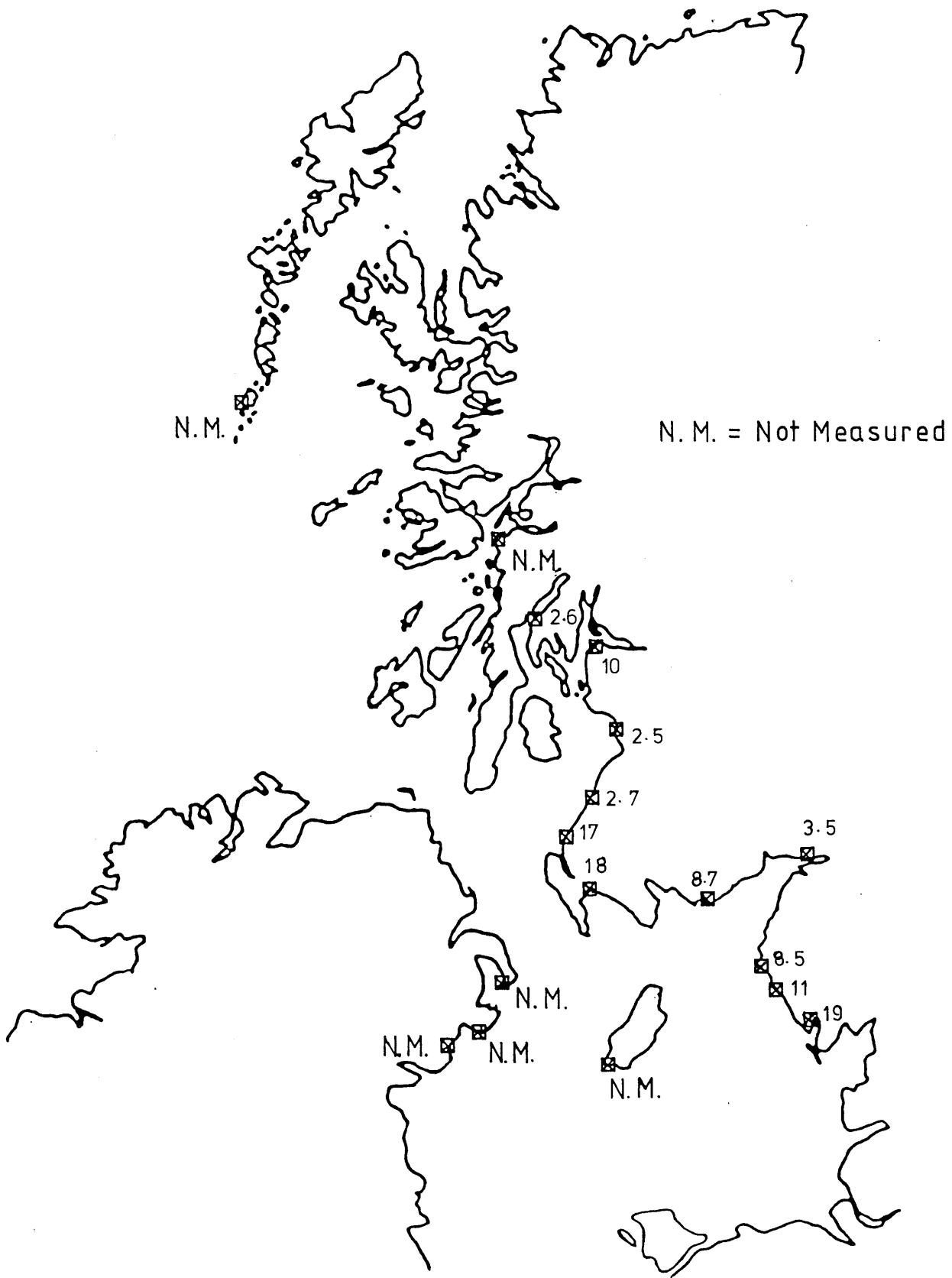
$^{239/240}\text{Pu}$ Reduction Factors* Compared to
 ^{137}Cs Reduction Factors*

<u>SITE</u>	<u>$\frac{^{239/240}\text{Pu Reduction}}{^{137}\text{Cs Reduction}}$</u>
Ravenglass	0.714
Sellafield	1.300
St. Bees	1.600
Annan	3.843
Balcary Bay	1.531
Sandhead	0.753
Ballantrae	0.783
Turnberry	4.980
Saltcoats	5.438
Gourock	1.331
Loch Fyne	5.201

*Reduction of Pu activities compared with activities found in Ravenglass seaweed and of Cs activities compared with activities found in Sellafield seaweed.

Figure 5.9

$$\frac{^{239,240}\text{Pu}}{^{137}\text{Cs}} \text{ Ratios in Seaweeds } (\times 10^2)$$



For radiocaesium, then, a half-distance of ~ 10 km has been estimated for the Cumbrian coast (from Sellafield to St. Bees) where the decrease in levels was very sharp. For the region from Sellafield to Sandhead - i.e. encompassing the north - eastern Irish Sea - $d_{1/2}$ was found to be 30 km, whilst for the North Channel to Saltcoats (CSA) and to Loch Fyne (CSA) the $d_{1/2}$ values were 93 and 155 km respectively. For the path of the plume passing to the west of Mull of Kintyre - i.e. bypassing the CSA - the seaweed collected from Dunstaffnage 6 months later was used to derive an approximate $d_{1/2}$ value of 210 km from the North Channel. For comparison, from seaweeds collected in 1982, Dahlgaard et al. (1984) calculated ^{137}Cs half-distances of 40 km in the Irish Sea and 430 km along the Scottish coast.

Corresponding values for Pu have been estimated as 26 km in the Irish Sea and 55 km for the North Channel to the CSA. Dahlgaard et al. (1984) estimated 23 km for the Irish Sea and 260 km along the Scottish coast.

Variations in radionuclide discharges have not been accounted for here but agreement between the data sets for the two different years is remarkably close in the Irish Sea sector. The observed values north of the North Channel suggest (from the above data) that the paths to the east and west of Mull of Kintyre are not directly comparable for there is a twofold difference between the two estimated half-distances for the Scottish coast. Taking into account the 7-month difference in sampling times between the Dunstaffnage seaweed and the others, a revised $d_{1/2}$ value for the "western" path of the plume (i.e. the Scottish coastal current) was derived as follows. Assuming a 6-month time-lag from Sellafield to Dunstaffnage (which is on the edge of Loch Etive) - see Section 3.2, Chapter 3 - a 1.5 times higher discharge level corresponds to seaweeds if sampled at Dunstaffnage in January

1983 (125 TBq discharged in February 1983 corresponds to August 1983 levels found at Dunstaffnage whilst 182 TBq discharged in July 1982 corresponds to January 1983 levels at Dunstaffnage). Hence the Dunstaffnage normalised ^{137}Cs level can be corrected from 0.101 to 0.152. This then gives a $d_{1/2}$ of 390km which compares well with the 430km estimated by Dahlgaard et al. (1984).

In comparing the $d_{1/2}$ values, radiocaesium and plutonium distributions indicate 2.5 - 4.6 and 4.8 times slower reduction rates respectively for the main plume along the Scottish coast than for the North Channel to the CSA. This finding agrees with the longer transit time found to the CSA (from Sellafield) than to the equivalent distance along the "western path", hence some residence / mixing of waters within the CSA has led to some reduction in levels.

The faster - approximately double - reduction of Pu compared with that of radiocaesium reflects the more conservative nature of the latter. By assuming radiocaesium to be perfectly conservative (i.e. its reduction is due solely to dilution) the reduction rate of Pu can be used to calculate (the lower limit of) the removal rate of Pu from the water column. Dahlgaard et al. (1984) estimated such a "half-life" of Sellafield Pu in Scottish waters to be 8 - 10 months. From the relationship between Pu and radiocaesium (Figure 5.10) the $^{239/240}\text{Pu}$: ^{137}Cs ratio seems to have approximately halved from Sellafield to the CSA. From Chapter 3 the transit time between Sellafield and reach the CSA has been calculated as 4.8 +/- 0.3 months; hence the reduction rate of Pu - over and above the inherent reduction also affecting radiocaesium which is partly due to dilution - corresponds to a half-life of ~4.8 months. From Chapter 3, however, an overall residence time of radiocaesium in the northern Irish Sea (and North Channel) has been estimated as 10 months which brings about an overall half-life of

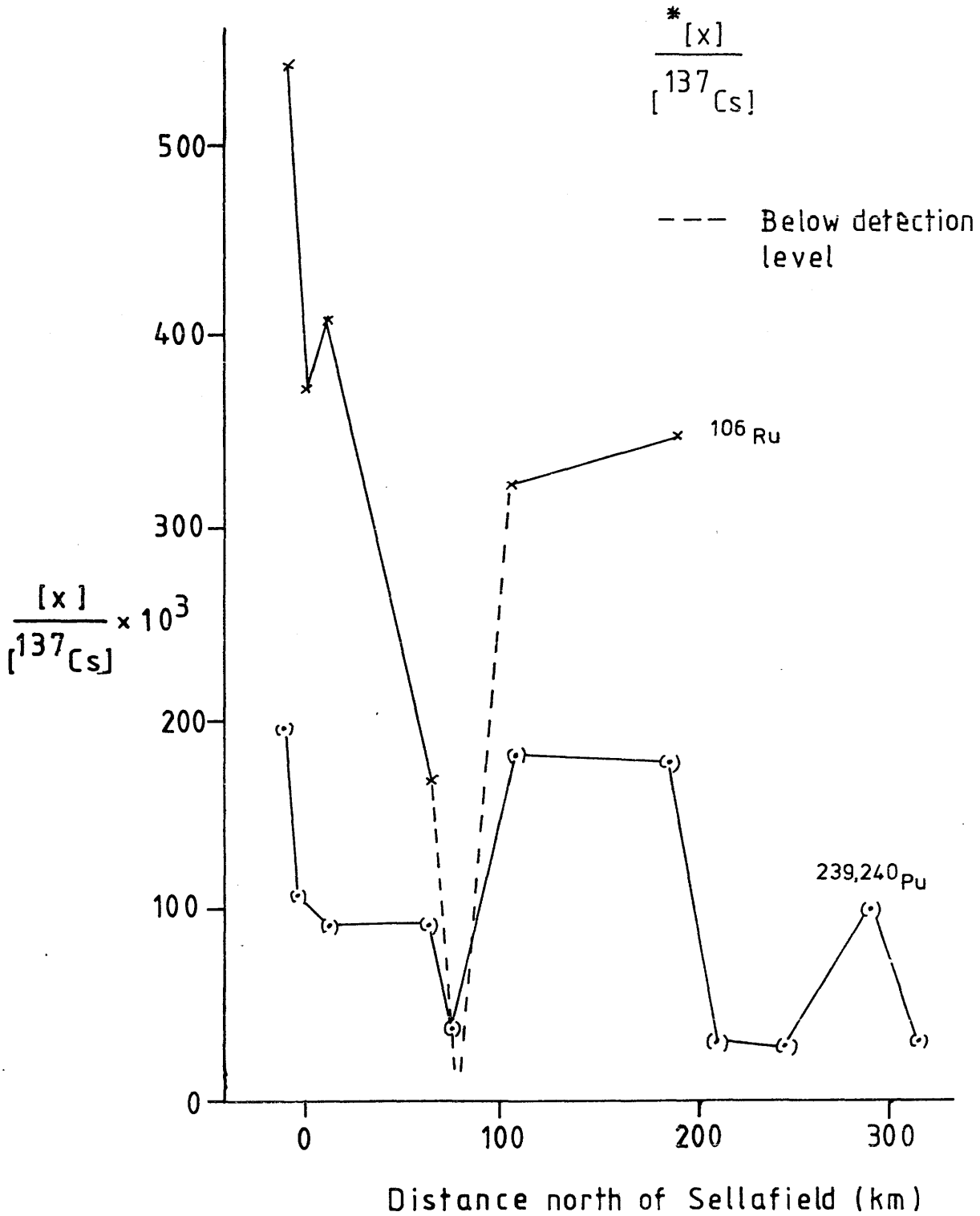
3.2 months for Pu as far as the CSA.

By comparing radiocaesium levels in sea water (against distance from Sellafield) for May 1983 - Figure 4.2a9, Chapter 4 - with those in seaweeds, the former give faster reduction rates, i.e. shorter $d_{1/2}$'s - 70km for the North Channel and 137km along the Scottish coastal current. For August 1983, however, the overall $d_{1/2}$ was estimated as 340km; hence variations are due partly to changes in discharge levels and also to varying hydrographic conditions - such as incursion of Atlantic water into the HSA causing increased dilution of the radioactive plume - as discussed in Chapter 4. However, comparison of actual radiocaesium levels in the sea water to those in the seaweeds gives concentration factors of radiocaesium from the ambient sea water by the seaweeds. For example, the CSA water in January 1983 contained ~ 0.75 Bq/l (Appendix I.1) whilst the activities of three CSA seaweeds - from Saltcoats, Gourock and Loch Fyne - averaged 18.5 Bq/Kg wet weight. This observation gives a concentration factor of 25; the value suggested by IAEA is 10 - Table 1.5. A further set of seaweeds from the CSA (October 1984) gave, from 8 samples, a range of radiocaesium concentration factors of 22 - 61 (MacKenzie, 1986, pers.comm.). From data of Dahlgaard et al. (1984), the concentration factors for Fucus seaweeds along the west Scottish coast lie mostly in the range $2-4 \times 10^3$; IAEA suggest 10^3 (Table 1.5).

At three sites, more than one species of seaweed was collected in order to investigate variations in concentration factors of radiocaesium by the various species. From Dunstaffnage, the normalised ^{137}Cs data shows F. spiralis to have higher concentration factors, by 1.3 and 1.13 times, than Pelvetia caniculata and Ascophyllum nodosum respectively (Table 5.2). At Portaferry, the two Fucus samples were very similar with F. vesiculosus exhibiting a slightly (<1.1 times)

Figure 5.10

$^{239,240}\text{Pu}$ and ^{106}Ru Levels in Seaweeds -
 [x] - Standardised Against $^{137}\text{Cs}^*$ Plotted
Against Distance from Sellafield



higher concentration factor than F.serratus (Table 5.2). Finally, at Ravensglass, F. vesiculosus showed an approximately 1.5 times higher concentration factor than Ascophyllum nodosum.

5.5 Summary and Conclusions

The pathway of radionuclide transfer to man via consumption and / or use of seaweeds and their products has been investigated. In radiological protection terms there is negligible risk but if Fucus seaweeds from the Cumbrian coast were to be consumed in the quantities which Porphyra has been known to be consumed in the past, an exposure equivalent to ~6% of the ICRP-recommended permissible intake, for members of the public, of 5mSv (or ~30% of the principal limit of 1mSv year⁻¹, see section 1.3, Chapter 1) would be experienced by critical group members.

Analyses of gamma-emitting and Pu alpha-emitting nuclide activities of seaweeds from the west coast of Britain have been carried out. The results have allowed estimation of transit times of water from the Sellafield pipeline to the various sites by using decay of the ¹³⁴Cs: ¹³⁷Cs ratio. These transit times indicate relatively long residence times within the Irish Sea and hence support similar findings in Chapter 3 from radiocaesium levels in sea water.

¹³⁷Cs was detected furthest from the source whilst short-lived radionuclides and those of high particle-reactivity of low discharge were reduced below detection levels nearer the source point. In order to make direct comparisons of levels of any radionuclide between the various seaweed samples the observed radionuclide levels were normalised with respect to ⁴⁰K levels. These "normalised" values allowed comparison between reduction rates of the radionuclides along

the path of the radioactive plume. Maximum (normalised) levels of Cs, Zr, Co, Ag and Ce radionuclides were found at the Sellafield site whereas maximum Ru, Nb, Eu, Mn and Sb occurred at Ravenglass. The only consistent results when compared with other workers were those of Cs and Ru.

Generally low radionuclide levels - measured and normalised - and a low $^{134}\text{Cs} : ^{137}\text{Cs}$ value for the Annan seaweed indicate that the radioactive plume of water bypasses the upstream region of the Solway Firth, taking a more direct route (from St. Bees) to Balcarry Bay. The relatively low radioactivity levels can be attributed at least partly to radioactive decay during the relatively long transit time and also possibly to greater scavenging of the radionuclides from the water column by sediment particles. Such enhanced scavenging of radionuclides obviously affects the non-conservative elements - such as Pu - more than radiocaesium; this fractionating effect would explain why the decrease in radiocaesium levels at Annan was not as obvious as the corresponding decreases in Pu and ^{106}Ru .

The decrease in Pu:Cs ratios with increasing distance from Sellafield demonstrates the relatively conservative behaviour of Cs. By assuming the latter to be perfectly conservative, a removal rate of Pu was estimated, giving a "half-life" of ~ 4.8 months for transit as far as the CSA. This value corresponds to an overall 3.2 month half-life when the inherent Cs "half-life", which has earlier been estimated as 10 months (Chapter 3), is accounted for. From a comparison of the Pu and Cs reduction rates, Pu is estimated to be removed 5 times faster than Cs.

Half-distances of 30km and 26km have been estimated for radiocaesium and Pu respectively in the Irish Sea; corresponding values for the North Channel to CSA region are ~ 120 km and 55km. Along

the main Scottish coastal current (bypassing the CSA), the half-distance for Cs was estimated as 390km, which compares well with a value of 430km determined by Dahlgard et al. (1984).

An estimate of the concentration factor by Fucus for radiocaesium was ~ 25 , within the range found by MacKenzie (1986) and close to the general value suggested by IAEA, 10, for all seaweeds (Table 1.5). Comparison between species at three different sites indicates that the Fucus seaweeds have higher concentration factors than Ascophyllum nodosum and Pelvetia caniculata.

Fucus seaweeds have been used successfully as indicators of radionuclide levels and behaviour in sea water and have provided useful information on the movement of the sea water. The transport data obtained here could be used for predictive purposes in assessing the dispersion of any future accidental or planned releases from Sellafield.

Time trends of radionuclide levels in seaweeds could be used in a similar manner to the radiocaesium time trends in sea water (as in Chapter 4, section 4.3) to obtain transit times for Sellafield water to reach various regions along the path of the radioactive plume. From radionuclide time trends in seaweeds, transit times for each nuclide could be deduced and subsequent comparison of transit times could further reveal differences in the physico-chemical behaviour of the effluent radionuclides.

CHAPTER 6

Overview

By recourse to several forms of data presentation throughout this study, various aspects of water movement in the HSA and nearby waters have been recognised.

Matching of the CSA radiocaesium record with the Sellafield discharge pattern suggests a Sellafield - CSA transit time of 4.8 months. From a single-box model, a residence time for water in the Irish Sea / CSA system of 14.4 months is estimated, whilst a maximum decay-time between Sellafield and the CSA is assessed at 17 months; most (>50%) of this residence seems, from E_a values (see below), to occur close to the Cumbrian coastline.

Further matching of radiocaesium time-trends at various transects throughout the HSA has allowed estimation of transit times between stations. Since such matching is at all possible, it is suggested that no thorough mixing of waters occurs during the plume's journey from Sellafield to The Minches (including the path to the CSA). However, since the Irish Sea is generally regarded as a well-mixed region, it is proposed that, within the northern Irish Sea, a fraction of the Sellafield discharge escapes thorough mixing, probably by remaining in surface waters (as implied by subsurface radiocaesium levels), whilst the remainder may be quite extensively mixed. Thereafter, data on radiocaesium levels throughout the water column indicate transport, without extensive mixing, of the surface, relatively undiluted

Sellafield discharge along the eastern side of the North Channel and northward along the west Scottish coast. The deduced transit times are, therefore, probably more representative of surface waters than of either deeper waters or the entire water column. From these transit times, E_a values of radiocaesium at each transect were obtained.

Comparison of the E_a values between sites gives an indication of radiocaesium dilution between these stations. Such dilutions are low ("threefold) along the main path of the plume along the west Scottish coast (between the North Channel and The Minches) and relatively high ("twentyfold) within the Irish Sea (from near Sellafield to the North Channel). Dilutions observed from actual radiocaesium levels were also low ("twofold) along the Scottish coastal current and those deduced from radiocaesium levels in seaweed were $\times 16 - 23$ for the Cumbria - CSA route. Half-distances obtained from seaweed radionuclide levels indicate faster dilution rates within the Irish Sea and CSA than along the west Scottish coast, i.e. 4 and 13 times faster from the North Channel to the CSA and in the Irish Sea respectively relative to that observed along the Scottish coastal current. Thus agreement is excellent between observed sea water and indicator seaweed radiocaesium levels.

Comparison of E_a variations with time at one transect with those elsewhere reflects the relative importance of water residence / mixing in the various regions. For example, water residence was found to be greater in the Irish Sea than in the North Channel / CSA, which, in turn, is greater than that occurring along the Scottish coastal current. This observation complements the above findings of greater dilution rates in the Irish Sea relative to the North Channel / CSA, which, in turn, exceed those along the Scottish coastal current.

^{134}Cs : ^{137}Cs ratio values in seaweeds from the west coast of Britain

also indicate relatively long residence times within the Irish Sea.

Spatial distributions of surface radiocaesium levels and salinities assist in defining Atlantic water influxes into the southern HSA; strong influx events (May 1982, August 1983 and June / July 1984) were found to correspond to periods of confinement of the radioactive plume to the Scottish coast, whereas weak influxes (May 1983 and April / May 1984) led to less pronounced restriction of the plume to the coast. The degree of coastal restriction of the plume seems to influence the proportions of Irish Sea-derived water flowing to the west and to the east of the Outer Hebrides. Except for inshore regions where fresh water dilution is also important, radiocaesium levels are largely dependent on salinity, i.e. on the degree of dilution of the radiocaesium plume by Atlantic waters. However, purely from salinity levels, it is not possible to describe accurately the movement of Atlantic water. For example, high salinities may be a reflection of an earlier Atlantic incursion (and a current withdrawal) or of a present incursion. The distribution of salinity and radiocaesium levels, e.g. the Islay Front's intensity, are found to be more useful in characterising Atlantic water behaviour. For example, whereas a westerly position of the front indicates current or recent withdrawal of Atlantic water, an accompanying weak radiocaesium / salinity gradient across the front (e.g. May 1982, May 1983 and October 1983) corresponds to fast currents at Tiree (accompanying strong winds here), thus implying a present incursion.

Also recognised from spatial water property distributions is the blockage of the northward-flowing Irish Sea / CSA water through the North Channel (August 1983) by Atlantic water flowing south along the coast of N.Ireland.

^{137}Cs / salinity plots indicate the relative influences exerted

by fresh water and saline Atlantic water in diluting the radiocaesium plume during its journey; the response of an area to variations in Sellafield discharge or in dilution by Atlantic water can therefore be partially recognised. Thus, peaks in radiocaesium levels at different times and places could be related and a transit time from the southern HSA (transect D) to The Minches (transect K) was estimated at $\sim 3-4$ months, in excellent agreement with the lag-time (3.5 months) derived from matching of the radiocaesium time-trends.

^{137}Cs / distance plots reflect the reduction in the plume's radiocaesium levels during its transport, whereas the same plot as a function of time provides a picture of temporal variation of radiocaesium levels throughout the area, thus illustrating the effects, with time and distance, of Atlantic water influence and of variation in Sellafield discharge levels.

Subsurface radiocaesium levels indicate that marked reductions, often to <10% surface values, occur in water below the halocline; this is attributed to greater subsurface (than surface) dilution by Atlantic waters. Atlantic water influence in the southern HSA, on two occasions, however, appeared to be more pronounced at the surface than at depth. The region of most extensive vertical mixing is found to be The Minches.

From the Sellafield - CSA lag-time, a mean current velocity of 1.7 km day⁻¹ is estimated. After identifying the north and south flowing water fractions within the North Channel, the above mean velocity is applied to the north-flowing water fraction to obtain a northward water flux of 5-10 km³ day⁻¹. Corresponding radiocaesium fluxes of $1.2 - 4.2 \times 10^{14}$ dpm day⁻¹ (June 1984 - February 1985) are derived, with reduced subsurface radiocaesium levels being accounted for. Southward and thus net (northward) North Channel flow is unknown.

More detailed ("monthly) radiocaesium time-trends at each transect could, in future, provide more precise estimates of lag-times and therefore more accurate mean current velocities between sites. The resulting current velocities could then be used to calculate radiocaesium / water fluxes through the various transects of the HSA.

Radionuclide activities in seaweeds indicate that the radioactive plume of water, during its journey from Sellafield to the North Channel, bypasses, to some extent, the upstream region of the Solway Firth. From Pu:Cs ratios of the seaweeds, a lower limit for the rate of removal of Pu from the water column is estimated at 4.8 months "half-life" (assuming perfectly conservative behaviour of Cs) during the Sellafield - CSA journey. From the observed reduction rates, Pu is estimated to be scavenged from the water column ~ 5 times faster than Cs during the Sellafield - CSA journey. Half-distances imply faster Pu (relative to Cs) removal outwith the Irish Sea (i.e. in the North Channel / CSA region) than within it.

Fucus seaweed is found to concentrate radiocaesium ~ 25 times relative to ambient sea water levels; on three occasions, this uptake factor is found to be higher than those for Ascophyllum nodosum and Pelvetia canaliculata. Because of such accumulation of radionuclides by seaweeds, the radioactivity is more easily detected in the latter than in sea water. Thus time-trends of radionuclide levels in seaweeds at each site could be used to obtain transit times between sites (as performed with sea water radiocaesium time-trends). Comparison, then, between transit times of the various radionuclides could reveal further differences in their physico-chemical behaviour.

During 1982 - 1985, 30-55% of the Sellafield - discharged radiocaesium is estimated to have passed through the CSA, diluted ~ 20 times relative to near-pipeline levels. This trend indicates that,

although the U.K. collective dose, when averaged to dose per person, is negligible, mean individual doses of ~ 10 times the UK-average are delivered to the locals population of the CSA.

Exposures of $\sim 6\%$ of the ICRP-recommended permissible annual intake, 5mSv, or $\sim 30\%$ of the principle limit of 1mSv year⁻¹, for members of the public, would be experienced by critical group members if Fucus seaweeds from Cumbria were consumed in the quantities in which Porphyra has been known to be consumed in the past.

REFERENCES

- Aarkrog, A., Dahlgaard, H., Hallstadius, L., Hansen, H. and Holm, E. (1983). Radiocaesium from Sellafield effluents in Greenland waters. Nature, 304, 49-51.
- Atherton, R.S. (1982-1986). BNF. Health and Safety Directorate, Risley, Warrington, UK. Pers. commⁿ.
- Aston, S.R. and Fowler, S.W. (1984). Experimental studies on behaviour of long-lived radionuclides in relation to deep-ocean disposal of nuclear waste. IAEA-CN-43/6, 339-354, Vienna, IAEA.
- Aston, S.R. and Stanners, D.A. (1979). The determination of estuarine sedimentation rates by $^{134}\text{Cs}/^{137}\text{Cs}$ and other artificial radionuclide profiles. Estuarine and Coastal Marine Science, 9, 529-541.
- Aston, S.R. and Stanners, D.A. (1981). Plutonium transport to and deposition and immobility in Irish Sea intertidal sediments. Nature, 289, 581-582.
- Barnes, H. and Goodley, E.F.W. (1961). The general hydrography of the Clyde Sea Area, Scotland. Part 1: Description of the area; drift bottle and surface salinity data. Bull. Mar. Ecol., 5, 112-150.
- Baxter, M.S and McKinley, I.G. (1978). Radioactive species in sea

- water. Proc. R. Soc. Edin., 76B, 17-35.
- Baxter, M.S., McKinley, I.G., MacKenzie, A.B. and Jack, W. (1979).
windscale radiocaesium in the Clyde Sea Area. Mar. Poll. Bull., 10,
116-120.
- Beasley, T.M., Carpenter, R. and Jennings, C.D. (1982). Plutonium,
 ^{241}Am and ^{137}Cs ratios, inventories and vertical profiles in
Washington and Oregon continental shelf sediments. Geochim.
Cosmochim. Acta., 46, 1931-1946.
- B.N.F.L., Health and Safety Directorate (1984). Annual report on
radioactive discharges and monitoring of the environment 1983.
Issued by Director of Health and Safety, August 1984.
- B.N.F.L., Health and Safety Directorate (1985). Annual report on
radioactive discharges and monitoring of the environment 1984.
Issued by Director of Health and Safety, August 1985.
- Bowden, K.F. (1950). Processes affecting the salinity of the Irish
Sea. Mon. Not. R. Astron. Soc., Geophys. Suppl., 6 (2), 63-90.
- Bowden, K.F. (1955). Physical oceanography of the Irish Sea. Fish.
Invest., Lond., Ser. 2, 18 (8), 67pp.
- Buchanan, M. (1983). Isle of Barra, Outer Hebrides, UK. Pers. commⁿ.
- Burton, J.D. (1975). Radioactive nuclides in the marine environment.
In Chemical Oceanography, ed. by J.P. Riley, and G. Skirrow, 2nd

- edn., vol. 3, 91-191, London, Academic Press.
- Carpenter, R. and Beasley, T.M. (1981). Plutonium and americium in anoxic marine sediments: evidence against remobilization. Geochim. Cosmochim. Acta., 45, 1917-1930.
- Clifton, R.J. and Hamilton, E.I. (1982). The application of radioisotopes in the study of estuarine and sedimentary processes. Estuar. Coast. Shelf Sci., 14, 433-446.
- Clokier, J. (1986). J. & J. Clokier, Manse Hse., Tain, Ross-shire, UK. Pers. commⁿ.
- Coughtrey, P.J. and Thorne, M.C. (1983). Radionuclide distribution and transport in terrestrial and aquatic ecosystems. A Critical Review of Data. Vol. 1, 496pp, Rotterdam, A.A. Balkema.
- Craig, R.E. (1959). Hydrography of Scottish coastal waters. Mar. Res., 1958 (2).
- Craig, R.E. and Slinn, D.J. (1957). Hydrographic observations off the Scottish west coast and northern Irish Sea, autumn 1955. Annls. Biol. Copenh., 12, 59-63.
- Cross, J.E. and Day, J.P. (1981). Plutonium and americium in seaweed from the Channel Islands. Environ. Pollut., 2B, 249-257.
- Dahlgaard, H., Aarkrog, A., Hallstadius, L., Holm, E. and Rioseco, J. (1984). Radiocaesium transport from the Irish Sea via the North Sea

- and the Norwegian coastal current to East Greenland. Symposium on Contaminant Fluxes through the Coastal Zone, Nantes, May 1984.
- Duursma, E.K. (1976). Radioactive tracers in estuarine chemical studies. In *Estuarine Chemistry*, ed. by J.D. Burton and P.S. Liss, chapter 6, 159-183, London, Academic Press.
- Duursma, E.K. and Eisma, D. (1973). Theoretical, experimental and field studies concerning reactions of radioisotopes with sediments and suspended particles of the sea. Part C: Applications to field studies. Neth. J. Sea Res., 6, 265-324.
- Eastmond, D. (1985). *The Scottish Farmer*, August 17, 1985, p20.
- Edwards, A. (1986). SMBA, Oban, UK. Pers. commⁿ.
- Ellett, D.J. (1978). Temperature and salinity conditions in the Sea of the Hebrides, 25-29 May 1976. Annls. Biol., Copenh., 33, 28-30.
- Ellett, D.J. and Edwards, A. (1983). Oceanography and inshore hydrography of the Inner Hebrides. Proc. R. Soc. Edin., 83B, 143-160.
- Faires, R.A. and Boswell, G.G.J. (1981). *Radioisotope Laboratory Techniques*. 4th edn., London, Butterworths.
- Fearnhead, P.G. (1975). On the formation of fronts by tidal mixing around the British Isles. Deep Sea Res., 22, 311-321.

- Fowler, S., Heyraud, M. and Beasley, T.M. (1975). Experimental studies on plutonium kinetics in marine biota. In *Impacts of Nuclear Releases into the Aquatic Environment*, IAEA-SM-198/23, 157-177, Vienna, IAEA.
- Friedlander, G., Kennedy, G.W. and Miller, J.M. (1964). *Nuclear and Radiochemistry*. 2nd edn., London, Wiley.
- Hallstadius, L., Aarkrog, A., Dahlgaard, H., Holm, E., Boelskifte, S., Duniec, S. and Persson, B. (1986). Plutonium and americium in Arctic waters, the North Sea and Scottish and Irish coastal zones. J. Environ. Radioactivity, (in press).
- Handyside, I., Hunt, G.J. and Partington, C. (1982). Control of radiocaesium discharges to the Irish Sea: ICRP-26 in Practice. In *The Dose Limitation System in the Nuclear Fuel Cycle and in Radiation Protection*, IAEA-SM-258/32, 325-345, Vienna, IAEA.
- Harvey, J. and Buchan, S. (1963). Hydrographic observations in North Channel, Irish Sea. Admiralty Marine Science Publication, No.12, 10pp.
- Hetherington, J.A. (1976a). The behaviour of plutonium nuclides in the Irish Sea. In *Environmental Toxicity of Aquatic Radionuclides: Models and Mechanisms*, ed. by M.W. Miller and J.N Stannard, 81-106, Mich., Ann Arbor Science.
- Hetherington, J.A. (1976b). Radioactivity in surface and coastal waters of the British Isles 1974. Tech. Rep. FRL., MAFF Direct.

- Fish. Res., Lowestoft, 11, 35pp.
- Hetherington, J.A. (1978). The uptake of plutonium nuclides by marine sediments. Mar. Sci. Commun., 4 (3), 239-274.
- Hetherington, J.A. and Harvey, B.R. (1978). Uptake of radioactivity by marine sediments and implications for monitoring metal pollutants. Mar. Poll. Bull., 9, 102-106.
- Hetherington, J.A., Jefferies, D.F. and Lovett, M.B. (1975). Some investigations into the behaviour of plutonium in the marine environment. In Impacts of Nuclear Releases into the Aquatic Environment, IAEA-SM-198/29, 193-212, Vienna, IAEA.
- Hetherington, J.A., Jefferies, D.F., Mitchell, N.T., Pentreath, R.J. and Woodhead, D.S. (1976). Environmental and public health consequences of the controlled disposal of transuranic elements to the marine environment. In Transuranium Nuclides in the Environment, IAEA-SM-199/11, 139-154, Vienna, IAEA.
- Howarth, M.J. (1982). Non-tidal flow in the North Channel of the Irish Sea. In Hydrodynamics of Semi-enclosed Seas, ed. by J.C.J. Nihoul, 205-242, Oxford, Elsevier.
- Hughes, D.G. (1976). A simple method for predicting the occurrence of seasonal stratification and fronts in the North Sea and around the British Isles. ICES, CM 1976/C:1.
- Hunt, G.J. (1983). Radioactivity in surface and coastal waters of the

- British Isles, 1981. Aquat. Environ. Monit. Rep., MAFF Direct. Fish. Res., Lowestoft, (9), 36pp.
- Hunt, G.J. (1984). MAFF, FRL, Lowestoft, UK. Pers. commⁿ.
- Hunt, G.J. (1985). Radioactivity in surface and coastal waters of the British Isles, 1983. Aquat. Environ. Monit. Rep., MAFF Direct. Fish. Res., Lowestoft, (12), 46pp.
- Hunt, G.J. and Jefferies, D.F. (1981). Collective and individual radiation exposure from discharges of radioactive waste to the Irish Sea. IAEA-SM-248/101, 535-570, Vienna, IAEA.
- Hunter, J.R. (1972). An investigation into the circulation of the Irish Sea. Oceanography Report 72-1, U.C.N.W., Marine Science Labs.
- I.A.E.A. (1976). Effects of ionizing radiation on aquatic organisms and ecosystems. Tech. Rep. Ser., No. 172, 131pp, Vienna, IAEA.
- I.C.R.P. (1985). Statement from the 1983 meeting of the International Commission on Radiological Protection. Annal. ICRP 14(1), ICRP Publ. (39), 8pp, Oxford, Pergamon Press.
- Jefferies, D.F. (1986). MAFF, FRL, Lowestoft, UK. Pers. commⁿ.
- Jefferies, D.F., Preston, A and Steele, A.K. (1973). Distribution of Caesium-137 in British coastal waters. Mar. Poll. Bull., 4, 118-122.
- Jefferies, D.F., Steele, A.K. and Preston, A. (1982). Further studies

- on the distribution of ^{137}Cs in British coastal waters - I. Irish Sea. Deep Sea Res., 29 (6a), 713-738.
- Johnston, P. (1983). Marine Biology Station, (Queens University) Portaferry, N.Ireland. Pers. commⁿ.
- Kautsky, H. (1973). The distribution of the radionuclide Caesium-137 as an indicator for North Sea watermass transport. Dt. Hydrogr. Z., 26, 241-246.
- Kautsky, H. (1976). The Caesium-137 content in the water of the North Sea during the years 1969-1975. Dt. Hydrogr. Z., 29, 217-221.
- Kautsky, H. (1985). Distribution and content of different artificial radionuclides in the water of the North Sea during the years 1977 to 1981 (complemented with some results from 1982 to 1984). Dt. Hydrogr. Z., 38, 193-224.
- Kautsky, H. and Eicke, H.F. (1982). Radiological investigations in the western Baltic Sea and the Baltic proper, including the Danish Straits, during 1981. Dt. Hydrogr. Z., 35, 211-221.
- Kautsky, H., Jefferies, D.E. and Steele, A.K. (1980). Results of the Radiological North Sea Programme RANOSP 1974 to 1976. Dt. Hydrogr. Z., 33, 152-157.
- Kershaw, P.J., Swift, D.J., Pentreath, R.J. and Lovett, M.B. (1983). Plutonium redistribution by biological activity in Irish Sea sediments. Nature, 306, 774-775.

- Knudsen, M. (1907). Some remarks about the currents in the North Sea and adjacent waters. *Cons. Int. Explor. Mer., Public. de Circ.*, 39.
- Lally, A.E. and Eakins, J.D. (1978). Some recent advances in environmental analysis at AERE Harwell. in Symposium on the Determination of Radionuclides in Environmental and Biological Materials, CEGB, Sudbury House, 9-10 October, 1978.
- Lee, A. (1960). Hydrographical observations in the Irish Sea, January - March 1953. *Fish. Invest., Lond., Ser. 2*, 23 (2).
- Livingston, H.D. (1981). Woods Hole Oceanographic Institution, Woods Hole, Massachusetts, USA. *Pers. commⁿ*.
- Livingston, H.D. and Anderson, R.F. (1983). Large particle transport of plutonium and other fallout radionuclides to the deep ocean. *Nature*, 303, 228-231.
- Livingston, H.D. and Bowen, V.T. (1977). Windscale effluents in the waters and sediments of the Minch. *Nature*, 269, 586-588.
- Livingston, H.D. and Bowen, V.T. (1979). Pu and ¹³⁷Cs in coastal sediments. *Earth Planet. Sci. Lett.*, 43, 29-45.
- Livingston, H.D., Bowen, V.T. and Kupferman, S.L. (1982a). Radionuclides from Windscale discharges I: nonequilibrium tracer experiments in high-latitude oceanography. *J. Mar. Res.*, 40 (1), 253-272.

- Livingston, H.D., Bowen, V.T. and Kupferman, S.L. (1982b). Radionuclides from Windscale discharges II: Their dispersion in Scottish and Norwegian coastal circulation. J. Mar. Res., 40 (4), 1227-1258.
- Lyman, J. and Fleming, R.H. (1940). Composition of sea water. J. Mar. Res., 3, 134-146.
- MacKenzie, A.B. (1977). A radionuclide study of the Clyde Sea Area. Ph.D. Thesis, University of Glasgow.
- MacKenzie, A.B. (1986). SURRC, East Kilbride, UK. Pers. commⁿ.
- MacKenzie, A.B., Baxter, M.S., McKinley, I.G., Swan, D.S. and Jack, W. (1979). The determination of ^{134}Cs , ^{137}Cs , ^{210}Pb , ^{226}Ra and ^{228}Ra concentrations in nearshore marine sediments and sea water. Journal Radioanalytical Chemistry, 48, 29-47.
- Mauchline, J. (1980). Artificial radioisotopes in the marginal seas of north-western Europe. In *The Northwest European Shelf Seas: The Seabed and the Sea in Motion II. Physical and Chemical Oceanography and Physical Resources*, ed. by F.T. Banner, M.B. Collins and K.S. Massie, Elsevier Oceanography Series 24B, 517-542, Oxford, Elsevier.
- Mauchline, J. and Templeton, W.L. (1964). Artificial and natural radioisotopes in the marine environment. Oceanogr. Mar. Biol. Ann. Rev., 2, 229-279.

- McKay, W.A. (1983). Marine chemistry and tracer applications of radiocaesium. Ph.D. Thesis, Universtiy of Glasgow.
- McKay, W.A. and Baxter, M.S. (1985a). Water transport from the north-east Irish Sea to western Scottish coastal waters: further observations from time-trend matching of Sellafield radiocaesium. Estuar. Coast. Shelf Sci., 21, 471-480.
- McKay, W.A. and Baxter, M.S. (1985b). The partitioning of Sellafield-derived radiocaesium in Scottish coastal sediments. J. Environ. Radioactivity, 2 (2), 93-114.
- McKay, W.A., Baxter, M.S., Ellett, D.J. and Meldrum, D.T. (1986). Radiocaesium and circulation patterns west of Scotland. J. Environ. Radioactivity, (in press).
- McKinley, I.G. (1975). Unpublished data, B.Sc. Thesis, University of Glasgow.
- McKinley, I.G. (1979). Tracer applications of radiocaesium in a coastal marine environment. Ph.D. Thesis, University of Glasgow.
- McKinley, I.G. and Baxter, M.S. (1980). A radiotracer study of water renewal and sedimentation in a Scottish Fjord. Fjord Oceanography, NATO Conference Series, 4, 539-545, New York, Plenum Press.
- McKinley, I.G., Baxter, M.S., Ellett, D.J. and Jack, W. (1981a). Tracer applications of radiocaesium in the Sea of the Hebrides. Estuar. Coast. Shelf Sci., 13, 69-82.

- McKinley, I.G., Baxter, M.S. and Jack, W. (1981b). A simple model of radiocaesium transport from Windscale to the Clyde Sea Area. Estuar. Coast. Shelf Sci., 13, 59-67.
- Mitchell, N.T. (1967). Radioactivity in surface and coastal waters of the British Isles. Tech. Rep. FRL., MAFF Direct. Fish. Res., Lowestoft, 1, 45pp.
- Mitchell, N.T. (1975). Radioactivity in surface and coastal waters of the British Isles 1972-73. Tech. Rep. FRL., MAFF Direct. Fish. Res., Lowestoft, 10, 40pp.
- Mitchell, N.T. (1977). Radioactivity in surface and coastal waters of the British Isles 1976. Part 1: The Irish Sea and its environs. Tech. Rep. FRL., MAFF Direct. Fish. Res., Lowestoft, 13, 15pp.
- Mitchell, N.T. (1983). MAFF, FRL, Lowestoft, UK. Pers. commⁿ.
- Murray, C. N., Murray, L. and Huynh-Ngoc, L. (1973). Var-river sediment interactions of ^{65}Zn , ^{60}Co , ^{51}Cr and ^{110}Ag . In Radioactive Contamination of the Marine Environment, IAEA-SM-158/7, 105-124, Vienna, IAEA.
- Nelson, D.M. and Lovett, M.B. (1978). Oxidation state of plutonium in the Irish Sea. Nature, 276, 599-601.
- Onishi, Y., Serne, R.J., Arnold, E.N., Cowan, C.E. and Thompson, F.L. (1981). Critical review: radionuclide transport, sediment transport

- and water quality mathematical modeling and radionuclide adsorption / desorption mechanisms. PNL-2901, 512pp, Washington, Battelle Pacific Northwest Labs.,
- Perkins, E.J., Bailey, M. and Williams, B.R.H. (1964). The biology of the Solway Firth in relation to the movement and accumulation of radioactive materials VI. General Hydrography, with an appendix on meteorological observations. UKAEA, PG Rep. 604 (CC), 8pp.
- Pentreath, R.J. (1985). Radioactive discharges from Sellafield (UK). In Behaviour of Radionuclides Released into Coastal Waters, ed. by R.J. Pentreath, IAEA-TECDOC-329, Annex 1, 67-110, Vienna, IAEA.
- Pentreath, R.J., Harvey, B.R. and Lovett, M.B. (1985). Chemical speciation of transuranium nuclides discharged into the marine environment. CEC/NRPB Speciation-85 Seminar, Oxford, April 1985.
- Pentreath, R.J., Lovett, M.B., Jefferies, D.F., Woodhead, D.S., Talbot, J.W. and Mitchell, N.T. (1984a). The impact on public radiation exposure of transuranium nuclides discharged in liquid wastes from fuel element reprocessing at Sellafield, U.K. Radioactive Waste Management, 5, 315, Vienna, IAEA.
- Pentreath, R.J., Woodhead, D.S., Kershaw, P.J., Jefferies, D.F. and Lovett, M.B. (1984b). The behaviour of plutonium and americium in the Irish Sea. Proc. ICES Symp. on Contaminant Fluxes through the Coastal Zone, Nantes, No. 21.
- Pingree, R.D., Holligan, P.M. and Mardell, G.T. (1978). The effects of

- vertical stability on phytoplankton distributions in the summer on the northwest European shelf. Deep Sea Res., 25, 1011-1028.
- Prandle, D. (1984). A modelling study of the mixing of ^{137}Cs in the seas of the European continental shelf. Phil. Trans. R. Soc. Lond., 310A, 407-436.
- Preston, A., Jefferies, D.F. and Pentreath, R.J. (1972). The possible contributions of radioecology to marine productivity studies. Symp. zool. Soc. Lond., 29, 271-284.
- Proudman, J. (1939). On the currents in the North Channel of the Irish Sea. Mon. Not. R. Astron. Soc., Geophys. Suppl., 4 (6), 387-403.
- Ramster, J.W. and Hill, H.W. (1969). Current system in the northern Irish Sea. Nature, 224, 59-61.
- Sager, G. and Sammler, R. (1968). Atlas der Gezeitenströme für die Nordsee, den Kanal und die Irische See. 2nd edn., Rostock, Seehydrographischer Dienst der DDR.
- Santschi, P.H., Li, Y.-H., Adler, D.M., Amdurer, M., Bell, J. and Nyffeler, U.P. (1983). The relative mobility of natural (Th, Pb and Po) and fallout (Pu, Am, Cs) radionuclides in the coastal marine environment: results from model ecosystems (MERL) and Narragansett Bay. Geochim. Cosmochim. Acta, 47, 201-210.
- Santschi, P.H., Li, Y.-H., O'Hara, P. and Amdurer, M. (1984). Removal and backdiffusion processes of radiotracers in shallow coastal

marine ecosystems (MERL) of Narragansett Bay, R.I., USA. Symposium on Contaminant Fluxes Through the Coastal Zone, Nantes, May, 1984, No. 51.

Sholkovitz, E.R., Cochran, J.K. and Carey, A.E. (1983). Laboratory studies of the diagenesis and mobility of $^{239,240}\text{Pu}$ and ^{137}Cs in nearshore sediments. Geochim. Cosmochim. Acta, 47, 1369-1379.

Sholkovitz, E.R. and Mann, D.R. (1984). The pore water chemistry of $^{239,240}\text{Pu}$ and ^{137}Cs in sediments of Buzzards Bay, Massachusetts. Geochim. Cosmochim. Acta, 48, 1107-1114.

Simpson, J.H., Edelsten, D.J., Edwards, A., Morris, N.C.G. and Tett, P.B. (1979). The Islay Front: physical structure and phytoplankton distribution. Estuar. Coast. Shelf Sci., 9, 713-726.

Stanners, D.A. and Aston, S.R. (1981a). An improved method of determining sedimentation rates by the use of artificial radionuclides. Estuar. Coast. Shelf Sci., 13, 101.

Stanners, D.A. and Aston, S.R. (1981b). Factors controlling the interactions of ^{137}Cs with suspended and deposited sediments in estuarine and coastal environments. In Impacts of Radionuclide Releases into the Marine Environment, IAEA-SM-248-141, 131-142, Vienna, IAEA.

Stanners, D.A. and Aston, S.R. (1982). Desorption of ^{106}Ru , ^{134}Cs , ^{137}Cs , ^{144}Ce and ^{241}Am from intertidal sediment contaminated by nuclear fuel reprocessing effluents. Estuar. Coast. Shelf Sci., 14,

687-691.

Templeton, W.L. and Preston, A. (1966). Transport and distribution of radioactive effluents in coastal and estuarine waters of the United Kingdom. In *Disposal of Radioactive Wastes into Seas, Oceans and Surface Waters*, IAEA-SM-72/16, 267-289, Vienna, IAEA.

Thompson, N., Cross, J.E., Miller, R.M. and Day, J.P. (1982). Alpha and gamma radioactivity in *Fucus vesiculosus* from the Irish Sea. *Environmental Pollution*, 3B, 11-19.

U.N.S.C.E.A.R., (1981). Environmental Behaviour and Dosimetry of Radionuclides. A/AC.82/R.407, 185pp.

Walton, A. (1983). Marine Biology Station, Port Erin, (University of Liverpool) Isle of Man. Pers. commⁿ.

Williamson, D.I. (1956). Planktonic evidence for irregular flow through the Irish Sea and North Channel in the autumn of 1954. *J. Mar. Biol. Assoc. UK*, 35, 461-466.

Wilson, T.R.S. (1974). Caesium-137 as a water movement tracer in the St. George's Channel. *Nature*, 248, 125-127.

Woodhead, D.S. (1984). Contamination due to radioactive materials. *Marine Ecology*, 5, Ocean Management, Pt. 3, 1111-1287.

APPENDIX I

Radiocaesium Levels in Surface Waters
of Clyde Sea Area and Loch Etive

1.1. Clyde Sea Area

<u>Date</u>	<u>^{137}Cs (dpm/l)</u>	<u>Salinity (‰)</u>	<u>$^{134}\text{Cs}/^{137}\text{Cs}$</u>
11.3.82	51.9 ± 0.5	28.15	0.049 ± 0.004
22.4.82	67.1 ± 0.7	31.45	0.054 ± 0.003
5.5.82	68.8 ± 0.7	32.17	0.047 ± 0.003
4.10.82	42.0 ± 0.4	23.76	0.030 ± 0.004
30.11.82	59.8 ± 0.6	31.00	0.046 ± 0.003
2.12.82	50.8 ± 0.5	26.50	0.043 ± 0.003
27.3.83	37.7 ± 0.4	23.84	0.038 ± 0.003
14.4.83	47.6 ± 0.5	31.72	0.040 ± 0.003
21.4.83	39.1 ± 0.8	30.50	0.047 ± 0.004
12.5.83	37.7 ± 0.4	29.27	0.037 ± 0.004
8.6.83	40.5 ± 0.8	31.79	0.046 ± 0.004
24.6.83	39.8 ± 0.4	30.75	0.036 ± 0.004
25.8.83	43.7 ± 0.6	31.58	0.038 ± 0.004
6.9.83	41.6 ± 0.4	32.36	0.042 ± 0.004
24.10.83	26.6 ± 0.4	21.84	0.038 ± 0.006
22.11.83	34.5 ± 0.5	30.72	0.049 ± 0.004
25.1.84	32.8 ± 0.5	27.12	0.048 ± 0.004
9.2.84	27.0 ± 0.4	28.34	0.047 ± 0.005
9.2.84	33.0 ± 0.5	32.54	0.035 ± 0.004

cont.'d

Clyde Sea Area cont'd.

<u>Date</u>	<u>^{137}Cs (dpm/l)</u>	<u>Salinity (‰)</u>	<u>$^{134}\text{Cs}/^{137}\text{Cs}$</u>
28.2.84	32.8 ± 0.5	26.53	0.048 ± 0.005
15.3.84	31.2 ± 0.5	30.89	0.035 ± 0.005
17.4.84	31.2 ± 0.5	28.16	0.032 ± 0.004
1.5.84	32.0 ± 0.5	31.96	0.046 ± 0.005
27.5.84	32.5 ± 0.5	33.26	0.037 ± 0.004
10.6.84	30.7 ± 0.4	33.81	0.039 ± 0.005
13.6.84	35.7 ± 0.5	31.30	0.044 ± 0.004
21.7.84	37.3 ± 0.5	33.08	0.040 ± 0.004
1.8.84	32.2 ± 0.5	31.94	0.045 ± 0.004
13.9.84	30.4 ± 0.4	32.47	0.036 ± 0.005
11.10.84	29.9 ± 0.4	30.29	0.042 ± 0.005
26.10.84	26.3 ± 0.4	28.39	0.033 ± 0.005
28.11.84	27.7 ± 0.4	29.74	0.038 ± 0.005
18.12.84	22.7 ± 0.3	23.72	0.039 ± 0.006
25.1.85	30.9 ± 0.4	29.69	0.040 ± 0.004
19.2.85	28.7 ± 0.4	28.09	0.033 ± 0.004
28.2.85	31.4 ± 0.4	31.40	0.050 ± 0.003
24.3.85	30.3 ± 0.4	31.67	0.037 ± 0.004
12.4.85	24.1 ± 0.4	26.41	0.045 ± 0.005
8.5.85	24.0 ± 0.4	29.91	0.049 ± 0.005
6.6.85	22.0 ± 0.3	30.48	0.053 ± 0.005
25.6.85	22.9 ± 0.3	30.06	0.039 ± 0.005

I.2. Loch Etive - (Aird's Bay)

<u>Date</u>	<u>^{137}Cs (dpm/l)</u>	<u>Salinity (‰)</u>	<u>$^{134}\text{Cs}/^{137}\text{Cs}$</u>
26.4.83	16.8 \pm 0.5	23.46	0.052 \pm 0.004
2/6/83	17.7 \pm 0.4	27.47	0.041 \pm 0.004
19/7/83	19.5 \pm 0.4	27.90	0.045 \pm 0.003
16.8.83	24.7 \pm 0.5	29.29	0.043 \pm 0.003
26.9.83	23.2 \pm 0.7	28.07	0.039 \pm 0.003
17.11.83	17.9 \pm 0.5	24.88	0.040 \pm 0.004
15.12.83	13.9 \pm 0.4	25.59	0.041 \pm 0.005
24.2.84	10.6 \pm 0.2	24.26	0.044 \pm 0.006
2.4.84	12.4 \pm 0.2	27.63	0.038 \pm 0.007
10.4.84	12.2 \pm 0.2	28.43	0.047 \pm 0.008
18.6.84	14.5 \pm 0.2	29.78	0.056 \pm 0.006

APPENDIX II

Radiocaesium and Salinity Levels in Sea Water
for Research Vessel Cruises

II.1. May 1983 - Surface Samples

<u>Station</u>	<u>^{137}Cs (dpm/l)</u>	<u>$^{134}\text{Cs}/^{137}\text{Cs}$</u>	<u>Salinity (‰)</u>
A1	44.8 ± 0.5	0.045 ± 0.003	33.794
A2	42.9 ± 0.5	0.048 ± 0.004	33.810
A3	46.4 ± 0.5	0.055 ± 0.003	33.716
A4	53.1 ± 0.6	0.063 ± 0.004	33.594
A5	42.3 ± 0.4	0.053 ± 0.004	33.537
B1	39.3 ± 0.4	0.047 ± 0.004	33.720
B2	47.0 ± 0.5	0.053 ± 0.003	33.698
B3	35.5 ± 0.4	0.051 ± 0.004	33.804
B4	35.4 ± 0.4	0.048 ± 0.004	33.822
B5	34.1 ± 0.4	0.046 ± 0.004	33.863
D1	9.1 ± 0.1	0.046 ± 0.008	34.613
D2	35.5 ± 0.4	0.045 ± 0.002	33.912
D3	41.1 ± 0.4	0.044 ± 0.002	33.832
D4	41.8 ± 0.4	0.047 ± 0.002	33.814
D5	43.2 ± 0.4	0.046 ± 0.002	33.791
D6	39.7 ± 0.4	0.046 ± 0.002	33.786
D7	42.2 ± 0.4	0.047 ± 0.002	33.782
D8	41.9 ± 0.4	0.048 ± 0.002	33.808
G1	24.0 ± 0.3	0.045 ± 0.003	33.76
G2	27.4 ± 0.3	0.044 ± 0.003	33.99

II.1. May 1983 - Surface Samples. cont.'d.

<u>Station</u>	<u>^{137}Cs (dpm/l)</u>	<u>$^{134}\text{Cs}/^{137}\text{Cs}$</u>	<u>Salinity (‰)</u>
G3	21.3 ± 0.2	0.051 ± 0.003	34.21
G4	20.8 ± 0.2	0.046 ± 0.003	34.23
G5	19.1 ± 0.2	0.050 ± 0.004	34.358
G6	16.7 ± 0.2	0.052 ± 0.004	34.394
G7	19.0 ± 0.2	0.050 ± 0.004	34.363
G8	24.5 ± 0.3	0.050 ± 0.003	34.186
G9	22.9 ± 0.2	0.050 ± 0.003	34.132
G10	29.5 ± 0.3	0.044 ± 0.002	34.040
G11	27.8 ± 0.3	0.044 ± 0.003	33.98
G12	18.7 ± 0.2	0.046 ± 0.004	34.42
G13	31.4 ± 0.3	0.047 ± 0.003	34.31
G14	25.0 ± 0.3	0.049 ± 0.003	34.238
G14	25.0 ± 0.3	0.049 ± 0.003	34.238
G15	2.0 ± 0.1	B.D.L.	35.189
G16	0.1 ± 0.1	B.D.L.	35.406
J1	8.1 ± 0.1	0.080 ± 0.040	34.856
J2	6.8 ± 0.1	B.D.L.	34.959
J3	5.8 ± 0.1	B.D.L.	35.019
J4	5.5 ± 0.1	B.D.L.	35.065
J5	4.9 ± 0.1	B.D.L.	35.072
J6	1.6 ± 0.1	B.D.L.	35.334
J7	0.4 ± 0.1	B.D.L.	35.394
J8	0.3 ± 0.1	B.D.L.	35.408

cont.'d

II.1. May 1983 - Surface Samples. cont.'d

<u>Station</u>	<u>^{137}Cs (dpm/l)</u>	<u>$^{134}\text{Cs}/^{137}\text{Cs}$</u>	<u>Salinity (‰)</u>
K1	12.4 ± 0.1	0.045 ± 0.006	34.571
K2	12.3 ± 0.1	0.056 ± 0.006	34.555
K3	12.2 ± 0.1	0.042 ± 0.006	34.595
K4	11.2 ± 0.1	0.060 ± 0.010	34.563
K5	10.6 ± 0.1	0.047 ± 0.007	34.578
K6	12.0 ± 0.1	0.051 ± 0.006	34.566
K7	11.9 ± 0.1	0.051 ± 0.006	34.539
K8	10.9 ± 0.1	0.056 ± 0.007	34.585
K9	10.9 ± 0.1	0.070 ± 0.007	34.575
Z1	40.3 ± 0.4	0.052 ± 0.004	33.856
Z2	50.2 ± 0.5	0.055 ± 0.003	33.723
Z3	52.9 ± 0.6	0.051 ± 0.003	33.685
Z4	86.9 ± 0.9	0.056 ± 0.002	33.346
Z5	95.7 ± 1.0	0.034 ± 0.002	33.214
Z6	92.8 ± 0.9	0.055 ± 0.002	33.314
BN1	N.M.	N.M.	34.868
BN2	N.M.	N.M.	34.911
BN3	N.M.	N.M.	35.062
BN4	N.M.	N.M.	35.304
BN5	N.M.	N.M.	35.221
BN6	N.M.	N.M.	35.373
BN7	N.M.	N.M.	35.407
BN8	N.M.	N.M.	35.418
DO	N.M.	N.M.	35.180

II.1 May 1983 - Surface Samples. cont.'d

<u>Station</u>	<u>^{137}Cs (dpm/l)</u>	<u>$^{134}\text{Cs}/^{137}\text{Cs}$</u>	<u>Salinity (‰)</u>
M	N.M.	N.M.	35.433
N	N.M.	N.M.	35.430
O	N.M.	N.M.	35.439
Q	N.M.	N.M.	35.405
S	N.M.	N.M.	35.394
T	N.M.	N.M.	34.904
MOOR A3	N.M.	N.M.	35.412
MOOR HS1	N.M.	N.M.	34.396
MOOR Y	N.M.	N.M.	34.011
MOOR M2	N.M.	N.M.	33.843
MOOR J	N.M.	N.M.	33.883
<u>LAT N</u>	<u>LONG W</u>		
55°42'	6°32'	N.M.	33.787
55°32'	6°22'	N.M.	33.748
55°24'	6°10'	N.M.	33.699
55°16'	6°00'	N.M.	33.819
55°10'	5°49'	N.M.	33.835
55°07'	5°50'	N.M.	33.805
55°05'	5°40'	N.M.	33.677
55°00'	5°47'	N.M.	33.860
55°00'	5°29'	N.M.	33.454
54°53'	5°41'	N.M.	33.877
54°54'	5°21'	N.M.	33.610
54°52'	5°12'	N.M.	33.073

B.D.L. = Below Detection Level

N.M. = Not Measured

II.2a. August 1983 - Surface Samples

<u>Station</u>	<u>^{137}Cs (dpm/l)</u>	<u>$^{134}\text{Cs}/^{137}\text{Cs}$</u>	<u>Salinity (‰)</u>
A1	35.5 ± 1.1	0.074 ± 0.004	33.944
A2	27.3 ± 0.8	0.044 ± 0.009	33.966
A3	21.4 ± 0.7	0.047 ± 0.007	34.221
A4	22.2 ± 0.7	0.044 ± 0.010	34.243
A5	20.3 ± 0.6	0.036 ± 0.007	34.248
B1	32.0 ± 1.0	0.045 ± 0.002	33.784
B2	31.9 ± 1.0	0.044 ± 0.002	33.759
B3	32.2 ± 1.0	0.040 ± 0.002	33.758
B4	29.8 ± 0.9	0.039 ± 0.003	33.785
B5	30.7 ± 0.9	0.044 ± 0.002	33.790
D0	1.1 ± 0.1	0.130 ± 0.070	35.315
D1	0.6 ± 0.1	0.021 ± 0.123	35.316
D2	0.5 ± 0.1	0.005 ± 0.177	35.201
D3	1.9 ± 0.1	0.129 ± 0.080	35.161
D4	21.5 ± 0.3	0.047 ± 0.004	34.226
D5	18.7 ± 0.3	0.048 ± 0.009	34.360
D6	19.9 ± 0.3	0.070 ± 0.009	34.298
D7	22.1 ± 0.3	0.048 ± 0.008	34.217
D8	21.3 ± 0.3	0.048 ± 0.004	34.202
E1	28.0 ± 0.4	0.040 ± 0.003	33.780
E2	27.8 ± 0.4	0.042 ± 0.003	33.762
E3	28.9 ± 0.4	0.047 ± 0.003	33.792
E4	29.7 ± 0.9	0.048 ± 0.003	33.756
E5	27.3 ± 0.4	0.048 ± 0.003	33.705

cont.'d

II.2a. August 1983 - Surface Samples . cont.'d

<u>Station</u>	<u>^{137}Cs (dpm/l)</u>	<u>$^{134}\text{Cs}/^{137}\text{Cs}$</u>	<u>Salinity (‰)</u>
G1	20.3 ± 0.3	0.038 ± 0.004	34.311
G2	19.7 ± 0.3	0.045 ± 0.004	34.320
G3	19.0 ± 0.6	0.049 ± 0.004	34.409
G4	18.0 ± 0.3	0.047 ± 0.005	34.391
G6	20.3 ± 0.6	0.044 ± 0.004	34.346
G7	21.1 ± 0.3	0.040 ± 0.004	34.278
G9	21.5 ± 0.3	0.044 ± 0.004	34.277
G10	19.8 ± 0.3	0.038 ± 0.004	34.288
G11	20.1 ± 0.3	0.046 ± 0.004	34.330
G12	18.2 ± 0.3	0.044 ± 0.005	34.424
G13	11.6 ± 0.2	0.052 ± 0.007	34.632
G14	5.4 ± 0.1	0.070 ± 0.015	34.958
G15	3.0 ± 0.1	0.084 ± 0.023	35.207
G16	0.7 ± 0.1	0.265 ± 0.227	35.359
J1	15.9 ± 0.5	0.048 ± 0.005	34.429
J2	15.4 ± 0.3	0.043 ± 0.004	34.542
J3	15.2 ± 0.5	0.045 ± 0.005	34.586
J4	14.0 ± 0.3	0.048 ± 0.004	34.628
J5	4.5 ± 0.1	0.039 ± 0.013	35.117
J6	0.2 ± 0.1	1.261 ± 0.923	35.404
J7	0.2 ± 0.1	0.568 ± 0.256	35.381
J8	0.1 ± 0.1	1.155 ± 0.630	35.342

cont.'d

II.2a. August 1983 - Surface Samples - cont.'d

<u>Station</u>	<u>^{137}Cs (dpm/l)</u>	<u>$^{134}\text{Cs}/^{137}\text{Cs}$</u>	<u>Salinity (‰)</u>
K1	14.0 ± 0.4	0.042 ± 0.005	34.607
K2	15.6 ± 0.3	0.044 ± 0.004	34.469
K3	14.8 ± 0.3	0.051 ± 0.004	34.541
K4	16.2 ± 0.3	0.048 ± 0.004	34.481
K5	16.4 ± 0.3	0.058 ± 0.004	34.476
K6	15.1 ± 0.3	0.040 ± 0.004	34.503
K7	14.2 ± 0.3	0.051 ± 0.004	34.496
K8	16.1 ± 0.3	0.047 ± 0.004	34.434
K9	16.4 ± 0.3	0.057 ± 0.004	33.840
MOOR J	28.6 ± 0.4	0.041 ± 0.003	33.755
MOOR Y	19.9 ± 0.6	0.045 ± 0.004	34.340
Y1	42.6 ± 1.3	0.041 ± 0.003	33.213
Y2	40.2 ± 1.2	0.046 ± 0.004	33.539
Y3	33.2 ± 1.0	0.046 ± 0.004	33.881
Y4	29.6 ± 0.9	0.044 ± 0.005	33.983
Y5	30.0 ± 0.9	0.043 ± 0.005	33.993
Z1	37.4 ± 0.5	0.042 ± 0.005	33.872
Z2	35.3 ± 0.5	0.038 ± 0.005	33.865
Z3	33.8 ± 0.5	0.041 ± 0.005	33.884
Z4	33.5 ± 0.5	0.062 ± 0.005	33.906
Z5	34.0 ± 0.5	0.040 ± 0.005	33.904
Z6	37.5 ± 0.5	0.050 ± 0.005	33.819

cont.'d

II.2a. August 1983 - Surface Samples. cont.'d

<u>Station</u>	<u>^{137}Cs (dpm/l)</u>	<u>$^{134}\text{Cs}/^{137}\text{Cs}$</u>	<u>Salinity (‰)</u>
a	N.M.	N.M.	35.271
b	N.M.	N.M.	35.284
c	N.M.	N.M.	35.412
d	N.M.	N.M.	35.439
e	N.M.	N.M.	35.466
f	N.M.	N.M.	35.401
g	N.M.	N.M.	35.253
h	N.M.	N.M.	35.261
BN4	N.M.	N.M.	35.063
BN5	N.M.	N.M.	35.396
BN6	N.M.	N.M.	35.102
BN7	N.M.	N.M.	35.414
BN8	N.M.	N.M.	35.383
G5	N.M.	N.M.	34.351
G8	N.M.	N.M.	34.278
L1	N.M.	N.M.	34.321
L2	N.M.	N.M.	34.190
L3	N.M.	N.M.	34.648
L4	N.M.	N.M.	34.633
L5	N.M.	N.M.	34.692
L6	N.M.	N.M.	34.688
M1	N.M.	N.M.	34.604
M2	N.M.	N.M.	34.788
M3	N.M.	N.M.	35.003
M4	N.M.	N.M.	35.282

cont.'d

11.2b. August 1983 - Subsurface Samples

<u>Station</u>	<u>Depth (metres)</u>	<u>^{137}Cs (dpm/l)</u>	<u>$^{134}\text{Cs}/^{137}\text{Cs}$</u>	<u>Salinity (‰)</u>
G7	136	2.0 ± 0.1	0.102 ± 0.042	35.228
J2	50	14.5 ± 0.3	0.046 ± 0.004	34.627
J2	90	8.4 ± 0.2	0.041 ± 0.007	34.926
J3	40	12.7 ± 0.4	0.045 ± 0.005	34.694
K3	60	14.6 ± 0.4	0.041 ± 0.005	34.549

II.2a. August 1983 - Surface Samples. cont.'d

<u>Station</u>	<u>^{137}Cs (dpm/l)</u>	<u>$^{134}\text{Cs}/^{137}\text{Cs}$</u>	<u>Salinity (‰)</u>
M5	N.M.	N.M.	35.356
M6	N.M.	N.M.	35.386
M7	N.M.	N.M.	35.397
MOOR HS1	N.M.	N.M.	34.033
MOOR M2	N.M.	N.M.	34.334
M	N.M.	N.M.	35.386
N	N.M.	N.M.	35.397
O	N.M.	N.M.	35.374
P	N.M.	N.M.	35.436
Q	N.M.	N.M.	35.387
S	N.M.	N.M.	35.234
U	N.M.	N.M.	35.353
V	N.M.	N.M.	35.335
W	N.M.	N.M.	35.395
<u>LAT N LONG W</u>			
58°09' 5°33'	N.M.	N.M.	34.578
58°01' 5°40'	N.M.	N.M.	34.137
57°55' 5°48'	N.M.	N.M.	34.011
57°47' 5°51'	N.M.	N.M.	34.153
58°00' 7°26'	N.M.	N.M.	34.443
57°56' 7°45'	N.M.	N.M.	34.477
57°51' 7°57'	N.M.	N.M.	34.488
57°46' 8°12'	N.M.	N.M.	34.755
56°31' 6°34'	N.M.	N.M.	34.325
56°23' 6°42'	N.M.	N.M.	34.336
56°14' 6°49'	N.M.	N.M.	34.582
55°41' 6°34'	N.M.	N.M.	34.163
55°34' 6°31'	N.M.	N.M.	34.314
55°30' 6°08'	N.M.	N.M.	34.046

II.3 January 1984 - Surface Samples

<u>Station</u>	<u>^{137}Cs (dpm/l)</u>	<u>$^{134}\text{Cs}/^{137}\text{Cs}$</u>	<u>Salinity (‰)</u>
A1	22.9 ± 0.7	0.048 ± 0.006	34.008
A2	25.3 ± 0.8	0.037 ± 0.005	33.884
A3	22.8 ± 0.7	0.043 ± 0.006	34.250
A4	11.2 ± 0.3	0.028 ± 0.011	34.500
A5	11.5 ± 0.4	0.032 ± 0.011	34.493
D1	1.1 ± 0.1	0.085 ± 0.057	35.233
D2	5.9 ± 0.2	0.038 ± 0.011	34.686
D3	8.6 ± 0.3	0.042 ± 0.007	34.809
D4	9.1 ± 0.3	0.038 ± 0.009	34.632
D5	11.0 ± 0.3	0.052 ± 0.008	34.516
D6	14.0 ± 0.4	0.040 ± 0.006	34.345
D7	15.6 ± 0.5	0.039 ± 0.007	34.325
G1	14.8 ± 0.5	0.042 ± 0.006	32.762
G2	13.7 ± 0.4	0.040 ± 0.006	34.425
G3	12.6 ± 0.4	0.034 ± 0.007	34.524
G4	9.5 ± 0.3	0.030 ± 0.009	34.670
G6	7.1 ± 0.2	0.042 ± 0.012	34.811
G7	6.1 ± 0.2	0.032 ± 0.013	34.905
G9	4.1 ± 0.1	0.028 ± 0.020	34.966
G10	5.0 ± 0.2	0.008 ± 0.018	34.918
G11	3.5 ± 0.1	0.050 ± 0.025	35.024
G12	3.0 ± 0.1	0.033 ± 0.029	35.111
G13	3.0 ± 0.1	0.045 ± 0.029	35.062
G14	1.0 ± 0.1	-0.016 ± 0.085	35.204

II.3. January 1984 - Surface Samples. cont.'d

<u>Station</u>	<u>^{137}Cs (dpm/l)</u>	<u>$^{134}\text{Cs}/^{137}\text{Cs}$</u>	<u>Salinity (‰)</u>
G15	0.3 ± 0.1	N.M.	35.323
G16	0.3 ± 0.1	0.003 ± 0.227	35.459
G5	7.6*	N.M.	34.750
G8	5.4*	N.M.	34.897
M	0.25*	N.M.	35.408
N	0.2*	N.M.	35.411
n	0.2*	N.M.	35.416
o	0.15*	N.M.	35.437
p	0.1*	N.M.	35.445
q	0.1*	N.M.	35.443
S	0.1*	N.M.	35.442

LAT N LONG W

57°09'	6°46'	11.8*	N.M.	34.484
56°58'	6°37'	13.3*	N.M.	34.411
56°47'	6°23'	N.M.	N.M.	33.965
56°36'	6°29'	13.2*	N.M.	34.416
56°24'	6°45'	13.6*	N.M.	34.400
56°15'	6°52'	6.9*	N.M.	34.791

N.M. = Not Measured

* = Extrapolated from ^{137}Cs /Salinity curve.

II.4a. April/May 1984 - Surface Samples

<u>Station</u>	<u>^{137}Cs (dpm/l)</u>	<u>$^{134}\text{Cs}/^{137}\text{Cs}$</u>	<u>Salinity (‰)</u>
A1	31.5 ± 0.5	0.053 ± 0.005	33.455
A2	32.3 ± 0.5	0.043 ± 0.004	33.698
A3	26.4 ± 0.4	0.052 ± 0.005	33.940
A4	27.3 ± 0.4	0.044 ± 0.005	33.931
A5	27.1 ± 0.4	0.041 ± 0.005	33.935
B1	30.5 ± 0.9	0.040 ± 0.004	33.769
B2	26.8 ± 0.8	0.050 ± 0.005	33.789
B3	26.0 ± 0.8	0.043 ± 0.005	33.806
B4	25.4 ± 0.8	0.045 ± 0.005	33.826
B5	23.7 ± 0.7	0.040 ± 0.005	33.838
E1	18.6 ± 0.3	0.051 ± 0.008	33.887
E2	17.2 ± 0.3	0.051 ± 0.008	33.858
E4	19.0 ± 0.3	0.064 ± 0.008	33.867
E5	16.1 ± 0.2	0.040 ± 0.009	33.542
E3	N.M.	N.M.	33.876
G1	15.5 ⁺	N.M.	33.989
G2	17.6 ⁺	N.M.	34.068
G4	11.3 ⁺	N.M.	34.503
G6	11.9 ⁺	N.M.	34.500

⁺ Extrapolated from Maff Data.

N.M. = Not Measured

II.4b. April/May 1984 - Subsurface Samples

<u>Station</u>	<u>Depth (metres)</u>	<u>^{137}Cs (dpm/l)</u>	<u>$^{134}\text{Cs}/^{137}\text{Cs}$</u>	<u>Salinity (‰)</u>
G1	10	17.6 ⁺	N.M.	N.M.
G1	30	17.0 ⁺	N.M.	N.M.
G1	70	17.0 ⁺	N.M.	34.124
G2	25	18.1 ⁺	N.M.	34.139
G4	75	9.8 ⁺	N.M.	N.M.
G4	100	7.2 ⁺	N.M.	34.775
G6	10	11.9 ⁺	N.M.	34.512
G6	30	9.8 ⁺	N.M.	34.619

N.M. = Not Measured

+ = Extrapolated from Maff Data

II.5a. June/July 1984 - Surface Samples

<u>Station</u>	<u>^{137}Cs (dpm/l)</u>	<u>$^{134}\text{Cs}/^{137}\text{Cs}$</u>	<u>Salinity (‰)</u>
A1	25.8 ± 0.4	0.056 ± 0.005	33.894
A2	26.1 ± 0.4	0.064 ± 0.005	33.923
A3	27.1 ± 0.4	0.056 ± 0.005	33.849
A4	23.5 ± 0.4	0.043 ± 0.006	34.083
A5	19.2 ± 0.3	0.067 ± 0.007	34.212
B1	23.2 ± 0.3	0.051 ± 0.006	33.873
B2	23.0 ± 0.3	0.045 ± 0.006	33.907
B3	22.5 ± 0.3	0.044 ± 0.006	33.907
B4	22.2 ± 0.3	0.050 ± 0.006	33.898
B5	22.4 ± 0.3	0.050 ± 0.006	33.928
D0	0.3 ± 0.1	0.434 ± 0.275	35.388
D1	0.3 ± 0.1	0.223 ± 0.322	35.339
D2	0.3 ± 0.1	0.424 ± 0.316	35.335
D3	0.3 ± 0.1	0.447 ± 0.232	35.183
D4	0.5 ± 0.1	0.277 ± 0.248	35.064
D5	19.3 ± 0.3	0.030 ± 0.007	34.237
D6	21.8 ± 0.3	0.031 ± 0.007	34.099
D8	22.7 ± 0.3	0.067 ± 0.008	34.081
E1	18.4 ± 0.6	0.037 ± 0.004	33.953
E2	19.6 ± 0.6	0.045 ± 0.004	33.944
E3	21.3 ± 0.6	0.052 ± 0.004	33.957
E4	19.7 ± 0.6	0.043 ± 0.005	33.942
E5	18.4 ± 0.6	0.046 ± 0.005	34.091

cont. id

II.5a. June/July 1984 - Surface Samples. cont.'d

<u>Station</u>	<u>^{137}Cs (dpm/l)</u>	<u>$^{134}\text{Cs}/^{137}\text{Cs}$</u>	<u>Salinity (‰)</u>
G9	5.7 ± 0.1	0.027 ± 0.015	34.932
G11	7.2 ± 0.1	0.053 ± 0.014	34.825
J1	6.0 ± 0.2	0.058 ± 0.009	34.803
J2	4.3 ± 0.1	0.043 ± 0.016	35.145
J4	4.7 ± 0.1	0.050 ± 0.012	35.006
J5	2.7 ± 0.1	B.D.L.	35.146
J6	2.2 ± 0.1	0.036 ± 0.019	35.209
J8	0.2 ± 0.1	0.060 ± 0.498	35.435
K1	6.8 ± 0.2	0.040 ± 0.009	34.785
K2	8.1 ± 0.2	0.042 ± 0.006	34.721
K3	7.7 ± 0.2	0.049 ± 0.008	34.661
K4	8.6 ± 0.3	0.043 ± 0.007	34.627
K6	8.0 ± 0.2	B.D.L.	34.603
K8	9.3 ± 0.3	0.057 ± 0.007	34.405
W1	44.1 ± 0.7	0.048 ± 0.005	33.667
W2	43.1 ± 0.6	0.051 ± 0.005	33.712
W3	44.0 ± 0.6	0.047 ± 0.005	33.610
W4	50.6 ± 0.7	0.054 ± 0.004	33.567
W5	45.9 ± 0.7	0.047 ± 0.005	33.600
T1	19.5 ± 0.3	0.047 ± 0.010	34.09
T2	25.3 ± 0.4	0.052 ± 0.008	33.99
T3	24.5 ± 0.4	0.054 ± 0.007	34.02
T4	17.7 ± 0.3	0.063 ± 0.012	34.17
T5	17.4 ± 0.3	0.049 ± 0.008	34.15
T6	21.0 ± 0.3	0.050 ± 0.009	34.08

11.5a. June/July 1984 - Surface Samples. cont.'d

<u>Station</u>	<u>^{137}Cs (dpm/l)</u>	<u>$^{134}\text{Cs}/^{137}\text{Cs}$</u>	<u>Salinity (‰)</u>
Y1	29.0 ± 0.9	0.038 ± 0.004	33.765
Y2	32.3 ± 1.0	0.050 ± 0.005	33.538
Y3	33.6 ± 1.0	0.041 ± 0.004	33.330
Y4	30.7 ± 0.9	0.036 ± 0.004	33.654
Y5	27.1 ± 0.4	0.043 ± 0.006	33.866
Z1	27.6 ± 0.4	0.042 ± 0.005	33.910
Z2	27.7 ± 0.4	0.044 ± 0.005	33.918
Z3	29.1 ± 0.4	0.036 ± 0.005	33.923
Z4	30.0 ± 0.5	0.049 ± 0.008	33.923
Z5	33.4 ± 0.5	0.045 ± 0.006	33.885
Z6	30.9 ± 0.5	0.039 ± 0.005	33.919
BN2	4.7*	N.M.	34.998
BN3	5.6*	N.M.	34.913
BN4	3.6*	N.M.	35.098
BN5	3.5*	N.M.	35.101
BN6	0.4*	N.M.	35.394
BN7	0.1*	N.M.	35.421
BN8	0.3*	N.M.	35.405
BN9	0.1*	N.M.	35.417
D7	21.0 ⁺	N.M.	34.120
G1	16.5 ⁺	N.M.	34.212
G2	16.5*	N.M.	34.309
G3	12.7*	N.M.	34.466
G4	11.3 ⁺	N.M.	34.571

11.5a. June/July 1984 - Surface Samples - cont.'d

<u>Station</u>	<u>^{137}Cs (dpm/l)</u>	<u>$^{134}\text{Cs}/^{137}\text{Cs}$</u>	<u>Salinity (‰)</u>
G5	10.5 [*]	N.M.	34.587
G6	4.7 ⁺	N.M.	34.994
G7	7.7 ⁺	N.M.	34.980
G8	10.4 [*]	N.M.	34.595
G10	6.6 [*]	N.M.	34.840
G12	6.2 [*]	N.M.	34.884
G13	7.2 ⁺	N.M.	34.818
G14	6.0 [*]	N.M.	35.006
G15	0.4 ⁺	N.M.	35.353
G16	0.3 ⁺	N.M.	35.393
J3	5.2 [*]	N.M.	34.976
J7	0.2 [*]	N.M.	35.424
K5	8.8 [*]	N.M.	34.597
K7	10.0 [*]	N.M.	34.504
K9	9.8 [*]	N.M.	34.375
L1	9.6 [*]	N.M.	34.250
L2	7.7 [*]	N.M.	34.662
L3	7.7 [*]	N.M.	34.663
L4	7.5 [*]	N.M.	34.710
L5	8.0 [*]	N.M.	34.652
L6	6.1 [*]	N.M.	34.855
M1	N.M.	N.M.	33.394
M2	5.0 [*]	N.M.	34.860
M3	2.2 [*]	N.M.	35.225

cont.'d

II.5a June/July 1984 - Surface Samples - cont.'d

<u>Station</u>	<u>^{137}Cs (dpm/l)</u>	<u>$^{134}\text{Cs}/^{137}\text{Cs}$</u>	<u>Salinity (‰)</u>
M4	0.2*	N.M.	35.410
M5	0.1*	N.M.	35.414
M6	0.3*	N.M.	35.396
M7	0.3*	N.M.	35.396
M8	0.6*	N.M.	35.386
M9	N.M.	N.M.	35.386
O	0.3*	N.M.	35.397
P	0.1*	N.M.	35.443
Q	0.2*	N.M.	35.405
S	0.7*	N.M.	35.379
T	5.7*	N.M.	34.916
X1	23.5*	N.M.	34.048
X2	31.4*	N.M.	33.884
X3	36.8*	N.M.	33.804
X4	34.0*	N.M.	33.854
X5	34.8*	N.M.	33.837

LAT N LONG W

58°53'	8°00'	0.7*	N.M.	35.376
58°42'	8°26'	0.6*	N.M.	35.389
58°10'	5°35'	8.9*	N.M.	34.431
58°01'	5°41'	6.2*	N.M.	34.865
57°39'	9°59'	0.1*	N.M.	35.433
57°33'	6°51'	9.0*	N.M.	34.675
57°19'	7°03'	9.2*	N.M.	34.655

N.M. = Not Measured

* = Extrapolated from ^{137}Cs /Salinity Curve

† = Extrapolated from NAFF data

II.5b. June/July 1984 - Subsurface Samples

<u>Station</u>	<u>Depth (metres)</u>	<u>^{137}Cs (dpm/l)</u>	<u>$^{134}\text{Cs}/^{137}\text{Cs}$</u>	<u>Salinity (‰)</u>
A2	50	24.8 ± 0.4	0.052 ± 0.006	33.940 ^(*)
A2	100	23.3 ± 0.3	0.051 ± 0.006	34.045
A4	100	18.8 ± 0.3	0.061 ± 0.009	34.221
B2	30	21.5 ± 0.3	0.047 ± 0.007	33.915 ^(*)
B2	60	23.3 ± 0.3	0.047 ± 0.006	33.917
B4	50	21.3 ± 0.3	0.055 ± 0.007	33.903 ^(*)
B4	112	24.2 ± 0.4	0.051 ± 0.006	33.907
D2	40	0.5 ± 0.1	0.221 ± 0.250	35.050
D4	40	1.8 ± 0.1	0.157 ± 0.087	35.011
D7	40	20.7 ± 0.3	0.075 ± 0.008	34.125
E3	80	19.0 ± 0.6	0.049 ± 0.004	33.982
J2	40	4.0 ± 0.1	0.072 ± 0.011	35.100 ^(*)
J2	60	3.8 ± 0.1	0.018 ± 0.013	35.065 ^(*)
J2	80	3.8 ± 0.1	0.042 ± 0.009	35.077
K2	100	7.8 ± 0.2	0.048 ± 0.006	34.738
W2	55	39.2 ± 0.6	0.040 ± 0.005	33.732
W4	55	46.3 ± 0.7	0.047 ± 0.004	33.561
Y2	40	28.6 ± 0.9	0.040 ± 0.005	33.857 ^(*)
Y4	60	28.4 ± 0.9	0.040 ± 0.004	33.838 ^(*)
Z2	50	25.7 ± 0.4	0.057 ± 0.007	33.95 ^(*)
Z2	100	26.3 ± 0.4	0.051 ± 0.007	33.937
Z4	100	25.1 ± 0.4	0.048 ± 0.008	33.98 ^(*)
Z4	200	22.7 ± 0.4	0.059 ± 0.010	34.00 ^(*)

cont.'d

Il.5b. June/July 1984 - Subsurface Samples. cont.'d

<u>Station</u>	<u>Depth (metres)</u>	<u>^{137}Cs (dpm/l)</u>	<u>$^{134}\text{Cs}/^{137}\text{Cs}$</u>	<u>Salinity (‰)</u>
G1	25	15.0 ⁺	N.M.	34.237 ^(*)
G1	55	15.0 ⁺	N.M.	34.263
G2	20	16.5 ⁺	N.M.	34.305
G2	40	16.5 ⁺	N.M.	34.302
G4	30	10.3 ⁺	N.M.	34.620 ^(*)
G4	75	6.7 ⁺	N.M.	34.920 ^(*)
G6	30	5.6 ⁺	N.M.	34.994
G7	60	7.7 ⁺	N.M.	35.020 ^(*)
G7	130	0.8 ⁺	N.M.	35.321
G9	75	0.04 ⁺	N.M.	35.390 ^(*)
G9	150	0.1 ⁺	N.M.	35.413
G11	30	7.2 ⁺	N.M.	34.828 ^(*)
G11	60	6.7 ⁺	N.M.	34.892
G13	40	5.1 ⁺	N.M.	34.970 ^(*)
G13	100	2.2 ⁺	N.M.	35.200 ^(*)
G15	100	0.4 ⁺	N.M.	35.369
G16	125	0.1 ⁺	N.M.	35.420

N.M. = Not Measured

+ = Extrapolated from Maff Data

(*) = Extrapolated from CTD Profile

11.6a. November 1984 - Surface Samples

<u>Station</u>	<u>^{137}Cs (dpm/l)</u>	<u>$^{134}\text{Cs}/^{137}\text{Cs}$</u>	<u>Salinity (‰)</u>
A1	30.5 ± 0.4	0.038 ± 0.003	32.820
A2	28.4 ± 0.4	0.034 ± 0.003	33.659
A3	27.6 ± 0.4	0.038 ± 0.003	33.970
A4	21.5 ± 0.3	0.044 ± 0.006	34.110
A5	23.3 ± 0.3	0.038 ± 0.004	34.091
B1	30.5 ± 0.4	0.041 ± 0.003	33.708
B2	27.8 ± 0.4	0.038 ± 0.003	33.797
B3	27.5 ± 0.4	0.046 ± 0.005	33.842
B4	21.1 ± 0.3	0.041 ± 0.008	33.971
B5	20.9 ± 0.3	0.044 ± 0.005	33.951
E1	13.9 ± 0.2	0.040 ± 0.005	34.025
E2	13.2 ± 0.2	0.042 ± 0.005	34.027
E3	13.1 ± 0.2	0.041 ± 0.005	34.018
E4	13.5 ± 0.2	0.030 ± 0.005	34.019
E5	13.4 ± 0.2	0.037 ± 0.005	34.033
F1	27.3 ± 0.4	0.037 ± 0.004	33.912
F2	24.9 ± 0.4	0.039 ± 0.004	33.988
F3	26.1 ± 0.4	0.038 ± 0.006	33.942
F4	28.5 ± 0.4	0.042 ± 0.005	33.861
F5	26.7 ± 0.4	0.043 ± 0.003	33.280
K1	6.2 ± 0.1	0.088 ± 0.011	34.655
K2	6.8 ± 0.1	0.036 ± 0.010	34.690
K3	6.2 ± 0.1	0.045 ± 0.010	34.680
K4	5.6 ± 0.1	0.055 ± 0.012	34.679

II.6a. November 1984 - Surface Samples. cont.'d

<u>Station</u>	<u>^{137}Cs (dpm/l)</u>	<u>$^{134}\text{Cs}/^{137}\text{Cs}$</u>	<u>Salinity (‰)</u>
K5	6.4 ± 0.1	0.066 ± 0.010	34.615
K6	6.3 ± 0.1	0.060 ± 0.011	34.617
K7	7.0 ± 0.1	0.052 ± 0.010	34.549
K8	7.0 ± 0.1	0.045 ± 0.009	34.561
K9	7.6 ± 0.1	0.045 ± 0.009	34.298
W1	100.1 ± 1.4	0.055 ± 0.001	31.929
W2	65.9 ± 0.9	0.054 ± 0.001	33.337
W3	51.3 ± 0.7	0.046 ± 0.002	33.683
W4	43.4 ± 0.6	0.041 ± 0.002	33.739
W5	30.5 ± 0.4	0.033 ± 0.003	33.845
X1	22.8 ± 0.7	0.035 ± 0.003	33.862
X2	23.5 ± 0.7	0.037 ± 0.003	33.880
X3	43.8 ± 1.3	0.047 ± 0.002	33.639
X4	68.1 ± 1.0	0.049 ± 0.002	33.108
X5	49.5 ± 0.7	0.049 ± 0.002	33.445
Y1	42.6 ± 1.3	0.049 ± 0.002	33.790
Y2	34.9 ± 1.1	0.042 ± 0.002	33.869
Y3	35.6 ± 1.1	0.039 ± 0.002	33.876
Y4	33.6 ± 1.0	0.041 ± 0.002	33.889
Y5	29.0 ± 0.9	0.037 ± 0.002	33.439
Z1	32.3 ± 1.0	0.040 ± 0.002	33.857
Z2	34.5 ± 1.0	0.039 ± 0.002	33.859
Z3	48.3 ± 1.5	0.046 ± 0.001	33.553
Z4	48.7 ± 1.5	0.046 ± 0.001	33.544

cont.'d

II.6a. November 1984 - Surface Samples . cont.'d

<u>Station</u>	<u>^{137}Cs (dpm/l)</u>	<u>$^{134}\text{Cs}/^{137}\text{Cs}$</u>	<u>Salinity (‰)</u>
Z5	44.5 ± 1.3	0.046 ± 0.002	33.687
Z6	52.6 ± 1.6	0.053 ± 0.001	33.535
G1	10.9 ⁺	N.M.	33.692
G2	11.6 ⁺	N.M.	34.360
G4	5.5 ⁺	N.M.	34.779
G5	N.M.	N.M.	34.815
G6	5.3 ⁺	N.M.	34.856
G7	0.4 ⁺	N.M.	35.073
G8	N.M.	N.M.	35.067
G9	1.7 ⁺	N.M.	35.048
G10	3.5*	N.M.	34.934
G11	2.8 ⁺	N.M.	34.962
G12	N.M.	N.M.	35.114
G13	1.2 ⁺	N.M.	35.158
G14	N.M.	N.M.	35.183
G15	0.7 ⁺	N.M.	35.191
G16	0.09 ⁺	N.M.	35.292
L1	7.4*	N.M.	34.402
L2	7.3*	N.M.	34.411
L3	7.2*	N.M.	34.549
L4	7.0*	N.M.	34.576
L5	6.5*	N.M.	34.606
L6	N.M.	N.M.	34.596

II.6a November 1984 - Surface Samples. cont.'d

<u>Station</u>	<u>^{137}Cs (dpm/l)</u>	<u>$^{134}\text{Cs}/^{137}\text{Cs}$</u>	<u>Salinity (‰)</u>
S	N.M.	N.M.	35.277
s	N.M.	N.M.	33.422
T	1.2 ⁺	N.M.	35.158
t	N.M.	N.M.	33.440
<u>LAT N</u>	<u>LONG W</u>		
55°32'	5°25'	N.M.	32.769
55°26'	5°02'	N.M.	32.750
55°18'	5°29'	21.6*	32.697
55°16'	5°09'	25.0*	33.023

* Extrapolated from ^{137}Cs /Salinity Curves

+ Extrapolated from Maff Data

II.6b. November 1984 - Subsurface Samples.

<u>Station</u>	<u>Depth (metres)</u>	^{137}Cs (dpm/l)	$^{134}\text{Cs}/^{137}\text{Cs}$	<u>Salinity (‰)</u>
A2	120	27.6 ± 0.4	0.039 ± 0.003	33.749
A4	125	23.5 ± 0.3	0.051 ± 0.004	34.124
K2	100	5.9 ± 0.1	0.045 ± 0.011	34.693
K8	140	6.8 ± 0.1	0.042 ± 0.009	34.561
W2	40	63.1 ± 0.9	0.048 ± 0.002	33.556
W4	30	33.9 ± 0.5	0.045 ± 0.003	33.780
X4	55	30.2 ± 0.4	0.038 ± 0.003	33.906
Z2	49	33.3 ± 1.0	0.039 ± 0.002	33.859 ^(*)
Z2	98	33.8 ± 1.0	0.041 ± 0.002	33.859 ^(*)
Z3	70	41.9 ± 1.3	0.041 ± 0.001	33.753 ^(*)
Z3	140	36.0 ± 1.1	0.042 ± 0.002	33.839 ^(*)
Z4	130	37.5 ± 1.1	0.045 ± 0.002	33.852 ^(*)
Z4	260	34.3 ± 1.0	0.048 ± 0.002	33.855
Z5	60	41.6 ± 1.3	0.041 ± 0.002	33.750 ^(*)
Z5	120	38.5 ± 1.2	0.044 ± 0.002	33.775 ^(*)
G1	60	10.7 ⁺	N.M.	34.221 ^(x)
G1	130	10.2 ⁺	N.M.	34.260 ^(*)
G2	30	11.3 ⁺	N.M.	34.356
G4	80	5.8 ⁺	N.M.	34.776 ^(*)
G6	25	4.9 ⁺	N.M.	34.864
G7	65	0.3 ⁺	N.M.	35.078 ^(*)
G7	130	0.4 ⁺	N.M.	35.082

cont.'d

II.6b. November 1984 - Subsurface Samples. cont.'d.

<u>Station</u>	<u>Depth (metres)</u>	<u>^{137}Cs (dpm/l)</u>	<u>$^{134}\text{Cs}/^{137}\text{Cs}$</u>	<u>Salinity (‰)</u>
G9	70	0.5 ⁺	N.M.	35.087(*)
G9	145	0.6 ⁺	N.M.	35.132(*)
G11	25	2.6 ⁺	N.M.	34.988(*)
G11	50	2.5 ⁺	N.M.	34.992
G15	120	0.4 ⁺	N.M.	35.241
G16	125	0.1 ⁺	N.M.	35.365

N.M. = Not Measured

+ = Extrapolated from Maff Data

(*) = Extrapolated from CTD Profile

11.7a. February 1985 - Surface Samples

<u>Station</u>	<u>^{137}Cs (dpm/l)</u>	<u>$^{134}\text{Cs}/^{137}\text{Cs}$</u>	<u>Salinity (‰)</u>
Z1	28.8 ± 0.4	0.052 ± 0.004	33.917
Z2	28.0 ± 0.4	0.049 ± 0.005	33.959
Z3	26.3 ± 0.4	0.041 ± 0.005	34.065
Z4	31.8 ± 0.5	0.042 ± 0.003	33.943
Z5	35.9 ± 0.5	0.044 ± 0.004	33.794
Z6	29.7 ± 0.4	0.045 ± 0.004	33.943

II.7b. February 1985 - Subsurface Samples

<u>Station</u>	<u>Depth (metres)</u>	<u>^{137}Cs (dpm/l)</u>	<u>$^{134}\text{Cs}/^{137}\text{Cs}$</u>	<u>Salinity (‰)</u>
Z2	50	26.7 ± 0.4	0.036 ± 0.005	34.020
Z2	85	19.6 ± 0.3	0.035 ± 0.007	34.269
Z3	75	16.5 ± 0.3	0.046 ± 0.009	34.385
Z3	150	15.2 ± 0.2	0.042 ± 0.009	34.428
Z4	100	13.7 ± 0.2	0.040 ± 0.010	34.422
Z4	185	13.2 ± 0.2	0.036 ± 0.010	34.459
Z5	70	23.6 ± 0.4	0.050 ± 0.006	33.960
Z5	140	30.2 ± 0.4	0.053 ± 0.005	34.223

Il.8 May 1982 - Surface Samples

<u>Station</u>	<u>^{137}Cs (dpm/l)</u>	<u>$^{134}\text{Cs}/^{137}\text{Cs}$</u>	<u>Salinity (‰)</u>
1	22.2 ± 0.2	0.045 ± 0.006	34.50
2	22.6 ± 0.2	0.045 ± 0.006	34.28
3	17.7 ± 0.2	0.055 ± 0.007	34.56
4	16.1 ± 0.2	0.049 ± 0.008	34.66
5	9.1 ± 0.1	0.013 ± 0.014	35.06
7	11.0 ± 0.1	0.021 ± 0.011	34.91
8	4.1 ± 0.1	0.041 ± 0.030	35.22
9	17.9 ± 0.2	0.050 ± 0.007	34.67
10	18.3 ± 0.2	0.047 ± 0.007	34.65
11	1.3 ± 0.1	B.D.L.	35.34
12	2.4 ± 0.1	0.004 ± 0.051	35.29
14	0.2 ± 0.1	0.014 ± 0.510	35.39
15	0.2 ± 0.1	0.014 ± 0.516	35.50
16	0.3 ± 0.1	0.493 ± 0.489	35.35
17	0.4 ± 0.1	0.217 ± 0.319	34.95
18	0.7 ± 0.1	0.429 ± 0.432	34.87
19	28.8 ± 0.3	0.054 ± 0.004	34.18
20	9.8 ± 0.1	0.058 ± 0.017	34.76
21	16.4 ± 0.2	0.039 ± 0.007	34.69
22	27.3 ± 0.3	0.041 ± 0.004	34.14
23	24.7 ± 0.3	0.053 ± 0.005	34.31
24	14.0 ± 0.2	0.046 ± 0.008	34.71
25	0.2 ± 0.1	0.186 ± 0.554	35.38
26	0.2 ± 0.1	0.388 ± 0.672	35.40

11.8 May 1982 - Surface Samples. cont.'d

<u>Station</u>	<u>^{137}Cs (dpm/l)</u>	<u>$^{134}\text{Cs}/^{137}\text{Cs}$</u>	<u>Salinity (‰)</u>
27	1.8 ± 0.1	0.029 ± 0.064	35.29
28	15.4 ± 0.2	0.030 ± 0.008	34.61
29	15.1 ± 0.2	0.053 ± 0.008	34.61
30	8.5 ± 0.1	0.071 ± 0.014	34.97
31	1.8 ± 0.1	0.156 ± 0.092	35.31
32	0.2 ± 0.1	0.531 ± 0.458	35.33
33	0.2 ± 0.1	0.571 ± 0.573	35.33
34	5.0 ± 0.1	0.071 ± 0.024	35.14
35	9.6 ± 0.1	0.029 ± 0.013	34.86
37	0.2 ± 0.1	0.067 ± 0.675	35.37
38	1.9 ± 0.1	0.033 ± 0.066	35.30
39	5.8 ± 0.1	0.045 ± 0.022	35.14
40	11.6 ± 0.1	0.048 ± 0.011	34.76
41	0.5 ± 0.1	0.135 ± 0.270	35.38
42	5.4 ± 0.1	B.D.L.	35.07
43	13.8 ± 0.2	0.037 ± 0.009	34.65
44	21.7 ± 0.2	0.039 ± 0.006	34.20
45	10.6 ± 0.1	0.054 ± 0.011	34.82
46	19.2 ± 0.2	0.042 ± 0.007	34.52
47	18.1 ± 0.2	0.037 ± 0.007	34.40
48	20.3 ± 0.2	0.029 ± 0.006	34.40
49	9.2 ± 0.1	0.003 ± 0.013	35.38
51	18.3 ± 0.2	0.021 ± 0.007	34.10
52	44.6 ± 0.5	0.042 ± 0.003	34.00

APPENDIX IIIEnvironmental Appearance Factors (Ea).

III.1. For Sellafield to the CSA for Transit Times
4.5 - 5.1 months. (mBq⁻¹/TBqdy⁻¹) .

<u>Date</u>	<u>Ea - 4.5 months</u>	<u>Ea - 5.1 months</u>
<u>1981</u>		
Nov.	0.215	0.230
Dec.	0.244	0.244
<u>1982</u>		
Jan.	0.217	N.A.
Feb.	N.A.	N.A.
Mar.	N.A.	N.A.
Apr.	N.A.	N.A.
May	0.196	0.196
June	0.178	0.186
July	0.185	0.185
Aug.	0.173	N.A.
Sept.	N.A.	N.A.
Oct.	0.169	0.169
Nov.	0.133	0.125
Dec.	0.165	0.159
<u>1983</u>		
Jan.	0.165	0.164
Feb.	0.164	0.164
Mar.	0.163	0.168

III.1. cont.'d.

<u>Date</u>	<u>Ea - 4.5 months</u>	<u>Ea - 5.1 months</u>
<u>1983</u>		
April	0.239	0.231
May	0.285	0.281
June	0.193	0.183
July	0.199	N.A.
Aug.	0.188	0.188
Sept.	0.155	0.148
Oct.	0.196	0.187
Nov.	0.348	0.364
Dec.	0.555	0.523
<u>1984</u>		
Jan.	0.330	0.336
Feb.	0.508	0.532
Mar.	0.799	0.755
Apr.	0.729	0.702
May	0.535	0.541
June	0.643	0.635
July	0.608	0.616
Aug.	0.501	0.523
Sept.	0.304	0.299
Oct.	0.318	0.309
Nov.	0.434	0.423
Dec.	0.450	0.421
<u>1985</u>		
Jan.	0.365	0.351
Feb.	0.321	0.326

N.A. = Not Available

III.2

Ea's for Loch Etive for Transit Times
 5.7 - 7.1 months ($\text{Bq l}^{-1}/\text{Tbq day}^{-1}$)

	<u>Month of Discharge</u>	<u>Ea - 5.7 months lag</u>	<u>Ea - 7.1 months lag</u>
<u>1982</u>	Sep.	N.D.	0.078
	Oct.	N.D.	0.071
	Nov.	0.066	N.D.
	Dec.	0.082	0.089
<u>1983</u>	Jan.	0.092	0.112
	Feb.	0.110	0.108
	Mar.	N.D.	N.D.
	Apr.	0.153	0.133
	May	0.167	0.126
	Jun.	0.092	N.D.
	Jul.	N.D.	0.080
	Aug.	N.D.	0.071
	Sep.	0.060	0.059
	Oct.	0.083	N.D.
	Nov.	N.D.	0.165
	Dec.	0.265	N.D.
<u>1984</u>	Jan.	N.D.	N.D.
	Feb.	N.D.	N.D.
	Mar.	N.D.	N.D.

N.D. = No data available for this month

111.3

Ea's for Transect Z for Transit Times
 0.4 - 2.4 months ($\text{Bq l}^{-1}/\text{TBq day}^{-1}$)

<u>Month of Discharge</u>		<u>Ea - 0.4 months lag</u>	<u>Ea - 2.4 months lag</u>
<u>1983</u>	Mar.	N.D.	0.165*
	Apr.	N.D.	N.D.
	May	0.305*	0.248
	Jun.	N.D.	N.D.
	Jul.	0.196	N.D.
	Aug.	N.D.	N.D.
	Sep.	N.D.	N.D.
	Oct.	N.D.	N.D.
	Nov.	N.D.	N.D.
	Dec.	N.D.	N.D.
<u>1984</u>	Jan.	N.D.	N.D.
	Feb.	N.D.	N.D.
	Mar.	N.D.	N.D.
	Apr.	N.D.	0.740
	May	N.D.	N.D.
	Jun.	0.671	N.D.
	Jul.	N.D.	N.D.
	Aug.	N.D.	N.D.
	Sep.	N.D.	0.460
	Oct.	N.D.	N.D.
	Nov.	0.721	0.491
	Dec.	N.D.	N.D.
<u>1985</u>	Jan.	0.501	N.D.

* = ^{137}Cs level corrected for fresh water dilution
 from ^{137}Cs /salinity curve

N.D = No data available

III.4

Ea's for Transect A for Transit Times
 1.3 - 3.3 months ($\text{Bq l}^{-1}/\text{TBq day}^{-1}$)

<u>Month of Discharge</u>		<u>Ea - 1.3 months lag</u>	<u>Ea - 3.3 months lag</u>
<u>1982</u>	Feb.	N.D.	0.140
	Mar.	N.D.	N.D.
	Apr.	0.142	N.D.
<u>1983</u>	Feb.	N.D.	0.198
	Mar.	N.D.	N.D.
	Apr.	0.281	N.D.
	May	N.D.	0.235
	Jun.	N.D.	N.D.
	Jul.	0.185	N.D.
	Aug.	N.D.	N.D.
	Sep.	N.D.	N.D.
	Oct.	N.D.	0.138
	Nov.	N.D.	N.D.
	Dec.	0.395	N.D.
<u>1984</u>	Jan.	N.D.	0.312
	Feb.	N.D.	N.D.
	Mar.	0.713	0.599
	Apr.	N.D.	N.D.
	May	0.452	N.D.
	Jun.	N.D.	N.D.
	Jul.	N.D.	N.D.
	Aug.	N.D.	0.592
	Sep.	N.D.	N.D.
	Oct.	0.381	N.D.
	Nov.	N.D.	N.D.
	Dec.	N.D.	N.D.
<u>1985</u>	Jan.	N.D.	N.D.

N.D. = No data available

III.5

Ea's for Transect B for Transit Times
 2.3 - 3.5 months ($\text{Bq l}^{-1}/\text{TBq day}^{-1}$)

<u>Month of Discharge</u>		<u>Ea - 2.3 months lag</u>	<u>Ea - 3.5 months lag</u>
<u>1982</u>	Feb.	N.D.	0.177
	Mar.	0.169	N.D.
<u>1983</u>	Jan	N.D.	N.D.
	Feb.	N.D.	N.D.
	Mar.	N.D.	N.D.
	Apr.	N.D.	0.170
	May	N.D.	N.D.
	Jun.	0.213	N.D.
	Jul.	N.D.	N.D.
	Aug.	N.D.	N.D.
	Sept.	N.D.	N.D.
	Oct.	N.D.	N.D.
	Nov.	N.D.	N.D.
	Dec.	N.D.	N.D.
<u>1984</u>	Jan.	N.D.	0.294
	Feb.	0.424	N.D.
	Mar.	N.D.	0.515
	Apr.	0.514	N.D.
	May	N.D.	N.D.
	Jun.	N.D.	N.D.
	Jul.	N.D.	N.D.
	Aug.	N.D.	0.451
	Sep.	0.266	N.D.

N.D. = No data available

III.6

Ea's for Transect D for Transit Times
 2.4 - 4.0 months ($\text{Bq l}^{-1}/\text{TBq day}^{-1}$)

<u>Month of Discharge</u>	<u>Ea - 2.4 months lag</u>	<u>Ea - 4.0 months lag</u>
<u>1982</u>		
Jan.	N.D.	0.090
Feb.	N.D.	N.D.
Mar.	0.099	N.D.
<u>1983</u>		
Jan.	N.D.	0.163
Feb.	N.D.	N.D.
Mar.	0.155	N.D.
Apr.	N.D.	0.117
May	0.146	N.D.
Jun.	N.D.	N.D.
Jul.	N.D.	N.D.
Aug.	N.D.	N.D.
Sep.	N.D.	0.061
Oct.	N.D.	N.D.
Nov.	0.151	N.D.
Dec.	N.D.	N.D.
<u>1984</u>		
Jan.	N.D.	N.D.
Feb.	N.D.	0.316
Mar.	N.D.	N.D.
Apr.	0.502	N.D.
May	N.D.	N.D.
Jun.	N.D.	N.D.
Jul.	N.D.	N.D.
Aug.	N.D.	0.420
Sep.	0.227	N.D.

N.D. = No data available

III.7

Ea's for Transect G for Transit Times
 3.7 - 5.1 months ($\text{Bq l}^{-1}/\text{TBq day}^{-1}$)

<u>Month of Discharge</u>	<u>Ea - 3.7 months lag</u>	<u>Ea - 5.1 months lag</u>
<u>1981</u>		
Nov.	N.D.	0.096 ^(M)
Dec.	0.101 ^(M)	0.092
<u>1982</u>		
Jan.	0.082	N.D.
Feb.	N.D.	N.D.
Mar.	N.D.	0.080 ^(M)
Apr.	0.077 ^(M)	N.D.
May	N.D.	N.D.
Jun.	N.D.	N.D.
Jul.	N.D.	N.D.
Aug.	N.D.	N.D.
Sep.	N.D.	0.079 ^(M)
Oct.	0.080 ^(M)	N.D.
Nov.	N.D.	N.D.
Dec.	N.D.	0.100
<u>1983</u>		
Jan.	N.D.	N.D.
Feb.	0.102	N.D.
Mar.	N.D.	0.077
Apr.	0.114	N.D.
May	N.D.	N.D.
Jun.	N.D.	0.067 ^(M)
Jul.	0.073 ^(M)	N.D.
Aug.	N.D.	0.068
Sep.	0.058	N.D.
Oct.	N.D.	N.D.
Nov.	N.D.	0.170
Dec.	N.D.	N.D.

III.7 cont.'d

Ea's for Transect G for Transit Times
 3.7 - 5.1 months ($\text{Bq l}^{-1}/\text{TB day}^{-1}$)

<u>Month of Discharge</u>	<u>Ea - 3.7 months lag</u>	<u>Ea - 5.1 months lag</u>
<u>1984</u> Jan	0.170	0.159
Feb.	N.D.	N.D.
Mar.	0.364	N.D.
Apr.	N.D.	N.D.
May	N.D.	N.D.
Jun.	N.D.	0.274
Jul.	N.D.	N.D.
Aug.	0.202	0.223
Sep.	N.D.	N.D.
Oct.	0.144	N.D.

N.D. = No data available

(M) = MAFF cruise

III.8

Ea's for Transect E for Transit Times
 3.9 - 5.5 months (Bq l⁻¹/TBq day⁻¹)

Month of Discharge	Ea - 3.9 months lag	Ea - 5.5 months lag
<u>1983</u> Feb.	N.D.	0.111
Mar.	N.D.	N.D.
Apr.	0.157	N.D.
May	N.D.	N.D.
Jun.	N.D.	N.D.
Jul.	N.D.	N.D.
Aug.	N.D.	N.D.
Sep.	N.D.	N.D.
Oct.	N.D.	N.D.
Nov.	N.D.	0.184
Dec.	N.D.	N.D.
<u>1984</u> Jan.	0.184	0.297
Feb.	N.D.	N.D.
Mar.	0.470	N.D.
Apr.	N.D.	N.D.
May	N.D.	N.D.
Jun.	N.D.	0.280
Jul.	0.265	N.D.

N.D. = No data available

III.9

Ea's for Transect K for Transit Times
 5.7 - 7.7 months ($\text{Bq l}^{-1}/\text{TBq day}^{-1}$)

<u>Month of Discharge</u>	<u>Ea - 5.7 months lag</u>	<u>Ea - 7.7 months lag</u>
<u>1982</u>		
Oct.	N.D.	0.039
Nov.	N.D.	N.D.
Dec.	0.045	N.D.
<u>1983</u>		
Jan.	N.D.	0.062
Feb.	N.D.	N.D.
Mar.	0.059	N.D.
April	N.D.	N.D.
May	N.D.	N.D.
Jun.	N.D.	N.D.
Jul.	N.D.	N.D.
Aug.	N.D.	N.D.
Sep.	N.D.	N.D.
Oct.	N.D.	N.D.
Nov.	N.D.	0.097
Dec.	N.D.	N.D.
<u>1984</u>		
Jan.	0.097	N.D.
Feb.	N.D.	N.D.
Mar.	N.D.	N.D.
Apr.	N.D.	0.169
May	N.D.	N.D.
Jun.	0.153	N.D.

N.D. = No data available

APPENDIX IV ^{137}Cs Data For MAFF/G.U. Calibration

<u>G.U (dpm/l)</u>	<u>MAFF (dpm/l)</u>
20.3 \pm 0.8	24.6
19.7 \pm 0.6	23.4
18.0 \pm 0.4	21.0
20.3 \pm 0.6	22.2
21.1 \pm 0.3	24.0
21.5 \pm 0.3	23.4
20.1 \pm 0.6	24.0
11.6 \pm 0.4	13.8
3.0 \pm 0.1	3.2
0.7 \pm 0.1	0.6
14.8 \pm 0.6	18.0
13.7 \pm 0.6	16.6
9.5 \pm 0.3	10.8
7.1 \pm 0.2	8.4
6.1 \pm 0.2	7.2
4.1 \pm 0.1	4.7
3.5 \pm 0.1	4.0
3.0 \pm 0.1	3.4
0.3 \pm 0.1	0.3
5.7 \pm 0.1	6.6
7.2 \pm 0.2	8.4

$$y = 1.1566x + 0.09374; y = \text{MAFF}, x = \text{G.U.}$$

APPENDIX VSeaweed DataAppendix V.1

Wet Weight : Dry Weight Ratios for Seaweeds
From North West Britain, 3/4 January 1983.

<u>SITE</u>	<u>Wet weight : Dry weight</u>
Ravenglass	6.67
Sellafield	5.08
St. Bees	5.91
Annan	10.00
Balcary Bay	6.04
Sandhead	4.17
Ballantrae	4.17
Turnberry	5.00
Saltcoats	6.65
Gourock	5.27
Loch Fyne	4.91

Appendix V.2

⁴⁰K Activities in Seaweeds From North West Britain
(3/4 January 1983)

<u>SITE</u>	<u>⁴⁰K (mBq/g dry weight)</u>
Ravenglass	1.44E 03 ± 5.70E 01
Sellafield	1.02E 03 ± 4.85E 01
St. Bees	1.24E 03 ± 5.25E 01
Annan	1.69E 03 ± 5.00E 01
Balcary Bay	1.41E 03 ± 5.44E 01
Sandhead	6.11E 02 ± 4.07E 01
Ballantrae	7.92E 02 ± 4.44E 01
Turnberry	1.06E 03 ± 4.66E 01
Saltcoats	1.24E 03 ± 4.96E 01
Gourock	5.62E 02 ± 4.96E 01
Loch Fyne	9.25E 02 ± 4.18E 01

APPENDIX VI - Computer Programmes*

VI.1 137 Cs Calculation Programme

```

0001 COMMON A(100),B(100),C7(100),CR(100),N,X(10,100),Y(10,100)
0002 COMMON JZ
0003 CALL PAPER(1)
0004 JZ#1
0005 RN#1,0
0006 READ(5,10)N
0007 WRITE(6,15)N
0008 FORMAT(I3)
0009 10 FORMAT(1H0,10X,I3)
0010 15 FORMAT(1H0,10X,I3)
0011 DO50 I=1,N
0012 READ(5,20) C7(I),CR(I)
0013 WRITE(6,30)C7(I),CR(I)
0014 50 CONTINUE
0015 WRITE(6,40)
0016 20 FORMAT(F5.1,F4.3)
0017 30 FORMAT(1H,10X,F8.2,5X,F8.4)
0018 40 FORMAT(1H1,80(1H*))
0019 CALL RMX
0020 DO 200 J=1,3
0021 DO 250 K=1,N
0022 C7(K)=X(J,K)
0023 CR(K)=Y(J,K)
0024 250 CONTINUE
0025 CALL RMX
0026 200 CONTINUE
0027 999 CONTINUE
0028 CALL GREND
0029 STOP
END

```

cont'd...

VI.1 cont'd

```

0001 SUBROUTINE BXMZ
0002 COMMON A(100),B(100),C7(100),CR(100),N,X(10,100),Y(10,100)
0003 COMMON JZ
0004 CALL BLKPEN
0005 CALL CTRHAG (12)
0006 CALL MAP(0,0,75,0,0,0,0,13)
0007 CALL SCALSI(12,0,0,0,025)
0008 DO00 K=1,16
0009 RN=FLOAT(K)
0010 TOT=81.3
0011 RTT=0.101
0012 FN=-0.693/IRN
0013 FR=EXP(FN)
0014 FR=1.0-FR
0015 DO100 I=1,N
0016 RTT=0.974*((1.0-FR)*RTT*TOT)+(FR*C7(I)*CR(I))
0017 TOT=((1.0-FR)*TOT)+(FR*C7(I))
0018 RTT=RTT/TOT
0019 WRITE(6,J0)TOT,RTT
0020 30 FORMAT(1H ,1UX,F0.2,0X,F0,4)
0021 A(I)=RTT
0022 B(I)=TOT
0023 IF(JZ.GE.2) GOTO 90
0024 X(K,I)=TOT
0025 Y(K,I)=RTT
0026 90 CONTINUE
0027 100 CONTINUE
0028 WRITE(6,40)
0029 40 FORMAT(1H1,80(1H*))
0030 IF(K.EQ.5)CALL REDPEN
0031 IF(K.EQ.9)CALL BLKPEN
0032 IF(K.EQ.13) CALL REDPEN
0033 NJ=N-1
0034 DO120 I=1,NJ
0035 F=FLOAT(I)
0036 CALL POINT (F,A(I))
0037 J=I+1
0038 G=F+1.0

0039 CALL JOIN(G,A(J))
0040 120 CONTINUE
0041 60 CONTINUE
0042 JZ=JZ+1
0043 CALL FRAME
0044 RETURN
0045 END

```

cont'd...

VI.1 cont'dVARIABLE NAMES

MCT	number of water profiles
TITLE	graph title
NX	number of samples in particular profile
TT	table heading
C7	number of counts in Cs-137 window
C4	" " " " Cs-134 "
DY	decay time (days)
IW	printout number
VL	sample volume (litres)
TM	count time (minutes)
T1 - T6	location and date
D	sample depth (metres)
S	" salinity (°/oo)
T	" temperature (C)
O	" D.O. concentration (°/oo)
B7	background in Cs-137 window (c.p.m.)
B4	" " Cs-134 " "
A	Cs-137 concentration (d.p.m.l ⁻¹)
E	error on Cs-137 "
B	Cs-134 concentration "
C	error on Cs-134 "
R	Cs-134/Cs-137 ratio
G	error on ratio
X	salinity corrected Cs-137 concentration (d.p.m.l ⁻¹)

* written by I. G. McKinley

VI. 2 Mixing - box Model Programme

```

0001 COMMON YSC9(20,20),XSC9(20,20),XERS(20,20),NX(20),TITLE(16),HCT
0002 DIMENSION A(99),B(99),C(99),S(99),T(99),D(99),E(99),F
1(99),G(99),R(99),X(99)
0003 CALL PAPER(1)
0004 READ(5,99) HCT
0005 99 FORMAT(12)
0006 IF(HCT.EQ.0.0) GOT0999
0007 READ(5,110)(TITLE(KX),KX=1,16)
0008 FORMAT(15A4)
0009 DO 800 IX=1,HCT
0010 READ(5,99) NX(IX)
0011 READ(5,110)(TT(K),K=1,15)
0012 WRITE(6,120)(TT(K),K=1,15)
0013 FORMAT(1H1,20X,15A4/20X/60(1H*))
0014 WRITE(6,130)
0015 130 FORMAT(/10X,'CODE1,4X,'DEPTH(M)',3X,'137(DPM/L)',5X,'134(DPM/L)',
15X,'RATIO1,7X,'SC7(DPM/L)' SAL(PH) TEMP(C) D.U.,(PH)')
K0=NX(IX)
0016 DO 100 J=1,K0
0017 READ(6,20) C7,C4,DY,1H,YL,1H,T1,T2,T3,T4,T5,T6,D(J),S(J),T(J),O(J)
0018 20 FORMAT(2(F10,2,10X),F10,2,18,F12,5,F5,2/3A4,2X,3A4/4F10,2)
0019 IF(T1.EQ.0.0) TM=1380
0020 IF(S(J).EQ.0.0) S(J)=0.00001
0021 IF(VL.EQ.0.0) VL=10.0
0022 87=17.72830*TM
0023 84=22.591*TM
0024 FC=EXP(0.0000629*DY)/(0.14829*TM*VL)
0025 F0=EXP(0.0009212*DY)/(0.2330*TM*VL)
0026 A(J)=((C7-B7)-0.33194*(C4-B4))/0.999893
0027 B(J)=((C4-B4)-0.00032*A(J))*FD
0028 A(J)=A(J)*FC
0029 R(J)=B(J)/A(J)
0030 X(J)=A(J)*(35.0/S(J))
0031 C7=C7+D7
0032 C4=C4+D4
0033 EC=SQRT((C7+0.11018*C4)*(FC/0.999893)
0034 ED=SQRT((C4)*FD)
0035 ER=SQRT((EC/A(J))*2)+(ED/B(J))*2)
0036 E(J)=SQRT((EC**2)+((0.074*A(J))*2))
0037

```

cont'd ...

VI. 2 cont'd

```

0038 F(J)=SQRT((ED**2)+((0.025*(J)**2))
0039 G(J)=ER*(J)
0040 XSCS(IX,J)=X(J)
0041 YSCS(IX,J)=Y(J)
0042 XERS(IX,J)=E(J)
0043 WRITE(6,60)T1,T2,D(J),A(J),E(J),B(J),F(J),R(J),S(J),X(J),8(J),T(J)
      1,0(J)
0044 60 FORMAT(/10X,2A4,F5,1,2(F6,1,1) +/- 1,F4,1),F7.3,1 +/- 1,F5,3,F7,1,6
      1X,3(F6,2,3X))
0045 100 CONTINUE
0046 WRITE(6,560)
0047 560 FORMAT(1H1,99(1H*))
0048 800 CONTINUE
0049 CALL DRAW
0050 CONTINUE
0051 CALL GREND

0001 SUBROUTINE DRAW
0002 COMMON YSCS(20,20),XSCS(20,20),XERS(20,20),NX(20),TITLE(15),MCT
0003 CALL CTRMAG(14)
0004 CALL PLOTCS(0,3,0,97,TITLE,60)
0005 CALL CYRMAG(12)
0006 CALL PLOTCS(0,75,0,05,ICS=137 PCI/L1,15)
0007 CALL PLOTCS(0,05,0,96,DEPTH (M),1,9)
0008 CALL MAP (75,0,150,0,85,0,=5,0)
0009 CALL SCALES
0010 D020 I=1,MCT
0011 INX=HX(I)
0012 0010 J=1,INX
0013 XU=XSCS(I,J)=XERS(I,J)
0014 XV=XSCS(I,J)+XERS(I,J)
0015 CALL POINT (XU,YSCS(I,J))
0016 CALL JOIN (XV,YSCS(I,J))
0017 10 CONTINUE
0018 IMX=INX-1
0019 D015 K=1,IMX
0020 CALL POINT (XSCS(I,K),YSCS(I,K))
0021 IK=K+1
0022 CALL JOIN (XSCS(I,K),YSCS(I,IK))
0023 15 CONTINUE
0024 20 RETURN
0025 END

```

APPENDIX VIIReference Standards for Ge (Li)VII. 1. Mixed Radionuclide Gamma-Ray Reference Standard.

<u>Radionuclide</u>	<u>Gamma-ray energy (MeV)</u>	<u>Overall Uncertainty (%)</u>
^{109}Cd	0.088	+/- 2.7
^{57}Co	0.122	+/- 2.0
^{139}Ce	0.166	+/- 2.8
^{203}Hg	0.279	+/- 2.1
^{113}Sn	0.392	+/- 3.5
^{85}Sr	0.514	+/- 2.0
^{137}Cs	0.662	+/- 3.2
^{88}Y	0.898	+/- 3.8
^{60}Co	0.1173	+/- 0.8
^{60}Co	1.333	+/- 0.8
88Y	1.836	+/- 2.8

VII. 2. ^{152}Eu Gamma Standard

<u>Gamma-ray energy (keV)</u>	<u>Relative Intensity (%)</u>
121.8	60
244.6	28
344.2	100
411.0	7
443.9	18
778.6	45
964.1	55
1086.0	45
1407.5	90
1457	
1528	

